Eindrapportage

Intelligente sturing van zonwering voor optimale gebouwprestaties

Auteurs: Roel Loonen (TU/e), Sam Kin (Kindow BV)

TKI Urban Energy – project 1621503

Mei 2021

Intelligente sturing van zonwering voor optimale gebouwprestaties

Samenvatting

Slimme aansturing van zonwering kan de energie-efficiëntie en het comfort in gebouwen flink verhogen. In bestaande gemotoriseerde systemen is de regelintelligentie echter beperkt. Dit vormt een gemiste kans voor energiebesparing, en een bron van klachten.

Het doel van dit project was de ontwikkeling van verbeterde intelligente aansturing voor gemotoriseerde zonwering. Daarnaast zijn de effecten van de regeling op de energie-efficiëntie en de kwaliteit van het binnenklimaat gekwantificeerd via een gevalideerd simulatiemodel en vervolgens vertaald in een gebruiksvriendelijke interface, zodat specifieke businessproposities in detail besproken kunnen worden met potentiële opdrachtgevers.

Kindow heeft zich binnen dit project met name toegelegd op de uitbreiding van regelalgoritmes met een focus op schaalbaarheid (minimaliseren van kosten en het benodigde handwerk voor installatie en updates) en koppeling met externe services om zelflerendheid (leren van gebruikersinteractie) en anticiperend vermogen (sturen op basis van verwachte weerspatronen) onderdeel te maken van de regeling. Verder is er aandacht geweest voor de productontwikkeling naar een praktijktoepassing die geschikt is voor meerdere, gangbare zonweringssystemen (rolgordijnen en lamellen) en naadloos ingepast kan worden in bestaande gebouwen en gebouwbeheersystemen. De opgedane kennis is toegepast in meerdere praktijkprojecten, zoals beschreven op: https://kindowblinds.com/projects/.

In samenwerking met Kindow heeft de TU/e zich gericht op de uitbreiding en praktische toepassing van een geïntegreerd simulatiemodel om de effecten van intelligente zonwering op energiebesparing en binnenmilieukwaliteit te kunnen kwantificeren. Er is uitvoerig onderzoek gedaan naar de verschillende effecten van binnen- en buitenzonwering, waarbij duidelijk gebleken is dat de veelgebruikte vuistregel “binnenzonwering is niet effectief voor energiemanagement, want de warmte is al binnen” niet van toepassing is voor binnenzonwering met reflecterende doeken en intelligente aansturing. Daarnaast is onderzoek gedaan naar optimale doekeigenschappen voor verticale lamellen (met reflecterende en absorberende zijde) en (dubbele) rolgordijnen. Ook is er een gebruiksvriendelijke en uitgebreide database ontwikkeld die de prestaties van Kindow in gebouwen met bijv. verschillende glaseigenschappen, geveloriëntatie, raamgrootte snel inzichtelijk maakt. In de vorm van afstudeerprojecten is (i) de synergie aangetoond tussen dynamische binnenzonwering en een slim gedimensioneerd gevelontwerp (bijv. via overstekken), (ii) de mogelijkheid van automatische detectie van schaduw door omliggende gebouwen uitgewerkt, en (iii) de mogelijkheid van de koppeling tussen zonwering en gevel-geïntegreerde HVAC-systemen uitgezocht.

De bevindingen uit het project hebben een actieve bijdrage geleverd aan IEA SHC Task 56: https://task56.iea-shc.org/. Daarnaast heeft het project ook geleid tot publiciteit in vakbladen en relevante websites zoals: Bouwwereld, Glas in Beeld en Solar Magazine.

Inhoudsopgave

Inleiding

De Nederlandse overheid wil een volledig energieneutrale gebouwde omgeving in 2050. Gezien de verwachting dat in 2030 80% van het gebouwenbestand zal bestaan uit gebouwen die vandaag de dag al bestaan en in 2050 nog steeds 50%, wordt het duidelijk dat de uitdaging rondom energiebesparing vooral bij de bestaande bouw ligt. Er moet dus vol ingezet worden op energiebesparing in bestaande gebouwen. Voor kantoren is ook in november 2016 bekend gemaakt dat ze verplicht zijn aan een c-label te voldoen in 2023. Uit de praktijk blijkt dat eenvoudige inpasbaarheid in de bestaande situatie een belangrijke succesfactor is voor besparings- maatregelen. Automatisering van de zonwering is zo'n maatregel waarmee in potentie ook een groot effect behaald kan worden. De effectiviteit is echter sterk afhankelijk van de regeling van de zonwering. Motorisering van zonwering is een sterke trend maar de intelligentie van de regeling blijft in de praktijk ver achter. Deze is vaak beperkt tot een zon-windmeter op het dak. Een reactieve regeling waarbij de zonwering volledig open of dicht gaat. Dit resulteert vaak in 'pendelende' systemen, wat als zeer storend ervaren wordt door de gebruikers. Moeilijkheid daarin is ook de regelmatige strijdigheid tussen energie-optimalisatie en optimalisatie van comfort. Verdere complexiteit wordt toegevoegd door de gebruiker die in de regel in staat is om de automatische regeling handmatig te 'overrulen' en dat vaak doet in strijd met de optimalisering van energiegebruik.

In de praktijk blijft de intelligentie van gemotoriseerde zonwering achter en daarmee wordt de potentiële energiebesparing en comfortverhoging niet goed ingevuld. In een voorgaand iDEEGO project is een intelligente regeling ontwikkeld voor de aansturing van gemotoriseerde rolgordijnen (binnenzonwering). De besparing met binnenzonwering wordt echter betwist door veel partijen in de markt. Daarnaast vertegenwoordigen gemotoriseerde rolgordijnen (binnen) slechts een klein deel van de gangbare zonweringsystemen die gemotoriseerd worden. De regeling die ontwikkeld is binnen iDEEGO biedt al veel meer intelligentie dan de "domme" open- dicht regeling die op dit moment standaard is, door o.a. zonpositie en aanwezigheid mee te nemen. Deze kan echter nog veel verbeterd worden door ook rekening te houden met gebruikersinteractie en weerpatronen. Dit zal nodig zijn voor echt onderscheidend vermogen en impact op energiebesparing en comfort

Doelstelling

De doelstelling van het in dit rapport beschreven onderzoeks- en ontwikkelingsproject is tweeledig. Enerzijds richt het zich op de uitbreiding en verbetering van door Kindow ontwikkelde zonvolgende regelalgoritmes voor binnenzonwering met een focus op schaalbaarheid (minimaliseren van kosten en het benodigde handwerk voor installatie en updates) en koppeling met externe services om zelflerendheid (leren van gebruikersinteractie) en anticiperend vermogen (sturen op basis van verwachte weerspatronen) onderdeel te maken van de regeling. Deze regelingen gebruiken geavanceerde algoritmes op basis van meerdere input parameters, zoals instraling, zonpositie, flux (warmtestroom tussen binnen en buiten), weertype, aanwezigheid, positie van gebruiker t.o.v. het raam, etc.

Dit werk is gecomplementeerd met de ontwikkeling en implementatie van een gebouwsimulatiemodel waarmee de effecten van zulke regelingen op het energiegebruik en de kwaliteit van het binnenklimaat gekwantificeerd kunnen worden. Belangrijke aandachtpunten hierbij waren (i) de uitbreiding van het model voor alle veelvoorkomende vormen van zonwering op basis van Complex Fenestration System modellen, (ii) een gedetailleerde vergelijking tussen de prestaties van binnen- en buitenzonwering, en (iii) het opzetten van een interactieve database waarin op gebruiksvriendelijke wijze de prestaties van Kindow in verschillende gebouwtypen inzichtelijk gemaakt worden.

Projectresultaten

Productontwikkeling en regelingen

Kindow heeft veel tijd en ontwikkeling gestoken in een infrastructuur voor het realiseren van projecten op een snelle en betaalbare manier. Het energieverbruik en het piekvermogen van de systemen is flink afgenomen en het is nu mogelijk om 24 systemen door te lussen op één voeding en communicatielijn (dat komt overeen met ca 60 strekkende meter gevel per voeding). Dat scheelt veel tijd en dus kosten voor de installateur (grote drempel voor toepassing van gemotoriseerde zonweringssystemen in het algemeen)

Kindow heeft een 'low-light' sensor ontwikkeld voor het detecteren van bewolking. De sensor is verbonden aan dezelfde voeding en communicatielijn als de systemen en is in te stellen en toe te wijzen aan individuele of groepen systemen. De bewolkingsmodus is uitvoerig getest, drempelwaardes bepaald en deze is nu ook operationeel in twee commerciële projecten met Kindow Verticals. Verder is de sturing van Kindow uitgebreid met een high-light modus (hoge kans op verblinding) een Energiemodus (wordt op gestuurd bij afwezigheid) - en een Zomer/Wintermodus (zonwerend materiaal laten reflecteren of absorberen).

Kindow heeft een Bootloader ontwikkeld in de firmware, dat wil zeggen dat de firmware van de systemen, over de lijn opnieuw geprogrammeerd kan worden voor het doorvoeren van updates. Voor het communiceren over de lijn voor aansturing en firmware updates is een complexe communicatie en berichten structuur vereist die is ontwikkeld. Deze hebben wij in de toekomst ook nodig om systemen te monitoren (status en gebruik) en op basis daarvan zelflerendheid toe te voegen aan de aansturing zoals omschreven in WP4.

Kindow heeft een gateway ontwikkeld met programmatuur voor het vertalen van commando's van het gebouwbeheersysteem (KNX of BACNET) naar aansturingscommando's voor individuele en groepen systemen (Figuur 1). Zo kan men de systemen centraal en als collectief aansturen en ook koppelen aan bijvoorbeeld het brand- en/of inbraakalarm, of allemaal openen voor de glazenwasser. Ook maakt dit het mogelijk om de systemen per ruimte te bedienen via eventuele wandschakelaars die ook aan het gebouwbeheersysteem zijn verbonden. Via het GBS wordt in feite de Kindow automatische aansturing overrruled, deze wordt dan 's nacht weer vrijgegeven. Hiermee hebben we voldaan aan WP5

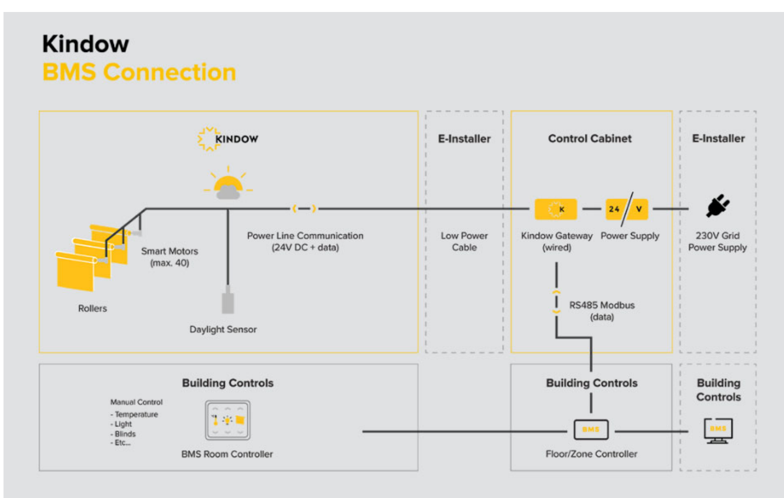

Figuur 1. Koppeling tussen Kindow regeling en gebouwbeheerssysteem.

Kindow ontwikkelt naast de het verticals systeem nu ook een rollers systeem (Figuur 2), om een totaaloplossing te kunnen beiden voor intelligente daglichtregeling in kantoren en utiliteitsgebouwen. Het rolgordijn past zich automatisch aan op de zonshoogte in relatie tot de afstand van het bureau/werkplek tot het raam. Kindow heeft een productontwerp en een functionerend prototype. Onderdeel van dit nieuwe prototype is ook een uitbreiding van de aansturing op basis van weerdata en aanwezigheid. Voor de aanwezigheid heeft Kindow een koppeling gemaakt met het platform van Mapiq (Yes!Delft bedrijf gespecialiseerd in lokaliseren en visualiseren van mensen in gebouwen). Mapiq registeert voor de ruimte van het prototype of er mensen aanwezig zijn en waar ze zich bevinden in de ruimte met eigen ontwikkelde sensoren. Door de koppeling maakt Kindow gebruik van deze data voor de aansturing, deze wordt vervolgens weer gevisualiseerd in de userinterface van Mapiq. Omtrent de online interface met weerdata maakt Kindow voor dit prototype nu gebruik van buitentemperatuur om te bepalen of er een koude- dan wel warmtevraag is voor de energiemodus (warmte weren vs. warmte toelaten). Anticiperend vermogen op basis van voorspeld weertype (zoals de bedoeling in WP3) is nog niet operationeel maar de basis voor dergelijke functionaliteit is voor een groot deel gelegd.

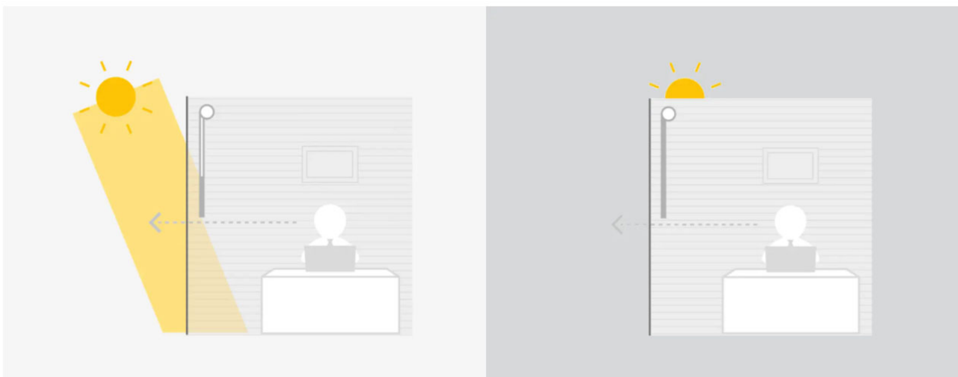

Figuur 2. Zonvolgend algoritme met Kindow rollers

Er is gezamenlijk een nieuwe methode ontwikkeld om gebouwspecifieke regelparamters te tunen op basis van gebouwsimulaties. Deze aanpak maakt gebruik van confusion matrices (Figuur 3) als een statistische classificatiemethode om (i) sensortypes te selecteren die een gunstige trade-off bieden, rekening houdend met meerdere prestatieaspecten en (ii) regelalgoritmen te identificeren die comfortcondities optimaliseren met gebruik van niet-ideale sensoren. De methode vergt relatief weinig inspanning van een ontwikkelaar, slechts een klein aantal simulaties en past goed binnen de huidige praktijk van de ontwikkeling van zonweringcontrole. De methode wordt getest met zonvolgende Kindow verticals. Voor meer details wordt verwezen naar het artikel de Vries et al. (2021) in Appendix A.

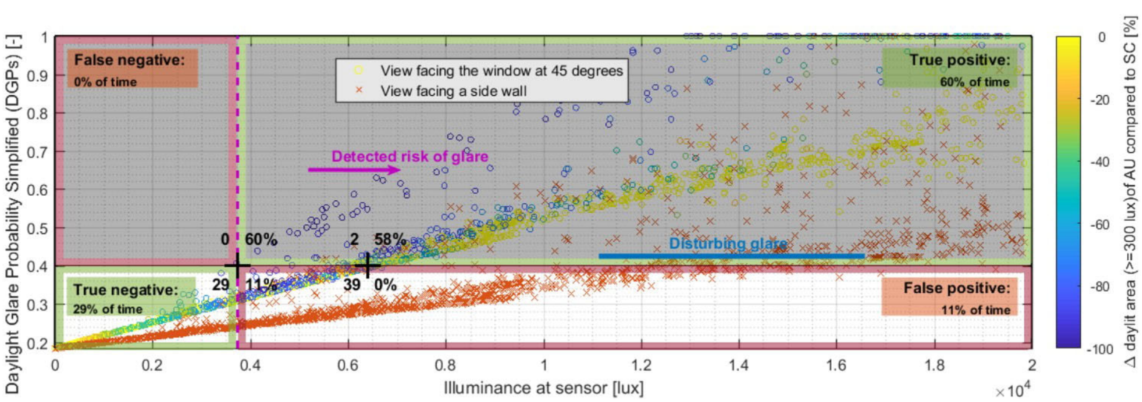

Figuur 3. Voorbeeld van een confusion matrix voor het verbeteren van Kindow regelingen

Prestaties en modellen

Het belangrijkste projectresultaat ten aanzien van prestaties en modellen staat uitvoerig beschreven in het PDEng rapport van Oindrila Ghosh (Appendix B).

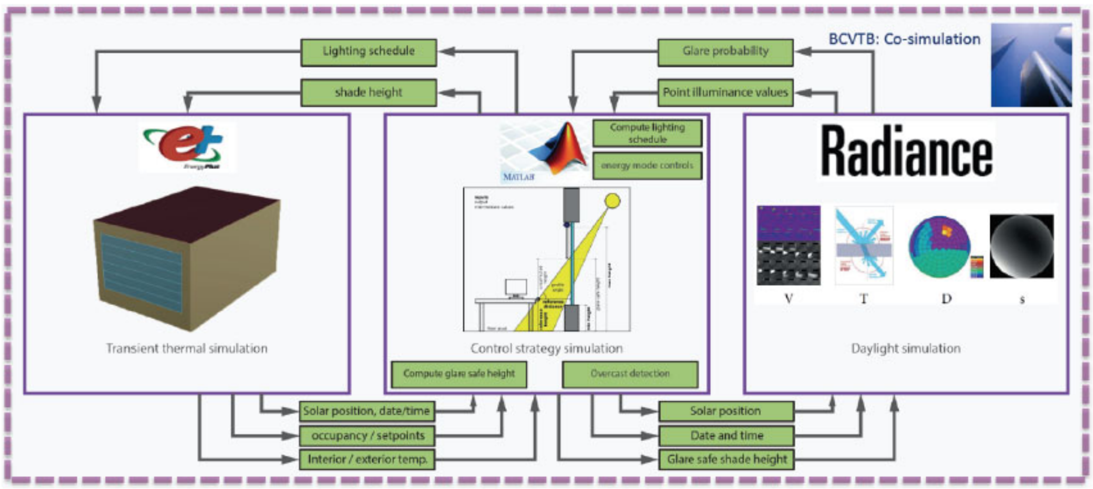

Figuur 4. Virtual testbed voor geïntegreerde simulaties (daglicht en thermisch) van geavanceerde zonwering.

Hierbij is het initieel ontwikkelde virtual testbed (Figuur 4) verder uitgebreid met focus op de volgende drie aspecten:

1. Prestatiebeoordeling voor Kindow producten en regelingen onder verschillende scenario's te onderzoeken. Daarnaast werden studies uitgevoerd om de meest efficiënte strategie te evalueren en na te gaan of er behoefte is aan verdere optimalisering.
2. Op basis van deze studies is een gebruiksvriendelijke en uitgebreide database opgezet met informatie over de energie- en comfortprestaties van Kindow voor in totaal 1440 verschillende opties voor invoerparameters (glaseigenschappen, gevelorientatie, raamgrootte, etc.) (Figuur 5). Deze opzoektabel drukt de prestaties uit in de vorm van relevante KPI's om vervolgens de interactie over overtuigende waardeproposities aan te gaan met potentiële klanten van Kindow.
3. Er zijn strategieën ontwikkeld om het marktbewustzijn van de mogelijkheden van binnenzonwering te stimuleren. Dit bestaat uit een reeks artikelen en interactieve blogs die snel en gemakkelijk inzicht geven in hoe het gebruik van Kindow producten de waarde van hun gebouwen kan verbeteren. Bovendien zijn korte artikelen in studententijdschriften en interviews in populaire bouwmagazines gepubliceerd, zoals zoals: Bouwwereld, Glas in Beeld en Solar Magazine.

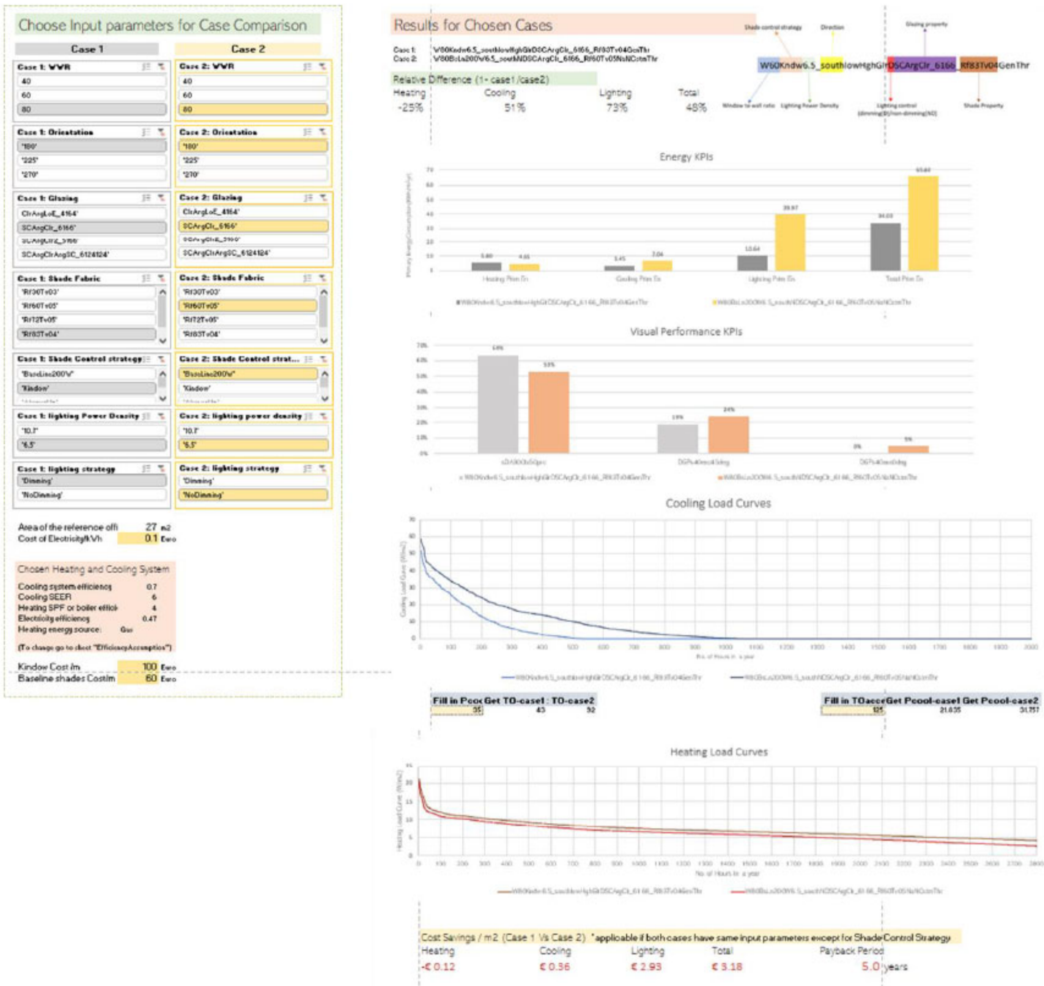

Figuur 5. Overzicht van de interactieve database

Kindow wordt regelmatig geconfronteerd met het standpunt: “waarom richten jullie je op binnenzonwering – iedereen weet toch dat dat niet effectief is voor energiemanagement, want de warmte is al binnen?”. Wat men zich vaak niet realiseert is dat deze vuistregel enkel inzoomt op de rol van zonwering voor het beperken van koellast, terwijl de werkelijke rol van zonwering veel complexer kan zijn wanneer het doelmatig wordt ingezet voor het balanceren van de energievraag voor verwarming, koeling en verlichting en tegelijkertijd beoogt het daglichtcomfort te verbeteren. Bovendien houdt de vuistregel geen rekening met de mogelijkheden die geboden worden door moderne spectraal-selectieve glastypen, reflecterende doeken en geavanceerde regelingen zoals Kindow. Om meer nuance aan te brengen in de discussie tussen de kampen binnen- vs. buitenzonwering, is de vergelijking tussen beide opties in detail bestudeerd, zoals beschreven in Appendix C. Uit deze studie kan geconcludeerd worden dat het gebruik van reflecterende materialen en de Kindow regeling voor rollerblinds het primaire energieverbruik kan reduceren met 6.5% in vergelijking met buitenzonwering met eenvoudige aansturing. Het gebruik van de Kindow Rollerblind-strategie verbetert bovendien de hoeveelheid daglicht die de ruimte binnenkomt aanzienlijk met een toename in Spatial Daylight Autonomy van 65%. Deze studie toont verder aan dat een zorgvuldige combinatie van beglazing en zonwering, en regelstrategieën belangrijk is voor het behalen van optimale prestaties. De vergelijking met standaard binnenzonwering is ook gemaakt, zoals weergegeven in Figuur 6.

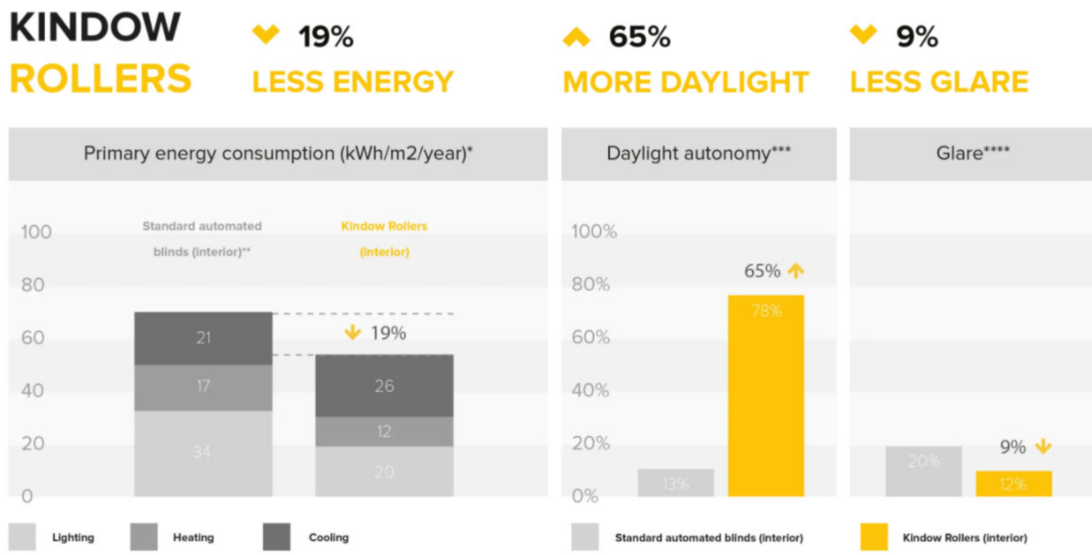

Figuur 6. Vergelijking tussen Kindow rollerblinds en rolgordijnen met standaard up-down regeling.

Om de resultaten van dit onderzoek in een bredere context te plaatsen, is actief deelgenomen aan discussies in werkgroepen van IEA SHC Task 56: Solar Building Envelopes. Deze interacties hebben onder andere geleid tot een verdiepende SWOT analyse die tot stand is gekomen met internationale expertfeedback tijdens een door de TU Eindhoven georganiseerde workshop (Figuur 7) http://task56.iea-shc.org/Data/Sites/1/publications/Task56--State-of-the-Art-SWOT.pdf. Een ander resultaat in de IEA SHC context is een studie naar de prestaties van Kindow in toekomstige scenario's, waarbij o.a. rekening gehouden is met een veranderende primaire energiefactor (PEF) als gevolg van een toename van hernieuwbare bronnen in de elektriciteitsmix. Uit deze verkenning, die beschreven staat in Appendix D, is aan het licht gekomen dat het verminderen van zonnewarmtewinsten in de toekomst een minder belangrijke rol heeft bij de keuze van beglazing en de regeling van zonweringssystemen, wanneer daglichtdimmersystemen en efficiëntere koelsystemen meer alomtegenwoordig zijn, en de aanwezigheid van hernieuwbare elektriciteit uit PV aanleiding geeft tot een gunstige PER in de zomermaanden. Dit is belangrijke informatie die gebruikt kan worden bij het maken slimme combinaties van beglazing en zonweringseigenschappen.

Figuur 7. Kindow SWOT-analyse als onderdeel van IEA SHC Task 56.

Tot slot is binnen de context van dit TKI Urban Energy project door drie afstudeerstudenten onderzoek gedaan naar gerelateerde onderwerpen die kunnen helpen bij de verdere opschaling van Kindow zoals optimalisatie van de gevel als geheel en koppeling met gevelgeïntegreerde HVAC systemen:

- Kim Bodde (2020) Coupled design optimization of façade design and automated shading control for improving visual comfort in office buildings. Appendix E.
- Wesley van der Sommen (2020) Context-aware solar shading strategies - performance potential and unsupervised machine learning approaches. Appendix F.
- Anqi Shi (2020) Simulation-based Performance Evaluation of Buildings with Window-frame Integrated Ventilation and Advanced Solar Shading. Appendix G.

Voor een uitgebreid overzicht van de bevindingen wordt in deze rapportage verwezen naar de afstudeerrapporten in de appendices.

JOURNAL OF BUILDING PERFORMANCE SIMULATION
https://doi.org/10.1080/19401493.2021.1887355

OPEN ACCESS Check for updates

Simulation-aided development of automated solar shading control strategies using performance mapping and statistical classification

Samuel B. de Vries, Roel C. G. M. Loonen and Jan L. M. Hensen

Unit Building Physics and Services, Department of the Built Environment, Eindhoven University of Technology, Eindhoven, The Netherlands

ABSTRACT
This paper presents a structured, generically applicable, method for using building performance simulation to aid the development of comfort-driven solar shading controls by mapping predicted occupant comfort conditions to sensor measurements. The method uses confusion matrices as a statistical classification approach to facilitate (i) selection of sensor deployment strategies that offer beneficial trade-offs considering multiple performance aspects and (ii) identification of control algorithms that optimise comfort conditions using non-ideal sensors. The support method requires relatively little effort from a developer, only a small number of simulations and fits well within the current practice of shading control development. The method is tested using a sun-tracking control strategy for indoor roller blinds as a case study, which demonstrates that the method can identify high-performance solutions. Finally, generally applicable features of the method are extrapolated from the case study, and alternative applications and the method's limitations are discussed.

ARTICLE HISTORY
Received 30 November 2020
Accepted 2 February 2021

KEYWORDS
Automated solar shading; control strategies; mapping; statistical classification; confusion matrix

1. Introduction

Automated solar shading systems are instrumental for improving indoor environmental quality and reducing building energy consumption (Beck and Dolmans 2010; Daum and Morel 2010; Konis and Selkowitz 2017; Kuhn 2017; Lee, DiBartolomeo, and Selkowitz 1998; Shen and Tzempelikos 2012). The performance of solar shading systems, however, greatly depends on how these screens or slats are operated (Correia da Silva, Leal, and Andersen 2015; Daum and Morel 2010; Gunay, O'Brien, and Beausoleil-Morrison 2016; Lee, DiBartolomeo, and Selkowitz 1998; Mahdavi et al. 2008; Shen and Tzempelikos 2012; Tzempelikos and Shen 2013; Yao et al. 2016). Conventional control systems, that are characterized by simple full open and close actions in response to a sensor and a control threshold (Tabadkani et al. 2020), often do not fulfil the comfort requirements of occupants and lead to occupant dissatisfaction (Bian, Leng, and Ma 2018; Meerbeek et al. 2014; Stevens 2001).

Developing control strategies for automated solar shading systems requires making decisions regarding a large number of design parameters involving the control logic, control sensors and the design of the shading device (Kuhn 2017). Additionally, the number of possible sequences of shading system actuations or states defines a vast control space. Leveraging these parameters in the development of comfort-driven control systems is complex because it requires insight into comfort conditions of occupants and trade-offs between conflicting performance aspects (Loonen et al. 2013). Additionally, these aspects are affected by highly dynamic environmental conditions and can interact differently depending on the specific application in terms of, for example, building type, facade properties and interior lay-out (Favoino et al. 2016; Kuhn 2017; Loonen et al. 2013; Loonen et al. 2014; Silva da, Leal, and Andersen 2012).

Shading control strategies rely on sensors to classify indoor comfort conditions and decide upon control actions (Beck and Dolmans 2010; Tabadkani et al. 2020). For instance, vertical outdoor irradiance and indoor convective temperature sensors are commonly used to detect conditions with a risk of glare and thermal discomfort and subsequently close shading devices. Sensors need to be non-intrusive to occupants and are usually placed in non-ideal locations. Therefore, they cannot measure comfort conditions of occupants and building performance indicators directly (Tzempelikos and Shen 2013; Yun et al. 2020). For detecting a risk of daylight glare discomfort, for instance, it is not practically feasible to use the luminance distribution and illuminance at

CONTACT Samuel B. de Vries s.b.d.vries@tue.nl Unit Building Physics and Services, Department of the Built Environment, Eindhoven University of Technology PO Box 513, 5600 MB Eindhoven, The Netherlands

Supplemental data for this article can be accessed here. https://doi.org/10.1080/19401493.2021.1887355

the position of occupants as direct control variables and only non-intrusive light sensors can be used. Additionally, it is important that a risk of glare resulting from a control action is predicted beforehand and prevented rather than retroactively corrected. The type of sensor that is used, its position and orientation influence the effectivity of the control strategy in addressing building performance aspects (Tzempelikos and Shen 2013; Yun, Park, and Kim 2017). In the development of a sensor strategy, a trade-off, therefore, must be made between the complexity and costs of the strategy on the one hand, and its positive effects on building performance on the other. An additional consideration is that, whilst control rules can always be easily changed, it is undesirable to change sensing equipment after it has been installed. There is therefore a need for new methods and tools to quantify the effectivity with which different sensor strategies influence whole building performance aspects.

Many studies that develop and test advanced control concepts rely on building performance simulation (BPS) (Atzeri et al. 2018; Coffey 2013; Daum and Morel 2010; Gunay et al. 2014; Huchuk et al. 2016; Seong et al. 2014a; Shen, Hu, and Patel 2014; Shen and Tzempelikos 2012; Tzempelikos and Shen 2013;Wienold 2007; Shen, Hu, and Patel 2014; Yun, Park, and Kim 2017). BPS can provide detailed insight into building performance aspects that are difficult and costly to measure or reproduce in experimental set-ups (de Klijn-Chevalerias et al. 2017). Additionally, with BPS, the effects of advanced control strategies can be evaluated for a large variety of buildings, climates and solar shading types (e.g. blinds, roller shades, shutters). This makes BPS a promising tool for exploring high potential control strategies and identifying risks in the context of automated solar shading (Loonen et al. 2017; Ochoa, Aries, and Hensen 2012). The use of BPS to inform the development of automated solar shading controls is, however, relatively new and there are several issues hindering BPS to be applied effectively in this context.

The development of solar shading controls using BPS currently follows a trial-and-error process where simulations are used to test a preconceived strategy using *post hoc* analyses (Loonen 2018). Although this process allows a developer to quantify the performance of a control strategy, it gives limited insight into how such a strategy can be improved further. Additionally, the knowledge obtained using this process tends to be case study specific and cannot be easily applied to a different type of solar shading system or a different building. There is therefore a need for generically applicable approaches that structure the use of BPS to identify high-performance solutions in an effective manner.

In recent years, many promising control strategies for solar shading systems have been proposed in scientific publications. There are explicit approaches, that prescribe control actuations under certain conditions. This group includes advanced rule-based control (RBC) algorithms that operate a shading system using knowledge about the sun's position (Jeong, Choi, and Sung 2016; Koo, Yeo, and Kim 2010; Seong et al. 2014a, 2014b; Tzempelikos and Shen 2013) and proportional control based approaches where the shading system's position is determined proportional to sensor measurements (Daum and Morel 2010; Kristl et al. 2008; Yun et al. 2020). Other strategies utilize an implicit performance weighing approach, where control actions are selected by comparing the effects that various possible control actions would have on weighted performance indicators. This group includes model predictive control (MPC) strategies, where control responses are optimized using built-in models (Xiong et al. 2019) and pre-defined performance goals (Huchuk et al. 2016; Mahdavi 2001; Mahdavi, Spasojevic, and Brunner 2005; Oldewurtel et al. 2012).

The literature on this topic also includes some generically applicable approaches for developing control strategies using BPS. For example, exhaustive-search simulation studies (Yun, Park, and Kim 2017) and self-learning methods (Gunay et al. 2014) have been applied to relate sensor measurements to performance goals by optimizing control thresholds for simple RBC strategies. This optimization does require, however, exploring a vast space of possible control thresholds. Additionally, the approach remains limited to the constraints of the initially assumed control concept and does not provide the deeper level of understanding that is needed to guide the development of a more advanced control logic. The MPC approach does not have this limitation. Although MPC has been shown to be a promising solution for high-performance building controls (Huchuk et al. 2016; Mahdavi 2001; Mahdavi, Spasojevic, and Brunner 2005; Oldewurtel et al. 2012), it is not commonly applied in practice (Coffey 2013; Piscitelli et al. 2019). A possible explanation can be found in the effort and skill that is required of a developer for every new type of solar shading system or when a system is commissioned into a new building. Potentially, self-learning behaviour can reduce this effort but setting up the model architecture and parametrizing the model remain costly. Additionally, MPC is computationally expensive and complex during operation. Researchers have developed techniques to significantly reduce the computational complexity of MPC by rule-extraction and the mapping of operational conditions to MPC control responses (Coffey 2013; Piscitelli et al. 2019). This process, however, requires more effort from developers and is computationally expensive in the preparation phase. Additionally, a fitness function with relative weights for different performance indicators must be defined beforehand when applying the MPC to the multi-objective solar shading control problem. This is not easily done based on engineering intuition and tuning these weights towards the desired performance outcomes therefore requires extensive sensitivity analyses (Mahdavi 2001; Oldewurtel et al. 2012).

This paper presents a simulation-based support method for the development of rule-based solar shading control strategies and the optimization of sensor selection, control thresholds and detection algorithms. The support method simplifies the task of developing an advanced control logic by guiding a developer in identifying a set of simple control actions, aimed at balancing trade-offs between a subset of performance aspects under specific representative environmental conditions. These control actions will later form the individual control modes of a multi-mode control strategy. The effects of these control modes on occupant comfort conditions are then graphically mapped to sensor measurements, such that the most beneficial conditions for activating each control mode can be identified. The effectivity of detection algorithms, sensors and control thresholds are then evaluated using statistical classification techniques and visualized in a confusion matrix. This allows the effectivity of non-intrusive sensors to be optimized. The graphic nature of this method allows the performance effects of all possible values for a single control threshold to be visualized in a single image using the results of only two full-year simulations. The method builds on, generalizes and structures some of the ad-hoc research tasks observed in literature on advanced solar shading case studies (Chan and Tzempelikos 2013; de Vries, Loonen, and Hensen 2019; Oh, Lee, and Yoon 2012; Shen and Tzempelikos 2017).

The support method gives detailed insight into how control decisions can be used to influence performance trade-offs and offers a structured approach for identifying high-performance solutions inside the design space. The goal of the support method is to assist the development of control solutions that are based on performance goals, yet easily implemented in simple control hardware. An additional requirement being that applying the method to a new case should require little effort from a developer and only a small number of simulations. This feature allows the method to be used to customize a control strategy for a particular building design. This is desirable because the relative weight of evaluation criteria can only be determined in relation to the building context (Kuhn 2017), for example, daylighting performance is more important in a building with small windows.

The support method will be illustrated and tested using a case study that develops a control strategy for an automated indoor roller blind system, with attention for the selection of sensors and control thresholds. The case study is used to show the structured approach and prove that the applied classification and visualization techniques identify high-performance solutions in a practical example. The control strategy was developed in collaboration with industry partners for whom simple control hardware and a limited time investment for each building design project are important considerations.

Section 2 of this paper will give a broad overview of the support method. The support method will be explained in more detail, using the case study, in section 3. The discussion in section 4 will evaluate the efficiency and shortcomings of the support method. Section 5 presents the conclusions of this research. These conclusions extrapolate the generic features and benefits of the support method from the case study and suggest promising future applications.

2. The computational shading control and sensor strategy development method

Figure 1 gives an overview of the proposed support method. A developer starts with five preparatory steps (1.1–1.5). These steps include defining a set of performance aspects, indicators and goals (1.3) that the control strategy will seek to balance. Additionally, the developer defines an initial set of control modes (1.1). In each of these control modes, the shading device is dynamically operated according to a distinct logic that focuses on pursuing a subset of the overall performance goals. The different control modes should vary in terms of how far the shading device is opened and, consequently, in the amount daylight, sunlight and solar radiation that is admitted. The developer then defines several potential sensors alternatives (1.2), that the multi-mode control strategy will use to switch between control modes. Additionally, the developer defines a description of a representative office space (1.4) that is considered representative for the final application of the system. A simulation model is then developed (1.5) to predict the performance of each of the control modes and the corresponding sensor readings for each sensor alternative.

A simulation of a typical year is executed for each of the initial control modes, where the specific control mode is followed continuously (2). These simulations offer the developer a quantification of the overall annual performance of each control mode, the instantaneous performance at each timestep and lists of corresponding simulated sensor readings.

The developer then evaluates, using annual performance indicators, if the individual performance goals

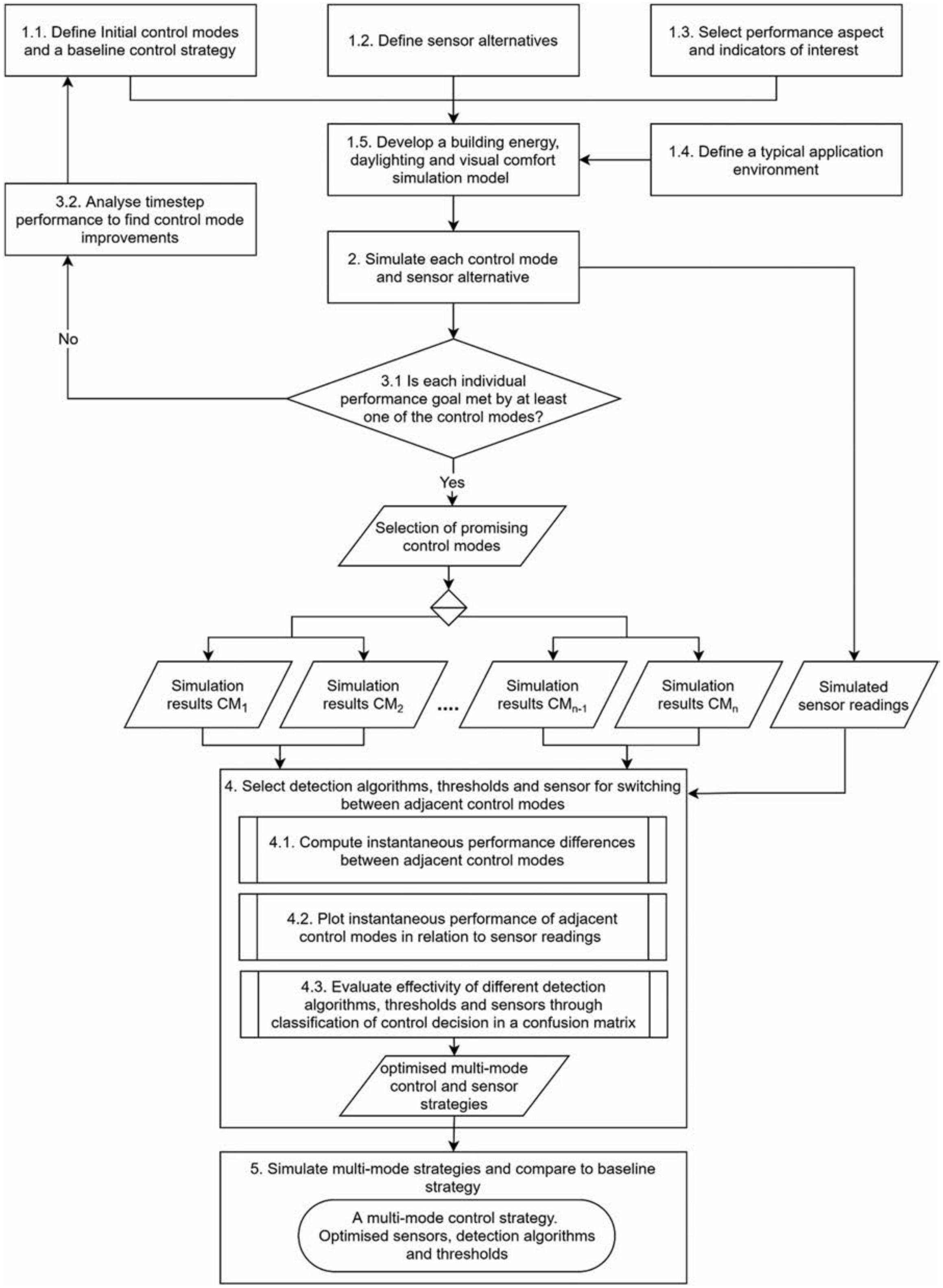

Figure 1. Overview of the computational method for developing high-performance solar shading control and sensor strategies.

are each met by at least one of the control modes and whether they provide the desired performance trade-offs (3.1). The most promising control modes are now selected and ordered in terms of the amount of solar energy that is admitted, with control mode 1 (CM_1) being the most open mode of operation and subsequent control modes

(CM_2 to CM_n) being more closed. If the initial control modes do not offer the desired performance, new control modes can be added. The developer can find possible improvements by analysing the instantaneous timestep performance of the initial control modes (3.2). If after multiple iterations of testing potential control modes the desired performance goals and trade-offs cannot be achieved, this gives reason to review the feasibility of the initially assumed goals, the proper functioning of the simulation model and the constraints that are posed by the selected dynamic shading system and its physical properties.

In the next step (4), a sensor strategy is developed. This strategy is defined by the detection algorithms, thresholds and sensors that are used to detect the boundaries of conditions where the control system will switch between two adjacent modes of operation. Adjacent here relates to the order in the admittance of solar energy. Each adjacent set of control modes will get a detection algorithm that determines when CM_n leads to poor performance and CM_{n+1} should be activated.

The approach in step 4 is to relate the instantaneous performance, or the performance difference, of two adjacent control modes to sensor readings (4.2) and test detection algorithms using statistical classification techniques. In this research, control decisions are classified in a confusion matrix (4.3) (Fawcett 2006). By relating the decisions of potential detection algorithms to simulated performance predictions, the effectivity of these algorithms can be evaluated. Potential sensor strategies can be evaluated from a multi-objective perspective by using the confusion matrix method for each performance indicator.

All steps will be graphically illustrated using the case study example. Additionally, a set of indicators that aid the developer in refining detection algorithms will be presented. This set includes indicators that are commonly used in the field of statistical classification as well as quantities developed in this research. The outcome of this process is a multi-mode control strategy, or multiple strategies, with optimised sensors and sensor thresholds. The performance of these strategies is then simulated and compared to a baseline strategy (5).

3. Case study: a sun-tracking control strategy for indoor roller blinds

This case study focusses on an automated indoor roller blind system that uses a metal-coated shading fabric with a high solar reflectance and low openness (Table 1). The shade is automated using a silent motor that allows its position to be varied continuously.

Table 1. Shade fabric properties.

	T_{vis}	$R_{vis;front}$	T_{sol}	$R_{sol;front}$	OF	ε_{front}	ε_{back}
Shade properties	0.013	0.719	0.025	0.740	0.008	0.230	0.858

3.1. Preparatory steps 1.1–1.5

3.1.1. Step 1.1: defining a set of initial control modes and a baseline strategy

In this case study, preventing daylight glare discomfort is the control goal with the highest priority. In this step, a large part of the control space will be excluded based on experience and the body of knowledge on preventing glare with shading devices. By assuming a set of rule-based control modes based on initial analyses in step 3 and optimizing the conditions under which they are activated in step 4, the control space is greatly decreased, and the problem made more manageable.

To maximize the admission of daylight and views, a developer can start with a control mode where the shading system is placed in the most open position. Here, this means fully raising the shade. To minimize cooling energy consumption and glare, a control mode is added where the shading system is placed in the most closed position. In this case, this means fully lowering the shade. An additional control mode is added that balances multiple conflicting performance objectives. Based on a review of literature, a promising sun-tracking algorithm was found (Tzempelikos and Shen 2013). This control logic, titled the solar cut-off logic, balances the goal of limiting daylight glare discomfort with the competing goal of admitting daylight and views to the outdoors. The algorithm controls the roller blind in relation to the sun's position to block direct sunlight from hitting an occupant's desk (Figure 2) using Equation (1). The edge of an occupant's desk is assumed to be at 75 centimetres height and positioned 75 centimetres from the façade. Solar cut-off algorithms can be geometrically defined for most commercially available products (Seong et al. 2014a; Tzempelikos, O'Neill, and Athienitis 2007) and are a good starting point in defining control modes.

$$sh = \frac{wpd}{\cos(\gamma - 180)} \cdot \tan\alpha + wph, \qquad (1)$$

where *wpd* is the distance between the edge of the work plane and the façade, *wph* is the height of the work plane from the floor; *sh* is the distance between bottom of the shade and the floor (shade height); γ is the solar azimuth in degrees (clockwise from North convention); and α is the solar altitude in degrees.

Previous research (Atzeri et al. 2018; de Vries, Loonen, and Hensen 2019; Tzempelikos and Shen 2013) showed that the sun-tracking strategy can lead to undesirable degrees of glare and cooling energy consumption

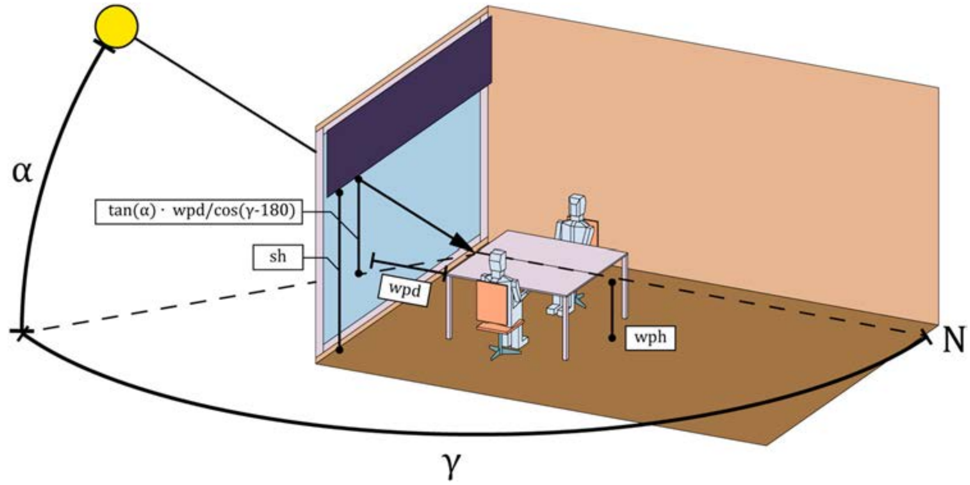

Figure 2. Parameters and solar position angles used in the solar cut off control logic.

because it causes the shade to be nearly fully raised at mid-day in summer when solar altitude is high. An additional control mode, titled EL, will therefore be included. The EL control mode follows the same sun-tracking behaviour as SC but now the maximum allowable shade height is limited to a seated eye-level height of 1.2 m.

A conventional control strategy for indoor roller blinds will be used as a benchmark. In this baseline strategy (BL), the roller blind is controlled using an outdoor global vertical irradiance sensor where the shade is either fully raised or lowered in response to a threshold of 200 W/m^2 (Beck and Dolmans 2010).

3.1.2. Step 1.2: defining potential sensor alternatives

In this study, the focus lies on sensors and algorithms for detecting different ranges in incident solar energy. In literature, a wide variety of sensors are used for this purpose, ranging from outdoor or indoor irradiance and illuminance sensors to glare sensors at the position of an occupant (Silva da, Leal, and Andersen 2012; Yun, Park, and Kim 2017). In this study, three sensors are evaluated: an exterior global horizontal irradiance sensor (E-$I_{g;h}$), an exterior global vertical irradiance sensor (E-$I_{g;v}$), and an indoor vertical illuminance sensor (I-$E_{g;v}$). The placement of these sensors is illustrated in Figure 3. The sensors are set up in an open-loop configuration and are selected because they are non-intrusive to occupants and easily commissioned on-site.

The outdoor irradiance sensors are chosen as this type of sensor is commonly installed for integration in building management systems. The indoor illuminance sensor is positioned in between the glazing and roller blind. This alternative is chosen because it is generally cheaper than the outdoor pyranometers. Additionally, this sensor is expected to better approximate the perception of daylight by occupants as it measures radiation in the visual spectrum, is affected by glazing characteristics, and its vertical position aligns reasonably well with the viewing direction of multiple occupants. Using this selection of sensors, the importance of both the positioning of a sensor and the part of the solar spectrum it measures, will be tested.

3.1.3. Step 1.3: selection of performance aspects and indicators

Explicitly stating performance goals, requirements and priorities beforehand facilitates decision making in the control development process. The performance aspects of interest in this study are daylight quality, visual comfort, view to the outdoors, and energy efficiency.

Spatial daylight autonomy is used as an indicator for daylighting performance, with 300 lux and 50% of occupied hours as cut-off criteria (sDA300/50%). This indicator is defined as the percentage of floor area that receives at least 300 lux for more than 50% of the occupied hours (Illuminating Engineering Society 2012) and has been shown to correlate well with subjective occupant assessments of daylight quality and quantity (Nezamdoost and Van Den Wymelenberg 2017). To be able to evaluate instantaneous daylighting performance, the daylit area fraction D_{300lx} is used. This indicator gives the percentage of floor area that receives at least 300 lux at a point in time.

Visual comfort is operationalized as the lack of visual discomfort and daylight glare probability simplified (DGPs) is used as a performance indicator. This metric was empirically derived by Wienold (2009) and relates the probability of the occurrence of glare to vertical illuminance at the eye of the observer. It has been shown that, although DGPs can accurately predict glare in instances where occupants are not exposed to direct sunlight and saturation is the dominant mechanism causing

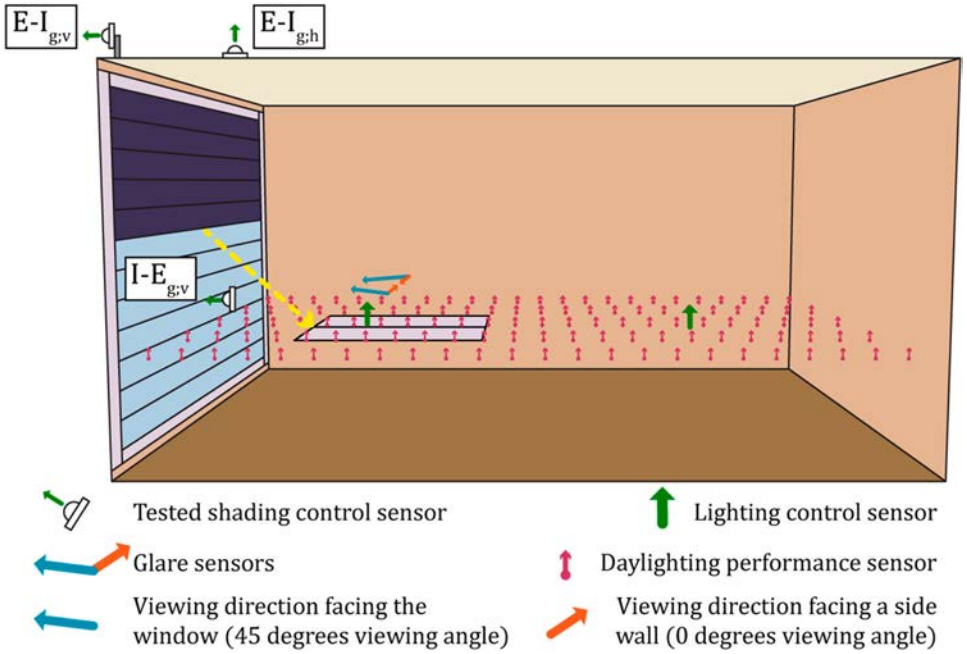

Figure 3. Overview of the reference office illustrating the placement of the investigated sensors and the set-up of the daylighting simulation model.

glare (Wienold, Iwata, and Sarey Khanie 2019), the metric performs less well when contrast glare is dominant. In this case study, DGPs is considered sufficiently reliable because the sun-tracking control strategy and low-openness fabric ensure that occupants are not exposed to sunlight.

Seating arrangements closest to the window are the most sensitive to the occurrence of glare (Giovannini et al. 2020). Additionally, the likelihood of glare discomfort is strongly influenced by viewing direction (Bian, Leng, and Ma 2018; Jakubiec and Reinhart 2012). To assess glare probability the two seating positions shown in Figure 2 are assumed. For each seating position, glare is assessed in two viewing directions (Figure 3): one where the occupant is facing a wall, and one where the occupant is facing the window at 45° as recommend in EN 14501 CEN (2017). Annual aggregated performance is quantified using the percentage of occupied hours that a DGPs of 0.40 (disturbing glare) is exceeded. This annual indicator is separately assessed for both viewing directions ($DGPs_{0.4;0deg;exc}$ and $DGPs_{0.4;45deg;exc}$), where at each timestep the maximum DGPs value of both occupant positions is used. $DGPs_{0.4;0deg;exc}$ thus gives the share of occupied hours that at least one of the two occupants perceives 'disturbing' glare if they were facing a wall (Figure 2) whilst $DGPs_{0.4;45deg;exc}$ assumes both occupants are facing the window at 45°. In this case study, $DGPs_{0.4;0deg;exc}$ is considered the most critical as it is representative for instances where the occupants are facing their computer monitors and cannot easily adjust their viewing direction. Disturbing glare in this viewing direction is likely to lead to occupants overruling the automated control system. Therefore, preventing disturbing glare in this viewing direction is stated as a performance goal of the strategy that is going to be developed. $DGPs_{0.4;45deg;exc}$ is considered less critical than $DGPs_{0.4;0deg;exc}$ because the occupants have more freedom to avert from this viewing direction. $DGPs_{0.4;45deg;exc}$ will therefore be treated as a performance indicator that is undesirable, but trade-offs with other aspects, such as daylighting performance, are considered acceptable.

The current state of the knowledge on view quality and quantity does not offer empirically supported performance indicators that are suited for evaluating the effects of dynamic solar shading devices (Hellinga and Hordijk 2014; Heschong 2003; Mardaljevic 2019; Pilechiha et al. 2020; Turan, Reinhart, and Kocher 2019). However, research investigating occupant operation of operable roller shades has shown that users tend to leave the lower portion of a window unshaded to maintain a visual connection with the outdoors (Haldi and Robinson 2010; Konis 2013; Sadeghi et al. 2016). In this study, view of the outdoors is assumed to be only dependent on the position of the shade. It is assessed as the percentage of occupied hours that the shade is positioned above the eye level of a seated occupant (1.2 m). This indicator will be abbreviated as $V_{1.2m;exc}$.

Energy performance is expressed in terms of primary energy consumption for cooling, heating and lighting and computed from simulated energy demand using

Table 2. Case study details and assumptions.

Geometry	Dimensions	width: 4.5 m; depth: 6 m; height: 3 m (27 m^2)
	Facade orientation	South
	Window to wall ratio:	80%
Fenestration	Type:	Low-E (pos. 3) double glazing with argon cavity filling
	Glazing:	U_{gl}: 1.2 W/m^2K, U_{frame}: 1.5 W/m^2K, T_{vis}: 0.82, SHGC: 0.62, CEN
Facade		Rc = 4.5 m^2K/W
Ceiling, walls, floor		Mixed: heavy weight floor/ceiling, lightweight walls
Internal gains	People:	3 (variable occupancy). 120 W/pers.
	Occupancy:	Weekdays: 8:00–19:00 (2860 h/year)
	Lighting:	10.9 W/m^2, closed loop linear dimming between 0–500 lux,Two sensors (Figure 1) that each control 50% of loads
	Equipment:	7.0 W/m^2
HVAC and settings	Infiltration:	ACH: 0.15
	Ventilation:	Demand driven, 40 m^3/(h∗pers.), ACH: 1 (average)
		Sensible heat recovery, efficiency: 70%
	Setpoints:	Lower set point: 21°C, Upper set point: 25°C (constant)
	System efficiencies (Beck and Dolmans 2010)	η_e: 0.39, η_{gas}: 1 (The Netherlands 2014)
		$\eta_{cool,deliv}$: 0.7 (Air-based cooling delivery system)
		COP_{cool}: 3 (Chiller with outdoor air condenser)
		η_h: 0.95 (Natural gas condensing boiler)
Weather		IWEC, Amsterdam, The Netherlands

Equation (2) from Beck, Dolmans, Dutoo, Hall and Seppänen (Beck and Dolmans 2010).

$$E_{prim.} = \frac{E_{light}}{\eta_e} + \frac{E_{cool}}{\eta_e \eta_c COP_{cool}} + \frac{E_{heat}}{\eta_h} \tag{2}$$

where $E_{prim.}$ is the primary energy consumption; E_{light} is the lighting energy demand; E_{cool} is the cooling energy demand; E_{heat} is the heating energy demand; η_e is the site to source primary energy ratio for electricity, $\eta_c$is the cooling delivery system efficiency; COP_{cool} is the chiller coefficient of performance, and η_h is the overall heating system efficiency

3.1.4. Step 1.4: defining a typical application environment

This study uses the reference office building for evaluating building-integrated solar envelope systems, developed within IEA SHC Task 56 (D'Antoni et al. 2019) with some minor adjustments. The details of this office cell and other modelling assumptions are given in Table 2.

3.1.5. Step 1.5: develop a simulation model

To account for the strong dependence of performance on interactions between the thermal and visual domains, this study relies on a co-simulation framework using Radiance (daylighting), EnergyPlus (thermal domain), Matlab (control logic) and BCVTB (information exchange). The Radiance three-phase method is used for daylighting and glare performance assessments as well as the prediction of indoor lighting energy consumption and associated heat gains. This approach has previously been validated for the performance assessment of advanced solar shading systems (McNeil and Lee 2013). BCVTB (Wetter 2011) directs the exchange of information between simulation environments. Matlab is used to describe the behaviour of the shading control logic and compute daylighting conditions and artificial lighting gains using a database with Radiance simulation results.

To simulate a variable height shading system using the Radiance three-phase method as well as EnergyPlus, the fenestration system needs to be divided into multiple horizontal segments which are either fully shaded or unshaded. To this end, the window is subdivided into 35 horizontally oriented window segments. This modelling resolution was chosen based on a sensitivity analysis presented in de Vries, Loonen and Hensen (de Vries, Loonen, and Hensen 2019).

Hourly weather data for Amsterdam (IWEC) is used in this study. For EnergyPlus, a 5-min time step is chosen, as a sub-hourly resolution helps to increase the reliability of the heat balance algorithms as well as limit the effect of errors deriving from BCVTB's loosely coupled co-simulation approach. Within Radiance an hourly time step is chosen to describe sky conditions because of the unavailability of sub-hourly weather data and the uncertainties associated with the creation of synthetic sub-hourly data for this location (Walkenhorst et al. 2002) (Table 3).

3.2. Step 2: simulate the performance of each control mode

The performance of the initial control modes is now simulated. In these simulations, the shading system follows one of the envisioned control modes continuously throughout the year. A case is simulated where the shades are always up (AU), one where the system follows the solar cut-off logic (SC), one where the shade is always down (AD) and one where the solar cut-off logic shade height is limited to the seated eye-level (EL).

Table 3. Simulation parameters and assumptions

	EnergyPlus	Radiance
Fenestration	Glazing optical properties from IGDB: Lay 1: IGDB# 1608 Lay 2: IGDB# 11560 Shade: anisotropic optical model with properties from CGDB# 20032	BSDF created with LBNL-Window Lay 1: IGDB# 1608 Lay 2: IGDB# 11560 Shade: CGDB# 20032
Interior surfaces		Lambertian reflectors: Ceiling, r_{vis}: 0.8, Wall, r_{vis}: 0.5 Floor, r_{vis}: 0.2
Simulation settings	Idealised HVAC system: unlimited capacity and ideal response	Sensor grid: 5 × 25 $V_{rcontrib}$: -ab 12 -ad 5 × 10^4 -lw 2 × 10^{-6}, $D_{rcontrib}$: -ab 2 -ad 10^3 -lw 5 × 10^{-4} -c 3000 s and D sky resolution: MF3
	5 min. time step	hourly time step

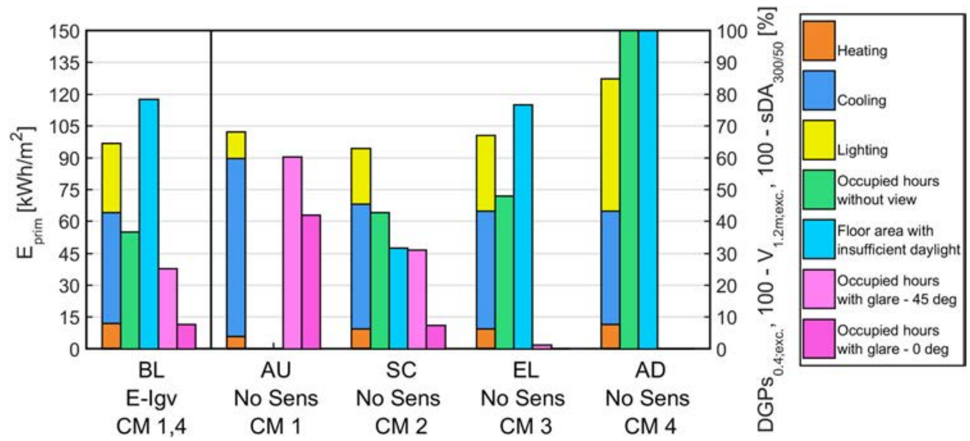

Figure 4. Summary of whole building performance for each control mode and the baseline strategy. BL: Baseline, AU: Always up, SC: Solar cut-off, EL: Solar cut-off with maximum height at eye level, AD: Always down.

3.3. Step 3: evaluate the performance of each control mode

Figure 4 shows the performance of each of the cases in relation to the baseline. Here, the performance indicators are reformulated such that the most desirable situation is reached if all performance indicators are as low as possible. View and glare performance is shown as the share of occupied hours that their required criterion was not met. Daylighting performance is presented as the complementary percentage to $sDA_{300/50}$: the floor area that does not receive at least 300 lux for 50% of occupied time.

The graph shows that each of the control modes successfully addresses a single performance aspect but performs badly on the other aspects. As expected, the AU case offers the best $sDA_{300/50}$ and $V_{1.2m;exc}$ but performs less well than the BL in terms of $DGPs_{0.4;exc}$ and E_{prim}. The SC case offers a more beneficial trade-off between the different performance aspects. Compared to the BL strategy it offers superior $sDA_{300/50}$ and a slight improvement in E_{prim} which can be attributed to reductions in lighting energy consumption. The SC logic performs similar to the BL strategy in terms of the other indicators, and does not satisfy the defined requirement of 0% $DGPs_{0.4;0deg;exc}$. The EL logic does fulfil the 0% $DGPs_{0.4;0deg;exc}$ requirement and greatly reduces $DGPs_{0.4;45deg;exc}$. With regards to daylighting and energy performance the EL strategy performance similar to the BL. The AD case fully eliminates disturbing glare in both viewing directions but performs very badly in all other performance indicators.

These results suggest that combining the AU, SC and EL control logics into a multi-mode control strategy could provide a strategy that performs significantly better than the baseline. In this multi-mode control strategy, the SC control mode would be activated under conditions where the AU mode leads to glare or an unacceptable amount of cooling energy consumption. Likewise, the EL strategy would be activated when excessive admission of solar energy in the SC mode would cause undesired performance. The AD case does not appear to offer any additional beneficial performance trade-offs in relation to the other cases and it will therefore not be considered as a potential control mode for the multi-mode strategy.

The development of more refined control actions can be supported by analysing the instantaneous timestep performance of the initially simulated cases (step 3.2). In this research, for instance, the EL strategy was added after analysing the contour plots in Appendix A. These

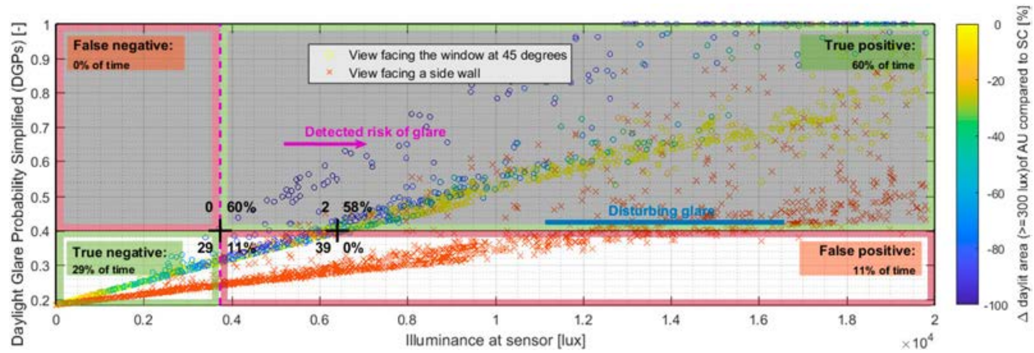

Figure 5. DGPs in relation to readings from the indoor vertical illuminance sensor. Simulated results for the AU case. $\Delta D_{t;300lx;2SC;1AU}$ is displayed using the colour of the circles for the 45-degree viewing angle.

plots show the timestep performance of the SC strategy and indicate that the EL strategy leads to excessive cooling energy consumption and glare when the shade is positioned very high at mid-day in summer.

The three most promising cases (AU, SC, EL) have now been identified. In Figure 4 these cases are ordered and numbered in terms of the amount of solar energy that they admit. As control modes in a multi-mode strategy, they will be respectively referred to as CM_{1AU}, CM_{2SC} and CM_{3EL}.

The analyses of the different cases in step 3 can also be used to verify the proper functioning of the simulation model. The results in Figure 4 show that as less solar energy is admitted, $sDA_{300/50,}$ lighting and cooling energy consumption decrease whilst heating energy consumption and $DGPs_{0.4;exc}$ rise. Additionally, analysing timestep (Appendix A) or monthly (Appendix C) aggregated simulation outputs can assist the modeller in verifying the simulation model.

3.4. Sensor strategy optimization: mapping of performance effects to sensor measurements and statistical classification of detection algorithms

The goal of this step is to develop a sensor strategy that identifies the most ideal conditions to activate each control mode. In the case study, two detection algorithms will have to be defined: one for activating CM_{2SC} and one for activating CM_{3EL}. The CM_{2SC} detection algorithm determines when the system will switch between the CM_{1AU} and the CM_{2SC} control modes. To develop this algorithm, instantaneous performance results from the AU and SC cases are related to the simulated sensor measurements and the effectivity of potential detections algorithms, and sensors, is evaluated using confusion matrices. The same approach is used to develop the CM_{3EL} detection algorithm that determines when the system switches between $CM_{2;SC}$ and $CM_{3;EL}$.

3.4.1. The confusion matrix approach: a detection algorithm for switching between the CM_{1AU} and the CM_{2SC} control mode

Figure 5 illustrates how the confusion matrix approach works using the CM_{2SC} detection algorithm and the I-$E_{g;v}$ sensor as an example. Simulated glare performance ($DGPs_{0.4;0deg}$ and $DGPs_{0.4;45deg}$) from the AU case is plotted in relation to the I-$E_{g;v}$ sensor measurements. Figures 6 and 7 show the same simulation results ($DGPs_{0.4;45deg}$ in relation to I-$E_{g;v}$) but underline the generic features of the approach and clarify the steps involved in making the confusion matrix. Earlier, we have defined $DGPs \geq 0.4$ as a criterion for undesired glare performance. Here, we will take a conservative approach and focus on preventing glare in the 45-degree viewing direction (coloured circles in Figure 5). Using the performance criterion, each instance is tested for the condition $DGPs_{45deg} \geq 0.4$ classifying them into 'positives' (P) or 'negatives' (N), where positive stand for the occurrence of glare. This classification is called the true performance classification (PC_{true}). In the images, it is represented by a horizontal line (Figure 6).

The goal of the sensor strategy is to predict this performance classification using a detection algorithm and sensor measurements S creating a $PC_{detected}$ that separates all instances into predicted P and N classes. An ideal sensor strategy (Figure 6) would be one that always classifies performance conditions correctly ($PC_{true} = PC_{detected}$). Actual sensor strategies are generally less effective and will classify some instances incorrectly. The effectivity of a sensor strategy can be evaluated by relating the detected classification to the true classification and binning all instances in one of the four cells of a confusion matrix. Figures 5 and 7 illustrate this graphically. Here, a potential detection algorithm that uses a single sensor threshold of 3700 lux is used, and $PC_{detected}$ can be represented by a vertical line. The two lines now graphically define a confusion matrix where all instances are contained within one of four quadrants:

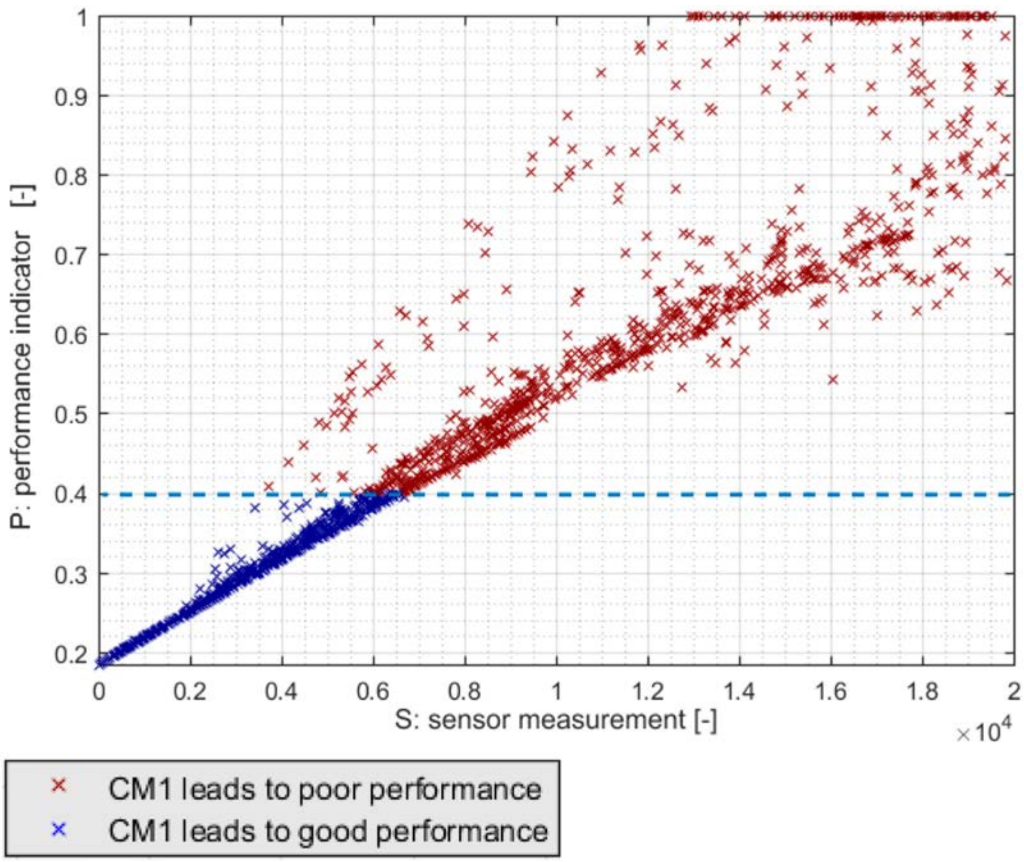

Figure 6. Actual performance classification of instantaneous performance of CM1 based on a performance criterion. Sensor: I-Eg;v, Performance indicator: DGPs45deg

- The true positives (TP): the sensor algorithm correctly detected glare in CM_{1AU}. CM_{2SC} is activated to prevent glare.
- The true negatives (TN): the sensor algorithm correctly detected no glare in CM_{1AU}. CM_{1AU} is activated to maximize the admission of daylight and views.
- The false positives (FP): the sensor algorithm wrongly detected glare in CM_{1AU}. CM_{2SC} is activated and the shade is lowered further than what would be necessary to prevent glare.
- The false negatives (FN): the sensor algorithm wrongly detected no glare in CM_{1AU}. CM_{1AU} is activated and this causes occupants to be exposed to glare.

The effectivity of different sensor strategies can be quantified by looking at the share of occupied hours that are contained in each confusion matrix region. The share of all positives that were detected by the sensor strategy, or true positive rate (TPR), gives an idea of how well the strategy detects conditions where the occupants perceive glare. Here, a TPR of a 100% means that all instances with disturbing glare where detected. The 'accuracy' (ACC) quantifies the frequency of the system making correct performance classifications and is defined as the ratio between the number of instances contained in the 'true' regions to the number of total instances. In this example, a greater ACC indicates better performance trade-offs between daylighting performance and visual comfort. The 3700-lux threshold that is evaluated in the confusion matrix in Figure 5 is defined such that false negatives, where activating $CM_{1;AU}$ would cause glare in the 45-deg viewing direction, never occur. The accuracy of this strategy is not ideal (89%) due to a substantial number of false positives (11%) that lead to an unnecessary decline in daylighting and view performance.

ACC and TPR only quantify the frequency of false control decisions but not the severity of the effects on other performance aspects. The impact of false control decisions can be large or small, however, depending on environmental conditions. More detailed insight into performance trade-offs can be obtained by looking at the effects of false control decisions on daylighting performance. To quantify these effects, the instantaneous difference in $D_{t;300lx}$ between the SC and AU cases is computed for each timestep (Equation (3)). This performance difference ($\Delta D_{t;300lx;2SC;1AU}$) is visualized in Figure 5 using the gradient colour scale of the 45-degree viewing angle. The dark blue colour of the instances contained in the FP

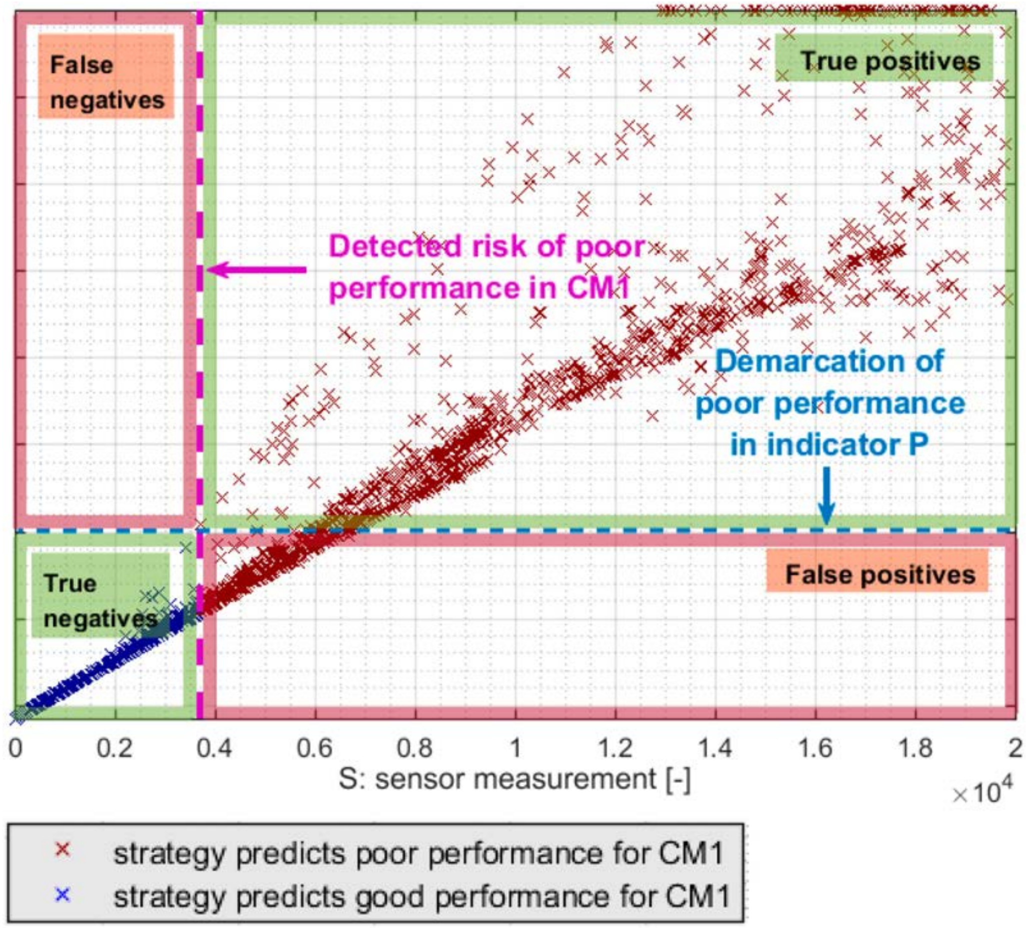

Figure 7. Performance classification by a simple detection algorithm (if: S > 3700 then: positive) and evaluation of its effectivity using a confusion matrix. Sensor: I-Eg;v, Performance indicator: DGPs45deg

region indicates that these instances will have a particularly strong negative effect on daylighting performance.

$$\Delta D_{t;300lx;2SC;1AU} = D_{t;300lx;SC} - D_{t;300lx;AU} \quad (3)$$

where $D_{t;300lx;SC}$ is the percentage of floor area that receives more than 300 lux, at time step *t*, for the SC case $D_{t;300lx;AU}$ is the percentage of floor area that receives more than 300 lux, at time step t, for the AU case; $D_{t;300lx;2SC;1AU}$ is the change in instantaneous daylighting performance when switching from $CM_{1;AU}$ to $CM_{2;SC}$

Table 4 summarizes the effectivity scores (TPR:100% and ACC:98%) associated to the 3700-lux threshold along with the resulting overall daylighting performance (sDA_{actual}: 74%) if this detection algorithm would be implemented in a two-mode strategy ($CM_{1;AU} + CM_{2;SC}$). In addition, the table shows the ideal daylighting performance that could be achieved (sDA_{ideal}: 100%) with a two-mode strategy if the detection algorithm would make no false classifications ($PC_{detected} = PC_{true}$). Together, the collection of indicators quantify how well the detection algorithm can isolate instances with undesired performance, what the effects are of wrong control decisions, and what could be gained by improving the algorithm further. By comparing sDA_{actual} to sDA_{ideal} it becomes clear that, although sDA_{actual} is significantly better than that of the BL (sDA:22%), there is still a lot of room for further improvement.

Figure 5 suggests that a better trade-off between glare and daylighting performance can be obtained by moving the threshold closer to the point where the linear regression line of the scatter plot intersects the 0.4 DGPs disturbing glare line. This approach is illustrated with the second cross. Here, the choice is made to accept that 3% of all $DGPs_{0.4;45deg}$ exceedance goes undetected (TPR: 97% and 2% FN) by using a control threshold of 6400 lux. The graph shows that this reduces the occurrence of FP to 0%. Table 4 summarises the positive effects of changing the detection threshold, where sDA_{actual} increases to 100%, matching sDA_{ideal}. Note that, although $DGPs_{0.4;45deg}$ increases, the more critical $DGPs_{0.4;0deg}$ indicator remains almost unchanged. This means that the disturbing visual discomfort that is introduced by this new threshold, could be mitigated by a change in the viewing direction of the occupant. In this case study, this

Table 4. Summary of the effectivity of tested sensors, thresholds and detection algorithms for switching between the CM_{1AU} and CM_{2SC} control modes.

Sensor:		Exterior horizontal irradiance				Exterior vertical irradiance				Interior vertical illuminance			
Threshold based on:		30 W/m²				50 W/m²				3700 lux			
$DGPs_{45\,deg}$ >= 0.4	Glare:	TPR:	100%	ACC:	78%	TPR:	100%	ACC:	91%	TPR:	100%	ACC:	89%
		$DGPs_{0.4;45deg}$	31%	$DGPs_{0.4;0deg}$	7%	$DGPs_{0.4;45deg}$	31%	$DGPs_{0.4;0deg}$	7%	$DGPs_{0.4;45deg}$	31%	$DGPs_{0.4;0deg}$	7%
	sDA:	Actual:	69%	Ideal:	100%	Actual:	78%	Ideal:	100%	Actual:	74%	Ideal:	100%
	E_{prim}:	Negative		Positive		Negative		Positive		Negative		Positive	
	kWh/m²	$\sum TN_e$:	1.1	$\sum FP_e$:	10.6	$\sum TN_e$:	4.7	$\sum FP_e$:	7.0	$\sum TN_e$:	4.5	$\sum FP_e$:	7.2
		$\sum FN_e$:	-0.5	$\sum TP_e$:	-8.7	$\sum FN_e$:	-0.9	$\sum TP_e$:	-8.3	$\sum FN_e$:	-0.7	$\sum TP_e$:	-8.4
		$totN_e$:	0.7	$totP_e$:	1.9	$totN_e$:	3.8	$totP_e$:	-1.3	$totN_e$:	3.8	$totP_e$:	-1.3
	Saved:	Actual:	0.7	Ideal:	11.7	Actual:	3.8	Ideal:	11.7	Actual:	3.8	Ideal:	11.7
Threshold based on:		80 W/m²				80 W/m²				6400 lux			
$DGPs_{45deg[2\%]}$ >= 0.4	Glare:	TPR:	97%	ACC:	87%	TPR:	97%	ACC:	97%	TPR:	97%	ACC:	98%
		$DGPs_{0.4;45deg}$	33%	$DGPs_{0.4;0deg}$	8%	$DGPs_{0.4;45deg}$	33%	$DGPs_{0.4;0deg}$	7%	$DGPs_{0.4;45deg}$	33%	$DGPs_{0.4;0deg}$	8%
	sDA:	Actual:	83%	Ideal:	100%	Actual:	99%	Ideal:	100%	Actual:	100%	Ideal:	100%
	E_{prim}:	Negative		Positive		Negative		Positive		Negative		Positive	
	kWh/m²	$\sum TN_e$:	5.5	$\sum FP_e$:	6.2	$\sum TN_e$:	7.2	$\sum FP_e$:	4.5	$\sum TN_e$:	7.9	$\sum FP_e$:	3.8
		$\sum FN_e$:	-0.7	$\sum TP_e$:	-8.5	$\sum FN_e$:	-1.2	$\sum TP_e$:	-8.0	$\sum FN_e$:	-1.1	$\sum TP_e$:	-8.1
		$totN_e$:	4.8	$totP_e$:	-2.3	$totN_e$:	6.0	$totP_e$:	-3.5	$totN_e$:	6.8	$totP_e$:	-4.3
	Saved:	Actual:	4.8	Ideal:	11.7	Actual:	6.0	Ideal:	11.7	Actual:	6.8	Ideal:	11.7

is considered an acceptable trade-off for improving daylighting performance.

The confusion matrix approach can also be used to assess how well the detection algorithm identifies instances where switching from the CM_{1AU} to CM_{2SC}, would improve energy performance. This process is visualized in Figure 8. In this case, control decisions are evaluated as if the only goal of the control is to minimize energy consumption. The effects of switching between the two control modes is quantified using the difference in instantaneous primary energy consumption for heating, cooling and lighting ($\Delta E_{t;\mathrm{prim}}$) between the AU and SC cases (Equation (4)).

$$\Delta E_{t;prim;2SC;1AU} = E_{t;prim;SC} - E_{t;prim;AU} \qquad (4)$$

where $E_{t;\mathrm{prim;SC}}$ is the instantaneous primary energy consumption for heating, cooling and lighting, at time step t, for strategy SC; $E_{t;prim;AU}$ is the instantaneous primary energy consumption for heating, cooling and lighting, at time step t, for strategy AU.

Instances where activating CM_{2SC} saves energy are now labelled as 'positives' and the PC_{true} is based on the performance criterion $\Delta E_{t;\mathrm{prim}} < 0$. This criterion is represented in the graph by the horizontal line at $\Delta E_{t;\mathrm{prim}} = 0$. The graph is used to evaluate the effectivity of the previously defined 6400-lux threshold from an energy perspective. This detection algorithm is again represented by a vertical line that defines PCdetected and the two lines delineate the regions of the confusion matrix. The colour scale is used to visualize $\Delta D_{t;300\mathrm{lx;2SC;1AU}}$ and highlights the relationship between energy and daylighting performance. To obtain a quantification of the total effects of the wrong and correct control decisions, the $\Delta E_{t;\mathrm{prim}}$ of all instances contained within each of the four regions of the confusion matrix are summed. The four regions, denoted with the subscript e, can be interpreted as follows:

- The true positives (TP_e): the sensor algorithm activates CM_{2SC}. This reduces $E_{t;\mathrm{prim}}$ compared to activating CM_{1AU}. A negative value for $\sum TP_e$ quantifies this reduction.
- The true negatives (TN_e): the sensor algorithm activates CM_{1AU}. This reduces $E_{t;\mathrm{prim}}$ compared to activating CM_{2SC}. A positive value for $\sum TN_e$ quantifies this reduction.
- The false positives (FP_e): the sensor algorithm activates CM_{2SC}. This increases $E_{t;\mathrm{prim}}$ compared to activating CM_{1AU}. A positive value for $\sum FP_e$ quantifies this increase.
- The false negatives (FN_e): the sensor algorithm activates CM_{1AU}. This increases $E_{t;\mathrm{prim}}$ compared to activating CM_{2SC}. A negative value for $\sum FN_e$ quantifies this increase.

The sums of two of the four matrix cells can be used to assess the effects that potential detection algorithms would have in a two-mode strategy ($CM_{1;AU} + CM_{2;SC}$) compared to the initial AU or SC cases. By summing all the detected 'negatives' ($totN_e$) the effects can be compared in relation to the SC case and by summing all

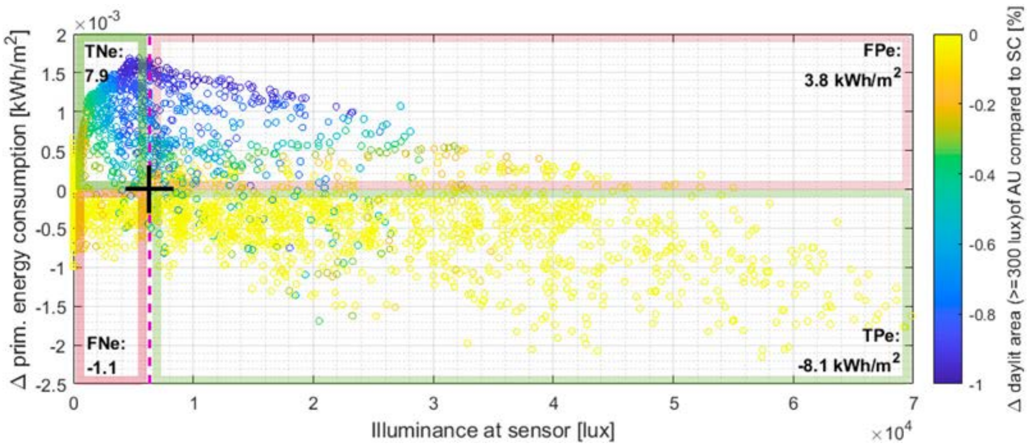

Figure 8. Evaluation of the effectivity of the illuminance sensor strategy in addressing energy performance. Vertical axis: difference in instantaneous primary energy consumption of AU and SC strategies. Colour: difference in instantaneous daylighting performance of AU and SC strategies.

the detected 'positives' ($totP_e$) the effects can be compared in relation to the AU case. The 6400-lux threshold $CM_{1;AU;2;SC}$ solution has a $E_{t;prim}$ that is 6.8 kWh/m^2 ($totN_e = TN_e + FN_e$) lower than that of the SC case. This net effect is a consequence of the instances where raising the shade saved energy (TNe: 7.9 kWh/m^2) and the instances where doing so would lead to more energy consumption (FNe: −1.1 kWh/m^2). For the initial 3700-lux threshold, the reduction in $E_{t;prim}$ compared to SC is only 3.8 kWh/m^2 (Table 4). This shows that the 6400-lux threshold is also more beneficial in terms of energy performance.

The four regions also allow the performance of a detection algorithm to be benchmarked against an ideal sensor strategy that always activates the CM with the lowest $E_{t;prim}$ ($PC_{detected} = PC_{true}$). With an ideal strategy $E_{t;prim}$ would be 11.7 kWh/m^2 ($TN_e + FP_e$) lower than that of the SC case. This means that 58% of the $E_{t;prim}$ reduction that could potentially be achieved by optimizing the detection algorithm has been realized with the 6400-lux algorithm. To facilitate these comparisons, the totNe score that is obtained by each sensor strategy is summarized under the header 'actual' next to the 'ideal' score.

Using these graphs and Table 4, some observations can be made. Figure 8 suggests that raising the shade fully saves energy in almost all instances where doing so would improve indoor daylighting conditions. In almost all instances where raising the shade would not cause such an improvement, the increase in solar heat gains would lead to an increase in total primary energy consumption. In this case, there appears to be little conflict between the goal of improving daylighting performance and the goal of improving energy performance.

The indicators in Table 4 show that compared to the original, 3700-lux threshold, the 6400-lux threshold offers more beneficial performance trade-offs between visual comfort and the other performance aspects. With this approach, both daylighting and energy performance come quite close to the ideal performance that is achievable using the selected control actuations. This suggests that there is little need for testing more complex detection algorithms.

To also be able to compare the effectivity of different sensors, control thresholds where determined for each type of sensor using both the 0% and the 2% $DGPs_{0.4;45deg}$ exceedance approaches. In Table 4, these thresholds are summarized along with the corresponding effectivity of each sensor strategy. The variation in daylighting and energy performance amongst the sensors shows that they vary in the effectivity with which they can classify instances with glare. It can be concluded that the E-$I_{g;h}$ sensor is less effective in classifying glare than the other sensors. Meeting the visual comfort requirement with this sensor leads to a 2 kWh/m^2 higher E_{prim} and a 17% lower $sDA_{300lx;50\%}$ than with the other sensors. Although the differences between the E-I_v and the I-$E_{g;v}$ are less pronounced, the I-$E_{g;v}$ sensor does perform better in terms of both daylighting (1%) and energy consumption (0.8 kWh/m^2).

3.4.2. A detection algorithm for switching between the CM_{2SC} and the CM_{3EL} control modes

In determining the detection algorithm for switching between $CM_{2;SC}$ and $CM_{3;EL}$, the goal of prohibiting glare discomfort is again given priority. Measurements from the three sensors are used to detect when $CM_{2;SC}$ leads to glare and decide that $CM_{3;EL}$ should be activated. Figure 9 shows simulated glare performance in relation to sensor measurements from the SC case. Here, two sensor

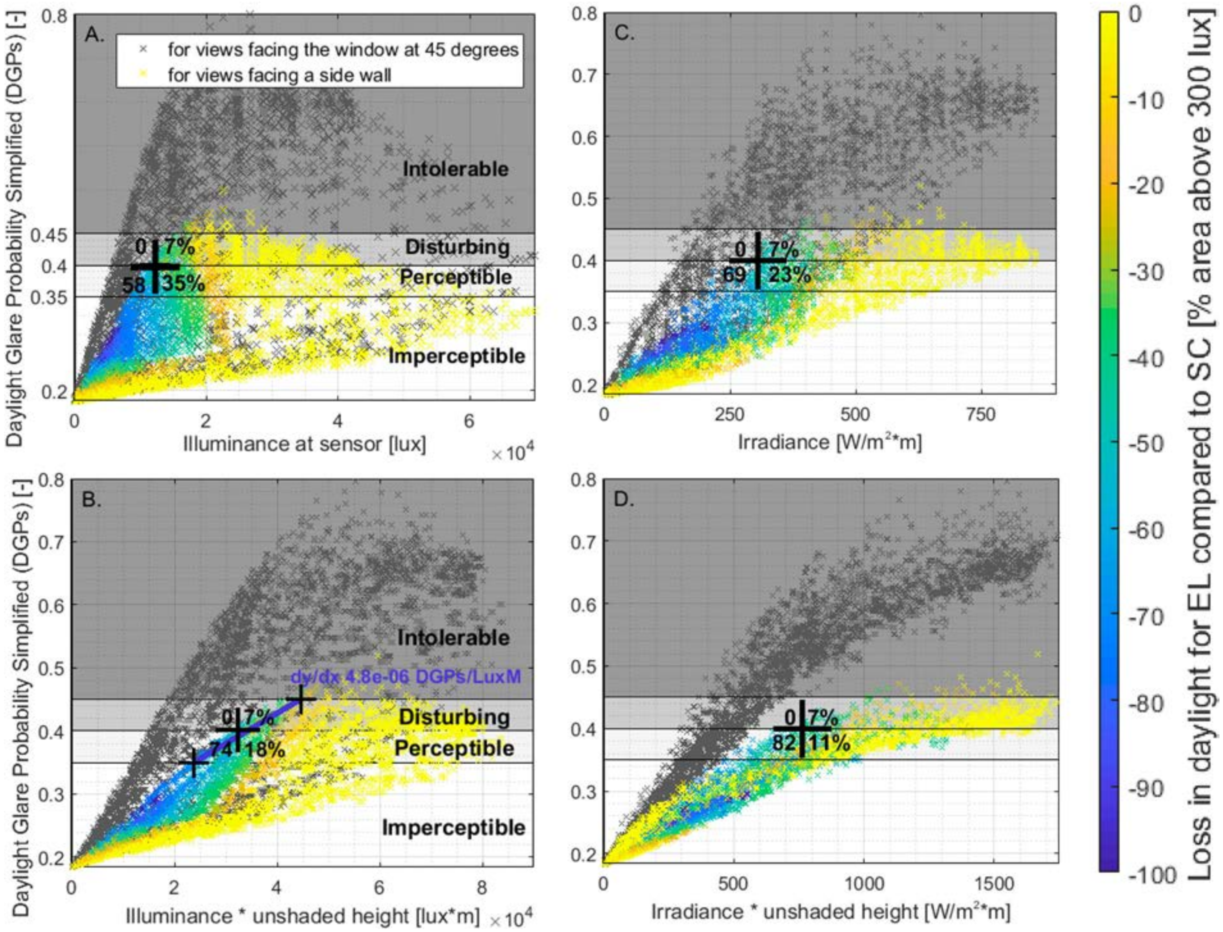

Figure 9. Simulated DGPs from the SC case in relation to: (A) Indoor vertical illuminance, (B) Indoor vertical illuminance multiplied by the unshaded window height. (C) Exterior horizontal irradiance, (D) Exterior horizontal irradiance multiplied by the unshaded window height. Colour represents the loss in daylit area

types are shown to illustrate the differences in the effectivity with which the sensors classify visual discomfort. A and B show results for the I-$E_{g;v}$ sensor. C and D show results for the E-$I_{g;h}$ sensor. The colour scale is again used to plot instantaneous effects on daylighting performance ($\Delta D_{t;300lx;3EL;2SC}$) of switching between the two control modes (Equation 5).

$$\Delta D_{t;300lx;3EL;2SC} = D_{t;300lx;EL} - D_{t;300lx;SC} \quad (5)$$

where $D_{t;300lx;EL}$ is the percentage of floor area that receives more than 300 lux, at time step t, for the EL case; $D_{t;300lx;SC}$ is the percentage of floor area that receives more than 300 lux, at time step t, for the SC case; $D_{t;300lx;3EL;2SC}$ is the change in instantaneous daylighting performance when switching from $CM_{2;SC}$ to $CM_{3;EL}$

The top graphs (A and C) show a detection algorithm where the control threshold is chosen such that disturbing glare is always prevented for the view facing the wall (0% FN). The relationship between glare probability and sensor measurements is less linear than in the previous example. As a result, there are many instances (35%) contained within the FP region. These instances have a strong negative effect on daylighting performance as can be seen from their negative $\Delta D_{t;300lx;3EL;2SC}$ values and the performance that is achieved compared to the ideal (Table 5).

The occurrence of glare in the SC case can be attributed to a large fraction of the window being exposed at high solar altitude giving occupants a large view of the sky. This situation can lead to glare at instances with high luminance sky conditions. A detection algorithm based on both illuminance and the amount of window area that is visible to the occupant, therefore, seems like a promising direction for further improvement. Figures C and D illustrate this approach. Here the illuminance, or irradiance, measured by the sensors is multiplied by the unshaded height of the window. The relationship between DGPs and these manipulated sensor measurements are more linear than in the cases using the unmanipulated sensor measurements. Consequently, the performance trade-offs that can be achieved are more beneficial as can be seen by the improvement in the effectivity indices shown in Table 5.

Table 5. Summary of the effectivity of tested sensors, thresholds and detection algorithms for switching between the CM2; SC and CM3;EL control modes.

		Exterior horizontal irradiance sensor				Exterior vertical irradiance sensor				Interior vertical illuminance sensor			
Threshold based on:		310 W/m²				150 W/m²				12000 lux			
DGPs0 deg >= 0.40	Glare:	TPR:	100%	ACC:	77%	TPR:	100%	ACC:	64%	TPR:	100%	ACC:	64%
		$DGPs_{0.4;45deg}$	7%	$DGPs_{0.4;0deg}$	0%	$DGPs_{0.4;45deg}$	7%	$DGPs_{0.4;0deg}$	0%	$DGPs_{0.4;45deg}$	7%	$DGPs_{0.4;0deg}$	0%
	sDA:	Actual:	57%	Ideal:	69%	Actual:	55%	Ideal:	69%	Actual:	53%	Ideal:	69%
	E_{prim}: kWh/m²	Negative		Positive		Negative		Positive		Negative		Positive	
		TN_e:	7.2	FP_e:	1.6	TN_e:	7.1	FP_e:	1.7	TN_e:	7.0	FP_e:	1.7
		FN_e:	0.0	TP_e:	-1.1	FN_e:	0.0	TP_e:	-1.1	FN_e:	0.0	TP_e:	-1.1
		totN_e:	7.2	totP_e:	-1.1	totN_e:	7.1	totP_e:	0.6	totN_e:	7.0	totP_e:	0.6
	Saved:	Actual:	-1.1	Ideal:	1.1	Actual:	-0.6	Ideal:	1.1	Actual:	-0.6	Ideal:	1.1
Threshold based on:		760 (W/m²)·m				380 (W/m²)·m				31600 lux·m			
DGPs0 deg >= 0.40 and sensor value * unshaded height	Glare:	TPR:	100%	ACC:	89%	TPR:	100%	ACC:	79%	TPR:	100%	ACC:	80%
		$DGPs_{0.4;45deg}$	14%	$DGPs_{0.4;0deg}$	0%	$DGPs_{0.4;45deg}$	11%	$DGPs_{0.4;0deg}$	0%	$DGPs_{0.4;45deg}$	11%	$DGPs_{0.4;0deg}$	0%
	sDA:	Actual:	61%	Ideal:	69%	Actual:	62%	Ideal:	69%	Actual:	63%	Ideal:	69%
	E_{prim}: kWh/m²	Negative		Positive		Negative		Positive		Negative		Positive	
		TN_e:	7.9	FP_e:	0.9	TN_e:	7.9	FP_e:	0.9	TN_e:	7.9	FP_e:	0.8
		FN_e:	-0.1	TP_e:	-1.0	FN_e:	0.0	TP_e:	-1.1	FN_e:	0.0	TP_e:	-1.1
		totN_e:	7.8	totP_e:	-0.1	totN_e:	7.9	totP_e:	-0.2	totN_e:	7.9	totP_e:	-0.3
	Saved:	Actual:	0.1	Ideal:	1.1	Actual:	0.2	Ideal:	1.1	Actual:	0.3	Ideal:	1.1

For assessing the effects of the different detection algorithms on energy performance, Equation (6) is used. Figure 10 visualizes these results for the detection algorithm where the I-$E_{g;v}$ sensor is used, and measurements are multiplied by the unshaded height. The net effects of each alternative, shown in Table 5, are again expressed relative to the SC case and are obtained by summing the instances contained in the TPe (switching to $CM_{3;EL}$ saved energy) and FPe (switching to $CM_{3;EL}$ used more energy) regions. This totP_e score is again summarized under 'actual' header.

$$\Delta E_{t;prim.;3EL;2SC} = E_{t;prim.;SC} - E_{t;prim.;EL} \tag{6}$$

where $E_{t;prim;EL}$ is the instantaneous primary energy consumption for heating, cooling and lighting, at time step t, for strategy EL and $E_{t;prim;SC}$is the instantaneous primary energy consumption for heating, cooling and lighting, at time step t, for strategy SC.

The energy and daylighting scores of the different sensors shown in Table 5 show that the I-$E_{g;v}$ sensor identifies visual discomfort most effectively. The differences between the sensors are less pronounced here than in the previous case with $CM_{1;AU}$ and $CM_{2;SC}$. By comparing the scores of the two approaches for switching between $CM_{2;SC}$ and $CM_{3;EL}$ it becomes clear that the most beneficial performance trade-offs can be achieved when sensor measurements are multiplied by the unshaded height of the window. Although there is some room for additional improvement, the achieved daylighting performance is reasonably close to the ideal. The graphs suggest that further improvements could be found by reducing the amount, or the negative effects, of the FP's shown in Figure 9. The amount of FP's can be reduced by improving the detection approach. Reducing the negative effects can be done by adjusting control response.

3.5. Step 5: simulate the performance of the developed multi-mode control strategies

A multi-mode control strategy with optimized detection algorithms has now been developed. The previous steps have focussed on evaluating and improving the performance of the individual detection and actuation algorithms. In this step, the performance of the complete multi-mode control strategy is assessed and compared to the baseline strategy. To evaluate if the confusion matrix method ranks the different sensors correctly, all sensors are included in this comparison. Only the best performing detection algorithms from the previous section are now evaluated. CM_{2SC} is activated using the 2% allowed $DGPs_{0.4;45deg}$ exceedance sensor threshold and the algorithm where the sensor measurements are multiplied by the unshaded height is used to activate CM_{3EL}.

Figure 11 presents a summary of whole building performance for the developed control strategies and sensor alternatives. The performance indicators are defined as in Figure 4 where the goal is to get each indicator as low as

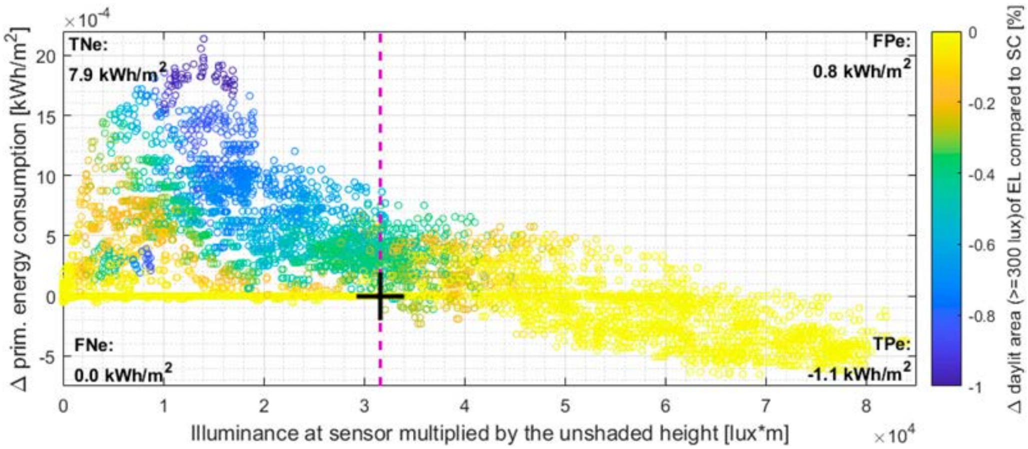

Figure 10. Evaluation of the effectivity of sensor strategy in addressing energy performance. Vertical axis: difference in instantaneous primary energy consumption of SC and EL strategies. Colour: difference in instantaneous daylighting performance of SC and EL strategies.

possible. To also evaluate the benefits of the individual control modes and detection algorithms, scenarios that include only two of the three proposed control modes are included for each sensor alternative.

For all sensor types, we see a similar pattern in performance improvements. Compared to the SC only strategy, fully raising the shade in the two-mode $CM_{1AU;2SC}$ strategies improve daylighting (by 16–32% $sDA_{300lx;50\%}$) and energy performance (by 6–11%) as well as the time with a view to the outdoors (by 24–27%) without causing a significant change in visual discomfort. The improvements in energy performance can be attributed to reductions in lighting energy consumption as well as to slight improvements in cooling energy consumption due to reduced lighting gains. The CM_{3EL} improves overall energy performance and reduces the time that the visual discomfort criterion is met to 0% (a 7% reduction) for the 0-degree viewing direction. These improvements do have a negative effect on daylighting performance (8-12% relative reduction in $sDA_{300lx;50\%}$). Compared to the SC only alternative, implementation of both the CM_{1AU} and CM_{3EL} control modes has a beneficial effect on all performance aspects. The only exception to this is the alternative using a horizontal irradiance sensor, where there is no improvement in daylighting performance.

Overall, substantial differences can be observed between the three sensors, where the indoor illuminance sensor stands out as the best performing alternative for all performance indicators. Compared to the worst performing alternative, the horizontal exterior irradiance sensor (E-Igh $CM_{1AU;2SC;3EL}$), the illuminance sensor (I-Ev $CM_{1AU;2SC;3EL}$) offers a 3% lower E_{prim}, a 9% higher $sDA_{300lx;50\%}$, 3% reduction in $DGPs_{0.4;45deg}$ exceedance and 3% more $V_{1.2m;exc}$. The large differences in daylighting performance between these two sensors can mainly be explained by the horizontal irradiance sensor's poor performance when it comes to detecting low-light conditions. This is not surprising as this threshold marks the lower boundary of conditions characterized as being partly cloudy or slightly overcast. Under such conditions, the contribution of the direct component will start becoming more significant in the overall sensor measurements and a vertically oriented sensor is better equipped to identify such instances.

Amongst the investigated alternatives I-Ev-$CM_{1AU;2SC;3EL}$ strategy offers the best trade-off in performance aspects. Compared to the conventional BL strategy it offers significant improvements for all indicators: 14% reduction in E_{prim}, a 56% higher $sDA_{300lx;50\%}$, 21% more $V_{1.2m;exc}$ and 15% reduction in $DGPs_{0.4;45deg}$ exceedance. Additionally, the I-Ev-$CM_{1AU;2SC;3EL}$ strategy can mitigate disturbing glare in the most critical viewing direction completely.

4. Discussion

This section evaluates the efficiency and limitations of the support method using the results of the case study. Additionally, this section discusses how the method can be used to customize controls for specific building applications.

In the confusion matrix method, instantaneous performance results of two separate simulations are used to identify ideal circumstances for switching between adjacent control modes. This approach has the limitation that it only quantifies the immediate performance effects of control actions. In assessing energy performance effects, this does not accurately describe the transient effects of shade actuations, and the admission of solar energy, on energy performance. This causes an error in the estimated energy reductions that are used to assess the individual control improvements. To explore the extent

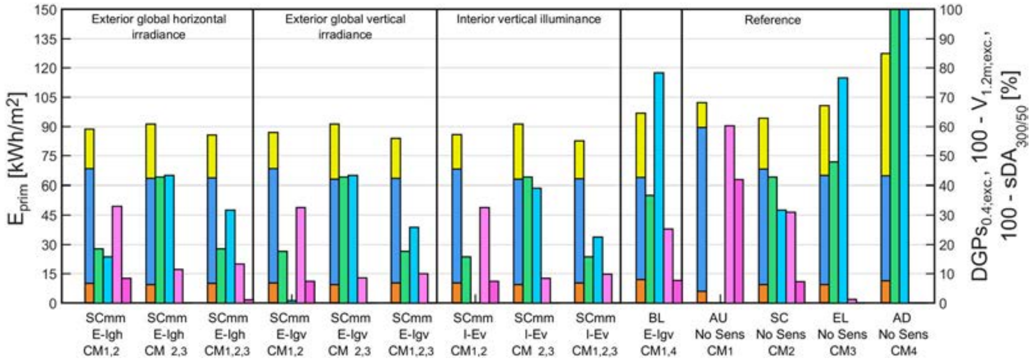

Figure 11. Summary of whole building performance predicted using simulations of the multi-mode SCmm strategy in combination with different sensors. Performance indices defined as in Figure 4.

to which this limitation influences the conclusions of the confusion matrix evaluations, the energy reductions that were estimated using this method are compared to the results from the multi-mode simulations (step 9). If we compare the energy performance results shown in Figure 11 to the estimated energy performance improvements, obtained by summing instantaneous E_{prim} in the confusion matrix quadrants (Tables 4 and 5), it can be seen that both evaluations lead to the same ranking of options for all sensors, detection algorithms and control mode alternatives. From this, it can be concluded that the confusion matrix approach can reliably rank amongst alternatives and identify high performing solutions.

Although the relative hierarchy of the different options is predicted correctly, the predicted energy savings are less accurate. The summation of confusion matrix quadrants suggests that the $CM_{1;AU,2;SC}$ strategy would have a 6.8 kWh/m^2 lower E_{prim} than the SC only strategy (Table 4) whereas the results from step 9 show this reduction to be 8.5 kWh/m^2 (Figure 11). The $CM_{2;SC,3;EL}$ strategy is estimated to lead to a 0.3 kWh/m^2 reduction in E_{prim} relative to SC whereas Figure 11 shows that this difference should be 3.2 kWh/m^2. Overall, the conclusions drawn from the multi-mode simulation study are in line with those based on the confusion matrix method. There are some discrepancies in predicted energy savings in absolute terms, but it is not the goal of the method to give an exact prediction of potential energy savings. Rather, the goal is to be able to rank the relative merits of different options and identify high performing solutions. This comparison showed that the confusion matrix method can meet this goal in a reliable way using only a very limited number of simulations.

The presented correlations between sensor measurements and performance effects depend on building design characteristics, occupant positions and contextual factors such as climate. Ideally, the proposed method is used to optimize control thresholds for specific building applications. To illustrate this, the support method was applied for three different buildings, varying in terms of their fenestration design and window-to-wall ratios (WWR: 40%, 60% and 80%). This additional study, shown in Appendix B, is not discussed in detail but the main conclusions can be summarized as follows. The scatter plots in Figure 14 show how the correlation between sensor measurements and glare and energy performance changes with the varying WWR. The graph shows that only the 40% WWR case leads to different conclusions regarding the control thresholds that are needed to satisfy required comfort conditions. In Figure 15, the I-Ev-$CM_{1AU;2SC;3EL}$ strategy is evaluated within the 40% WWR building using both generic control thresholds, defined using the initial 80%WWR case, and control thresholds customized to the specific building application. These results show that, although the I-Ev-$CM_{1AU;2SC;3EL}$ strategy with generic control thresholds gives significant performance improvements over the BL strategy, additional improvements in daylighting (18% higher $sDA_{300lx;50\%}$) and energy performance (8% lower E_{prim}) can be obtained by customizing control thresholds to the 40%WWR application.

5. Concluding remarks

This research presented a method that structures the use of BPS to support the development of comfort-driven control strategies for automated solar shading systems. The method is proposed as an alternative for the, often ad-hoc, approach that characterizes the current use of BPS in this field. The method was illustrated and tested using an automated indoor roller blind system as a case study where the structured method was used to guide the development of a multi-mode sun-tracking control strategy. Confusion matrices were used as a tool to assess the effectivity of control decisions and optimize the sensor strategy that is used to switch between control modes.

A series of scatter plots, relating sensor measurements to performance effects, combined with confusion matrices and a set of associated indicators were introduced to navigate the control space. These tools help quantify performance trade-offs and guide decision making in developing a sensor strategy. The mapping of sensor measurements to performance effects allows performance criteria to be directly translated to control thresholds. The visualization of this mapping in a set of scatter plots allowed the effects of moving control thresholds to be visualized in a single image and optimal control thresholds to be identified. The graphic nature of this mapping allows developers to investigate the performance effects of changing the relative weight of evaluation criteria without having to run additional simulations. Additionally, the plots visually support the developer in extracting detection algorithms from simulation data. Using the confusion matrix as a control decision classification tool, the performance of an existing concept could be analysed in a way that illustrated the constraints of a detection algorithm in relation to a more ideal unconstrained case. Being able to benchmark a potential concept in relation to an ideal control concept allows developers to weigh the costs of increasing control and sensor strategy complexity to potential gains in choosing research and development directions.

The most promising alternative that was identified in the case study, the SC_{mm}-$CM_{1AU;2SC;3EL}$ multi-mode strategy using an indoor illuminance sensor, offers a reduction of 14% in E_{prim}, 56% more $sDA_{300lx;50\%}$, and 8–15% reduction in $DGPs_{0.4}$ exceedance in relation to the conventional baseline solution (Figure 11). This shows that the support method can identify high-performance control rules, detection algorithms, thresholds and sensors using only a limited number of simulations. In this paper, many simulation results were presented to illustrate and test the proposed method. For identifying the best performing SC_{mm}-$CM_{1AU;2SC;3EL}$ alternative and comparing it against a baseline, only five simulations would have to be executed in practice.

The method was tested on three building designs with varying fenestration designs and offered significant performance improvements over the baseline strategies in all cases. The results showed that the performance improvements were largest when control thresholds were customized to the specific building application. By making scatter plots for multiple representative building applications, like in Figure 14, developers can also obtain insight and intuition into how the mapping of sensor measurements and performance effects are influenced by different building characteristics and adjust control thresholds on the basis of this insight.

The case study focussed on using single control thresholds for switching between control modes and only a single radiation sensor was used to inform the system in each alternative. Additionally, the actuation algorithms were intentionally kept simple and the study investigated a roller blind system with a limited degree of control freedom. It should be noted that the presented algorithms and sensor combinations are not part of the support method. The extent, however, to which the proposed method preserves its advantages when applied to systems with more control freedom should be tested in future research.

A few applications of the method, that go beyond the current case study, are recommended for further research. The performance mapping approach is not limited to using a single sensor and for developing detection algorithms based on multiple sensors, multi-dimensional plots can be used. Additionally, multiple performance criteria can be used with the confusion matrix method to identify threshold ranges that relate to different degrees of occupant sensitivities and comfort preferences. The 'disturbing' and 'perceptible' glare criteria can be used, for instance, to define the upper and lower boundaries of a threshold range that can be adjusted by users.

Different statistical classification techniques could be used as an alternative, or in addition to, the confusion matrices presented in this research. The confusion matrix approach has the advantage that different weights can be assigned to different types of false control decisions (e.g. causing glare is worse than decreasing the admission of daylight). A disadvantage of the current approach is that sensors are evaluated using specific control thresholds. For assessing sensors in a way that is not tied to a specific control threshold a ROC-curve could be used. The performance mapping approach also offers the possibility to develop detection algorithms based on machine learning techniques (Gunay et al. 2014). The PC_{true} and sensor measurements from the simulation results can be used in step 4 to train a classification tree or support vector machine, where, for example, the sensor measurements and solar position are used as predictors. This application could also provide opportunities to include user overrides, measured during control operation (Sadeghi et al. 2016), in the training data at a later stage.

In the support method, the control space of possible control actuations is constrained to a select number of control modes that are selected based on engineering knowledge and structured analyses. Hereby the control space is made smaller and more manageable. A disadvantage of this constraint is that, although the method leads to high-performance outcomes, ideal performance cannot be guaranteed. The support method is, however, also suited for developing actuation algorithms that exploit a larger part of the control space by using a proportional control approach (Shen and Tzempelikos 2017). To illustrate this point, Figure 9(B) illustrates how this could be approached in the case study. The graph indicates a slope that can be used in the $CM_{3;EL}$ mode to define the maximum shade height proportionally to sensor measurements, as an alternative to using seated eye level. Another possible application would be to discretize the control space and treat every shading system state as if it were a separate control mode. The mapping of sensor measurement to performance effects requires that distinct simulation alternatives are used but potentially a large number of control modes can be used. In the case study, this would mean using annual simulations of discrete shade height positions in step 2 and 3. In this application, the error in the assessment of instantaneous energy performance effects would have to be carefully assessed.

6. Data availability

The simulation toolchain and analyses functions that were developed for this study is publicly accessible and can be found in the following repository: https://gitlab.tue.nl/bp-tue/solarshading.

Disclosure statement

No potential conflict of interest was reported by the author(s).

Funding

This work was supported by the Rijksdienst voor Ondernemend Nederland through the TKI-Urban Energy consortium (TEID215059 and TKI-iDEEGO).

Nomenclature

RBC	Rule base control
MPC	Model predictive control
BPS	building performance simulation
wpd	Wor kplane distance
sh	shade height
α	solar altitude [°]
wph	Work plane height
γ	solar azimuth [°]
$E\text{-}I_v$	outdoor global vertical irradiance sensor
$E\text{-}I_{g;h}$	outdoor global vertical irradiance sensor
$I\text{-}E_{g;v}$	indoor vertical illuminance sensor
$sDA_{300/50\%}$	Spatial daylight autonomy 300 lux 50% of time
DGPs	daylight glare probability simplified
$DGPs_{0.4;45deg;exc}$	DGPS 0.4 exceedance for the 45° viewing direction
$V_{1.2m;exc}$	Share of occupied hours that sh $\geq$ 1.2 meters
$E_{prim.}$	Primary energy consumption for heating, cooling and lighting
η_e	Site to source primary energy ratio for electricity
η_c	Cooling delivery system efficiency
COP_{cool}	Chiller coefficient of performance
η_h	Overall heating system efficiency
IWEC	International Weather for Energy Calculations
BCVTB	Building controls virtual testbed
IGDB	International glazing database
CGDB	Complex glazing database
AU	Always up control logic
SC	Solar cut-off control logic
AD	Always down control logic
EL	Eye-level control logic
CM_{1AU}	Control mode nr. 1 following the AU logic as part of a multi-mode strategy
$CM_{1AU;2SC}$	A multi-mode control strategy with two control modes
PC_{true}	True performance classification
$PC_{detected}$	Detected performance classification
P and N	'Positive' and ' negative' classifications by the detection algorithm
TP	True positive Condition: $PC_{true} = P$ and $PC_{detected} = P$
TN	True negative Condition: $PC_{true} = N$ and $PC_{detected} = N$
FP	False positive Condition: $PC_{true} = N$ and $PC_{detected} = P$
FN	False negative Condition: $PC_{true} = P$ and $PC_{detected} = N$
sDA_{ideal}	sDA that of a two-mode control strategy assuming an ideal detection algorithm
sDA_{actual}	sDA that of a two-mode control strategy using the investigated detection algorithm
$\Delta D_{t;300lx;2CM;1CM}$	Difference in instantaneous daylighting performance of two simulated control modes
$\Delta E_{prim;2CM;1CM}$	Difference in instantaneous primary energy consumption of two simulated control modes
$\sum TNe$	Sum of all ΔE_{prim} contained in the true negative region
totNe	$TN_e + FP_e$
WWR	Window-to-wall ratio

ORCID

Samuel B. de Vries http://orcid.org/0000-0001-7906-299X
Roel C. G. M. Loonen http://orcid.org/0000-0001-6101-1449
Jan L. M. Hensen http://orcid.org/0000-0002-7528-4234

References

Atzeri, A. M., A. Gasparella, Cappelletti Francesca, Tzempelikos Athanasios. 2018. “Comfort and Energy Performance Analysis of Different Glazing Systems Coupled with Three Shading Control Strategies.” *Science and Technology for the Built Environment* 24 (5): 545–558.

Beck, W., D. Dolmans, G. Dutoo, A. Hall, and O. Seppänen. 2010. *Solar shading REHVA Guidebook 12*, edited by W. Beck. Forssa: REHVA.

Bian, Y., T. Leng, and Y. Ma. 2018. “A Proposed Discomfort Glare Evaluation Method Based on the Concept of ‘adaptive Zone’.” *Building and Environment* 143: 306–317.

CEN. 2017. *prEN 14501 Blinds and Shutters—thermal and Visual Comfort—Performance Characteristics and Classification*. Brussels: Comité Européen de Normalisation.

Chan, Y.-C., and A. Tzempelikos. 2013. “Efficient Venetian Blind Control Strategies Considering Daylight Utilization and Glare Protection.” *Solar Energy* 98: 241–254.

Coffey, B. 2013. “Approximating Model Predictive Control with Existing Building Simulation Tools and Offline Optimization.” *Journal of Building Performance Simulation* 6 (3): 220–235.

Correia da Silva, P., V. Leal, and M. Andersen. 2015. “Occupants’ Behaviour in Energy Simulation Tools: Lessons from a Field Monitoring Campaign Regarding Lighting and Shading Control.” *Journal of Building Performance Simulation* 8 (5): 338–358.

D’Antoni, M., P. Bonato, et al. 2019. *IEA SHC Task 56 – System Simulation Models, Part C Office Buildings*. Paris: International Energy Agency.

Daum, D., and N. Morel. 2010. “Assessing the Total Energy Impact of Manual and Optimized Blind Control in Combination with Different Lighting Schedules in a Building Simulation Environment.” *Journal of Building Performance Simulation* 3 (1): 1–16.

de Klijn-Chevalerias, M., R. Loonen, et al. 2017. Assisting the Development of Innovative Responsive façade elements using Building Performance Simulation. *Proceedings of the Symposium on Simulation for Architecture and Urban Design*, Society for Computer Simulation International, p. 27.

de Vries, S. B., R. C. G. M. Loonen, and J. L. M. Hensen. 2019. “Sensor Selection and Control Strategy Development Support for Automated Solar Shading Systems Using Building Performance Simulation.” In *Building Simulation*, edited by V. Corrado, E. Fabrizio, A. Gasparella, and F. Patuzzi, 4855–4862. Rome:
IBPSA.

Favoino, F., F. Fiorito, Cannavale Alessandro, Ranzi Gianluca, Overend Mauro 2016. “Optimal Control and Performance of Photovoltachromic Switchable Glazing for Building Integration in Temperate Climates.” *Applied Energy* 178: 943–961.

Fawcett, T. 2006. “An Introduction to ROC Analysis.” *Pattern Recognition Letters* 27 (8): 861–874.

Giovannini Luigi, Favoino Fabio, Lo Verso Valerio Roberto Maria, Serra Valentina, and Pellegrino Anna. 2020. “GLANCE (GLare ANnual Classes Evaluation): An Approach for a Simplified Spatial Glare Evaluation.” *Building and Environment* 186: 107375.

Gunay, H. B., W. O’Brien, and I. Beausoleil-Morrison. 2016. “Implementation and Comparison of Existing Occupant Behaviour Models in EnergyPlus.” *Journal of Building Performance Simulation* 9 (6): 567–588.

Gunay, H. B., W. O’Brien, Beausoleil-Morrison Ian, Huchuk Brent. 2014. “On Adaptive Occupant-learning Window Blind and Lighting Controls.” *Building Research & Information* 42 (6): 739–756.

Haldi, F., and D. Robinson. 2010. “Adaptive Actions on Shading Devices in Response to Local Visual Stimuli.” *Journal of Building Performance Simulation* 3 (2): 135–153.

Hellinga, H., and T. Hordijk. 2014. “The D&V Analysis Method: A Method for the Analysis of Daylight Access and View Quality.” *Building and Environment* 79: 101–114.

Heschong, L. 2003. *Windows and Offices: A Study of Office Worker Performance and the Indoor Environment*. Fair Oaks, CA: Energy Commission.

Huchuk, B., H. B. Gunay, O’Brien William, Cruickshank Cynthia A. 2016. “Model-based Predictive Control of Office Window Shades.” *Building Research & Information* 44 (4): 445–455.

Illuminating Engineering Society. 2012. *Approved Method: IES Spatial Daylight Autonomy (sDA) and Annual Sunlight Exposure (ASE)*. New York, NY: Illuminating Engineering Society.

Jakubiec, J. A., and C. F. Reinhart. 2012. “The ‘Adaptive Zone’ – A Concept for Assessing Discomfort Glare Throughout Daylit Spaces.” *Lighting Research & Technology* 44 (2): 149–170.

Jeong, K. Y., A. S. Choi, and M. Sung. 2016. “A Mock-up Study for Validation of an Improved Control Algorithm for Automated Roller Shade.” *Indoor and Built Environment* 25 (1): 17–28.

Konis, K. 2013. “Evaluating Daylighting Effectiveness and Occupant Visual Comfort in a Side-lit Open-plan Office Building in San Francisco, California.” *Building and Environment* 59: 662–677.

Konis, K., and S. Selkowitz. 2017. *Effective Daylighting with High-performance Facades*. Cham: Springer.

Koo, S. Y., M. S. Yeo, and K. W. Kim. 2010. “Automated Blind Control to Maximize the Benefits of Daylight in Buildings.” *Building and Environment* 45 (6): 1508–1520.

Kristl, Ž, M. Košir, Hensen Jan L.M., Overend Mauro. 2008. “Fuzzy Control System for Thermal and Visual Comfort in Building.” *Renewable Energy* 33 (4): 694–702.

Kuhn, T. E. 2017. “State of the art of Advanced Solar Control Devices for Buildings.” *Solar Energy* 154: 112–133.

Lee, E., D. DiBartolomeo, and S. E. Selkowitz. 1998. “Thermal and Daylighting Performance of an Automated Venetian Blind and Lighting System in a Full-scale Private Office.” *Energy and Buildings* 29 (1): 47–63.

Loonen, R. C. G. M. 2018. *Approaches for Computational Performance Optimization of Innovative Adaptive Façade Concepts*. Eindhoven: Department of the Built Environment, Eindhoven university of technology.

Loonen, R. C. G. M., F. Favoino, Hensen Jan L.M., Overend Mauro. 2017. “Review of Current Status, Requirements and Opportunities for Building Performance Simulation of Adaptive Facades.” *Journal of Building Performance Simulation* 10 (2): 205–223.

Loonen, R. C. G. M., S. Singaravel, Trčka M., Cóstola D., Hensen J.L.M. 2014. “Simulation-based Support for Product Development of Innovative Building Envelope Components.” *Automation in Construction* 45: 86–95.

Loonen, R. C. G. M., M. Trčka, Cóstola D., Hensen J.L.M. 2013. "Climate Adaptive Building Shells: State-of-the-art and Future Challenges." *Renewable and Sustainable Energy Reviews* 25: 483–493.

Mahdavi, A. 2001. "Simulation-based Control of Building Systems Operation." *Building and Environment* 36 (6): 789–796.

Mahdavi, A., A. Mohammadi, Kabir Elham, Lambeva Lyudmila 2008. "Occupants' Operation of Lighting and Shading Systems in Office Buildings." *Journal of Building Performance Simulation* 1 (1): 57–65.

Mahdavi, A., B. Spasojevic, and K. Brunner. 2005. "Elements of a Simulation-Assisted Daylight-Responsive Illumination Systems Control in Buildings." In *Building Simulation*, edited by I. Beausoleil-Morrison and M. Bernier, 15–18. Rome: IBPSA.

Mardaljevic, J. 2019. "Aperture-based Daylight Modelling: Introducing the 'View Lumen'." In *Building Simulation*, edited by V. Corrado, E. Fabrizio, A. Gasparella, and F. Patuzzi. Rome: IBPSA.

McNeil, A., and E. S. Lee. 2013. "A Validation of the Radiance Three-phase Simulation Method for Modelling Annual Daylight Performance of Optically Complex Fenestration Systems." *Journal of Building Performance Simulation* 6 (1): 24–37.

Meerbeek, B., M. te Kulve, Tommaso Gritti, Mariëlle Aarts, Evert van Loenen, and Emile. Aarts. 2014. "Building Automation and Perceived Control: A Field Study on Motorized Exterior Blinds in Dutch Offices." *Building and Environment* 79: 66–77.

Nezamdoost, A., and K. Van Den Wymelenberg. 2017. "A Daylighting Field Study Using Human Feedback and Simulations to Test and Improve Recently Adopted Annual Daylight Performance Metrics." *Journal of Building Performance Simulation* 10 (5–6): 471–483.

Ochoa, C. E., M. B. C. Aries, and J. L. M. Hensen. 2012. "State of the Art in Lighting Simulation for Building Science: A Literature Review." *Journal of Building Performance Simulation* 5 (4): 209–233.

Oh, M. H., K. H. Lee, and J. H. Yoon. 2012. "Automated Control Strategies of Inside Slat-type Blind Considering Visual Comfort and Building Energy Performance." *Energy and Buildings* 55: 728–737.

Oldewurtel, Frauke, Alessandra Parisio, Colin N. Jones, Dimitrios Gyalistras, Markus Gwerder, Vanessa Stauch, Beat Lehmann, and Manfred. Morari. 2012. "Use of Model Predictive Control and Weather Forecasts for Energy Efficient Building Climate Control." *Energy and Buildings* 45: 15–27.

Pilechiha, Peiman, Mohammadjavad Mahdavinejad, Farzad Pour Rahimian, Phillippa Carnemolla, and Saleh Seyedzadeh. 2020. "Multi-objective Optimisation Framework for Designing Office Windows: Quality of View, Daylight and Energy Efficiency." *Applied Energy* 261: 114356:1–23.

Piscitelli, M. S., S. Brandi, G. Gennaro, A. Capozzoli, F. Favoino, and V. Serra. 2019. "Advanced Control Strategies for the Modulation of Solar Radiation in Buildings: MPC-enhanced Rule-based Control." In *Building Simulation*, edited by V. Corrado, E. Fabrizio, A. Gasparella, and F. Patuzzi, 869–876. Rome: IBPSA.

Sadeghi, S. A., P. Karava, Konstantzos Iason, Tzempelikos Athanasios. 2016. "Occupant Interactions with Shading and Lighting Systems Using Different Control Interfaces: A Pilot Field Study." *Building and Environment* 97: 177–195.

Seong, Y.-B., M.-S. Yeo, and K.-W. Kim. 2014a. "Corrections for Minimizing Solar Profile Prediction Errors and Methods for Preventing Direct Glare on the Workplane in Blind Control." *Indoor and Built Environment* 23 (8): 1060–1079.

Seong, Y. B., M. S. Yeo, and K. W. Kim. 2014b. "Optimized Control Algorithm for Automated Venetian Blind System Considering Solar Profile Variation in Buildings." *Indoor and Built Environment* 23 (6): 890–914.

Shen, E., J. Hu, and M. Patel. 2014. "Energy and Visual Comfort Analysis of Lighting and Daylight Control Strategies." *Building and Environment* 78: 155–170.

Shen, H., and A. Tzempelikos. 2012. "Daylighting and Energy Analysis of Private Offices with Automated Interior Roller Shades." *Solar Energy* 86 (2): 681–704.

Shen, H., and A. Tzempelikos. 2017. "Daylight-linked Synchronized Shading Operation Using Simplified Model-based Control." *Energy and Buildings* 145: 200–212.

Silva da, P. C., V. Leal, and M. Andersen. 2012. "Influence of Shading Control Patterns on the Energy Assessment of Office Spaces." *Energy and Buildings* 50: 35–48.

Stevens, S. 2001. "Intelligent Facades: Occupant Control and Satisfaction." *International Journal of Solar Energy* 21 (2-3): 147–160.

Tabadkani, A., A. Roetzel, Li Hong Xian, and Tsangrassoulis Aris. 2020. "A Review of Automatic Control Strategies Based on Simulations for Adaptive Facades." *Building and Environment* 175: 106801:1–19.

Turan, I., C. Reinhart, and M. Kocher. 2019. "Evaluating Spatially-distributed Views in Open Plan Work Spaces." In *Building Simulation*, edited by V. Corrado, E. Fabrizio, A. Gasparella, and F. Patuzzi, 1098–1105. Rome: IBPSA.

Tzempelikos, A., B. O'Neill, and A. Athienitis. 2007. Daylight and Luminaire Control in a Perimeter Zone using an Automated Venetian Blind. *Conference on Building Low Energy Cooling and Advanced Ventilation Technologies in the 21st Century*, Crete island, Greece.

Tzempelikos, A., and H. Shen. 2013. "Comparative Control Strategies for Roller Shades with Respect to Daylighting and Energy Performance." *Building and Environment* 67: 179–192.

Walkenhorst, Oliver, Joachim Luther, Christoph Reinhart, and Jens. Timmer. 2002. "Dynamic Annual Daylight Simulations Based on One-hour and One-minute Means of Irradiance Data." *Solar Energy* 72 (5): 385–395.

Wetter, M. 2011. "Co-simulation of Building Energy and Control Systems with the Building Controls Virtual Test Bed." *Journal of Building Performance Simulation* 4 (3): 185–203.

Wienold, J. 2007. "Dynamic Simulation of Blind Control Strategies for Visual Comfort and Energy Balance Analysis." In *Building Simulation*, edited by Yi Jiang, 1197–1204. Beijing: IBPSA.

Wienold, J. 2009. "Dynamic Daylight Glare Evaluation." In *Building Simulation*, edited by P. A. Strachan, N. J. Kelly, and M. Kummert, 944–951. Glasgow: IBPSA.

Wienold, J., T. Iwata, M. Sarey Khanie. 2019. "Cross-validation and Robustness of Daylight Glare Metrics." *Lighting Research & Technology*. doi:1477153519826003.

Xiong, J., A. Tzempelikos, Ilias Bilionis, and Panagiota. Karava. 2019. "A Personalized Daylighting Control Approach to Dynamically Optimize Visual Satisfaction and Lighting Energy use." *Energy and Buildings* 193: 111–126.

Yao, J., Chow, D.H.C., Zheng, R.-Y., Yan, C.-W. 2016. "Occupants' Impact on Indoor Thermal Comfort: a Co-simulation Study on Stochastic Control of Solar Shades." *Journal of Building Performance Simulation* 9 (3): 272–287.

Yun, S.-I., H.-R. Kim, Doo Yong Park, and Jae-Weon Jeong. 2020. “Sensor Minimization Method for Integrated Daylighting Control by a Mathematical Approach.” *Energy and Buildings* 214: 109891-1–11.

Yun, G., D. Y. Park, and K. S. Kim. 2017. “Appropriate Activation Threshold of the External Blind for Visual Comfort and Lighting Energy Saving in Different Climate Conditions.” *Building and Environment* 113: 247–266.

Strategies for stimulating market penetration of advanced solar shading systems

Oindrila Ghosh
02.03.2021

EINDHOVEN UNIVERSITY OF TECHNOLOGY

Stan Ackermans Institute

SMART BUILDINGS & CITIES

Strategies for stimulating market penetration of advanced solar shading systems

By

Oindrila Ghosh

A thesis submitted in partial fulfillment of the requirements for the degree of Professional Doctorate of Engineering

The design described in this thesis has been carried out in accordance with the TU/e Code of Scientific Conduct

Roel G.C.M. Loonen, university coach

Sam kin, company coach

Eindhoven, the Netherlands

March, 2021

This thesis has been established in collaboration with

A catalogue record is available from the Eindhoven University of Technology Library

SAI-report: 2021/022

Executive summary

There is a growing urgency towards designing energy efficient buildings that focus on occupant comfort and wellbeing. State-of the-art dynamic façade components like automated solar shading systems can actively contribute towards solving this need and therefore are gaining increased attention due to their performance promise. However, due to a lack of comprehensive performance information, these façade systems still face some major barriers towards market integration.

The solutions that were developed in this PDEng project take place in this context, which was carried out in collaboration with Kindow BV, an advanced interior shading systems supplier. Kindow is a successful niche start-up which is growing towards becoming a scale up. During this phase of growth, Kindow realized it is facing two major barriers as follows:

1. The performance information on these advanced shading systems are available but limited. There is a need to understand how Kindow's products perform under varying scenarios and have different input parameter combinations tested to help Kindow create convincing business propositions for their clients.

2. There is also a lack of practitioner-oriented literature that highlights the performance benefits of advanced shading systems. For example, quantitative insights into the advantages of designing an integrated façade through careful combination of state-of-the-art façade components such as glazing, shading, or lighting systems are unavailable. Such lack of learning avenues makes it harder for Kindow to create enough market pull for its product.

Therefore, the goal of this PDEng project was to provide solutions to these problems using a systems thinking approach and resources from the building performance simulation workflow which are otherwise complicated for industrial use. Figure 1 shows the project workflow. The solutions provided to meet Kindow's needs were as follows:

1. Performance assessment was carried out for Kindow products to investigate their performance under varying scenarios. In addition, studies were done to evaluate the most efficient strategy and if there is a need for further optimisation.

2. An easy-to-use and comprehensive database was populated with energy and visual performance information for Kindow with various options of input parameters. This look-up table expresses performance with suitable KPIs to make convincing business propositions for Kindow's clients.

3. Strategies for stimulating market awareness were developed by creating different learning avenues targeted towards Kindow's different market stakeholders. The first one is a scientific, peer-reviewed publication that legitimizes the performance benefits of Kindow products. The second product created consists of a couple of articles and interactive blogs that provide quick and easy insights as to how using Kindow products can improve their building's value proposition. Finally, through short articles in student magazines and interviews in popular construction magazines.

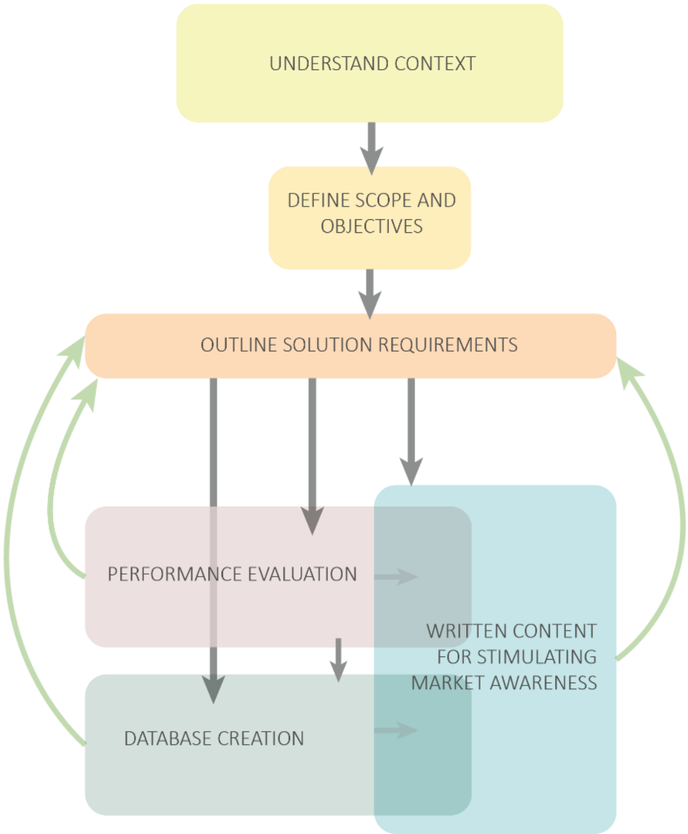

Figure 1: Project Workflow

In order to design and finalise these solutions, the CAFCR framework was used. This helped underline Kindow's barriers, understand their context and scope out the goals and objectives for the PDEng project. Then with the help of requirements engineering, the solution requirements were outlined and finally worked on to provide the final deliverables.

The first phase of the project focused on understanding and analysing the performance of Kindow Rollers blinds and Verticals. Up until the beginning of the project, Kindow products were only tested for a specific location and orientation and were not comprehensively benchmarked with other competing shading systems available in the market. Therefore, in this phase, the objective was to test which control strategy available for Kindow products provides the best trade-off in terms of conflicting performance goals such as daylight access and energy consumption. For Kindow roller blinds, the strategy with sun-tracking and cloudy and bright sky condition sensing turned out to be the most efficient in balancing the trade-offs as mentioned earlier. For Kindow Verticals, the retract control strategy which was most open to the view outdoors and retracts early morning to have clear view to the outdoors was found to be the most efficient in balancing trade-offs. It was also analysed how Kindow's control strategy performs in different climate conditions and façade orientation in comparison with industry standard automated shading systems. At the end of these studies, the control strategy with the most balanced trade-offs were selected and further optimized to perform better in orientations other than the South. These optimized strategies were then selected to be used for Kindow's second and third phase of solutions in the PDEng project. Additionally, these studies also highlighted the need to test Kindow's shading systems with respect other varying façade components such as glazing properties and Lighting systems.

In the next phase, studies were carried out to test the impact of different combinations of façade components and the insights from the resulting studies were compiled in preparation for a peer reviewed scientific publication. In addition, certain prevailing notions about shading performance were also tested and published on Kindow's website; most notably, the rule of thumb suggests that "only exterior shading is useful, because it can actually keep the sun out". Such notions do not hold true, since careful combination of internal shading with glazing and lighting systems can perform equally well or even outperform standard external shade combinations.

The final phase of the project was to create a database which Kindow could use for its client consultations. Owing to time limitations and greater interest towards roller blinds in the current market, it was finalised that the database would be created for Roller blinds. An easy to use Excel database was created where a Kindow employee could select desired facade component combinations (glazing, shading and lighting system properties) and get results that could be readily used to quantify Kindow's performance (primary energy consumption, daylight autonomy, glare, view, cost savings, load curves etc.) as compared to industry standard systems (Basic automated, manual, no shade at all) available in the market. The options chosen for each input parameter was selected according to the common installations done in the construction industry and feedback from kindow's clients. 1440 cases were simulated for the database, and it was built in a way to be easy updatable with new information in the future.

The data analysed from this large scale simulation set was used to create more insights which were used to create practitioner oriented design online content, such as interactive blogs which can grab a lot of attention and could be easily shared over social media for quicker information spread amongst Kindow's key stakeholders. In addition, all studies carried out throughout the project enabled creation of smaller avenues for market awareness such as interview with popular construction magazines as well as an article in the university student magazine. The idea was to be able to gain more web traffic for Kindow, such that it can slowly over time create enough market pull that clients already know about the benefits of Kindow's products and come to Kindow to start their customer journey from the 'request for purchase' stage.

This project managed to achieve the objectives of comprehensive evaluation of Kindow's performance in varying conditions and utilize that information to create a database as well as avenues to help stimulate market awareness for its products. Although there were minor limitations in terms of not producing a database for Kindow verticals due to lack of time, the current simulation framework had been setup in a way that it can be easily simulated by another skilled user in future. Also, the insights regarding the performance of the shading system will hopefully get further published in more magazines and articles than what was planned at the time of writing this thesis report.

Acknowledgements

It feels like yesterday, that I started my PDEng journey on a surprisingly warm and sunny February morning. It has been a whirlwind of two years since then, filled with warmth, friendship and good times and also some ‘pandemicky’ ones. I am grateful for all the knowledge and skills I have gained through this PDEng programme and more so for the awesome people that I have befriended. So, here goes a vote of thanks to all the people who made these last two years memorable.

First of all, a huge thank you to Roel, my university advisor for all the support and meticulous guidance for this PDEng project. You have always been there making sure I don’t go all over the place and work with restraint and foresight. Thank you for being so accommodating, especially me with my last minute feedback requests. Also, I would like to thank Samuel for putting up with my incessant coding related queries and always providing me with a plethora of information to any question that I asked. Thanks for the unwavering support

I would also like to thank Jan, his insight into the project has always pushed me to look at it from a different perspective. More so, I would like to thank him for creating this wonderful and nurturing environment that is the Building Performance group. I would also like to thank Lada , as it was a delight working with her as a student representative for the Smart Cities and Buildings programme.

Working in collaboration with Kindow, especially with my company advisor Sam Kin was a great learning experience. Thank you for being pragmatic and as well as flexible with your requirements from this project.

Thanks to all the wonderful souls I met during my time at TU/e, it would never have been this fun without the BPS group. Christina (my meme dealer), Zahra (my teasing machine), Afaq (thanks for listening to all my gibberish), Johann, Adam, Christos, Toon, Agatha, Bin, Pieter Jan, Dimitry, Rajesh, Luyi and Hemshikha - Thanks so much for making me feel so welcome and also thanks for the fun nights and summer trips outside of work!

Dear Julien and Waqas, still remember the first day we all started at 6th floor. Thank you for bringing so much joy and coffee breaks in my life. From attempting to watch Game of Thrones in Zwart Doos auditorium to fun road trips across the Netherlands we have really made some fun memories. Thanks Sonya, for being my workout buddy and introducing me to bouldering. A big thanks to you Liz and also Geri for not giving up on me since I left Singapore and always reaching out and keeping in touch no matter the distance.

The past two years would not be the same without you Antia. I will need to write another report to enumerate our little adventures and shenanigans, haha. So, I will just say this – thank you for existing in my life, you made it a happier place.

Finally, my family - Maa, Baba and Dada, thank you for your relentless support, enthusiasm and fangirl attitude. It is because of you that I am where I am and I am who I am.

Acronyms

BPS	Building performance simulation
BSDF	Bidirectional scattering distribution function
EU	European Union
HVAC	Heating, ventilation and air conditioning
KPI	Key performance indicator
LBNL	Lawrence Berkeley National Laboratory
MLP	Multi-level perspective
PDEng	Professional doctorate in engineering
SB&C	Smart buildings and cities
SDA	Spatial daylight autonomy
WWR	Window-to-wall ratio

Table of Contents

1. Introduction

1.1 Background

There is an increasing awareness of wellbeing and health in offices and public spaces, with good daylighting being considered as one of its important contributors. It was found that daylight is the preferred light source by humans. Surveys conducted show that 70% of office occupants believe there is a connection between the amount of natural light in the office and their work performance. Moreover, 87% believe there is a connection between office morale and the amount of daylight they receive in their office (View, Inc, 2019). Therefore, all of this indicates the growing awareness towards the socio-economic benefits of daylight in indoor spaces. Furthermore, daylight is also source for reducing lighting energy consumption. Electric lighting accounts for approximately 15% of the total electrical power consumption and 5% of greenhouse gas worldwide (IEA-SHC, 2019). Therefore, appropriate control of the daylight inside buildings can really benefit not only energy efficiency but also quality of wellbeing in occupants.

In addition to the need for appropriate daylighting indoors, it is important to note that there is also a growing demand for increasing the thermal efficiency of buildings. So, one of the first steps in improving energy efficiency is upgrading the building envelope and there is already a huge market for building refurbishment. We know this from the fact that 85-95% of buildings in the EU are expected to still be standing in 2050; renovating them is essential to reducing emissions and energy use. The European green deal Renovation Wave aims to double its current renovation rate and has set targets to refurbish 35 million inefficient buildings by 2030 (European Commission, 2020).

Total envelope refurbishment of existing buildings is often ideal from an energy efficiency perspective, but it is also more expensive and takes more construction time/workers. 'Light' refurbishments like retrofitting fenestration systems are gaining interest in the construction industry. Therefore, this has created a greater interest towards building integrated solar envelope systems (C. Maurer, 2018). Shading systems are one such an example that can help optimize building energy performance, on the condition that they are considered as an integral part of the indoor climate control system. There are advanced automated shade systems available in the market that dynamically respond to the outdoor environment. Thereby managing solar heat gains, daylight utilization and glare mitigation in buildings all while providing views to the outdoors with minimal occupant intervention. They are also a comparatively cheaper alternative to whole envelope insulation retrofits. In addition to the retrofit market, the value proposition of automated shade systems can also offer plenty of opportunities for new buildings, especially when these systems are carefully considered and integrated during the early design phases.

Automated solar shading systems are gaining increased attention due to their performance promise, but it faces some major barriers towards market integration. The main problem is that solar shading[1] still tends to be approached as an optional window dressing. In the majority of cases, it is considered as a soft furnishing rather than an integral part of façade design that can be deployed as an effective passive solar control and daylight management tool. The type of and properties of shading systems tend to be selected after all façade components (glazing properties, WWR, interior lighting properties

[1] The focus of this PDEng report is mostly on interior shading systems. The barriers mentioned here may be less pertinent for the market segment of exterior solar shading systems. However, the deployment of exterior shading systems faces many other challenges, related to e.g. wind loads, maintenance and cleaning, obtrusiveness, and costs. Moreover, as opposed to popular belief, the performance of modern interior shading is not necessarily inferior to the performance of exterior systems. More details on this topic are presented in section 4.3.1.

etc.) have already been decided. This happens in current practice because glazing, shading, and lighting are often not treated as one integrated system. Traditionally, each of these components are designed and commissioned by separate decisionmakers (lighting designer, façade engineer for glazing and interior designer for shades) and their performance is often measured and evaluated separately from each other. This segregation leads to missed opportunities, since the performance of these components are interdependent and its combined effect on admitting controlled amount of solar energy is critical to the whole building performance success.

Additionally, since insulation and airtightness in new buildings are getting better over the days, it makes such buildings more susceptible to overheating issues because of climate change, even in temperate climates (Dengel, 2012); (Aste, Leonforte, Manfren, & Mazzon, 2015); (Brambilla, Bonvin, Flourentzou, & Jusselme, 2018). This makes the control of solar gains through fenestration systems even more critical. All these siloed sectors (glazing, shading and lighting) are paying attention to this issue and create state-of-the-art products like spectrally selective glazing, reflective shade fabrics, advanced dimming lighting systems, sensor, actuators and smart controls etc. All these products provide new opportunities and careful combination of these advanced systems can considerably improve energy efficiency as opposed to the reductions made through common practices in designing façade component combinations.

Despite the advantages of automated shades, manual roller blinds are cheaper, therefore they end up garnering higher interest from practitioners. Research on occupant interaction with manual blinds demonstrates that once lowered/rotated to avoid glare or excess light into the workspace, they are rarely put back up when the discomfort is over, resulting in higher lighting energy demands (Reinhart, 2003); (Gunay, 2014); (Haldi, 2010). Therefore, in recent times, there is a shift towards adoption of dynamic solar shading systems. These systems can automatically regulate the entry of heat and light into the building by continuously responding to the outdoor environmental stimuli as well as indoor occupant behaviour. First generation automated shading devices have not been particularly successful. Occupant feedback suggested negative experiences with automated shading systems (Haldi, 2010) (Meerbeek, 2014). But with advancement of technology, these systems within the niche, now come with a variety of material properties, sensor-actuator systems and control mechanisms.

1.2 Kindow solar shading systems

Kindow BV is the developer of some of these niche innovative shading system technologies currently available in the market. Kindow's product is an automated interior shading system that is dynamically controlled based on real-time outdoor environmental information. Kindow has successfully launched themselves into the market with a few projects in the Benelux region. They have mature commercial products, but are continuously seeking to evolve and upgrade the technology, customization options and proposition. Currently, Kindow's sales approach has been very personal and proactive, through one-on-one client consultation in individual customer journeys (technology push). To be able to reduce this technological push through personal consultations and grow their business from a start-up phase to a scale-up where they concentrate only on incoming sales and customer support (figure 2), they need to have enough performance information about their technology already available in the market so that relevant stakeholders for their product like architects, energy consultants, contractors etc. are already aware of the benefits of adopting this technology and therefore come to Kindow directly for purchase (market pull).

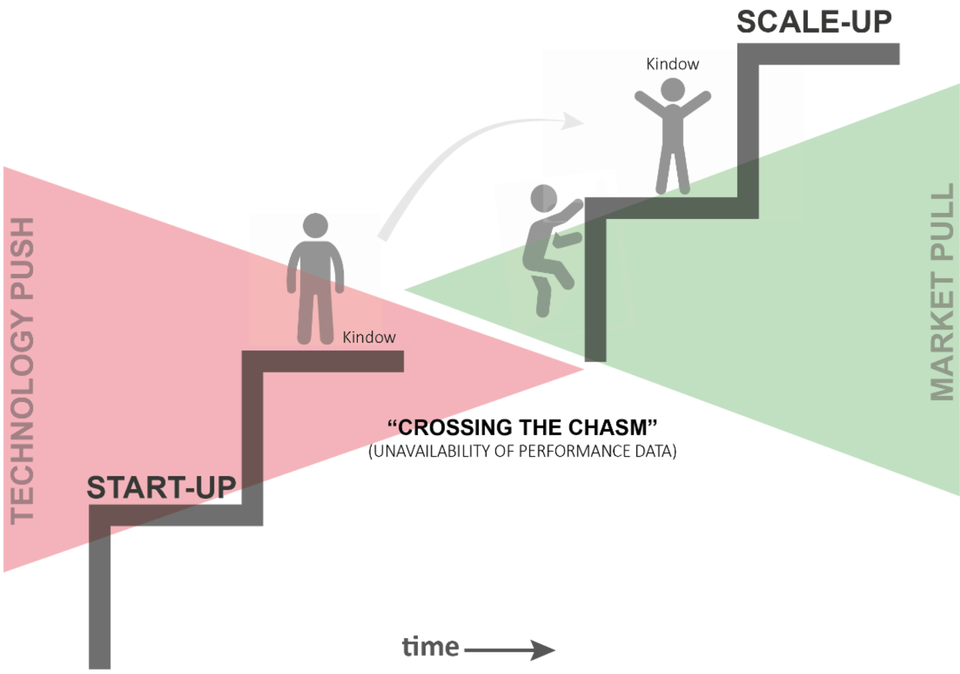

Figure 2: Kindow's transition from a start-up to scale up.

The lack of insight into operational performance and the risks associated is limiting Kindow from giving guarantees about the performance of their products, resulting in lacking market adoption of promising technologies, hence prohibiting company growth (Federizzi, 2017). Previous studies (although limited in the number of cases simulated) have already investigated the performance of Kindow shading systems (de Vries S. B., 2019); (F. Ochs M. M.-M., 2020); (F. Ochs M. M.-C.-M., 2020) and found that it can lead to superior daylighting (26-42%), visual comfort (19-21%) and energy performance (1-4%) compared to conventional automated solar shading solutions. Despite its promising performance, these advanced shading systems still requires further comprehensive performance assessments to create the market pull required to make it a mainstream product. For example, there is a lack of knowledge regarding the performance of advanced shading systems in combination to other state of the art façade components like glazing and lighting systems. In addition, advanced automated shading systems also needs to overcome other barriers such as compliance with both construction codes and energy-related norms. The lack of consolidated international standards and test methods devised for building integrated component makes it hard for these products to penetrate the market and consequently create awareness among practitioners regarding the benefits or trade-offs of advanced shade systems and their appropriate combinations with other façade components. The scientific and the business case for shading is poorly understood by building professionals (BNEF, 2018). Therefore, the advanced solar shading industry has not managed to turn façade industry (retrofit + new builds) into a more tangible business.

The goal of this PDEng project is to design ways to penetrate the shading systems market to create market pull for Kindow products. It aims to do so by providing detailed performance assessment of Kindow products. Then, utilize this information to create separate curated learning avenues targeted towards Kindow's market stakeholders. The objective of these solutions is to contribute to Kindow's transition to large scale "off the shelf" sales where the client is already aware of Kindow' s benefit over other available shading products in contrast to its current one-on-one client sales and communication which involves a lot of duplicated efforts in fostering awareness in clients and resources to carry out such consultations.

1.3 Design approach: Systems Thinking

To be able to achieve the various objectives, the overarching methodology that was used to deal with the design of this project is a Systems thinking approach (Arnold R. D., 2015). The core idea behind this approach is that it examines problems more completely and accurately before arriving at a solution. More specifically it follows a CAFCR framework which forms the backbone of the project design. Additionally, Requirements engineering and certain theories in system innovation (e.g., Strategic Niche Management, lean business model) were used to understand the context and subsequently design the deliverables for the project.

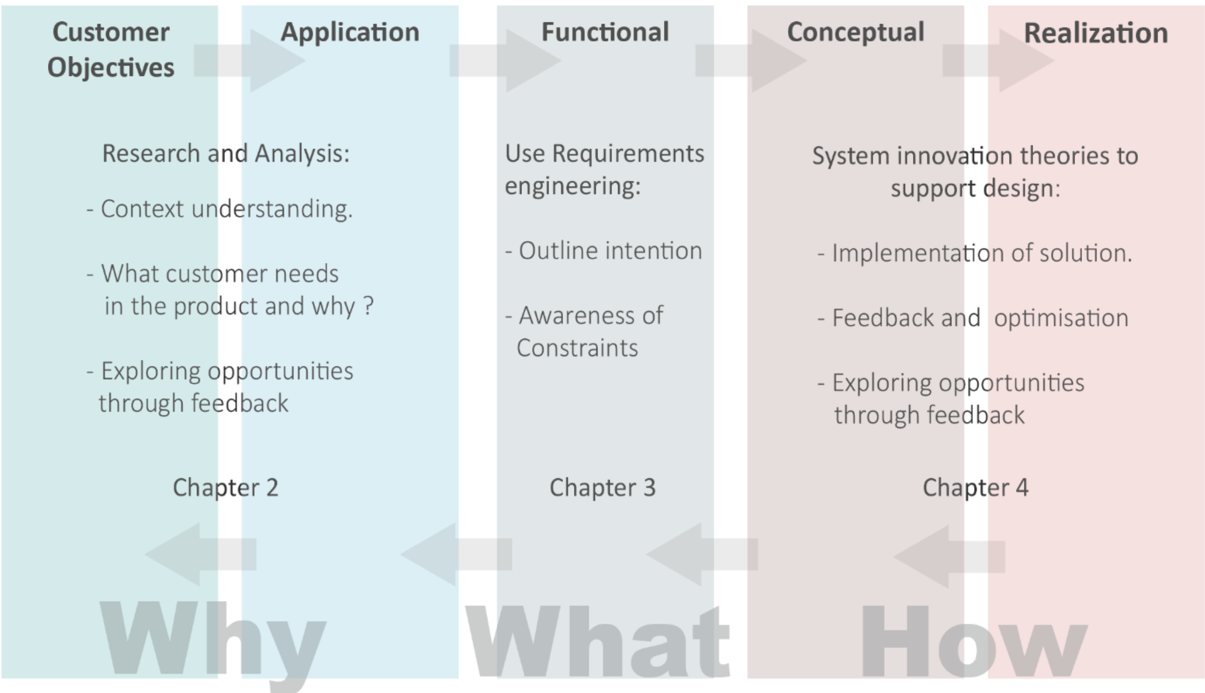

Figure 3: CAFCR framework + requirements engineering + system Innovation theories that have been combined and used in the project. The back arrows defines the feedback loop among each views and how it facilitated re-adjustment of requirements and design of the deliverables.

CAFCR framework: The CAFCR model (Muller, 2020) decomposes the overall structure of a project into five views (Figure 3). A short explanation of the five views and how they are used in this report are outlined below:

1. <u>The Customer Objectives and Application view:</u> These two sections look at what the customer wants to achieve. It analyses the needs of the customer, understands the landscape context that the customer (Kindow) is embedded in and provides the justification of '*why*' a specific design or solution should be carried out in order to be able to solve the customer's problems. **"Chapter 2 – Analysis"** in this report will cover the first two views. It will provide a quick description of the company and its products followed by what were the initial

objectives/needs from Kindow. After that, the background context specific to Kindow and its current barriers in the construction sector is explored. Finally, the specific scope and objectives of the PDEng project are identified and the tools and resources to be used for the project are selected.

2. The Functional view: This view of the CAFCR framework is where the scope and objectives set in the previous view are categorized into specific, measurable, achievable, realistic and time-bound (SMART) deilverables. Requirements engineering will be used here to set out '*what*' are the necessary functions and attributes for our final deliverables. **"Chapter 3 – Design Requirements"** will cover the functional view or the requirements section. The project objectives are clearly categorized into three target solution areas and the design requirements for these target areas are specified in a table.

3. The Conceptual and Realisation View: The last two views are conceptual and realization views which describe *'how'* the product was designed and implemented. The product is then further optimized after feedback from the client. **"Chapter 4 - Implementation"** provides a description of these last two views. It will showcase the detailed design of the deliverables that correspond to the target solution areas. Progress of the solution deliverables described in this section was not linear. They overlapped each other or were executed simultaneously depending on client feedback and strategic re-adjustment of project goals (figure 3).

2. Analysis

Up until now, the report outlined the general landscape for advanced solar shading systems within the construction industry. Section 1.2 shortly highlights the company Kindow and then proceeds to outline the design approach that will be used for executing the PDEng project. From this chapter onward, we will zoom in on Kindow in more detail and proceed with the application of the CAFCR framework.

2.1 Company Introduction

The PDEng project is carried out in collaboration with the company Kindow. It is a supplier and producer of daylight-controlled interior blinds, an innovative system in which the blinds are dynamically controlled based on real-time outdoor environmental information. It has two main products:

1. **Roller Blinds:** Kindow Rollers (Figure 4) adapt to the position of the sun, going up or down to an optimal height automatically, to prevent direct sunlight from a desk and computer screen. This way the unwanted glare and overheating are prevented, while daylight admission and view are optimized. When cloudy, Kindow Rollers are fully retracted to have a full unobstructed view and allow for maximum daylight access. Kindow Rollers will prevent glare. When it’s sunny and the sky is bright, their height will be capped to eye level, preventing glare while allowing view. Also, when the sun is not directly on the façade, skies can be too bright and they will close to eye level. Closing to eye level also results in less cooling load during summer. An optimal option for installation within window frames (Kindow, 2019).

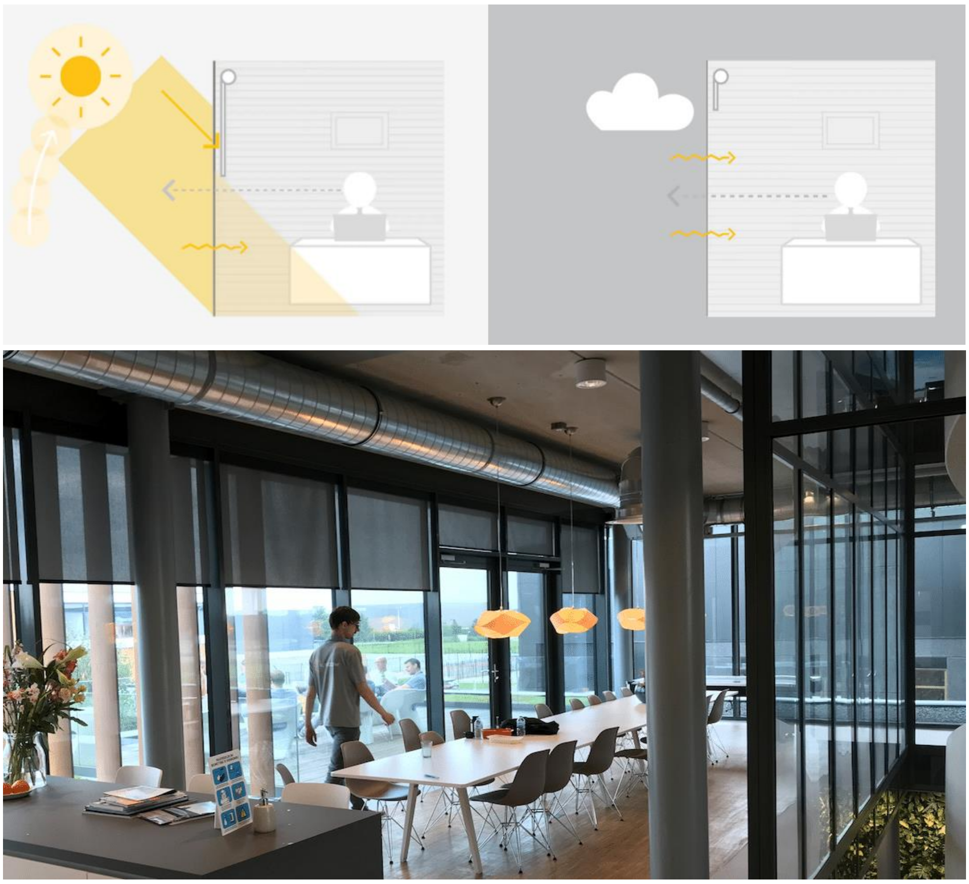

Figure 4: Kindow rollers. Source: Kindowblinds.com

2. **Verticals:** Kindow Verticals (Figure 5) track the sun automatically, facing the sun. The blinds prevent glare from direct sunlight while creating more openness during the day to allow for more view and diffuse daylight to enter. The blinds open automatically when cloudy. Both sides of the vertical blinds can be used effectively. In summer the reflective side of the blinds will face the sun in order to keep out heat, while in winter the absorptive side will be used to harvest heat. Resulting in a lower cooling load during summer as well as a lower heating load during winter. Kindow Verticals are optimal for full glass facades, allowing for daylight transmission from floor to ceiling. A great choice for buildings situated in countries further from the equator. Here the sun will be positioned low at the horizon over long periods of the year and our sun tracking verticals will still allow openness over the full height of the glass (Kindow, 2019)

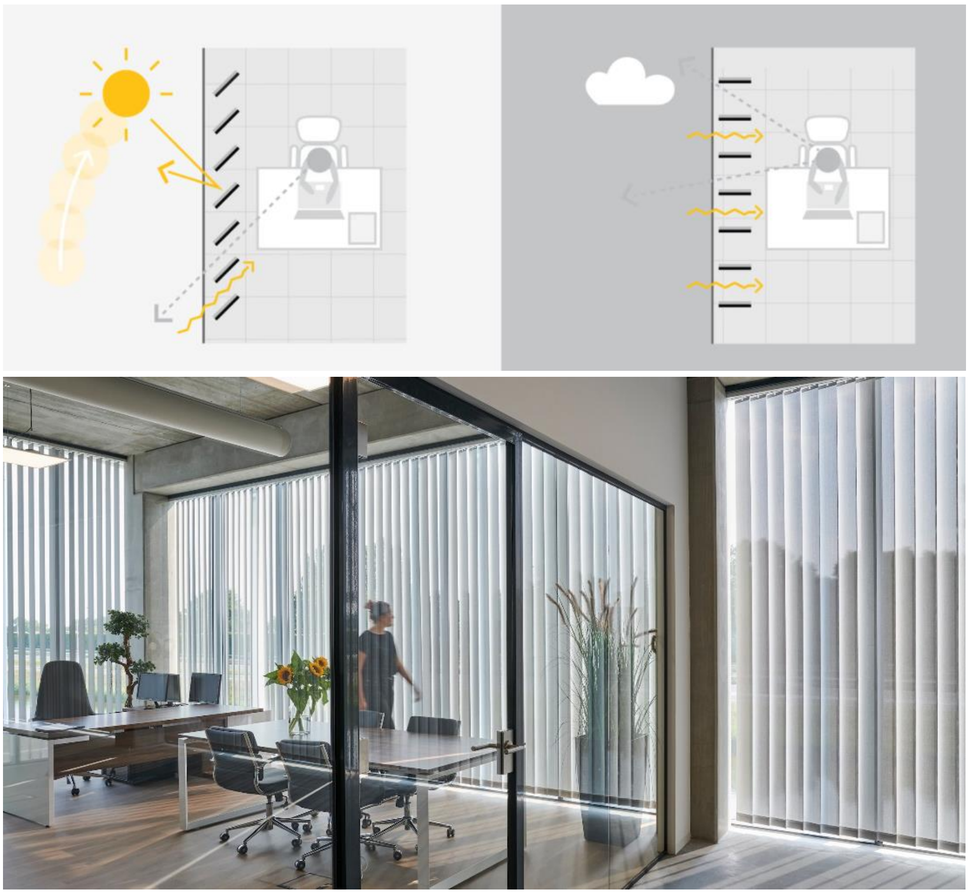

Figure 5: Kindow Verticals. Source: Kindowblinds.com

It must be noted that current market feedback from practitioners has showed greater interest towards roller blinds than verticals albeit overall better visual performance of Kindow verticals. Therefore, currently, Kindow's development strategy heavily leans towards Roller Blinds.

2.2 Client Objective

As mentioned before Kindow is at the end of its start-up phase and scaling up. It is currently struggling with limited market access and integration due to lack of performance information. Overcoming this barrier will allow it to successfully grow as a scale-up. Therefore, at the start of this collaboration, Kindow came in with two key expectations from this PDEng project. They are outlined below:

1. The added value of Kindow products needs to be quantified to be convincing. It needs to stand out from its competition which may have lower costs but are incomparable or have inferior performance. Additionally, performance quantification is also necessary for having realistic expectations from the product and not publicise something that Kindow cannot meet. As mentioned before, the building industry in general has a poor understanding of the business case of using advanced solar shading. The effect of shades on costs are twofold, energy efficiency as well as added value of improved comfort on the health and productivity of occupants. Although, the latter has a much higher financial impact, it is also an indirect effect and hard to substantiate. Although, there is the growing trend in health and well-being in buildings, Kindow wants to create a business case in which increased energy efficiency is considered. Therefore, it requires performance assessments and benchmarking done for its products to create convincing and tailored pitches to its clients.

2. In addition, Kindow's products are niche innovative products in the shading market. There is a constant struggle where Kindow needs to explain its clients the importance of considering the product in early stages of building design. Furthermore, in the public domain, there is not enough existing available information regarding such advanced systems. Especially not in combination with other façade elements such as advanced glazing and lighting systems. Having such information analysed and published to create strategic learning avenues can be a helpful tool to gain further credibility amongst building professionals and in market penetration. Attaining this second objective, would allow Kindow to create a market pull rather than the technology push it must go through during its sales process.

2.3 The background Context

Kindow is an innovative technology provider that is trying to transition from a niche towards mainstream products in the solar shading industry. In this section, we examine Kindow from a so-called Multi-Level Perspective (MLP). It is a means for explaining how technological transitions come about and facilitates a way to understand the interaction between actors, environment and innovation (Geels, 2002). As the name implies, MLP posits that transitions come about through interaction processes within and among three analytical levels: niches, socio-technical regimes and a socio-technical landscape (Bilali, 2019). It organizes innovative technologies (such as Kindow) in the lowest level: niches. These are the 'incubation rooms' from normal market forces to allow research and learning and creation of support networks. The well-set industries that are currently based on stabilized practices are generally called the Regime (Geels, 2002). In this project, we will be referring to 'creating comfortable thermal and lighting conditions in offices' as the Regime. This is because our niche technology actively affects indoor lighting conditions and solar heat gains entering a building. Therefore, all sectors responsible for Indoor lighting and solar heat gains in the built environment: 1. Façades & glazing 2. Shading systems 3. Indoor artificial lighting are considered as part of the transitioning socio-technical regime. There are standard (rule-set) practices in terms of façade component selection, stages within the design process when different façade components are considered and other compartmented processes embedded in the regime (Geels, 2002). Kindow, together with other innovative tech companies in the glazing and lighting industry, can slowly trigger a cascade of changes in these 'rules sets' to fundamentally change the regime over time. The landscape context, which involves changes in policies, awareness on sustainability and environmental problems etc. can also play a role in starting changes both within regime and niche systems.

The three sectors – glazing, shading and lighting together form the larger socio-technical system (regime) that deals with indoor lighting of the built environment and there is a plethora of promising technologies to deal with that. Currently, these three sectors function in a siloed manner, with building industry stakeholders considering them at different times during the building life cycle despite the fact that they are related to each other. Pressure from the landscape context as well as the advent of new innovations in each of these sectors are slowly prompting them to morph into one integrated system. For the purpose of this report, we are going to concentrate on the shading systems regime, because this is where the PDEng project innovation lies. The way solar shading systems are used to control solar gains entering the indoor spaces of the building lies the main challenge. The advanced intelligent control strategy used for shading systems is the niche (Figure 6: The multilevel perspective on Kindow's transition.Figure 6).

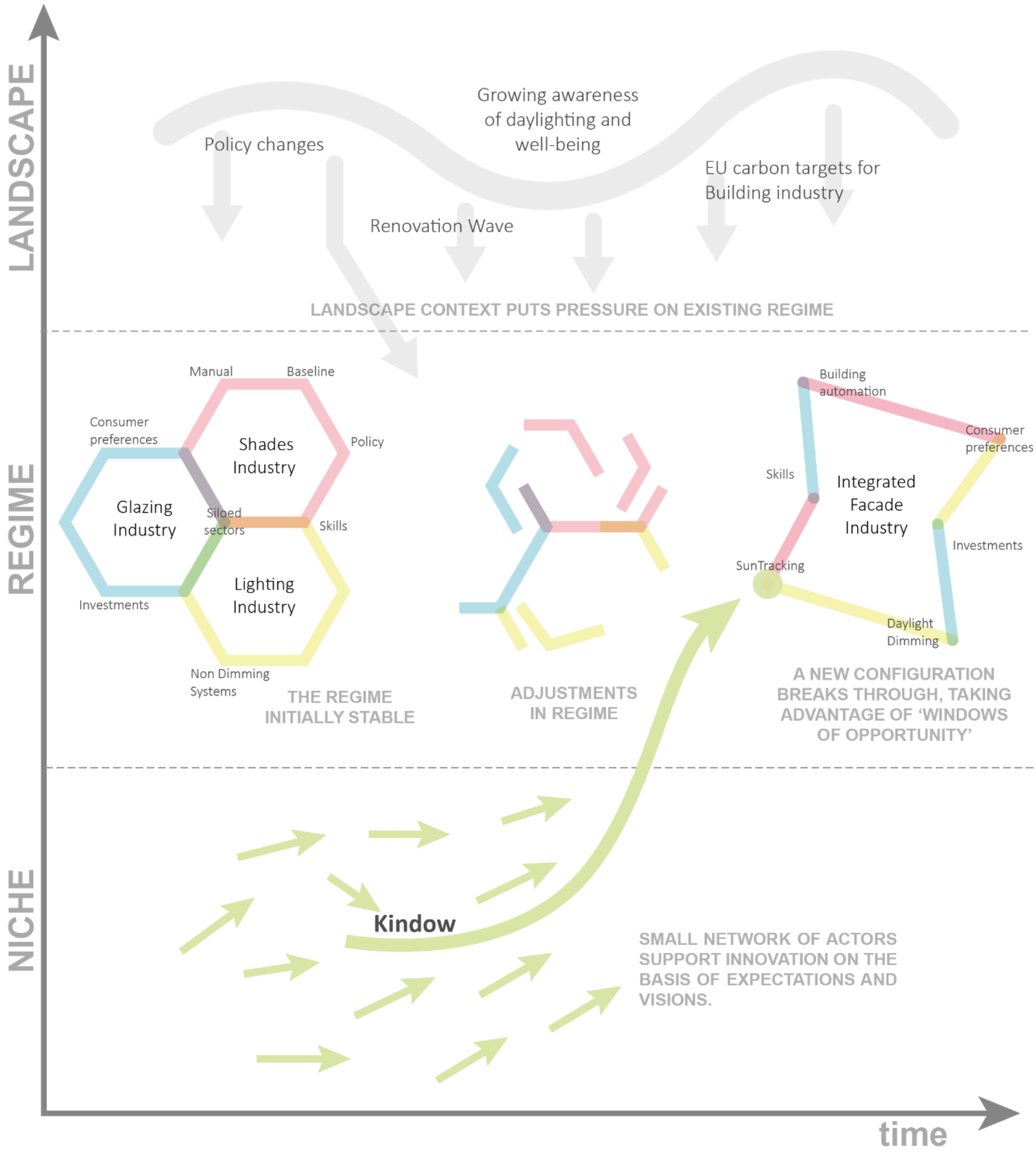

Figure 6: The multilevel perspective on Kindow's transition. Source: adapted from (EEA, 2017).

2.4 Current Barriers for Kindow

To understand the barriers and challenges faced by Kindow, it is important to know the market actors that affect Kindow's sales. As shown in Figure 7, the usual stakeholder or actors influencing sales of Kindow or any shading system in the market are in the operation or maintenance phase of a building lifecycle. This is because they are considered as an interior design product rather than an active component that affects the whole building performance and costs. In order to be considered during the design phase of the building lifecycle, Kindow actively engages with its 'target' stakeholders.

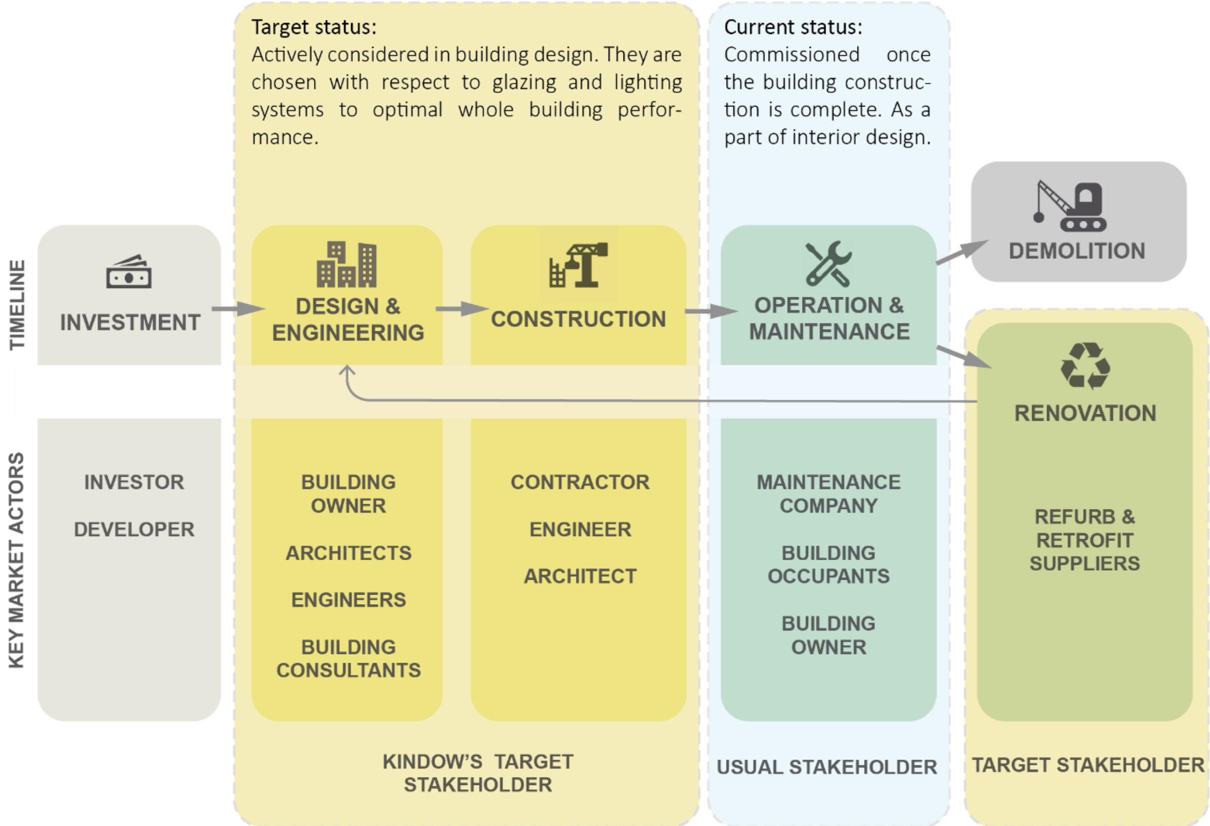

Figure 7: Market actors for Kindow. Stages at which shades are currently considered and where it needs to be considered.

During these interactions, Kindow faces the following barriers:

1. **Lack of performance assessment of advanced shading systems:** Although there are state-of-the-art dynamic shading systems available in the market, Kindow and similar products lack research in terms of benchmarking and quantifying the impact of its performance on Indoor Environmental Quality through extensive simulations of varying practical operating conditions. It is fundamentally impossible to consider the performance of shading systems individually without considering the effects of other façade parameters like WWR, glazing and lighting. This also means that component-level performance metrics that are used for conventional solar shading systems, such as solar heat gain coefficient (g-value) and visible light transmittance, are only of limited value for communicating the effect of advanced shading systems on building performance. This lack of knowledge regarding their operational performance and related risks prohibits Kindow from successfully selling its technology to its target stakeholders.

2. **Market Awareness:** All target actors look at shading systems (especially internal shades) in a very siloed manner. Something that is chosen in the end during the operation and maintenance phase. Architects and energy consultants spend considerable time designing for optimal WWR in combination with correct external façade elements and glazing properties to optimise daylighting and minimise glare (Peters et. al., 2018). Considering shading systems at this stage can remarkably change their design options by providing a leeway in choice of their façade components like glazing properties, lighting systems as well as sizing their heating and cooling systems. This lack of awareness is again fuelled by dearth of information regarding the performance of existing advanced shading systems. In addition, currently, most performance information regarding shades is based on anecdotal knowledge from practitioners' education or past experience. For example, one of the common aphorisms goes as follows: "external shades are always better than internal shades, as they keep the sun out". Architects and Consultants would install low g-value glazing and leave it to the building owners to install manual shades for glare prevention, disregarding the fact that automated shades can provide better daylighting conditions and reduce lighting consumption all while giving the opportunity to use a comparatively 'cheaper' glazing.

3. **Building regulations and energy certifications:** The solar shading industry has lobbied less successfully in comparison to insulation and glazing industries (Seguro, 2016). Therefore, installation of shading systems is not directly accounted for in most regulations and certifications, making it a less attractive option to investigate for building performance improvement. The scientific and the business case for shading is poorly understood by building professionals, institutions, consumers, and, to some extent, the industry itself.

4. **Other barriers:** Higher upfront costs, 'not so trendy' aesthetics of verticals, lack of easy design support tools that can accurately simulate these dynamic shades, mismatch between design budget and construction budget etc. are some of the other barriers Kindow faces (C. Maurer, 2018). These along with policy and regulatory barriers are out of scope for this PDEng project.

It can be summarized that the overarching issue that limits market penetration of advanced shading system technology is a lack of performance assessment information and the related awareness of shading systems as an active component that needs to be considered in early stages of façade design. Kindow and the shading industry as a whole needs to overcome this by gradually shifting the market's understanding on advanced shading systems.

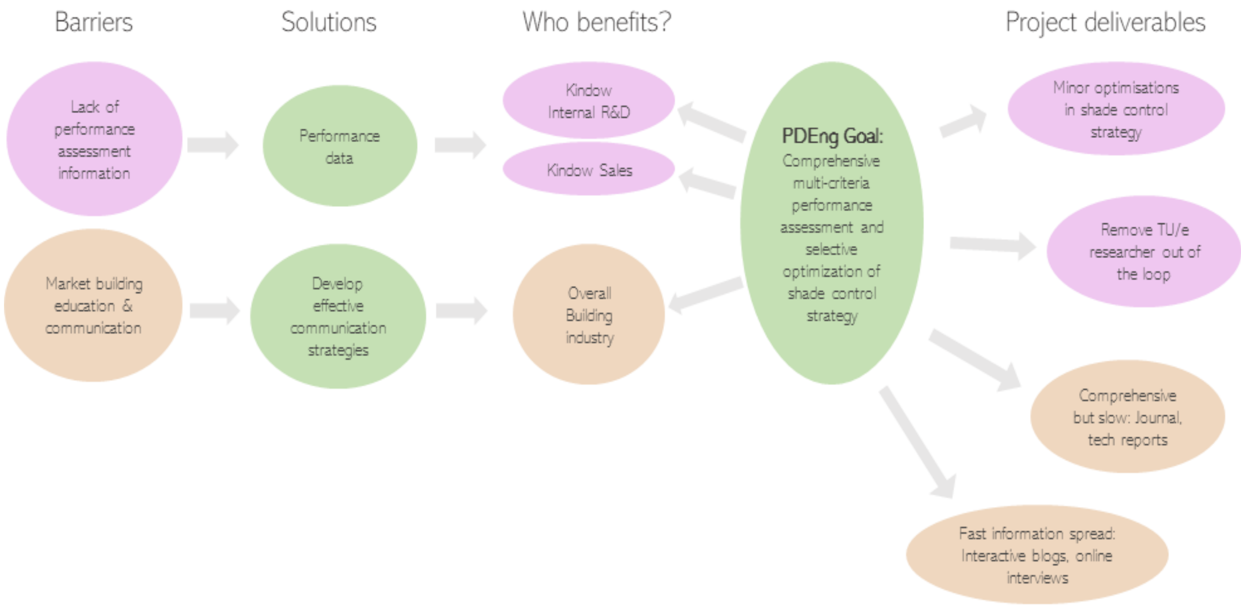

Figure 8:Summary of Kindow barriers, their solutions and how it translates into the PDEng project goal and deliverables

2.5 Scope of the project

After the initial company feedback and getting a deeper understanding of the complex ecosystem in which this innovation is embedded, it was clear that Kindow was working on two development directions:

1. Roller Blinds: This product line had stronger focus from Kindow. Its control strategy was more or less established and only required minor adjustments. Industry feedback indicated stronger inclinations for roller blinds, partly due to its aesthetics. Therefore, Kindow prioritized the comprehensive performance assessment of this product to assist their current client consultations as well as create material for market building education and communication. Kindow preferred that this PDEng project primarily work on this direction.

2. Verticals: This product required further strategic research and development of its control strategies and blind property selection. Due to lesser demands from the industry, its development was limited to smaller studies related to control strategy optimization. Comprehensive performance assessment for verticals were planned to be executed after Roller blinds (this part is out of scope for the PDEng project due to time limitations).

2.6 Overall project objective

The main objective of this project is to design strategies to stimulate better market penetration of Kindow products. To do so, performance evaluation and benchmarking of Kindow Shading systems in different scenarios of climate, orientation as well as with other controlled parameters like various glazing options, lighting systems and shade properties is carried out. The goal is to utilize this knowledge base to address the different problem areas identified within Kindow's socio-technical ecosystem. With help of these targeted solutions, the project aims to accelerate the process of market integration for Kindow.

2.7 Tools and resources for the project

The execution of this project was dependent on the use of multiple software tools and resources. The main goal of the project provided with an opportunity to extensively use building performance simulations for Kindow's complex shading systems. Commonly used modelling methods in Building Performance Simulation are not sufficient to provide performance assessment of products with such complex physical behaviour. Therefore, a custom co-simulation framework was developed at the BPS unit at TU/e (de Vries S. B., 2021). The co-simulation model (Figure 9) uses a link between four existing software environments where information is exchanged between the different models during simulation. EnergyPlus, a dynamic building simulation program developed on behalf of the U.S. Department of Energy, is used to simulate the thermal behaviour and energy performance of the building. The co-simulation model uses Radiance to describe the behaviour of daylight. Radiance is a collection of programs which uses 'backward raytracing' to make accurate predictions about daylight access, glare and the amount of artificial lighting required. Matlab, a mathematical programming environment, was used to implement the Kindow control algorithm. The information exchange within the co-simulation model is made possible by the software environment BCVTB.

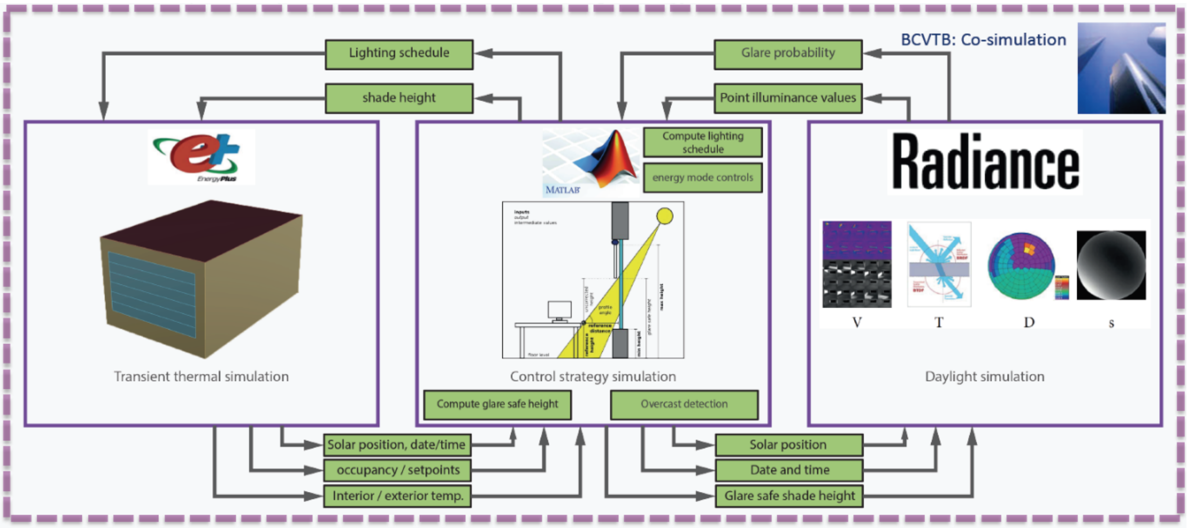

Figure 9: Co-simulation framework used in the project. (Source: Vries, 2018)

This project takes advantage of the initial framework that was specifically developed for a PhD project that is also carried out in collaboration with Kindow. However, the outputs of this framework were not readily usable for the purpose of creating reports to assist market adoption (or market awareness) and client interaction. In addition, it is a complicated framework that requires a certain amount of expertise rendering it an unfeasible option for current market actors to use. Therefore, it was also the purpose of this PDEng project to bridge the gap between academia and the industry by modifying the current framework to produce results that are readily usable for market actor's consumption.

Here, some of the Key Performance Indicators that will be used to explain results of simulation studies are outlined below:

Energy performance is assessed based on the energy demand for lighting, cooling and heating at room level in combination with an estimate of the primary energy consumption based on a number of system efficiency assumptions. The energy demand at room level provides an insight into the savings potential in general. The following reference figures have been used for this purpose. (Beck, 2010); .

$$E_{Prim} = \frac{E_{Light}}{\eta_e} + \frac{E_{Cool}}{\eta_e \eta_c COP} + \frac{E_{Heat}}{\eta_h} \qquad with: \eta_e = 0.39, \eta_c = 0.7, COP = 3, \eta_{h=} 0.95 \tag{2}$$

In order to quantify the degree of daylight access, this project will use daylight autonomy (DA) and spatial daylight autonomy (sDA). Daylight autonomy can be interpreted as the percentage of time that a measuring point receives 'sufficient' daylight. For this indicator, the abbreviation DA300lx is often used, where 300 stands for the number of lux that is set as a limit value. Spatial daylight autonomy enables us to express daylight access to a room as a whole in one number. It is defined as the percentage of the floor area with a daylight autonomy higher than fifty percent. Spatial daylight autonomy can be interpreted as the fraction of the floor area that receives sufficient daylight most of the time (Reinhart, Mardaljevic, and Rogers 2006). For this indicator, the abbreviation sDA 300/50 is often used, where 300 stands for the limit value in lux and 50 for the required exceeding percentage of the usage time.

In this report, 'daylight glare probability simplified' (DGPs) is used as an indicator to assess the risk of glare (Wienold, 2009). Although much is still unknown in the field of glare perception and assessment, it is certain that glare is associated with high luminance differences in the field of view, with the total luminance at eye level, as well as with the position of glare sources in relation to the focus area of the eye task. The DGPs indicator is primarily based on vertical illuminance but neglects the influence of peak glare sources. In this report, a DGPs limit of 0.40 has been considered for occupied hours when the glare is weaker than 'disturbing'. And the DGPs values are considered at the two sensor points as shown in figure 10, one has a viewing angle of 45 degrees and the other at 0 degrees meaning it is directly facing the wall.

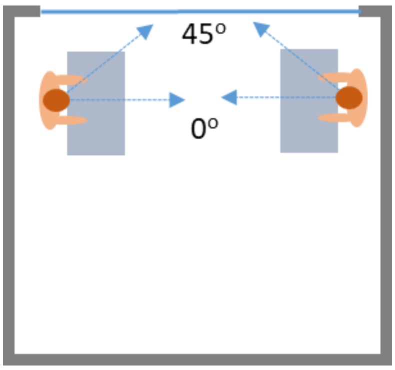

Figure 10:Positioning of the sensor point and the viewing angles considered for DGP calculations

3. Design Requirements

It is clear why Kindow faces these obstacles and what it needs from this PDEng project to help solve this. There are two major requirements from Kindow that can be summarised as follows:

1. Create performance results for advanced shading systems that can be used to significantly boost Kindow's business case towards its clients.

2. Address the lack of performance information about advanced shade systems in the building industry through creation of strategic learning avenues, such that it creates a market pull for Kindow products.

The design of the solution for these two major requirements were categorized into three main solution areas:

3.1 Product performance analysis and strategic shade control optimization

The first solution area (table1) was carried out in the first phase of the project. It helped understand Kindow's products better and facilitated the process of designing the requirements for the next two solution areas. Implementation of these requirements is elaborated in section 4.1.

Table 1: Requirements for Product performance analysis and strategic shade control optimization.

1.	Evaluate product performance under a strategic set of conditions.
2.	Set those conditions such that it addresses the commonly requested information by the market actors.
3.	These conditions should include environmental scenarios (e.g., location, orientation) as well as other parameters that can be manipulated at the design phase of a building (e.g., glazing properties, fabric properties etc.).
4.	The knowledge obtained should be used as feedback to optimize product performance.
5.	It should aid the design and modification of requirements for other solution areas.

3.2. Extensive performance analysis and benchmarking to aid sales process

This solution area was essentially designed and executed shortly after beginning the third solution area – educating the market (section 4.3).

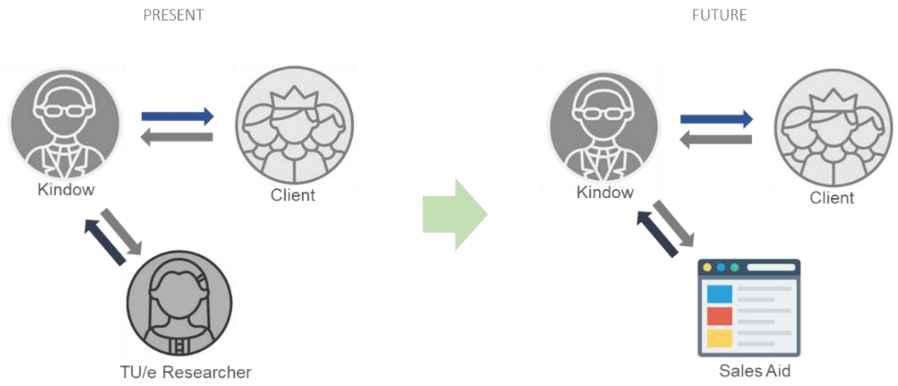

Figure 11: TU/e researcher replaced by sales aid tool in future client interactions.

The main idea was to create a solution that would utilize the simulation framework but eliminate the need of a TU/e researcher for every performance assessment for Kindow's future client consultations (figure 11). Table 2 outlines the requirements for this solution area, its implementation is elaborated in section 4.2.

Table 2: Requirements for Extensive performance analysis and benchmarking to aid sales process

1.	After finalization of the control strategies, extensive performance analysis needs to be executed with an extended set of conditions.
2.	These set of conditions should represent current trends in the industry.
3.	A generic example of Kindow's existing competitors are required to be analyzed under the same set of conditions for comparison.
4.	The results from all the simulations should be reliable. It also needs to be compiled in a database.
5.	The database will be for internal use only and should be based on Microsoft Excel.
6.	The database needs to have a fairly easy interface so that the user can quickly find the results it needs.
7.	The results in the database should be represented through simple Key Performance Indicators that can be easily translated to monetary terms. If not monetarily quantifiable, it should be strongly indicative of Kindow's added value to its clients.
8.	When input conditions are chosen through the database interface, the output should also include comparative analysis that Kindow can easily use in their client interactions.
9.	All detailed information related to case simulations that are not included in the database should be accessible to Kindow.
10.	The database should be easy to upgrade with new simulation cases if needed in future.

3.3 Market building education and communication

The solution area requirements of this section were outlined right after section 3.1 was implemented. And it got updated and progressed simultaneously with section 3.2. The overall aim of this solution area was to analyse all data carried out in multiple simulation studies in section 3.1 and 3.2 and design way to create learning avenues for Kindow's market actors. Implementation of these requirements is elaborated in section 4.3.

1.	With the information accumulated from the extensive performance assessment of Kindow products, it needs to be analysed for overall trends.
2.	Once clear conclusions and trends have been drawn from the data, it needs to be published in different formats to maximise reach to different market actors that could affect Kindows sales as well as the Advanced shading systems segment itself as a whole.
3.	One channel of information spread needs to be validated by the scientific community to add credibility to Kindow. This approach is slow but comprehensive.
4.	Another method is to interactively engage industry professionals through blogs or articles. It can include dynamic data visualization for ease of consumption online.
5.	Another knowledge dissemination method should be directed towards students who are the future professionals in the building industry.
6.	It should be able to generate enough interest in social media platforms to bring in more online traffic to Kindow and generate an overall awareness on Shade performance.
7.	Create enough content so that it can be used for industry interviews and magazine articles for quicker consumption and impact.

4. Implementation

In this section, the design solutions that were proposed in response to the requirements outlined in the previous chapter are elaborated.

4.1. Control Optimization feedback

The overarching goal of this solution was to understand how Kindow products perform under a specific set of scenarios and if there is a strategic need for improvement in their control strategies. This exercise would result in the selection of the updated control strategy for use in the upcoming solution deliverables (section 4.2 and 4.3). The studies carried out in this section would also provide insights if there are any knowledge gaps that needs to be explored.

The current construction industry is seeing a plethora of state-of-the-art dynamic shading systems, but the problem is these shading systems lack research in terms of benchmarking and quantifying the impact of their performance on Indoor Environmental Quality. For Kindow, the problem gets more complicated. Due to its advanced sun tracking technology, its performance is very case specific. Relationships between its material properties and control strategies are not linearly connected to energy costs and comfort improvements. It is impossible to extrapolate the findings of one scenario to a different scenario application. Almost all the current R&D work for Kindow at TU/e has been done considering a south-facing office space in Amsterdam, the Netherlands. It was unsure if the current concept would also perform well for other applications (climate, orientation, building type). It was important to understand if the current approach would be flexible enough to accommodate the needs of different situations or if Kindow would need to diversify their portfolio of control strategies to achieve the same.

Therefore, to begin with the analysis, three different locations in different climate zones were chosen: Amsterdam, Rome and Stockholm. Each location for both south and the west orientation. The roller blinds were simulated with the following control strategies (**Error! Reference source not found.**) and c ompared. The reasoning behind the sensor value selection for the following strategies is based on the studies conducted by de Vries (2019).

1. **The Baseline control strategy:** The roller blind is controlled using an outdoor global vertical irradiance sensor where the shade is either fully raised or lowered in response to a threshold of 200 W/m^2 (Beck et al. 2010; de Vries, 2019)

2. **The Kindow strategy:** This strategy seeks to balance the admission of daylight and views while trying to limit daylight glare discomfort. To achieve this, the roller shade movement is based on sun tracking and a combination of other senses such as high light and low light conditions to control shade movement. To analyse which combination of sensing works best, the following sub control strategies were examined.

    a. ***Only Sun tracking***: The roller blind is controlled in relation to the sun's position to block direct sunlight from hitting an occupant's desk in an office space using the relation shown in Eq.1. The edge of an occupant's desk is assumed to be at 75 cm height and positioned 75 cm from the façade. If the sun is not in direct view of the façade, the shade is fully raised (de Vries S. B., 2019).

    $$\frac{wpd}{\cos\gamma} \times tan\alpha + wph = sh \qquad (1)$$

    wpd: distance between workplane and façade, wph: height of workplane, γ: solar azimuth (west from south convention), α: solar altitude.

    b. ***Sun tracking + low light condition sensing***: It tracks the sun as well as uses an indoor vertical illuminance sensor at the window to detect for cloudy sky conditions. If the Illuminance levels are below 6400lx, it considers the outdoor sky condition to be low light and the shades are fully raised.

    c. ***Sun tracking + high light condition sensing:*** It tracks the sun as well as uses an vertical illuminance sensor at the window to detect for clear bright sky conditions. If the Illuminance levels are higher than 12300lx, it considers the outdoor sky condition to be too bright and susceptible to cause glare. Therefore, the shades light and the shades are lowered to 1.2m which is approximately the eye level of the occupant (de Vries S. B., 2019).

    d. ***Sun tracking + high light + low light condition sensing:*** This control strategy combines all the above-mentioned outdoor sky sensing. This is the most comprehensive control strategy option provided by Kindow.

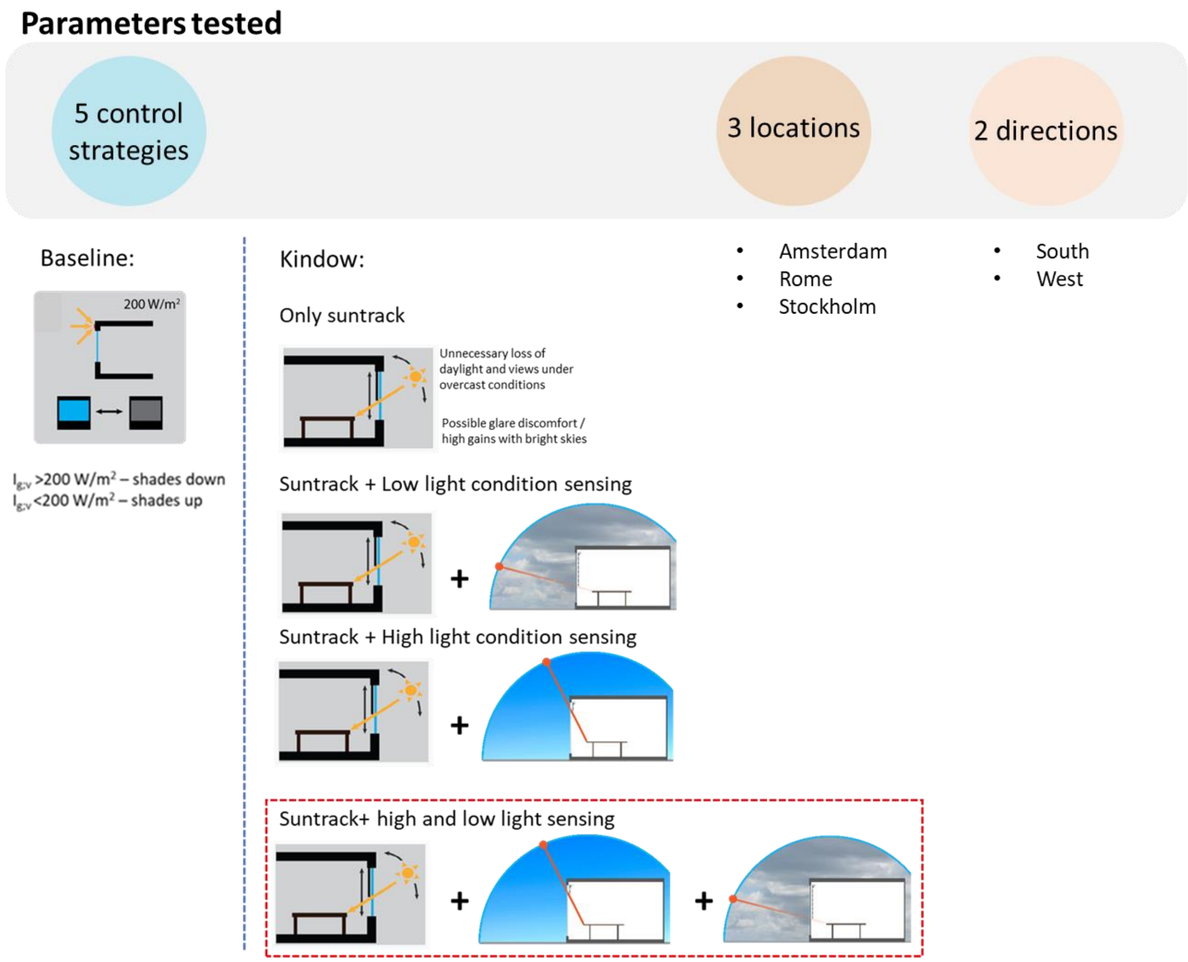

Figure 12: Different shade control strategies tested. Input parameters chosen for the study. Adapted from de Vries,2020

A total of 12 cases were simulated as shown in Figure 12. A reference office with interior dimensions of 4.5m x 6m x 3m was chosen unobstructed by any urban context. An Argon filled double glazed window with LowE coating was considered with an 80% window to wall ratio. The key results of the study (fig 12) are summarized as follows:

1. Out of the four Kindow Control strategy tested, 'Suntrack+lowlight' had the lowest total (heating+cooling+lighting) primary energy consumption closely followed by 'Suntrack+highlight+lowlight' strategy.
2. In terms of visual performance, 'Suntrack+highlight+lowlight' performs the best in terms of glare and views. It had 50% lower DGPs values than 'Suntrack+lowlight' strategy for both 45- and 0-degree viewing angles.
3. These results were consistent for all locations and orientations. Therefore, it was concluded that the 'Suntracking + low lighting and highlight sensing' strategy had the best balance between primary energy consumption and visual comfort.
4. This Shade strategy was then further optimised to reduce glare for façade orientations other than south. This updated shade strategy was then finalised for future use in all simulation studies for the project. For more details regarding this optimisation process, please refer to appendix 1.

Now that the Kindow Control strategy was finalised, the next simulation study was done to benchmark the Kindow control strategy with industry standard automated shades which we are referring to in this report as the Baseline strategy. It was again carried out for differing scenarios like orientation and location and two main conclusions were drawn about their performance:

1. There was an overall reduction in heating and lighting demand when the control strategy was changed from Baseline to Kindow. Figure 13 illustrates the annual energy demand for baseline and Kindow strategies. The red (heating), blue (cooling) and yellow (lighting) dot represents percentage difference in energy demand when the baseline (Bsln) strategy is swapped with Kindow (Kndw) control strategy. The major benefits of using Kindow control strategy come from the reductions in lighting energy demand (57% - 5.8%). Due to system efficiencies, reduction in lighting demand is proportionally more impactful than heating and cooling on total primary energy consumption. As Kindow allows the blinds to stay more “open” while trying to provide better daylight access, it reduces the requirement of artificial lighting.

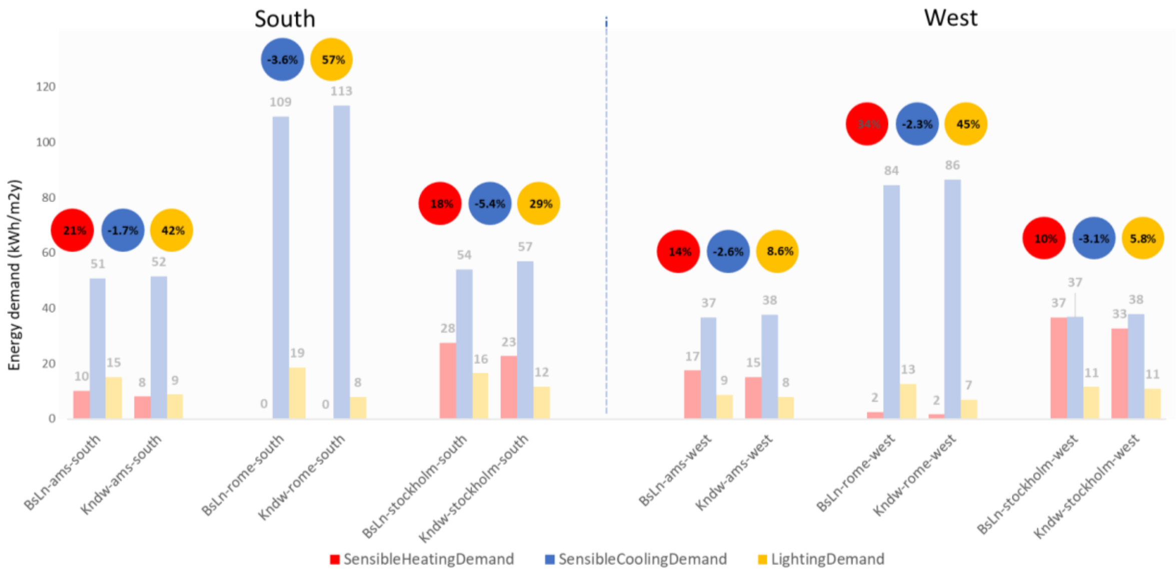

Bsln = Baseline, the blinds are completely up/down, sensor used façade irradiance.
Kndw = Kindow strategy with sun-tracking and with highlight and low light condition activated.

Figure 13: Energy Performance evaluation of Kindow shades against baseline shades for different scenarios.

2. There was also significant reduction in glare values from baseline to Kindow. It ranges from 30 – 9%, with highest reductions noted for Stockholm, where due to its high latitude, the sun is always much lower and in view of the occupant than other locations. Additionally, the reductions were overall higher for south than west orientation (Figure 14). Again, we can see the added value of dynamic sun tracking as it effectively reduces visual discomfort while providing views and daylight access.

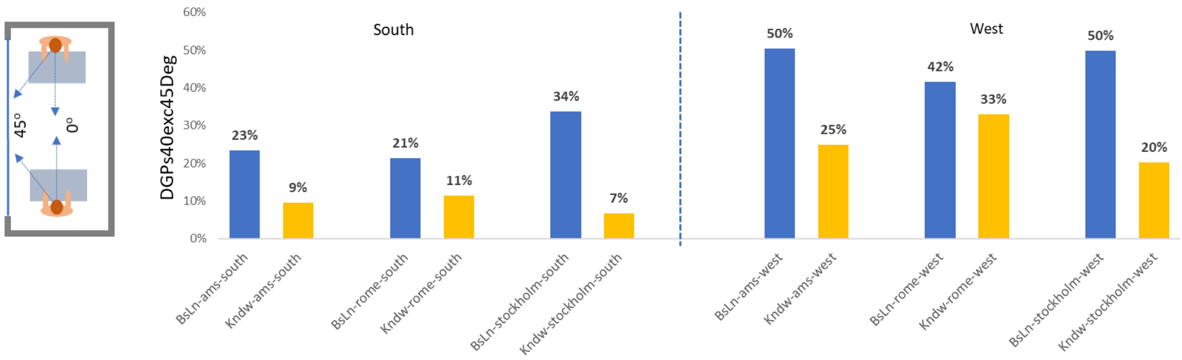

Bsln = Baseline, the blinds are completely up/down, sensor used façade irradiance.
Kndw = Kindow strategy with sun-tracking and with highlight and low light condition activated.

Figure 14: Visual Performance evaluation of Kindow shades against baseline shades for different scenarios.

After this step, it was realized that there were other questions/aspects to these studies that needed further exploration. For example, the concept of shading as an active component of an integrated façade system. The next study was therefore, set to test these shades in comparison to different glazing, shading and lighting properties and to assess how they influence each other. This study facilitated the development of other project deliverables for market building education and awareness (Section 4.3).

Throughout this process, the co-simulation framework was also modified to automate the whole process of input parameter selection and file pre-processing before the cases can be run in multiple batch files.

Kindow Verticals:

Another case study was done to evaluate different control strategies for verticals. Initially (before the start of the PDEng project) only two control strategies had been explored. They are:

1. Perpendicular strategy: In this strategy, the vertical blinds are always perpendicular to the incident sun rays (figure 15). They tend to be more "open" when the sun angle is low (e.g. mornings and sunset times).
2. Minimum cut-off strategy: The alternate edge of two consecutive vertical blinds are aligned with the incident sun ray (figure15). In general, it is more "open" when the sun angle is large (e.g around noon).

Now for this part of the study, nine additional control strategy options including the perpendicular and minimum cut off strategy were explored and benchmarked. For simplicity, only the two important ones will be outlined. They are :

3. Most Open: This is the combination of perpendicular and minimum cut-off strategy to create a new control that provides maximum view to the outdoors and daylight access while blocking glare. This strategy uses perpendicular strategy during low sun angles and Minimum cut-off strategy during high sun angles (figure 15).
4. Retract: This is a combination of most open and retract, where the vertical blinds stay retracted util the illuminance values exceed 6000lux (below this number there are no chances of glare to the occupant). Then it expands and does sun tracking using the most open strategy for the

entire day. When the occupant leaves, the blinds close and retracts again early morning at 6:00 hrs (figure 15).

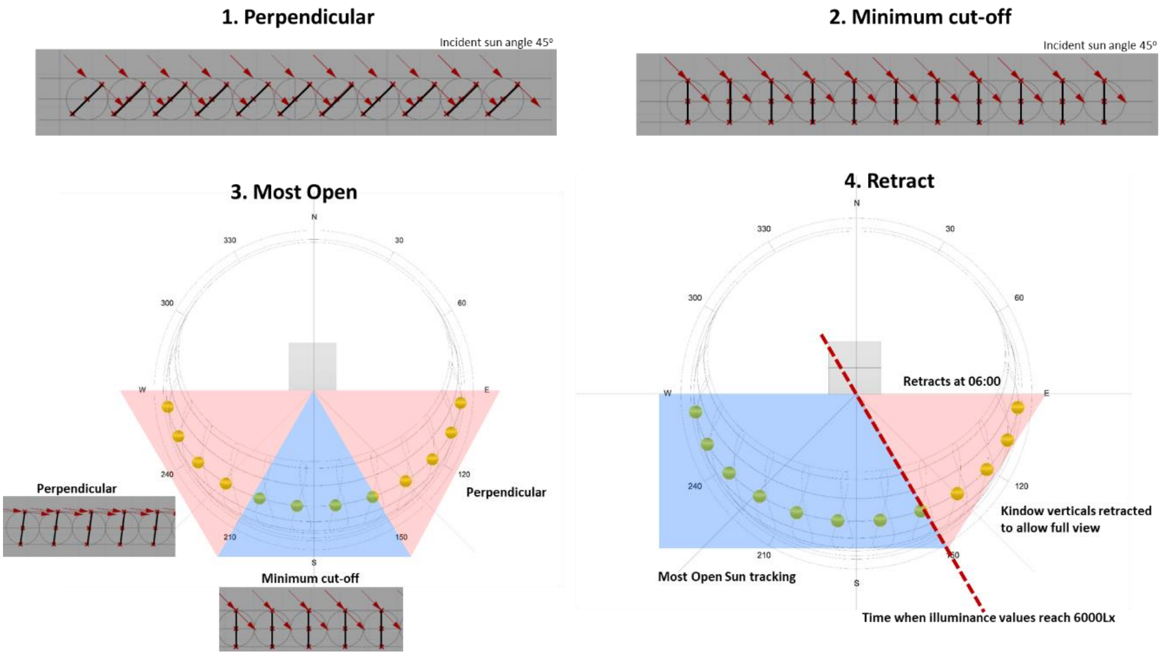

Figure 15: Four important vertical blind control strategy that were tested for optimisation feedback. The array of thick black lines is the cross-sectional view of the vertical blind fins.

The control strategies were only tested for south orientation and Amsterdam. The simulation uses the same co-simulation framework as mentioned in section 2.7. The key insights from the study illustrate that:

1. The 'retract' control strategy has the highest reduction in primary energy consumption (22%) when compared to Baseline roller blinds.
2. Moreover, the 'retract' strategy had the highest spatial daylight autonomy (89%) out of the 4 strategies mentioned and compared to the baseline, it also has a 4% reduction in DGPs value for a 0-degree viewing angle.
3. The study included a control strategy that was a variation of 'Retract' called 'retract_annoying'. This strategy would retract throughout the whole occupies period s whenever it would detect a low light condition. This allowed it to have the least primary energy consumption and the highest spatial daylight autonomy values. But in a realistic scenario, constant retraction and expansion of vertical blinds would be annoying for the occupant. Therefore, for the purpose of any further simulation studies, the retract only strategy was finalised to be considered.

Not only did this study help provide useful insights on the performance of different controls strategies but also suggested a direction for strategic implementation of some of the features explored for Kindow Vertical controls. For example, the actual application of retraction is not yet available in Kindow verticals and currently the company is working towards making it possible. Further details regarding that study can be found in appendix 2.

These shade control optimisation studies carried out for Kindow roller blinds and verticals allowed a better understanding of product performance in different scenarios. For Kindow roller blinds, it was found that the most comprehensive strategy allowed for best trade-offs in terms of the conflicting performance goals of reducing heat gains and glare while provide maximum daylight access indoors. For Verticals, different combinations were tested and a new optimised control strategy was developed. These studies also paved the path for the need to understand the implications of changing other input parameters that can be controlled by designers or practitioners at the design stage (e.g., glazing properties, shade fabric properties, lighting system properties etc). All these aspects are going to be analysed in the next sections.

4.2. Database for client interaction assistance.

Once the final shade control strategy was confirmed for roller blinds, the next phase was to create a knowledge base which Kindow can refer to depending on the unique needs of their clients. During the PDEng project, Kindow had to rely on TU/e to provide them with the performance information to create a customized value proposition for their clients. It was clear that they wanted to replace the TU/e researcher from their client consultation loop and the efficient way to do so was by creating a database that allows for comparing Kindow in combination with a representative variety of commonly used façade elements.

As mentioned in section 3.2, Kindow wanted an easy to use database in Excel that they can use to look -up reliable performance information about their roller blinds product under different scenarios and input parameter assumptions. One use case would be that a client comes to Kindow with some of its building information such as orientation, glazing property etc. Then Kindow looks up the nearest match in the database and compares it with different shade properties such as a manual shade or a baseline shade and Kindow. Once selected, the Excel database would produce performance results that can be readily used as input for their proposition to clients.

Inputs: To be able to provide accurate assessments to its future clientele, it was clear that multiple input parameters needed to be simulated to cover a wide variety of client requests that may come in. Figure 16 shows the different input parameters chosen to be simulated. Furthermore, 2-4 different options within these parameters were chosen that were in line with the current trends of what materials are getting used in the industry. These options were finalised after close consultation with Kindow based on their previous client consultation experience. A total of 1440 different cases were simulated.

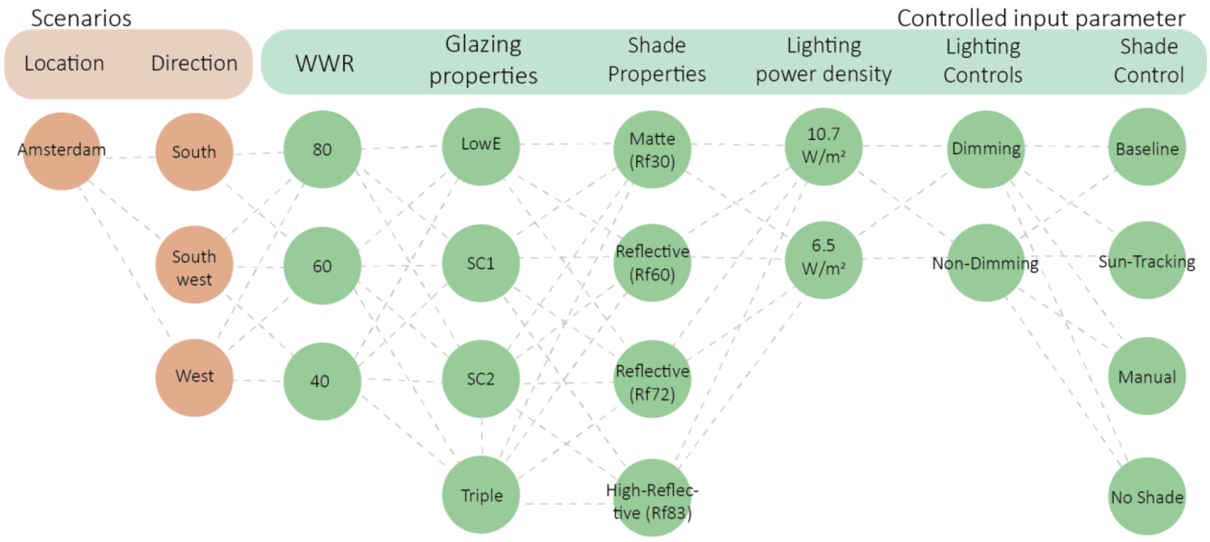

Figure 16: Final selection of input parameter options. All of these combinations provided for 1440 cases.

Each case roughly had a simulation time of 30 minutes, excluding the pre- and post-processing times for them. Therefore, we had to be careful with the addition of each option, as it would considerably increase the number of cases, and thus simulation time. To limit the computation time, some input choices were scoped out. For example, orientation was limited to South, Southwest and west, limited fabric options and only dimming lighting option for manual shade control strategy. Always quick simulation studies were done before limiting the options. Input parameter options like HVAC COP were calculated directly inside the Excel database. The database is setup in a way that Kindow has the option to choose any heating and cooling system efficiencies they want.

Tool setup: The same co-simulation framework as mentioned in section 2.7 was used for simulations. However, since it would be impossible to simulate all cases one by one, the framework was modified in order to automate the whole process. Although it was entirely possible to run all cases at one go, care was taken to break it up in batches, so the computer does not run out of memory.

The co-simulation framework was also updated to accomodate the Complex Fenestration method for modelling the glazing and blinds in EnergyPlus. This update in the framework was done in collaboration with the PhD student, who is also researching on Kindow products. This update was carried out for better accuracy of simulation results as well as for consistency between the verticals and roller blinds model.

Outputs/results: Kindow's main objective was to be able to utilize this performance data to create convincing value propositions for its clients. For example, by comparing Kindow with a baseline or manual shade strategy, the user can investigate the amount of savings a client can get in terms of energy and cost. The database also provides comparisons of load-duration curves to suggest smaller investment in cooling capacity, return on investment etc. Also, Kindow wanted to be able to substantiate the qualitative benefits of its products in terms of visual performance such as daylighting, view etc. (figure 17). The database also provides these visual comfort KPIs as results.

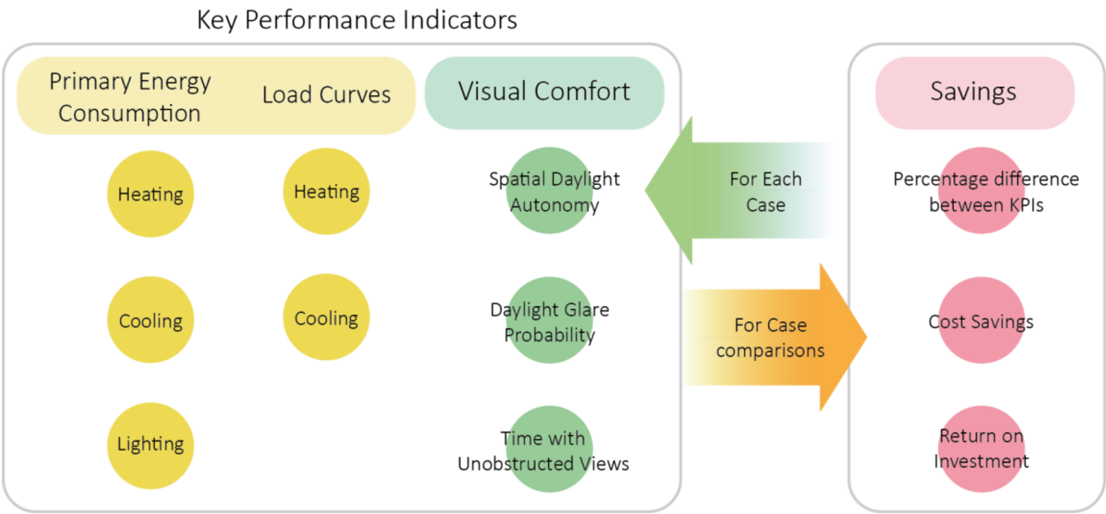

Figure 17: Outputs finalised for the Excel database.

The database was designed to be kept as simple as possible. If necessary, it can be seamlessly updated to extend the database with more options in future. Figure 18 shows a screenshot of the interface of the database. The left-hand side of the interface (outlined with a green dotted line) is where the user would select their input options and that will dynamically change all results that are mapped out on the right-hand side. For the output section which is denoted by 'results for the chosen cases'; first the full names of the cases are outlined followed by their percentage difference and bar chart comparisons of the energy and visual performance KPIs. Then comes the cooling and heating load curves. For the cooling load curves there is an option where the user can fill in the cooling system sizing and get the temperature exceedance hours and vice versa. This feature helps Kindow to quantify savings in terms of HVAC sizing and temperature exceedance hours. Finally, the last section shows cost savings and return on investment.

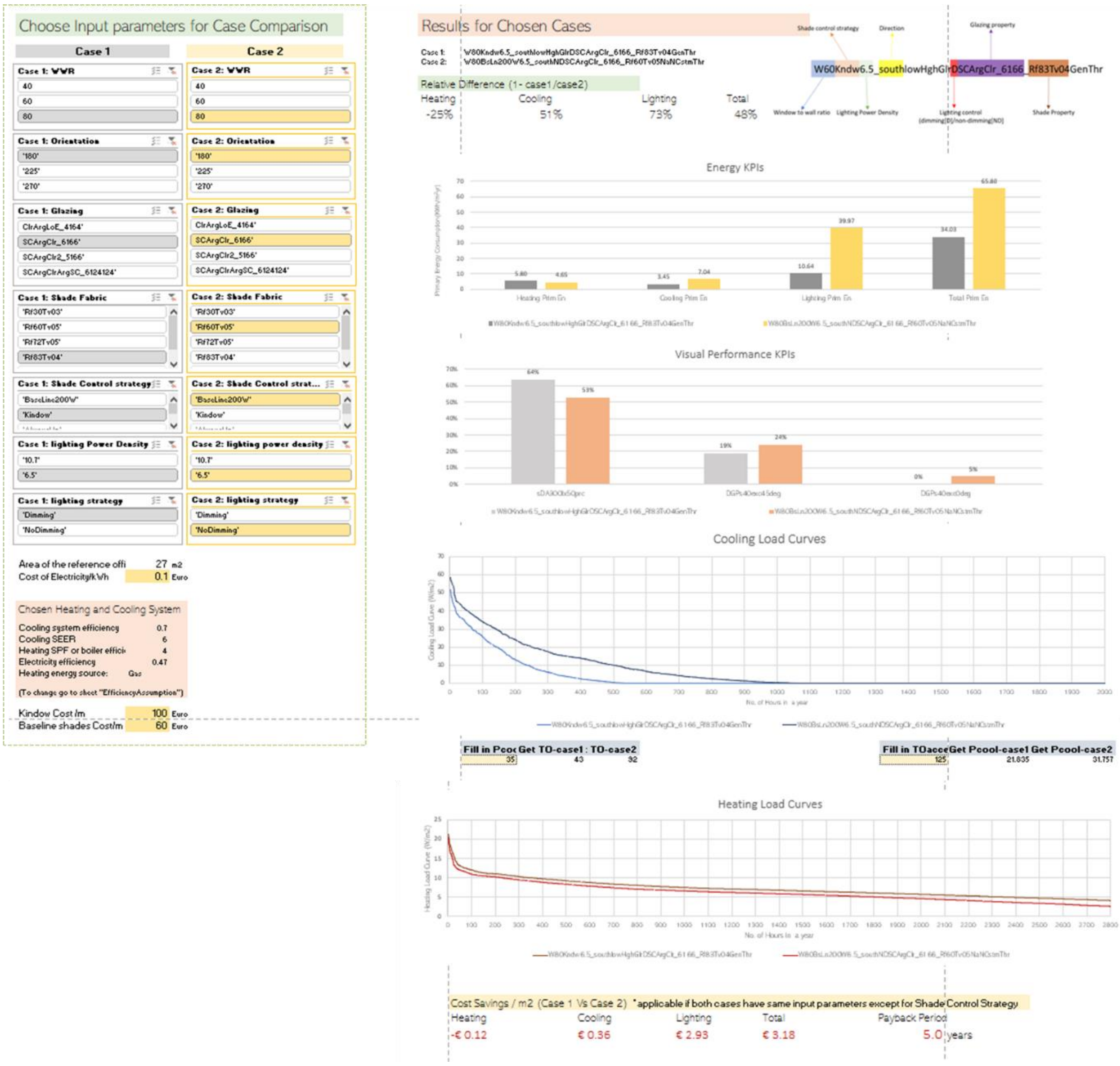

Figure 18: User Interface of the database

This video <click here> gives a brief overview of the interface of the database and a quick example to illustrate how to use it.

Key features of the database can be summarized as follows:

1. It has an easy to use and intuitive interface, keeping in mind that it is developed for an informed user within Kindow.
2. A clear and holistic performance assessment and quantification of Kindow's benefits is instantaneously available on the interface page. Further detailed information about chosen cases are available in separate worksheets in case the user wants to create their own graphs and outputs.
3. The data provided is consistent and comprehensive. It covers all relevant KPIs requested by Kindow in order to help with their business propositions.
4. The tool can also be used to suggest design options for the client during the concept design phase of a building. For example, proposing the use of alternative glazing or a different lighting

system and how such design decisions can bring greater benefits and savings than just solely implementing Kindow rollers.

There are certain points the user needs to keep in mind while using this tool:

1. Cost prices of glazing, lighting systems etc. are not considered. Therefore, to get reliable results on cost savings and return on investment KPIs, the cases chosen for comparison should only differ in terms of shade property (fabric type and control strategy). The user needs to do their own cost calculations if they want to compare changes in other controlled input parameters such as glazing, lighting systems etc.
2. All calculations are based on a test space of $27m^2$ floor area. Therefore, it will be unwise to extrapolate cost savings for any given dimension of office space.
3. The dashboard feature that allows choice of temperature exceedance hours and output sizing for cooling systems or vice versa are rather simplistic. Therefore, they should be only considered as suggestions. Again, keeping in mind, these are simulated for a small test space and further extrapolation of information may not be reliable.

Therefore, this database was created with enough input parameter options that Kindow can comfortably address most of its client's needs. All simulations results have been checked for consistency, and the database can conveniently replace the need for a TU/e researcher to carry out simulations for Kindow on a case by case basis.

4.3. Market building communication and education:

Kindow is an innovative technology provider that is trying to transition from a niche towards mainstream products in the solar shading industry. Kindow consistently needs to campaign towards it clients to explain the importance of considering the product in early stages of building design. There is not enough awareness in the market about the benefits of including smart shading systems in building facade design. Therefore, following measures were taken to stimulate the process of educating the market which include stakeholders such as architects, façade engineers, energy consultants etc.:

1. Use the simulation studies done during the PDEng project and analyse that data to come up with fresh insights regarding the performance benefits of using advanced shading systems like Kindow.
2. Translate these insights in specific formats to create learning avenues for Kindow's target stakeholders/actors.
    a. Comprehensive and detailed analysis of results and submitting to a peer reviewed scientific journal. This will provide Kindow with a scientific backing for its product performance. Online technical reports on Kindow website for quicker access to scientific information.
    b. Faster information spread through interactive blogposts that discuss key insights from the studies. Showcasing complex information though interactive graphs embedded in online blogs would provide quick access to relevant performance and design optimisation insights. Furthermore, it is engaging and transforms data into various visualisations which is otherwise not possible through traditional methods. It is more casual, quick and to the point and has a broader reach amongst practitioners.
    c. Through interviews and short articles in university magazines – In order to morph the current siloed regime to an integrated façade industry (figure 6) where current state

of the art technologies like Kindow become the main players, it is important to invest in creating awareness amongst students who would become next generation practitioners. Short articles in student magazines would allow graduates to already be aware of the latest insights on advanced shading products before they enter the construction industry.

These steps will contribute towards creating more awareness among practitioners in the building industry. Hopefully, over the years, this will facilitate a change in Kindow's customer journey. From being a one-on-one sales process, which requires duplicated efforts to gain customers to an off-the-shelf sales process where relevant stakeholders are already aware of the product benefits and directly approach Kindow to start the process of purchase.

When we apply concepts of strategic niche management (Schot & Geels, 2008) to propose stragies for scaling up Kindow's business, it can be seen that there is a lot of potential in nuturing the business through continued feedback from its market actors. Being able to provide the missing performance information and creating learning avenues for relevant actors are crucial to create a suitable environemnt for Kindow's scale up (figure 19).

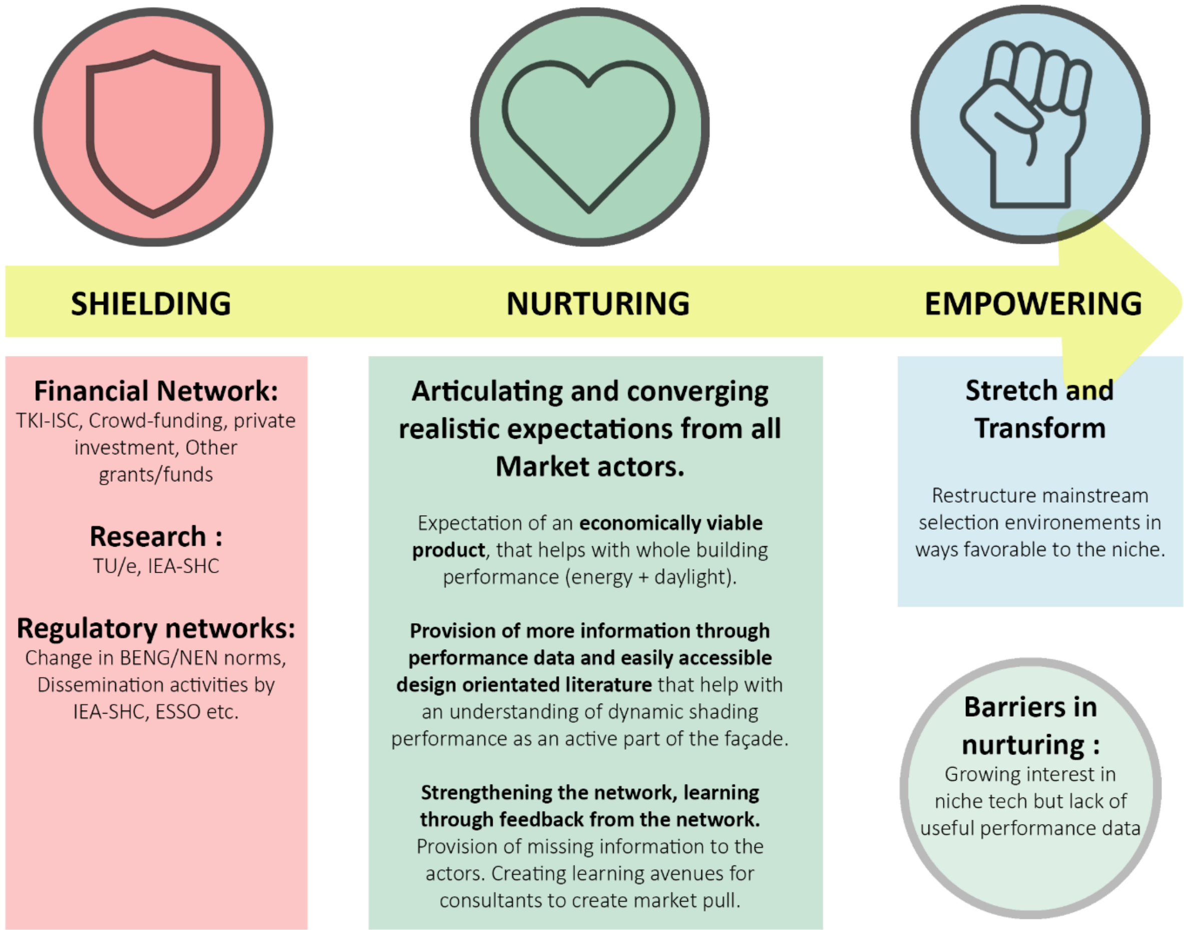

Figure 19: Strategic niche management showcasing the environment needed for company scale-up.

Therefore, there were two broad learning avenues that were implemented through this PDEng project:

4.3.1. Article and reports (Detailed and slow market assimilation)

<u>Online Report for Kindow:</u> During client interactions within Kindow's network, feedback is consistently received that internal shades are not as energy efficient in comparison to external shades. Kindow's market actors (such as architects, building consultants etc) have been operating with a prevailing idea that "only exterior shading is useful, because it can actually keep the sun out". This preconceived notion focuses on the component level (e.g. minimizing g-value of glazings) rather than the whole building level and undermines the potential value and impact of intelligent solar shading on occupant comfort and energy savings.

So, it was important to carry out another study to unpack this prevailing notion and test if it holds true. In the study, external shades were compared to automated shade control strategies such as the baseline (industry standard) and Kindow for a south facing test space with a 80% WWR in Amsterdam. The cases that were compared as follows:

- Case 1: External roller shades with reflective material properties.
- Case 2: External roller shades with non-reflective material properties.
- Case 3: Internal roller blinds with reflective material properties.
- Case 4: Internal roller blinds with non-reflective material properties.
- Case 5: Internal roller blinds with the Kindow control strategy.

The results (figure 20) show that careful combination of shade materials with reflective properties and the Kindow Rollerblind control strategy can lead to 6.5% energy savings compared to external shading and 20% against industry standard automated internal shading systems.

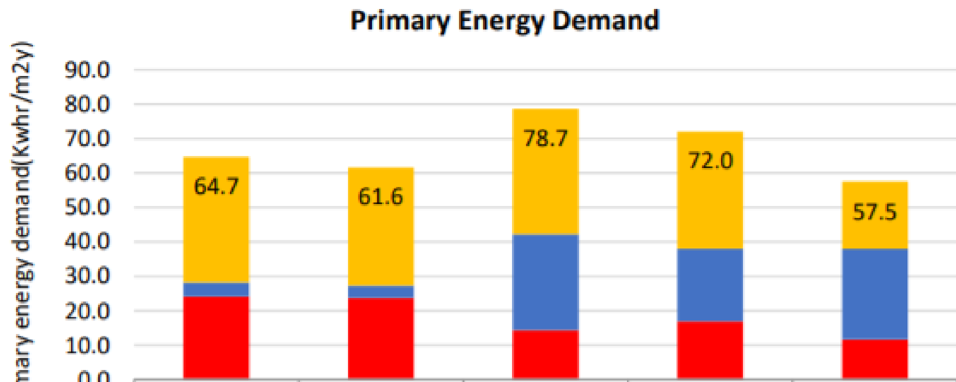

	Case 1 (ext_non-reflective)	Case 2 (ext_reflective)	Case 3 (int_non-reflective)	Case 4 (int_reflective)	Case 5 (int_reflective_Kindow)
LightingPrimEn	36.4	34.3	36.4	34.0	19.6
SensibleCoolingPrimEn	4.1	3.6	27.9	21.1	26.3
SensibleHeatingPrimEn	24.1	23.7	14.3	17.0	11.7

SensibleHeatingPrimEn SensibleCoolingPrimEn LightingPrimEn

Figure 20: Comparison of primary energy demand between External and internal shades.

This data provided clear indications that commonly held beliefs such as 'external shades are always better performing than interior shades' can be refuted with carefully chosen material properties and modern-day control technology. A detailed report of this study can be found on the Kindow Website (Click here) and in appendix 3.

Article for peer-reviewed scientific journal: In addition to this report, our initial studies on performance assessment and optimisation of shade control strategies (section 4.1), had already highlighted the need to further analyse the effect of shade properties (shade position, fabric type), lighting systems and glazing combinations. In other words, Kindow would benefit from such information and have it validated by the scientific field. This knowledge would act as a base for market awareness amongst academics and professionals alike. Although its rate of dissemination can be slow, this solution will increase Kindow's product performance credibility and facilitate the shift in current thinking towards advanced shades being an active component to façade design.

Studies were done to develop a better understanding of shading systems and were then written down in the form of a paper. It scrutinized conventional notions and illustrated the complex interdependencies of glazing, shading and lighting systems and how variation of these parameters under specific scenarios (location, orientation) can significantly alter the energy performance and visual comfort in buildings. The objective of this article is not to provide trends or guidelines for shade systems but to highlight the need for careful evaluation of each façade combination for best results. This study considered the following input parameter choices as shown in figure 21.

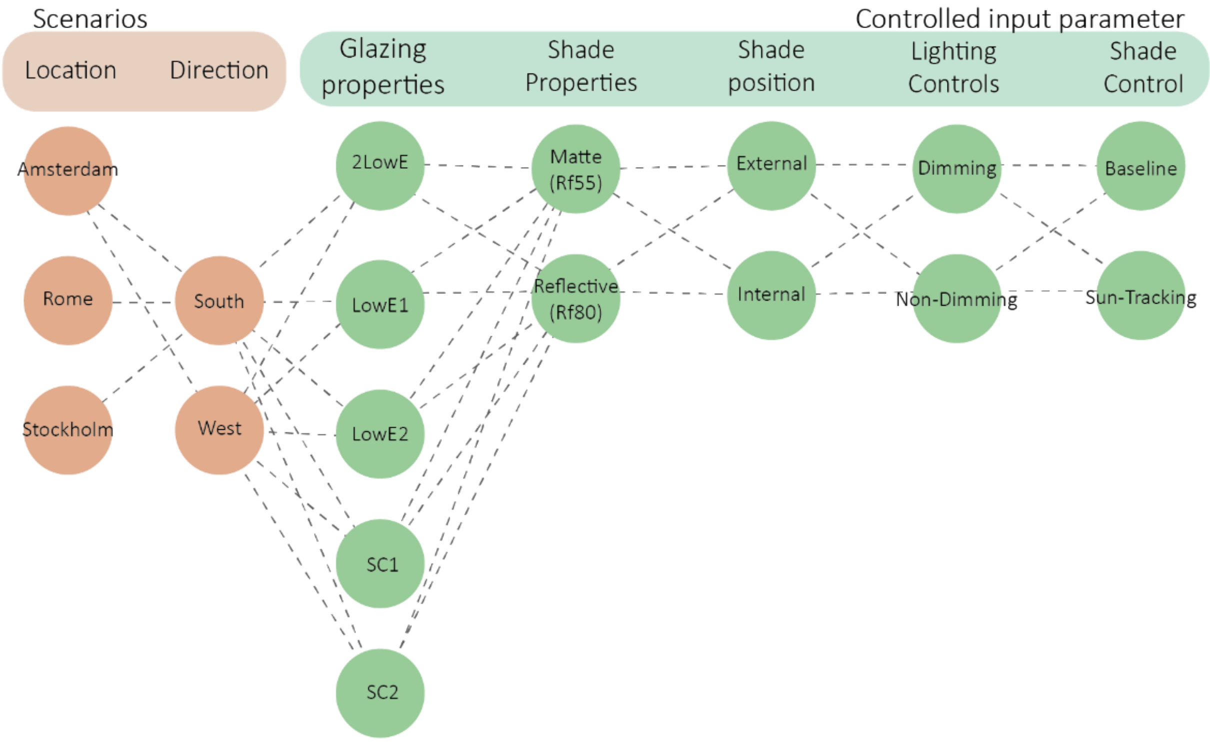

Figure 21: Input choices considered for the study.

The key conclusions from this study are:

1. Out of all the combinations of external shade cases, only 27% had lower primary energy consumption than an ideal internal shade-glazing and lighting system combination. Therefore, it can be postulated that a carefully chosen internal shade combination outperforms external shade combinations in most cases.
2. Exterior cases when combined with Sun tracking shade control outperforms all internal shade cases, making it a lucrative feature for future shading systems products.
3. An automated shading system in combination with dimming lighting controls optimises daylight harvesting in indoor spaces. As the lighting control strategy is changed from non-dimming to dimming type, primary energy consumption for lighting gets reduced by 32% up to 77%.
4. It is beneficial to choose reflective shading as it reduces overall cooling demand by a range of 10 - 22%.
5. In terms of visual performance, the sun-tracking control strategy showcases a marked improvement. There is an average relative increase of 49% in percentage time with unobstructed views and 41% increase in spatial daylight autonomy.

The manuscript is nearing completion, but is still undergoing final revisions at the time of writing this PDEng report. For full details about the draft manuscript, please refer to appendix 4.

4.3.2. Interactive Blogpost (Overall behavioral trends, quicker information spread)

Figure 22 shows a modified version of the lean business model to explain how and why an interactive blogpost that is consistently shared on professional social media platform can bolster Kindow's image and bring in more online traffic to its website.

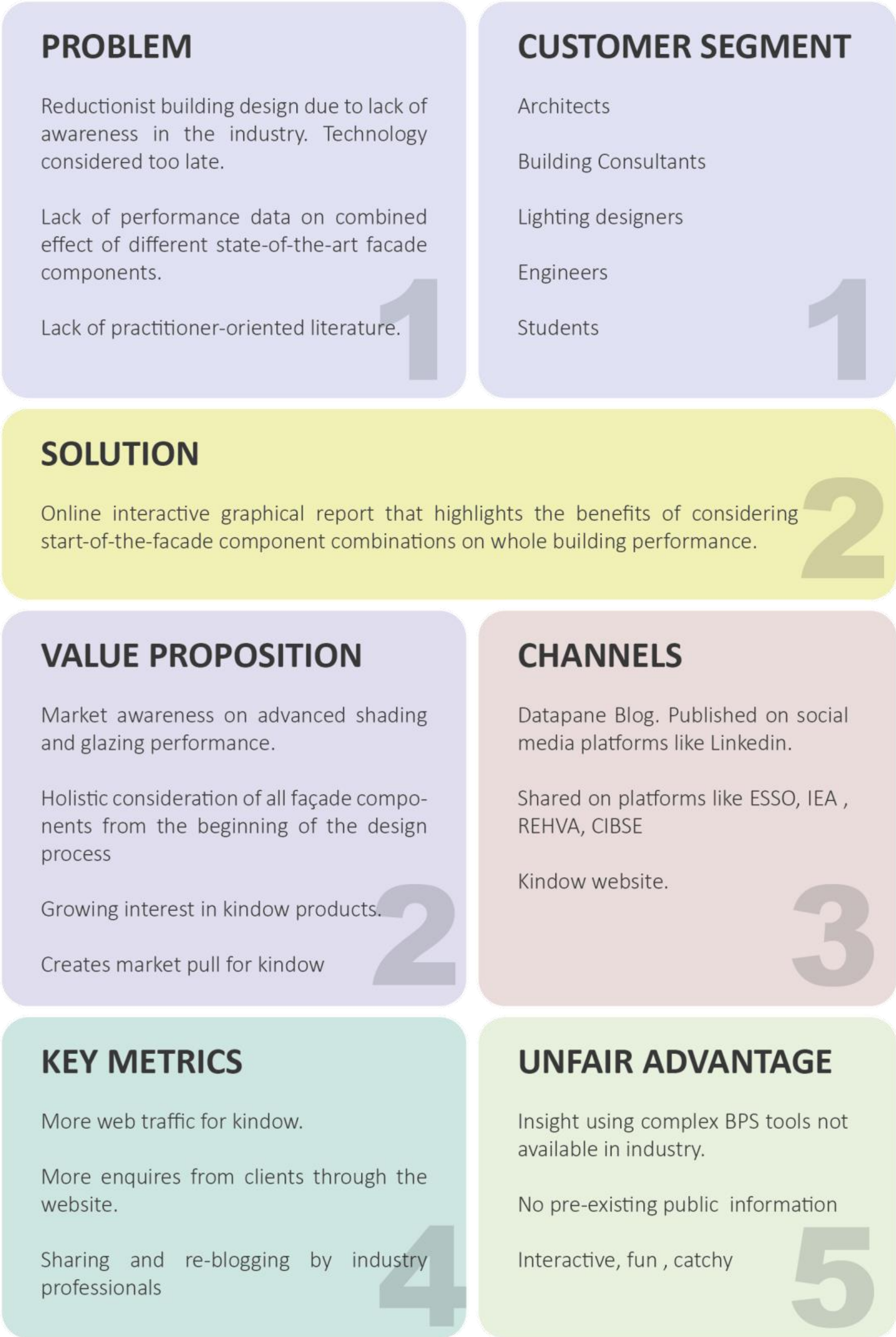

Figure 22: Lean Business Model canvas for online interactive blog idea for creating market awareness.

The large database created with 1440 cases is primarily intended to provide assistance with one-on-one client consultation. This large dataset was analysed and used to create graphs and relevant practitioner-oriented performance insights for the interactive blog. After data analysis, five main conclusions were postulated, drawing attention towards the benefits of considering appropriate combinations of façade systems (geometry + shading + glazing + lighting) at early stage design in order to maximise on cost and energy savings. This interactive blog attempts to repackage information from all the studies carried out in the PDEng project into practitioner-oriented online content. Interactive data visualization is attractive and grabs attention. c, which at times can be difficult to put down to specific in a text or a standard graph. It is quicker in exploring insights and facilitates easier assimilation of the study results.

The interactive blog is currently planned to be hosted as a blog on datapane.com, which is a python framework for building data science documents. According to the author's knowledge, this was one of the only free platforms that would allow seamless hosting of interactive plots without losing out on quality. The report published in this website can be easily shared through social media platforms like Linkedin. This way would ensure quicker information spread and aims to bring in more internet traffic to Kindow Website.

Follow this link to check out the whole Medium blog draft (figure 23).

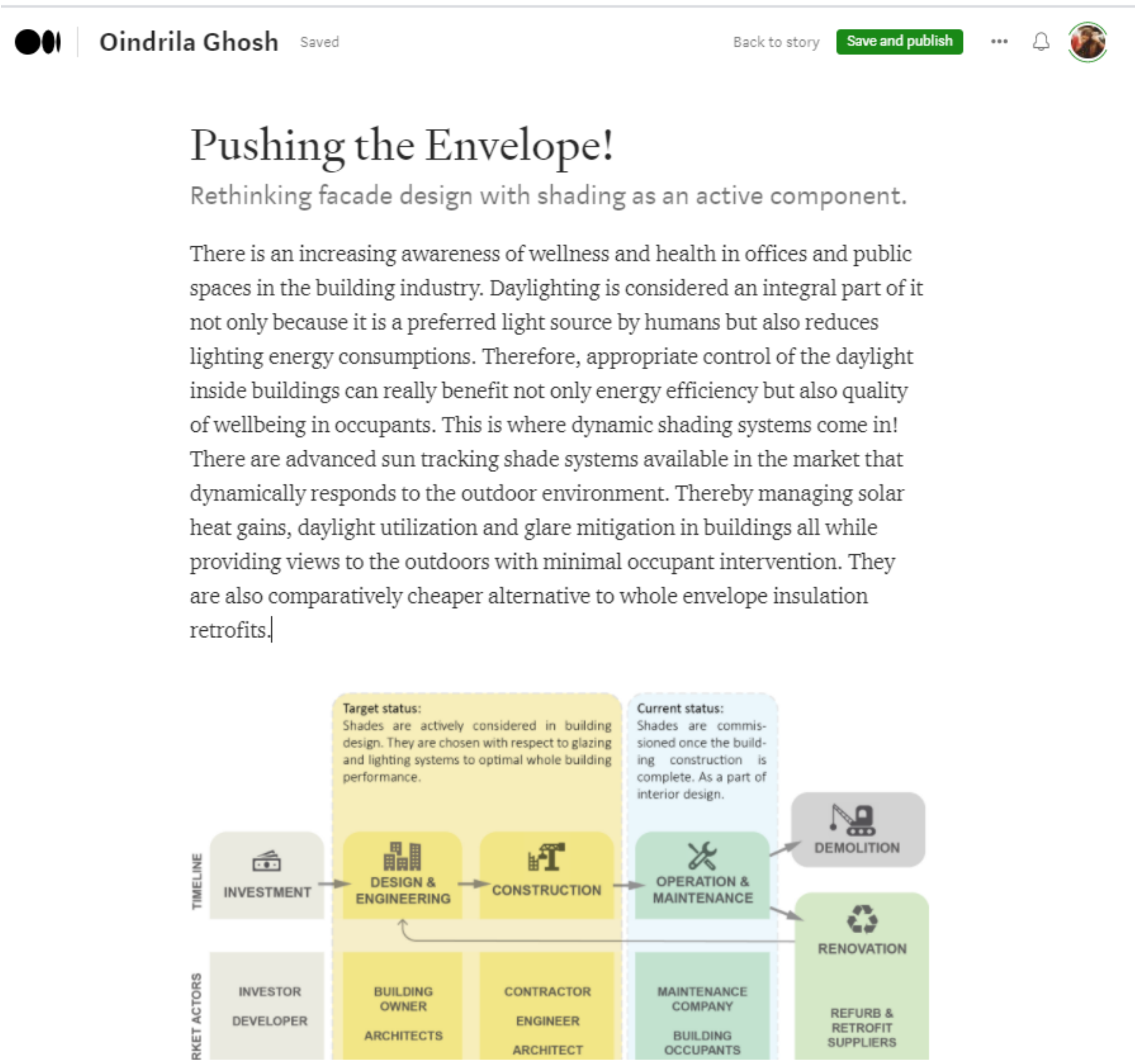
Oindrila Ghosh Saved Back to story Save and publish

Pushing the Envelope!

Rethinking facade design with shading as an active component.

There is an increasing awareness of wellness and health in offices and public spaces in the building industry. Daylighting is considered an integral part of it not only because it is a preferred light source by humans but also reduces lighting energy consumptions. Therefore, appropriate control of the daylight inside buildings can really benefit not only energy efficiency but also quality of wellbeing in occupants. This is where dynamic shading systems come in! There are advanced sun tracking shade systems available in the market that dynamically responds to the outdoor environment. Thereby managing solar heat gains, daylight utilization and glare mitigation in buildings all while providing views to the outdoors with minimal occupant intervention. They are also comparatively cheaper alternative to whole envelope insulation retrofits.

Figure 23: partial screenshot of whole content available as a medium blog).

Follow this link for part 1 of the datapane report. (fig 24).

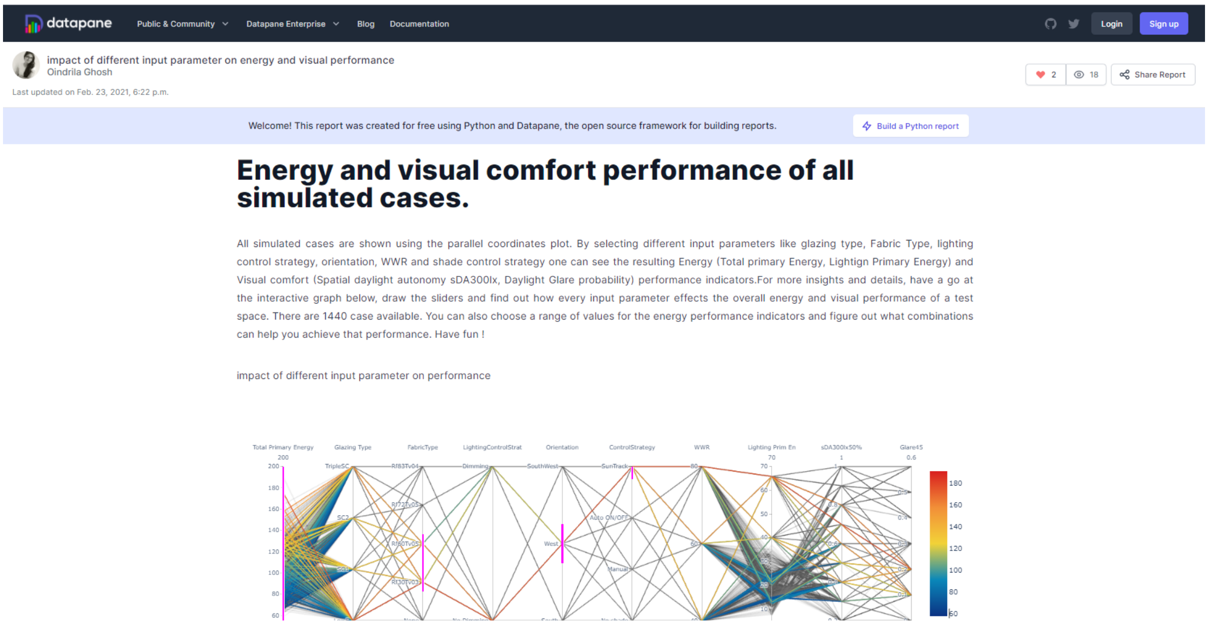

Figure 24: Datapane report. draft version.

It must be noted that this document is a beta version. If Kindow wants host this information in its own platform or some place else for better user experience. They can easily do so using the materials compiled for this beta version. But implementation of that is out of scope for this PDEng project.

4.3.3 Interviews and short articles in magazines

Based on studies carried out in this PDEng project, an interview was conducted for the Bouw Wereld magazine by the project advisors Roel and Sam. A link to the interview can be found here <click here> as well as in appendix 5.

Also, a short article was published in the University magazine for Built Environment students. This is again a strategic way to inform next generation industry professionals about the benefits of advanced shading systems <click here>.

5. Maintainence

BCVTB framework for Rollerblinds database: The Complete framework used for the studies in this project will be uploaded on Gitlab. With a user manual to run more input variations if required. The Excel datasheet is designed in a way, so that new data can be easily added to just one sheet. Separately, the database also has more detailed hourly information available as heatmaps that can be used if needed.

Interactive blog: all data is based on jupyterlab. The python-based information can be managed by Kindow's software dept and used to host it in their website.

5.1. Upgradability:

BCVTB framework for Verticals database: The synchronized CFS framework for verticals is also ready. Incase, the company needs to create a database for verticals, it can be easily used. With a user manual to run more input variations if required. Another (skilled) user required to run the framework.

Although currently out of scope, the Jupyterlab based graphs and charts can be easily used to create worksheets for student education at TU/e.

6. Conclusion

The aim of this PDEng project was to support the market penetration of Kindow by providing performance assessment of its products and by creating avenues to encourage market building communication and education. Based on the design requirement and feedback session with the company this project manages to achieve its goals that were outlined at the beginning of the project.

The systems thinking methodology was implemented to workout client needs, understand their context, and outline the solutions into discrete achievable deliverables. Following set of solution was proposed and implemented.

- The first step was to analyse Kindow's product performance and optimize their control strategy if necessary. Then the next step was to evaluate its performance in different contexts.
- This gave way to two large simulation sets. The analysis of the first simulation study led to the writing of peer reviewed publication illustrating the complex interdependencies of different façade elements. As well as a report testing existing notions about exterior and interior shading system performance.
- The second dataset which was the largest simulation set was used to create the database for Kindow's one-on-one client interaction.
- Analysis of the second dataset, also led to the creation of an interactive blog which is already hosted in an online platform (datapane) ready to be shared in a social media platform.

Although there were minor limitations in terms of not producing a database for Kindow verticals due to lack of time, the current simulation workflow has been setup in a way that it can be easily simulated by another skilled user in future. Also, the insights regarding the performance of the shading system will hopefully get further published in more magazines and articles than what was planned at the time of writing this thesis report.

References

Arnold R. D., W. J. (2015). A Definition of Systems Thinking: A Systems Approach. *Procedia Computer Science 44* , (pp. 669 – 678).

Aste, N., Leonforte, F., Manfren, M., & Mazzon, M. (2015). hermal inertia and energy efficiency—Parametric simulation assessment on a calibrated case study. *Applied Energy*, 111–123.

Beck, W. D. (2010). *Solar shading REHVA Guidebook 12.* REHVA; edited by W. Beck. Forssa:.

Bilali, H. E. (2019). The Multi-Level Perspective in Research on Sustainability Transitions in Agriculture and Food Systems: A Systematic Review. *MDPI Agriculture*.

Brambilla, A., Bonvin, J., Flourentzou, F., & Jusselme, T. (2018). On the Influence of Thermal Mass and Natural Ventilation on Overheating Risk in Offices. *Buildings , 8*(4).

C. Maurer, C. H.-C. (2018). *Report on barriers for new solar envelope systems: deliverable B1 - IEA SHC TASK 56 | building integrated solar envelope systems for HVAC and lighting.*

de Vries, S. B. (2019). Sensor selection and control strategy development support for automated solar shading systems using building performance simulation. *Building Simulation 2019: 16th Conference of IBPSA (BS2019),.* Rome.

de Vries, S. B. (2021). Simulation-aided development of automated solar shading control strategies using performance mapping and statistical classification. *Journal of Building Performance Simulation*, DOI: https://doi.org/10.1080/19401493.2021.1887355.

Dengel, A. &. (2012). *Overheating in new homes: A review of the evidence.* IHS BRE Press on behalf of the NHBC Foundation.

EEA. (2017). *Perspectives on transitions to sustainability.* Retrieved 02 25, 2021, from https://www.eea.europa.eu/publications/perspectives-on-transitions-to-sustainability/file

European Commission. (2020). *A Renovation Wave for Europe - greening our buildings, creating jobs, improving lives.* Brussels.

F. Ochs, M. M.-C.-M. (2020). *IEA SHC Task 56 - Design guidelines: Deliverable DC.3.* paris: International Energy Agency. https://task56.iea-shc.org/Data/Sites/1/publications/Task56-DC3-Design-guidelines.pdf.

F. Ochs, M. M.-M. (2020). *IEA SHC Task 56 - System Simulation Results: Deliverable DC2.* International Energy Agency. https://task56.iea-shc.org/Data/Sites/1/publications/Task56-DC2-System-simulation-results.pdf.

Federizzi, R. e. (2017). *Hurdles and opportunities offered by the exploitation of the solar source through multifunctional envelope technologies.* IEA SHC Task 56.

Geels, F. (2002). Technological transitions as evolutionary reconfiguration processes: a multi-level perspective and a case study. *Research Policy 31* , pp. 257-1273.

Gunay, H. e. (2014). On adaptive occupant-learning window blind and lighting controls. . *Building Research & Information, 42*(6), 739-756.

Haldi, F. a. (2010). Adaptive actions on shading devices in response to local visual stimuli. *Journal of Building Performance Simulation, 3*(2), 135-153.

IEA-SHC. (2019). *Daylighting of Non–Residential Buildings. Position Paper.* IEA.

Kindow. (2019). *products/kindow-rollers*. Retrieved from kindow.nl: https://kindowblinds.com/products/kindow-rollers/

Kindow. (2019). *Products/verticals*. Retrieved from Kindow.nl: https://kindowblinds.com/products/kindow-verticals/

Meerbeek, B. e. (2014). Building automation and perceived control: a field study on motorized exterior blinds in Dutch offices. *Building and Environment, 79*, 66-77.

Muller, G. (2020). *CAFCR: A Multi-view Method for Embedded Systems Architecting; Balancing Genericity and Specificity.* Delft: Technische Universiteit Delft.

NASA. (2012). *Technology Readiness Level*. Retrieved from https://www.nasa.gov/directorates/heo/scan/engineering/technology/txt_accordion1.html

Reinhart, C. a. (2003). Monitoring manual control of electric lighting and blinds. *Lighting research and technology, 35*(3), 243-258.

Schot, J., & Geels, F. W. (2008). Strategic niche management and sustainable innovation journeys: theory, findings, research agenda, and policy. *Technology Analysis & Strategic Management* , 20:5, 537-554.

Seguro, F. a. (2016). *Solar Shading Impact. Business case|Strategic Vision| Action Plan for British Blind and shutter Association.* Milton Keynes: National Energy Foundation.

Varela Souto, A. (2019). *Development of a design support tool for an innovative building-integrated.* Technische Universiteit Eindhoven.

View, Inc. (2019). *Future Workplace Wellness Study.* Future Workplace LLC.

Wienold, J. (2009). Dynamic Daylight Glare Evaluation. *n Building Simulation, edited by P. A. Strachan, N. J. Kelly, and M.* (pp. 944–951). Glasgow: IBPSA.

Appendix

1. Control optimization feedback:

As mentioned in section 4.1, four Kindow control strategies were tested. Here are the graph with the results for Primary energy consumption for all three locations and 2 orientations.

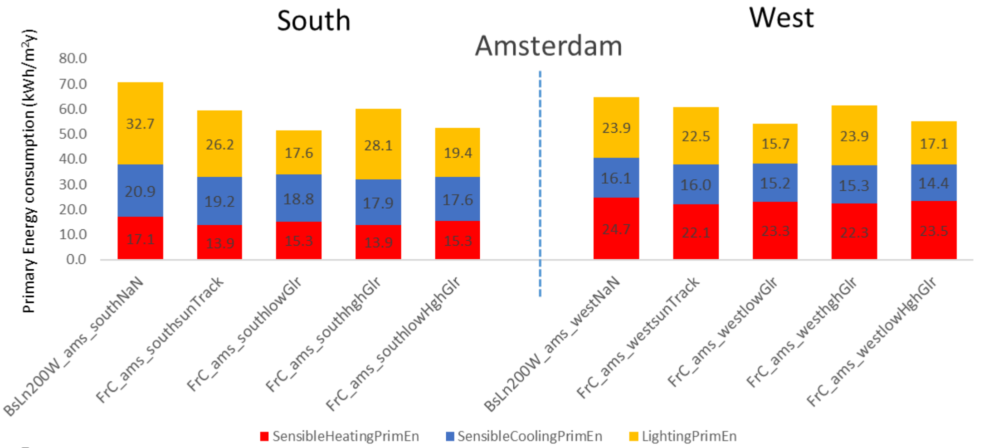

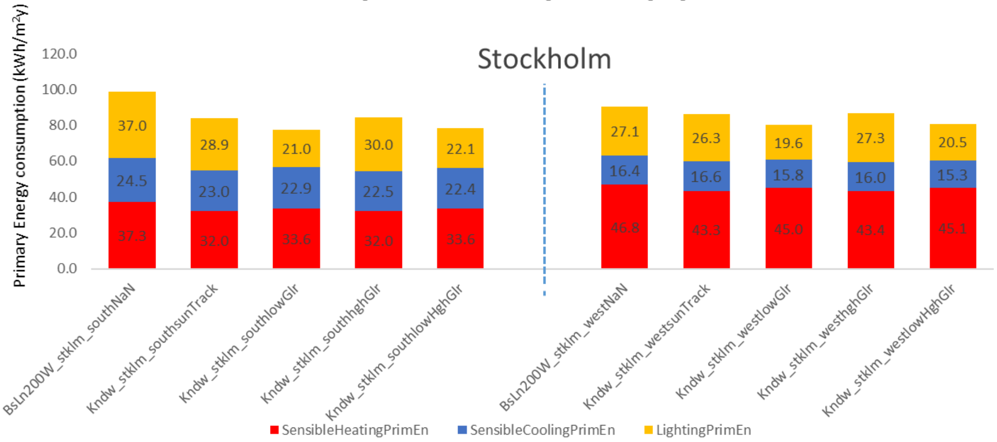

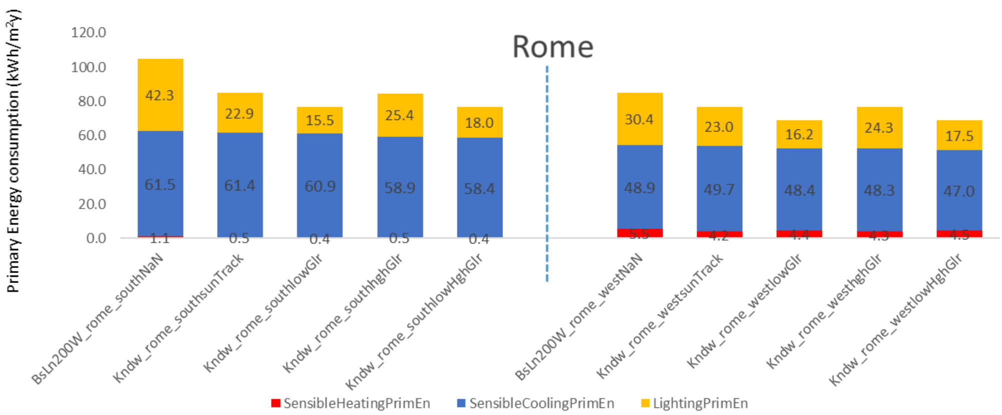

- General trends as expected due to climate: higher cooling gains in Rome, Higher heating gains in Stockholm and intermediate gains in Amsterdam as the climate is milder in comparison to the other two.
- Relative increased heat gains due to orientation change to west.

- In terms of impact of various control strategies tested: there is no specific trend noted. All had comparable performance and each case had its own trade-offs. Therefore, varying site conditions and client needs can allow choice of specific control strategies available.

Similarly, visual performance for all locations have similar trends. Here we are going to illustrate only for Amsterdam.

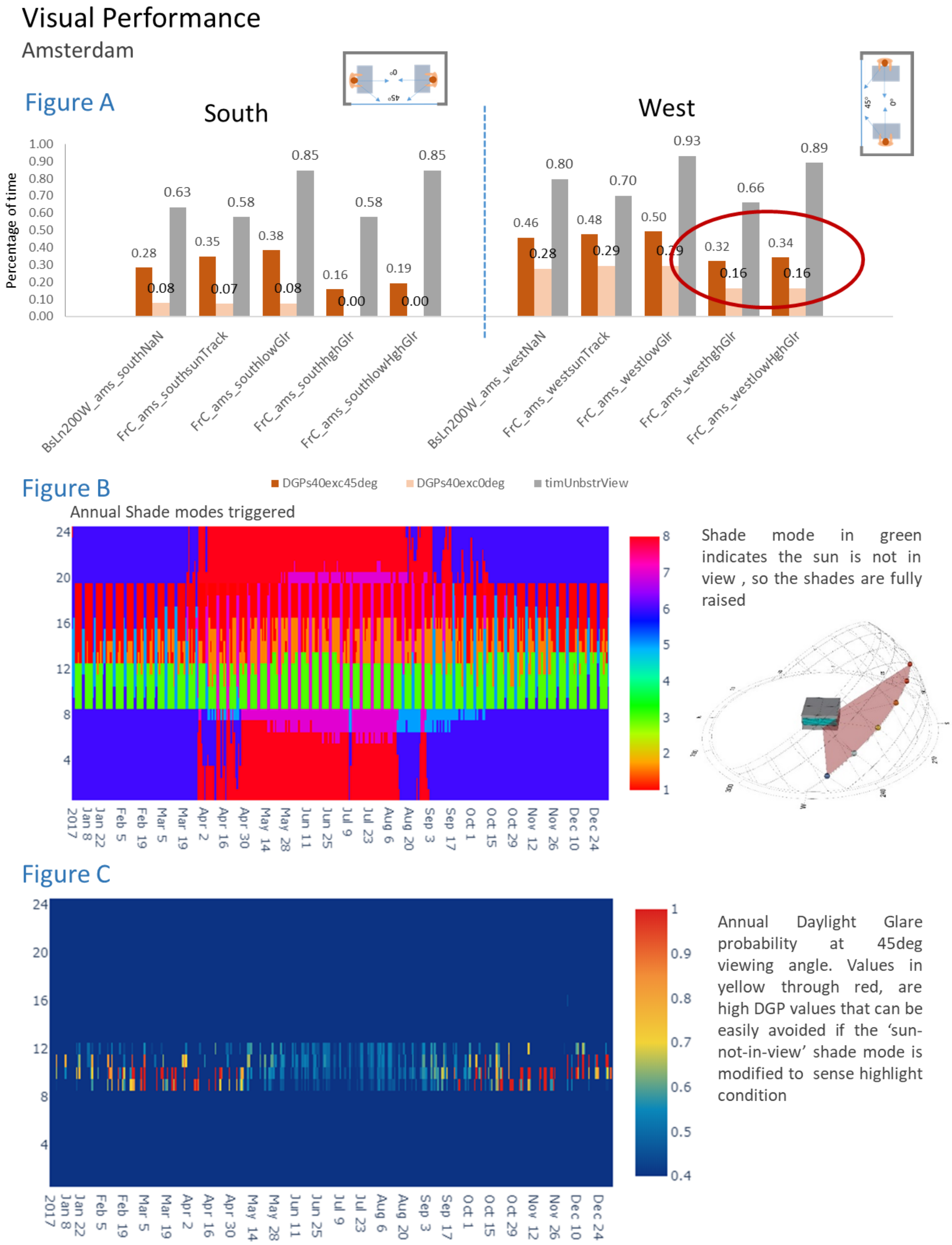

- It can be seen, the suntrack+low light sensing condition although performs comparatively better in terms of energy consumption, the DGPs values for viewing angle 45 and 0 degrees are twice as high as suntrack+low+high light sensing strategy. This is true for all locations.
- Also, the Highlight sensing strategies still do not manage to completely remove glare in the west oriented façade (circled in red in fig A). This is because the sun-track technology as mentioned in section 4.1 is programmed to raise the shade fully when the sun is not in view (fig B). For south orientation that is fine, but for west orientation atleast 4 hours when the office is occupied the sun is out of range and the sky is still too bright and can cause glare (fig C).

- Therefore, this control strategy was modified such that highlight sensing was on even when the sun is out of range. In doing so, DGPs values were finally considerable reduced (fig below).

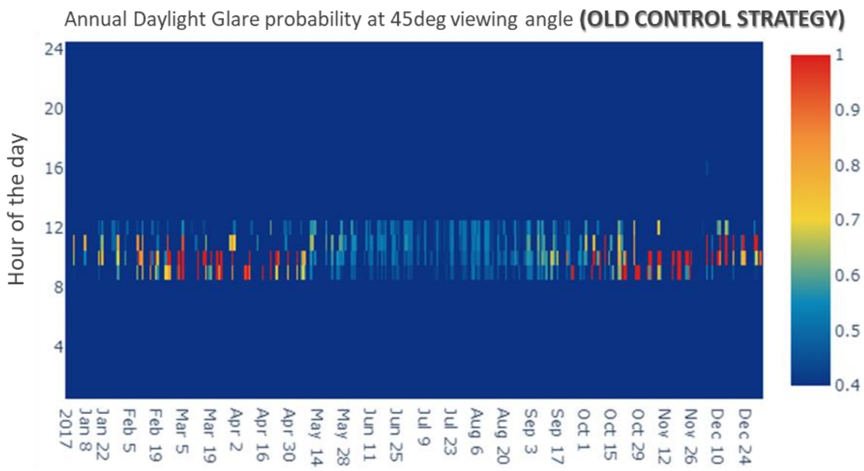

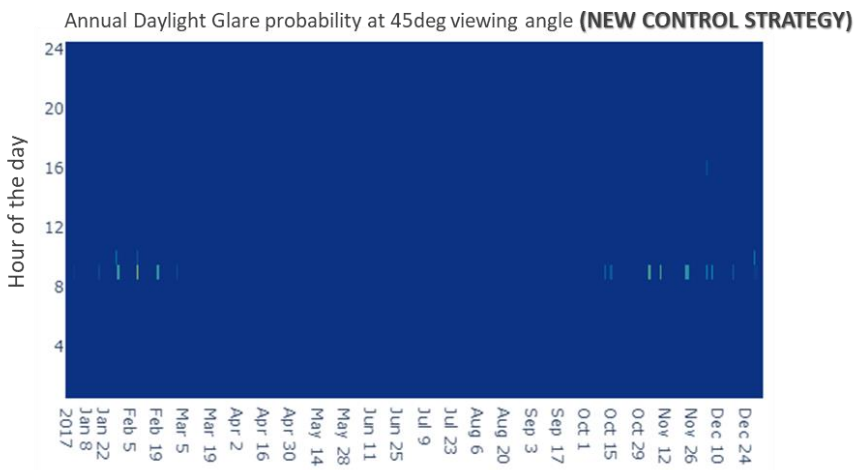

2. Vertical Blinds control strategy optimization:

As mentioned in section 4.1 the vertical blinds study has considered a total of 9 different vertical blind control strategy and compared them against the industry standard automated shading and a case with no shading at all. Below are the cases that were simulated:

1. Baseline: Up or down based on 200W irradiance threshold.
2. No Blinds

3. Perp2glazing_static : The vertical blinds are stationary and positioned 90 degress to the window.
4. Perpendicular: Perpendicular strategy: In this strategy, the vertical blinds are always perpendicular to the incident sun rays (figure 14). They tend to be more “open” when the sun angle is low (e.g. mornings and sunset times).
5. Minimum cut-off strategy: The alternate edge of two consecutive vertical blinds are aligned with the incident sun ray (figure14). In general, it is more “open” when the sun angle is large (e.g at noon).
6. Most Open: This is the combination of perpendicular and minimum cut-off strategy to create a new control that provides maximum view to the outdoors and daylight access while blocking glare. This strategy uses perpendicular strategy during low sun angles and Minimum cut-off strategy during high sun angles (figure 14).
7. Retract: This is a combination of most open and retract , where the vertical blinds stay retracted till the illuminance values exceed 6000lux (below this number there are no chances of glare to the occupant). Then it expands and does sun tracking using the most open strategy for the entire day. When the occupant leaves, the blinds close and retracts again early morning at 6:00 hrs (figure 14).
8. Retract_annoying: same as retract but it retracts whenever there is a low light condition.
9. Retract_highlight: same as retract but detects highlight condition when the sun is not in view and keeps sun tracking.
10. Retract_highlight_closed: Same as retract but detects highlight condition when sun is not in view and then the blinds are fully closed.
11. Retract_Flipped : same as retract strategy, but the shades flip to its absorbing side when the blinds are parallel to the window surface.

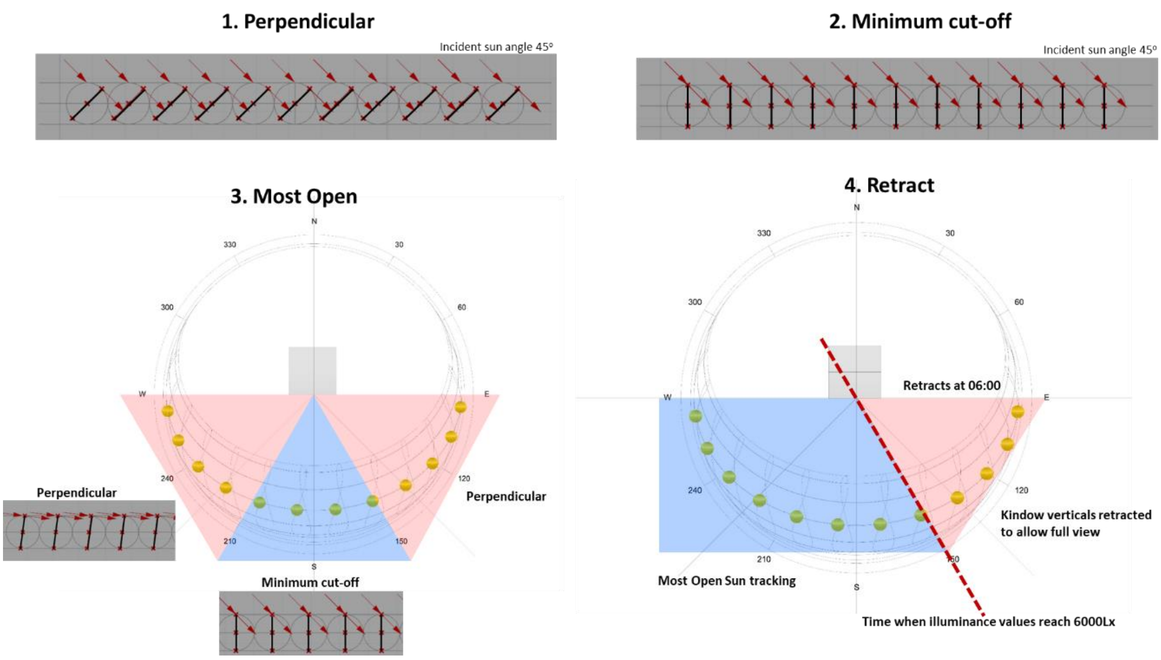

All these cases are simulated for the same test office space , south orientation and in Amsterdam. The following graphs shows their energy and visual performance.

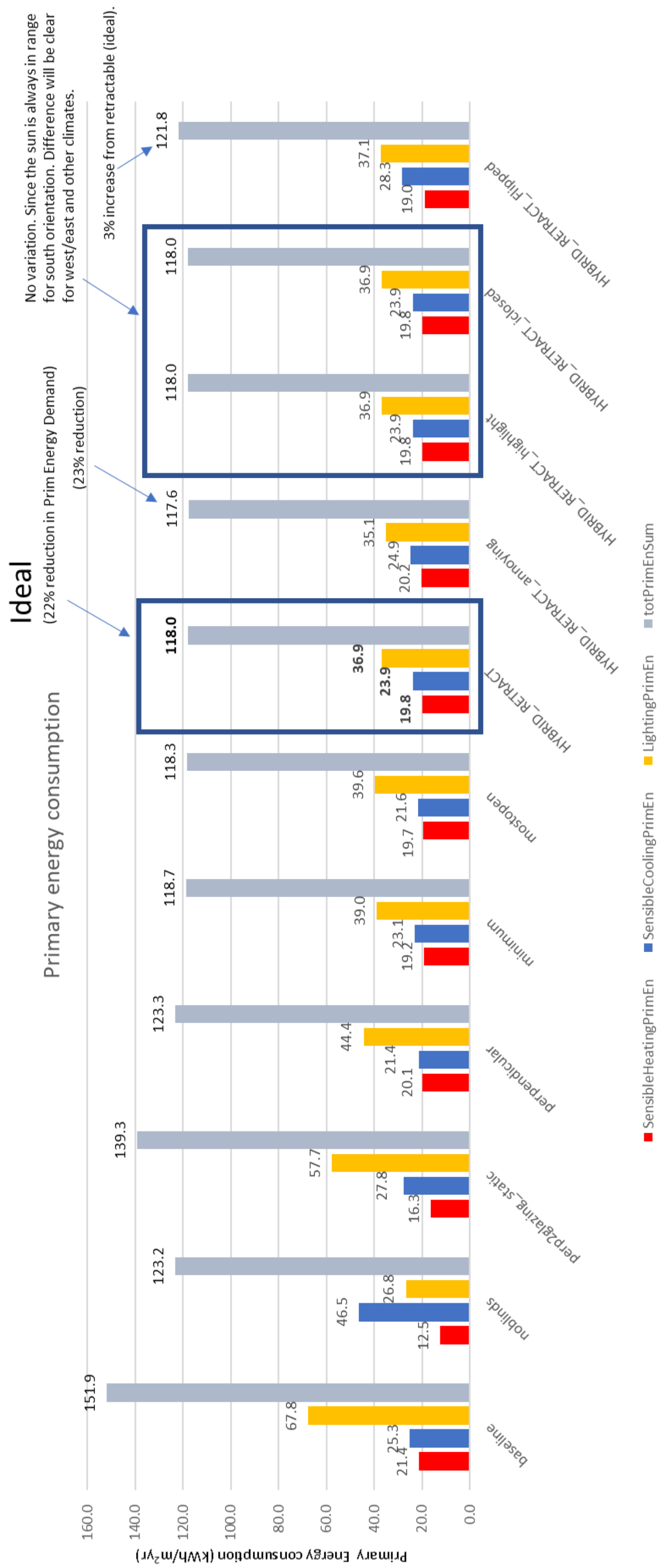

Figure 25: Energy performance of all control strategy variations for vertical blinds.

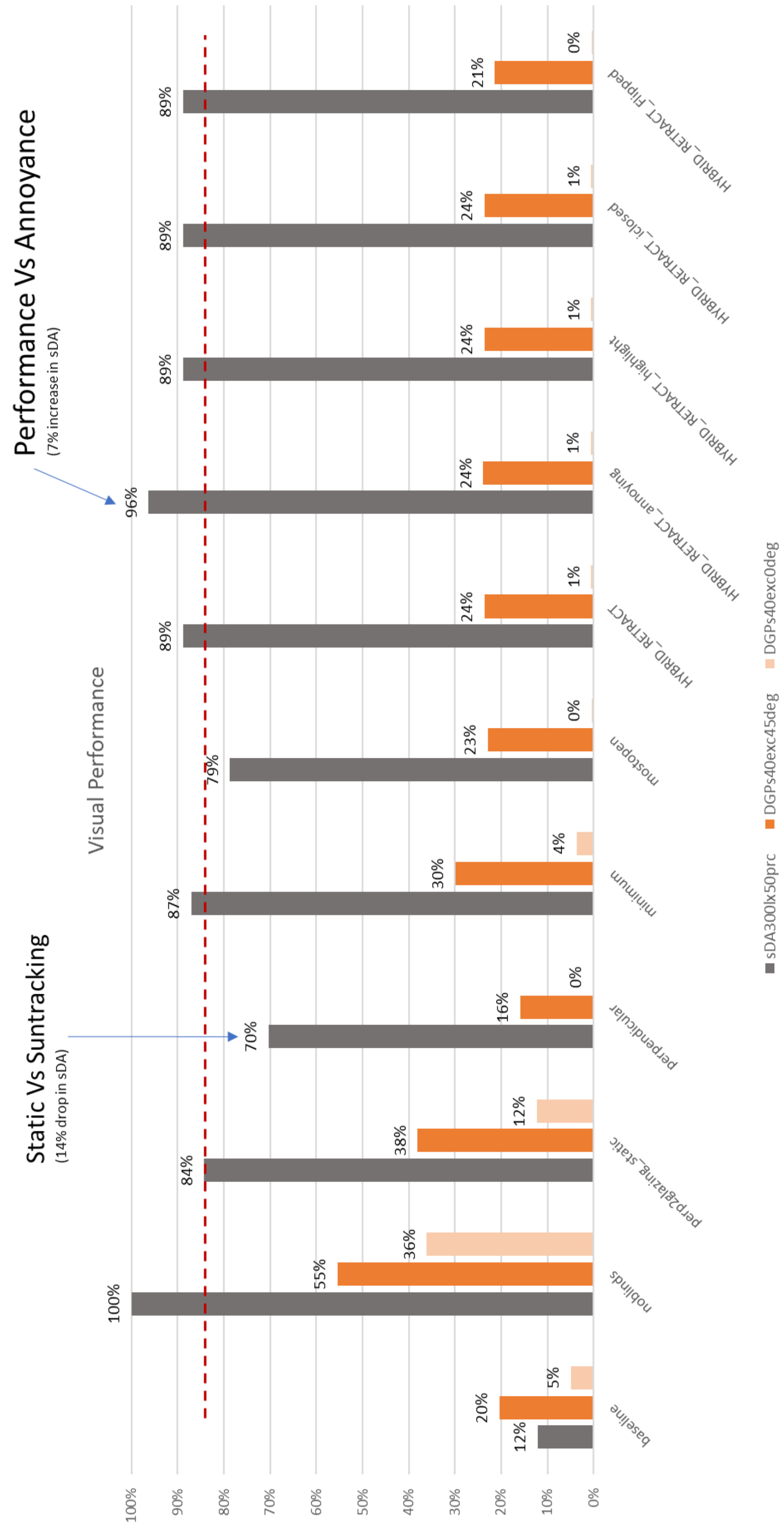

Figure 26: Visual performance performance of all control strategy variations for vertical blinds.

3. Report from the Kindow Website:

Energy performance analysis of advanced interior solar shading systems – Kindow Rollerblinds vs. state-of-the-art alternatives

Synopsis

This report discusses the results of a series of simulation studies carried out by researchers at Eindhoven University of Technology. The study analyses the performance of rollerblinds using an advanced solar-tracking control strategy – Kindow Rollerblinds [Kindow, 2019] – in comparison to commercially available automated shading systems like external and internal roller shades with façade irradiance sensors. The results are analysed in terms of energy consumption and visual comfort. The performance of the investigated system is examined in relation to shading material properties and settings for the control parameters. The simulations are run for a test office building of 27m^2 area and 80% WWR for a South orientation in Amsterdam.

The comparison with conventional shading systems shows that careful combination of shade materials with reflective properties and the Kindow Rollerblind control strategy can lead to 6.5% energy savings compared to external shading and 23.6% against conventional internal shading systems. A common rule-of-thumb in the building industry states that "indoor shading is not effective for reducing energy demand, because the heat is already trapped inside". This study provides clear indications that this conventional wisdom can be refuted with carefully chosen material properties and modern-day control technology. The results furthermore show that the application of the Kindow Rollerblind strategy can lead to an average increase of up to 65% (sDA300/50) in the amount of daylight entering the building. Furthermore, the simulation studies showed an increase of 22% in the operating time with an unobstructed view for the occupant. In terms of glare, the Kindow Rollerblind system has a 5 – 9% reduction to a conventional system.

Simulation Setup and Methodology

The reference office space developed by the International Energy Agency (IEA) Task 56 (2018) was used in this study [D'Antoni et al, 2018]. The office model has an area of 27m^2 and a South facing façade with a window to wall ratio of 80%. Table 1 illustrates all the assumptions made for the reference office. The differences amongst the cases are due to variations in shade materials, shade positioning and control strategy. In order to compare and benchmark the performance of Kindow Rollerblinds, the following case studies were considered.

- Case 1: External roller shades with reflective material properties (shade 1).
- Case 2: External roller shades with non-reflective material properties (shade 2).
- Case 3: Internal roller blinds with reflective material properties (shade 1).
- Case 4: Internal roller blinds with non-reflective material properties (shade 2).
- Case 5: Internal roller blinds with the Kindow control strategy (shade 1).

Cases 1 to 4 are the baseline cases which are chosen in such a way to represent the performance of conventional automated shading systems available in the market. Case 5 uses the same reflective shade material as case 1 and 3, but with the advanced Kindow control algorithm. The control strategies (Figure 27) are elaborated below:

3. The industry standard control strategy where the roller shades are either in up or down position based on a threshold value of 200W/m^2 façade irradiance value.
4. The latest Kindow Rollerblind control strategy where the rollerblind movement is based on sun tracking and senses high light and low light condition to control shade movement.
   To elaborate more on this, the system calculates the time and location of the sun at every moment. If the sun is behind the façade, the roller blind will be fully opened to allow daylight and view to enter. If the sun does fall into the field of vision of the facade, the system will try to determine whether there is a cloudy sky or a clear sky. If it is a cloudy sky, the blinds are fully opened. But when the sun is in sight and there is a clear sky, the system will lower the roller blind to such an extent that the sun is kept out of sight of the user. The height of the roller blind is determined based on the calculated position of the sun. This prevents glare from direct sunlight and reflections from the workplane. At the same time, the uncovered part of the window still allows daylight to enter the room and allows the user to retain part of his view to the outside. It is one of the more comprehensive control strategies available for Kindow products.

Performance of advanced solar shading systems depends on the interaction between the thermal and visual domains of physics. This study, therefore, uses a co-simulation method in which advanced models for thermal performance and daylight access are linked.

The co-simulation model (Figure 2) uses a link between four existing software environments where information is exchanged between the different models during simulation. EnergyPlus, a dynamic building simulation program developed on behalf of the U.S. Department of Energy, is used to simulate the thermal behaviour and energy performance of the building. The co-simulation model uses Radiance to describe the behaviour of daylight. Radiance is a collection of programs which uses 'backward raytracing' to make accurate predictions about daylight access, glare and the amount of artificial lighting required. Matlab, a mathematical programming environment, was used to implement the Kindow control algorithm. The information exchange within the co-simulation model is made possible by the software environment BCVTB (visualized by arrows in Figure 2).

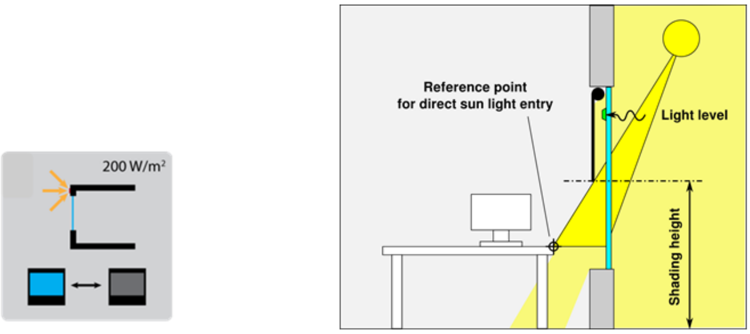

$I_{g;v}$ >200 W/m^2 – shades down
$I_{g;v}$ <200 W/m^2 – shades up

- Light level sunny: Dynamic shade height based on solar zenith and azimuth angle
- Light level cloudy: Shades are open

Figure 27: Baseline strategy and latest Kindow Rollerblind control strategy

Table 3: Modelling assumptions for the reference office for test cases.

		EnergyPlus	Radiance
	Dimensions	width: 4.5m; depth: 6m; height: 3m (27 m2)	
Geometry	**Window to wall ratio:**	80%	
	Type:	Solar Coating (pos. 3) double glazing with argon cavity filling,	
Fenestration	**Glazing:**	Ugl: 1.12 W/m2K Uframe: 1.5 W/m2K, SHGC: 0.306, CEN	Tvis: 0.688
	Shade 1 (Reflective):	Tsol: 0.02, Rsol: 0.74, Tvis: 0.01, Rvis: 0.72	
	Shade 2 (Non-Reflective):	Tsol: 0.02, Rsol: 0.48, Tvis: 0.01, Rvis: 0.45	
Facade		Rc = 4.5 m2K/W	rvis = 0.5
Ceiling, walls, floor		Mixed: heavy weight floor/ceiling, lightweight walls	Ceiling: rvis = 0.8, Wall: rvis = 0.5
			Floor: rvis = 0.2
	People:	3 (variable occupancy). 120 W/pers.	
Internal gains	**Occupancy:**	Weekdays: 8:00-19:00 (2860 hours/year)	
	Lighting:	10.9 W/m2 Dimming (linear between 0-500 lux) Two sensors (Figure 1) each control 50% of loads	
	Equipment:	7.0 W/m2	
	Infiltration:	ACH: 0.15	
	Ventilation:	Demand driven, 40 m3/(h*pers.), ACH: 1 (average)	
		Sensible heat recovery, eff: 70%	Sensor grid: 5x25
HVAC and settings	**Setpoints:**	Lower set point: 21°C, Upper set point: 25°C (constant)	V: -ab 12 -ad 5·104 -lw 2·10-6,
		Idealised: unlimited capacity and ideal response	D: -ab 2 -ad 103 -lw 5·10-4 -c 3000
	System efficiencies	ηe = 0.39, ηcool,deliv = 0.7, COPcool = 3, ηh = 0.95	
		Anisotropic optical model for shade	s and D: MF3
		5 min. time step	hourly time step
Weather		IWEC, Amsterdam	
Orientation		South	

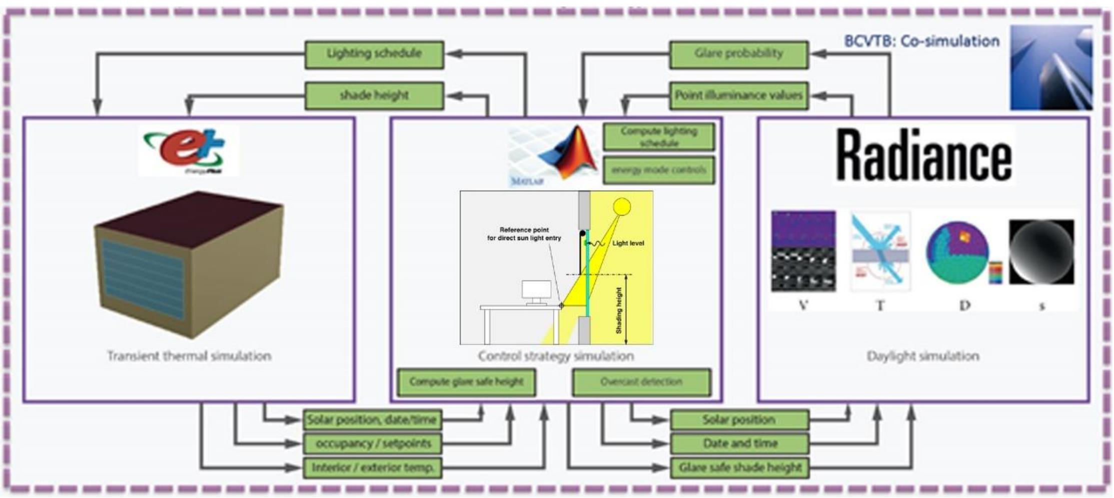

Figure 28: The co-simulation model

Performance indicators

In this study, energy performance is assessed on the basis of the energy demand for lighting, cooling and heating at room level in combination with an estimate of the primary energy consumption based on a number of system efficiency assumptions. The energy demand at room level provides an insight into the savings potential in general. It can be used to estimate the actual energy and cost savings when the Kindow Rollerblind control system is applied in combination with specific shade materials. In order to gain insight into the environmental savings potential, the primary energy consumption is also taken into account. The following reference figures have been used for this purpose. (Beck et al. 2010; Aa van der 2012).

$$E_{Prim} = \frac{E_{Light}}{\eta_e} + \frac{E_{cool}}{\eta_e \eta_c COP} + \frac{E_{heat}}{\eta_h} \quad \text{met: } \eta_e = 0.39, \quad \eta_c = 0.7, \quad COP = 3, \quad \eta_h = 0.95$$

In order to assess the performance of the shading systems, a series of performance indicators have been selected. In order to quantify the degree of daylight access, this study will use daylight autonomy (DA) and spatial daylight autonomy (sDA). Daylight autonomy can be interpreted as the percentage of time that a measuring point receives 'sufficient' daylight. For this indicator, the abbreviation DA300 is often used, where 300 stands for the number of lux that is set as a limit value. Spatial daylight autonomy enables us to express daylight access to a room as a whole in one number. It is defined as the percentage of the floor area with a daylight autonomy higher than fifty percent. Spatial daylight autonomy can be interpreted as the fraction of the floor area that receives sufficient daylight most of the time (Reinhart, Mardaljevic, and Rogers 2006). For this indicator, the abbreviation sDA 300/50 is often used, where 300 stands for the limit value in lux and 50 for the required exceeding percentage of the usage time.

In this report, 'daylight glare probability simplified' (DGPs) is used as an indicator to assess the risk of glare (Wienold 2009). Although much is still unknown in the field of glare perception and assessment, it is certain that glare is associated with high luminance differences in the field of view, with the total luminance at eye level, as well as with the position of glare sources in relation to the focus area of the eye task. The DGPS indicator is primarily based on vertical illuminance but neglects the influence of peak glare sources. In this report, a DGPs limit of 0.40 has been considered for occupied hours when the glare is weaker than ‘disturbing’. And the DGPs values are considered at the two sensor points as shown in figure 3, one has a viewing angle of 45 degrees and the other at 0 degrees meaning it is directly facing the wall. The maximum value out of the two sensor points is considered at each timestep and then the DGPs is evaluated for the whole year.

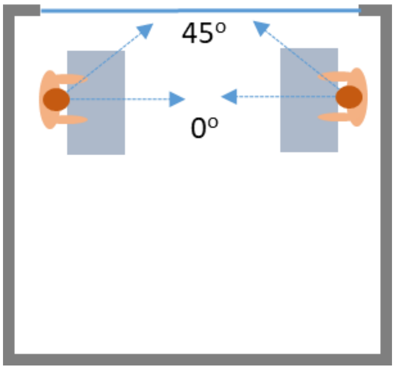

Figure 29: Positioning of the sensor point and the viewing angles considered for dgp calculations

Results

Energy Performance

Figure 4 shows the comparison of energy demand of the different cases considered for a south-facing office space in Amsterdam. The external shading system has much lower cooling demands in comparison to the internal shading systems as it can keep the solar radiation from entering the test space, but this also increases their heating demand considerably. Simple changes like the choice of using reflective shading material instead of the conventional non-reflective one can have quite an impact on the performance of these systems. For external shades (cases 1 and 2), this change accounts for 5.0% and 12.5% reduction in lighting and cooling demands. For internal shades (case 3 and 4), use of reflective shade material leads to 6.5% and 24.0% reduction in lighting and cooling demands respectively. The reductions seen in lighting demands is due to the angular behaviour of the reflective material which leads to difference in transmittance. And reduction in cooling is due to the reflectance property of the material, hence the reduction in cooling demand is more apparent for internal shades than external ones.

Since case 1 to 4 (conventional indoor and outdoor shading systems) use the same control strategy based on façade irradiance, the lighting demand is comparable for all these cases. Although at a closer look, one can notice a 5 – 6% reduction in lighting demand because of the use of reflective shades in cases 2 (baseline_externalshade) and 4 (baseline_internalshade) respectively. Case 5 (Kindow Rollerblind control), which uses the same reflective shading material as case 2 and 4, has an improved heating and lighting demand in comparison to the rest of the cases. For example, heating demand is reduced by an average of 25% in comparison to internal shades (case 3 and 4) and by an average of 50% against external shades (case 1 and 2). And lighting demand is reduced by an average of 44% against all cases 1 - 4. This improvement is because of its use of the complex sun tracking algorithm that considers sun position and sky brightness for its positioning during occupied hours.

On the other hand, there is also a 25% increase in cooling demand in comparison to case 4 (baseline_internalshade_reflective), as the current version of the control strategy allows more time with its shades up and unobstructed view of the outdoors to the occupant. This increase in cooling demands is less decisive for the total primary energy consumption and the influence of lighting is relatively large due to the system efficiency factors associated to meeting different types of loads.

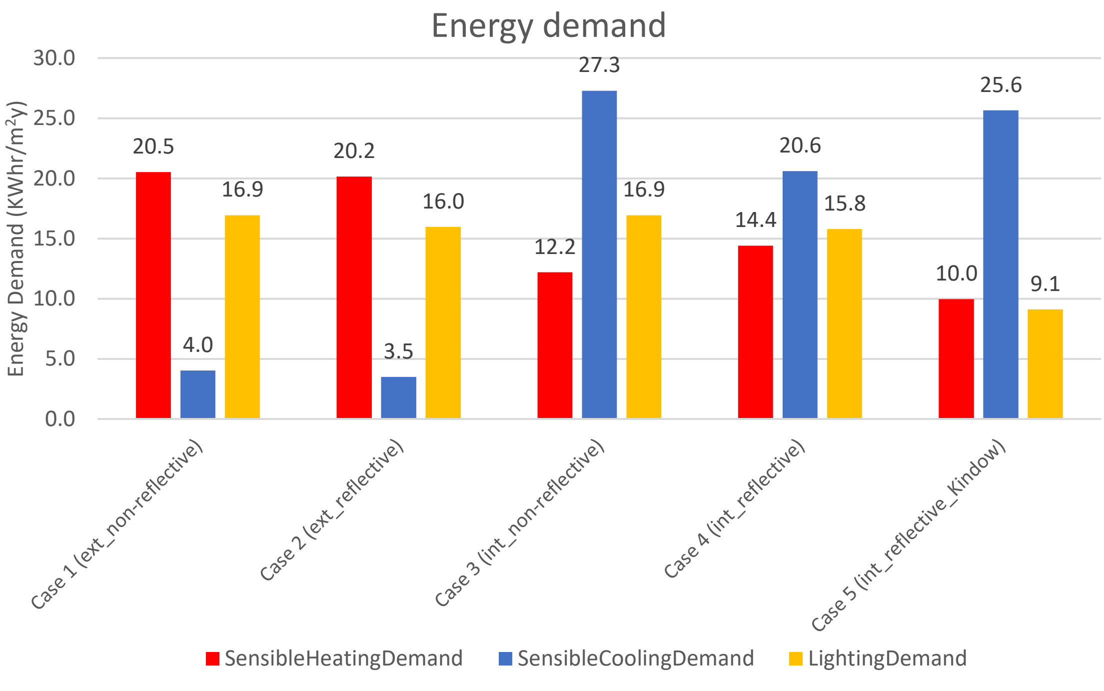

Figure 4: Annual energy demand comparison

As we can see in figure 5, the primary energy consumption shows that indoor shading systems with careful combination of shading material and control strategy (case 5) can outperform external shading systems (case 2) by a 6.5%.

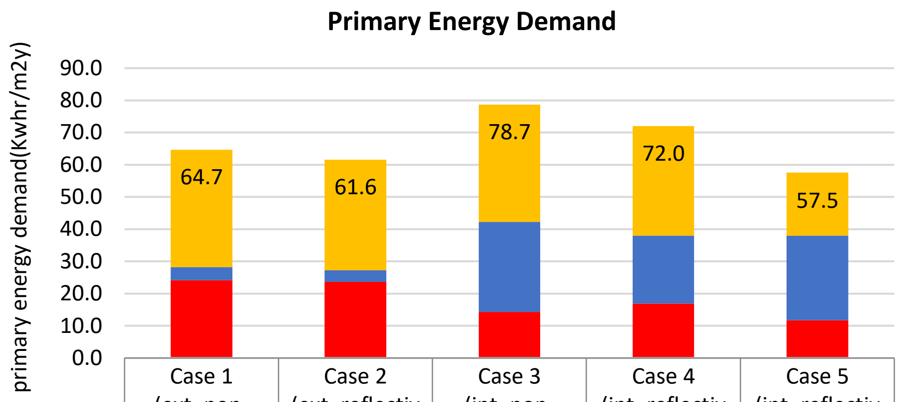

	Case 1 (ext_non-reflective)	Case 2 (ext_reflective)	Case 3 (int_non-reflective)	Case 4 (int_reflective)	Case 5 (int_reflective_Kindow)
LightingPrimEn	36.4	34.3	36.4	34.0	19.6
SensibleCoolingPrimEn	4.1	3.6	27.9	21.1	26.3
SensibleHeatingPrimEn	24.1	23.7	14.3	17.0	11.7

SensibleHeatingPrimEn SensibleCoolingPrimEn LightingPrimEn

Figure 5: Primary energy demand

It can also be seen that the use of Kindow Rollerblind control strategy (case 5) leads to an average 40% reduction in primary lighting energy demand in comparison to the rest of the cases. This also highlights that lighting energy has a greater influence on overall energy consumption compared to heating or cooling loads.

As the visible transmittance of both shade materials were kept identical at 0.012, the variation in reflective and non-reflective shading did not have a significant impact on visual performance. There is, however, a remarkable difference because of the change in control strategy.

Visual Performance

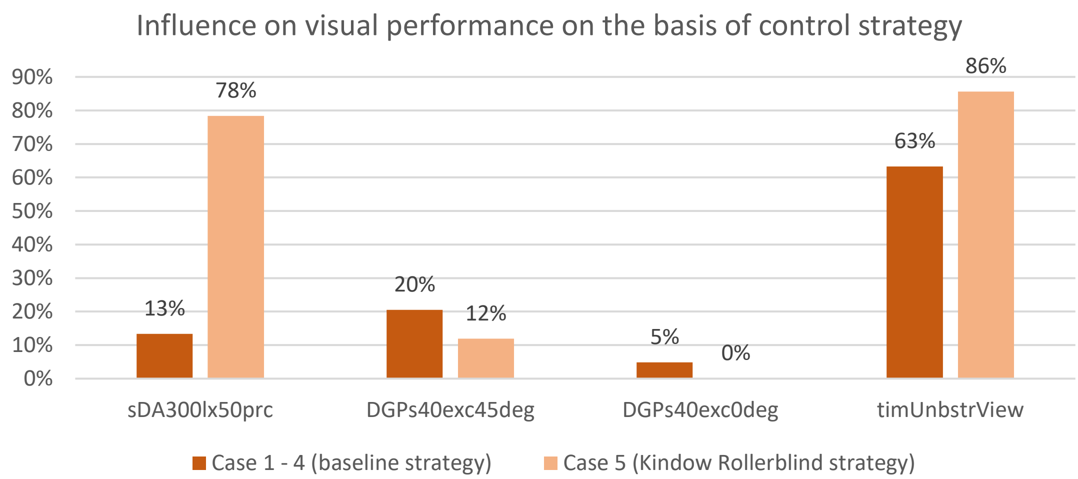

Figure 6: Influence of control strategy on visual performance.

There is a 65% increase in spatial daylight autonomy and 23% increase in percentage of time with an unobstructed view. An Unobstructed view means whenever the shades are above the height of the occupant's eyelevel. The Kindow Rollerblind strategy allows the shades to be more open than the baseline strategy thereby causing this remarkable improvement in the daylighting gains and view in the space. Also, its strategy for obstructing direct sun and instances of high illuminance sky conditions has resulted in 8% reduction in Glare values for 45^{o} viewing angle and complete removal of glare problems when the occupant is sitting parallel to the window (0^{o}).

Conclusion

From this study it can be concluded that use of reflective materials and the Kindow Rollerblind control strategy has great potential to optimise automated indoor shading systems according to building characteristics, user preferences and objectives. The possibilities in terms of energy saving and optimizing user comfort can be significantly increased. Primary energy consumption is reduced by 6.5% in comparison to external shading systems whereas there is a 23% drop in primary energy demand when compared to conventional indoor shading systems. The use of the Kindow Rollerblind strategy greatly improves the amount of daylight entering the space. As much as 65% increase in terms of spatial daylight autonomy and 9 and 5% decrease in glare probability for viewing angles 45 and 0 degrees respectively. It also questions the common rule-of-thumb that outdoor shading systems perform better as it keeps the solar radiation out before it enters the building through the glazing. And also illustrates that such conception doesn't necessarily guarantee good building performance. The study provides clear pointers that that careful combination of glazing and shading properties, and control strategies is important for optimal energy performance. Using reflective shade material instead of conventional non-reflective ones is likely the first step to improving energy demands. Consequently, major improvements in visual performance as well as energy demands can be obtained by using a refined and complex control strategy as used by Kindow.

Reference

1. Aa van der, R. 2012. "NEN 7120+ C2: Energieprestatie van gebouwen-Bepalingsmethode." In. Delft: Stichting Nederlands Normalisatie-instituut (NEN/CEN).
2. Beck, W, D Dolmans, G Dutoo, A Hall, and O Seppänen. 2010. "Solar Shading. REHVA Guidebook 12." In.: Forssa, Finland.
3. D'Antoni, Matteo, Paolo Bonato, David Geisler-Moroder, Roel Loonen, and Fabian Ochs. 2018. "IEA SHC T56 - System Simulation Models: part C." In. Paris: IEA.
4. Kindow B.V. 2019. Last accessed 27 august 2019. http://www.kindowblinds.com/
5. Reinhart, Christoph F, John Mardaljevic, and Zack Rogers. 2006. 'Dynamic daylight performance metrics for sustainable building design', Leukos, 3: 7-31.
6. Wienold, J. 2009. Daylight glare in offices. (Fraunhofer and Universität Karlsruhe (TH): Freiburg, Germany).

4. Peer Reviewed Scientific Publication Draft:

This has been removed from the SAI-report for restrictions

5. Interview at Bouwereld with Roel and Sam.

Binnenzonwering kan meer dan alleen zonlicht weren. Aangestuurd met een daglichtgestuurd systeem en gecombineerd met intelligente binnenverlichting kan binnenzonwering in kantoor- en utiliteitsgebouwen zelfs 40% besparing opleveren op het totale primaire energieverbruik. Dat is vergelijkbaar met conventionele energiebesparende maatregelen zoals gevelisolatie, met als groot voordeel dat het relatief betaalbaar en weinig ingrijpend is. Tot deze conclusie komt de TU Eindhoven naar aanleiding van een onderzoek dat ze hebben uitgevoerd in samenwerking met Kindow uit Delft.

Kindow is leverancier en producent van daglichtgestuurde binnenzonwering, een innovatief systeem waarbij de zonwering dynamisch wordt geregeld op basis van realtime informatie. “Per moment bekijkt het systeem hoe de zon staat ten opzichte van de gevel, wat de lichtintensiteit van de zon binnen is en of er mensen aanwezig zijn”, vertelt Sam Kin, CEO van Kindow. “Dit is wezenlijk anders dan een handmatig of geautomatiseerd open-dichtbuitenzonweringsysteem. Traditioneel gezien is zonwering alleen gericht op koeling en verlagen van de warmtelast en reageert dus alleen op zonlicht op de gevel. Maar als je kijkt naar de totaalbalans van verwarming, koeling en verlichting – dan is het in sommige gevallen wel heel gunstig om de zon gedeeltelijk binnen te laten.”

Onderzoek TU/e

Maar hoe gunstig het precies is om de zonwering intelligent aan te sturen was nog niet bekend. Vandaar dat Kindow samen met de TU Eindhoven onderzoek deed naar het effect van intelligente zonwering in combinatie met daglichtgestuurde verlichting. Volgens Kin was het een logische keuze om de verlichting bij het onderzoek te betrekken: “Bij intelligente verlichting beoordeelt een sensor in het plafond de lichtsterkte op het werkblad en op basis daarvan wordt het kunstlicht meer of minder sterk. Als er meer daglicht binnen komt, schakelt de verlichting terug. De verlichting geeft precies zoveel licht als nodig is. Als je dat combineert met daglichtgestuurde binnenzonwering dan heb je een win-win situatie, omdat de twee systemen reageren op elkaar.”

Energiebesparing

En die win-win situatie is niet mis. In het onderzoek werden verschillende gebouwen onderzocht die representatief zijn voor kantoorgebouwen van de afgelopen 15 jaar. Daaruit blijkt dat de intelligente zonwering en verlichting kan zorgen voor een energiebesparing van 40% op het primaire energieverbruik. Alleen de intelligente verlichting kan al een besparing van 18-32% opleveren ten opzichte van een klokschakeling. De combinatie van reflectieve binnenzonwering met intelligente daglichtsturing levert een besparing van 15-20% op het primaire energieverbruik. Een deel van die besparing zit in de koeling van een gebouw, mits aanwezig. Maar de besparingen op de energievraag voor koeling geven ook een indicatie van de verbeteringen in het thermisch comfort van gebruikers bij gebouwen waar geen koeling aanwezig is. Met andere woorden: is er geen koeling om op te besparen dan levert het in ieder geval een verhoogd comfort tijdens warme dagen.

Individueel kunnen de energiebesparingen niet zomaar bij elkaar opgeteld worden. Dat komt omdat het een het effect van intelligente zonwering anders is dan wanneer het gecombineerd wordt met verlichting. Vandaar dat de maximale energiebesparing van de combineerde systemen 40% is, en niet 52%. De genoemde besparingen gelden overigens voor gebouwen waar mensen overdag verblijven, dus vooral kantoor- en utiliteitsgebouwen.

Nieuwe wetenschappelijke inzichten

Het onderzoek is uitgevoerd met behulp van een subsidie van TKI Urban Energy. Een voorwaarde om gebruik te kunnen maken van de subsidieregeling is dat het moet leiden tot nieuwe wetenschappelijke inzichten. En die inzichten zijn er ook gekomen. Niet alleen was er überhaupt weinig bekend over de invloed van dit soort dynamische systemen, maar ook de conclusie dat binnenzonwering een positieve invloed kan hebben op de koeling mag toch wel een nieuw inzicht genoemd worden. “Wat veel mensen hebben geleerd in de collegebanken is dat buitenzonwering de warmte weert en binnenzonwering niet, want in het laatste geval is de warmte al binnen. Maar dit ligt duidelijk wat genuanceerder”, vertelt Roel Loonen, universitair docent aan de TU/e. “Modern dubbelglas laat zonnestraling door naar binnen, maar weerkaatst warmtestraling als het eenmaal binnen is. Normale zonweringsdoeken absorberen de zonstraling en zetten het om in warmtestraling, waardoor het inderdaad gevangen wordt in het gebouw. Maar reflecterende binnenzonwering weerkaatst een deel van het zonlicht, waardoor dat rechtstreeks weer naar buiten gaat. Uit het onderzoek en de productontwikkeling van Kindow blijkt dat binnenzonwering niet alleen decoratief hoeft te zijn, maar daadwerkelijk een sterke bijdrage kan leveren aan het energieverbruik van het gebouw. Dat inzicht is lang niet bij iedereen bekend.”

Zonwering zelden volledig dicht

De onverwacht goede werking van binnenzonwering hoeft volgens de onderzoekers overigens geen negatieve impact te hebben op de invloed van de zon in de wintertijd, wanneer de zon bij voorkeur juist fungeert als passieve verwarmingsbron. “Intelligente zonwering werkt niet met een open-dichtsturing, maar met een regeling die rekening houdt met de stand van de zon en weersomstandigheden. Dat betekent dat de zonwering zelden volledig gesloten zal zijn, maar altijd precies afgestemd op de gewenste situatie”, legt Loonen uit. “Schijnt de zon en er is een warmtevraag, dan gaat de zonwering open en kan de verlichting dimmen. Schijnt de zon en er is geen warmtevraag, dan kan de zonwering dicht. Ook houdt het systeem rekening met de stand van de zon. Laagstaande zon kan verblindend zijn en lastig tijdens het werk, dus in de winter kan dat betekenen dat de zonwering eerder dichtgaat, afhankelijk van de positionering van het glasoppervlak.”

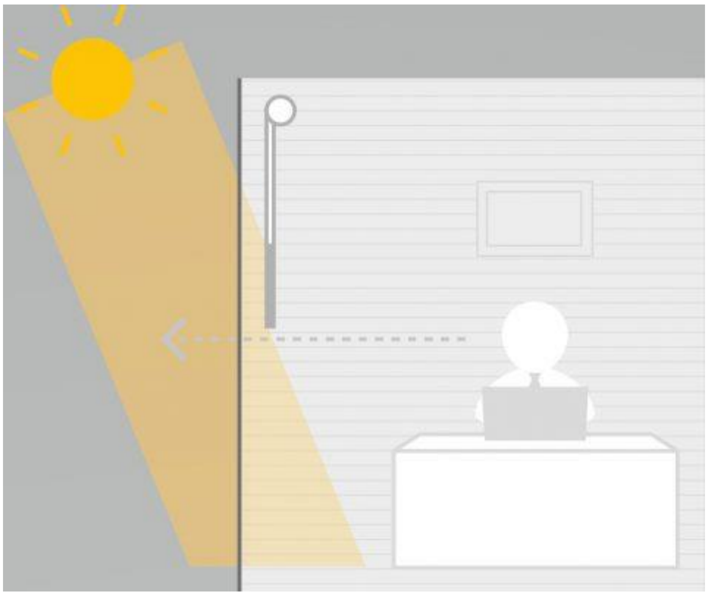

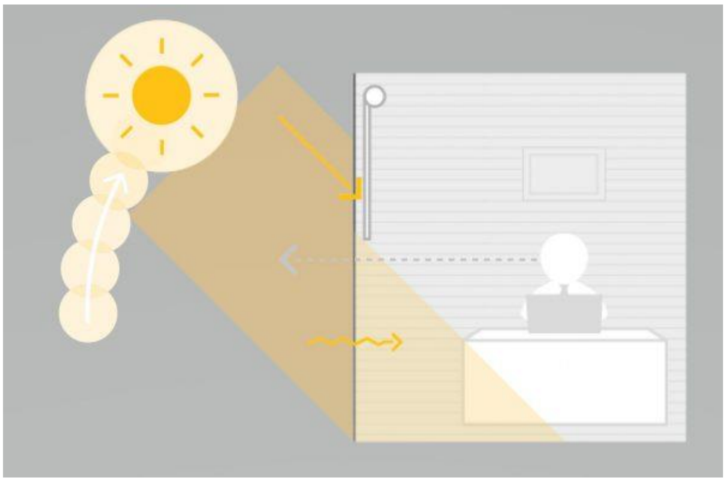

Buitenzonwering

Dat zonwering aan de binnenzijde van het glas wel werkt, neemt niet weg dat zonwering aan de buitenzijde in potentie efficiënter is, ware het niet dat er veel nadelen kleven aan dat soort systemen. Loonen: "Buitenzonwering wordt blootgesteld aan het buitenklimaat, het moet daarom bestand zijn tegen grote windbelasting, regen en temperatuurschommelingen. Dat maakt het systeem robuuster en tegelijkertijd minder geschikt voor de verfijnde aansturing die nodig is om de gunstige effecten op het binnenklimaat en energieverbruik te halen. Daarnaast is onderhoud ingewikkeld zodra het gebouw meer dan drie verdiepingen heeft. En bovendien heeft buitenzonwering ook veel invloed op het uiterlijk van het gebouw, wat niet altijd wenselijk is."

Transparanter glas

Het onderzoek leverde overigens ook nog een aanvullende conclusie op: bij intelligente zonwering kan het glas transparanter zijn dan normaal. Bij conventionele oplossingen in de markt wordt als aanvullende zonweringsmaatregel relatief donker glas toegepast met een lage zontoetredingsfactor (ZTA). "Het is een soort van compensatiemaatregel", vertelt Loonen. "Bij een slecht aangestuurde zonwering staat het systeem vaak of te ver open, of te ver dicht. Om negatieve effecten – met name met betrekking tot de koellast of oververhitting – te voorkomen wordt gekozen voor een relatief lage ZTA. Dat maakt de oplossing robuuster, maar de consequentie is dat op bewolkte dagen, of op momenten dat er geen zonnestraling op de betreffende gevel is, er ook veel minder daglicht wordt binnengelaten, met bijbehorende negatieve impact voor gezondheid, beleving en energieverbruik.”

Met een intelligente regeling is die lage ZTA volgens de onderzoekers niet nodig, omdat de zonwering dan actief is wanneer nodig en open gaat wanneer het kan. “De combinatie van reflecterende zonwering met transparant glas werkt bovendien beter, omdat op deze manier de warmte ook effectiever het gebouw kan verlaten.”

Nieuwe rekensoftware

Het doel van het onderzoek was overigens niet alleen het bepalen van de impact van intelligente zonwering en verlichting; het vormt ook de basis voor de ontwikkeling van nieuwe rekensoftware. “De bestaande rekentools zijn niet ontwikkeld met dit soort dynamische technieken in het achterhoofd, dus wij hebben gekeken welke aanpassingen daarvoor nodig zijn in de software”, legt Loonen uit. “Het onderzoek zelf is vrij gebouwspecifiek. We hebben geprobeerd een representatief gebouw te vinden, maar in Nederland zijn zoveel verschillende uitvoeringsvormen en er zijn zoveel knoppen waar je aan kunt draaien. Vandaar dat het voor de TU/e belangrijk is dat we een tool hebben waarmee we elk gebouw kunnen uitrekenen.”

Concurreren met gebruikelijke oplossingen

Vanwege de forse energiebesparing kan intelligente binnenzonwering en verlichting concurreren met gebruikelijke oplossingen zoals isolatie. Met als groot voordeel dat de implementatie van het slimme systeem eenvoudiger en goedkoper is dan bijvoorbeeld het isoleren van de schil. “We hebben veel tijd en moeite gestoken in een totaal, plug & play installatieconcept dat volledig uit te voeren is door de zonweringsmonteur en meerwerk voor een slim geautomatiseerde zonwering en opzichte van een handmatig systeem tot een minimum beperkt. Zo is voor zestig systemen maar een dubbel stopcontact nodig in de buurt van de gevel. Dat maakt het overzichtelijker en betaalbaarder”, zegt Kin. De maatregel kan dus voor kantoorgebouwen een interessante en laagdrempelige oplossing zijn en een alternatief voor andere energiebesparende maatregelen – zeker met oog op het verplichte energielabel C waaraan alle kantoorgebouwen vanaf 2023 moeten voldoen.

BENG en NTA 8800

Probleem is alleen dat slimme regeltechniek nog niet kan worden meegenomen in de BENG en NTA 8800. Dat betekent dat voor de BENG een automatisch open-dichtsysteem even goed scoort als een slim aangestuurd systeem, terwijl het onderzoek laat zien dat dit niet zo is. Kin en Loonen pleiten daarom voor een aanpassing in de BENG rekenmethodiek. Loonen: “Het grootste obstakel is de NTA 8800. Dat is een maandelijkse methode, dus één berekening per maand. Voor veel toepassingen gaat dat goed, maar hiermee is het fundamenteel onmogelijk om aan dit soort dynamische oplossingen te rekenen. Daarvoor is een uurlijkse berekening nodig. Je zou nog kunnen denken aan gelijkwaardigheidsverklaring, alleen dan krijgt het systeem een bepaalde vastgestelde score. We zijn naar de NTA gegaan om alles transparanter te maken, maar met zo’n verklaring gebeurt dat niet.”

Bewustwording

Met het onderzoek en de ontwikkeling van de software hopen Kin en Loonen bij te dragen aan de bewustwording dat je met dit soort slimme regeltechnieken veel kunt bereiken. “Het lijkt nu alsof zoveel mogelijk zonnestraling weren in kantoorgebouwen de beste oplossing is. Kleinere raamoppervlaktes en relatief dure buitenzonwering lijken dan de voor de hand liggende maatregelen om het energieverbruik te beperken. Maar dat is niet zo. Intelligente daglichtsturing kan een aantrekkelijk alternatief zijn en kan de ontwerpruimte van kantoorgebouwen vergroten en de energieprestaties verbeteren. Het maakt het mogelijk grotere ramen toe te passen voor meer uitzicht en daglicht. En omdat je geen dure buitenzonwering hoeft te plaatsen, kun je besparen op de stichtingskosten van de gevel en zo weer budget vrijmaken voor andere verbeteringen”, besluit Loonen.

Executive Board

Navigation address: De Zaale, Eindhoven
P.O. Box 513, 5600 MB Eindhoven
The Netherlands
www.tue.nl

Author
O. Ghosh
S.B. de Vries
R.C.G.M. Loonen

Date
27 August 2019

Version
1

Energy performance analysis of advanced interior solar shading systems – Kindow Rollerblinds vs. state-of-the-art alternatives

Where innovation starts

Technische Universiteit
Eindhoven
University of Technology

Table of contents

Title
Energy performance analysis of advanced interior solar shading systems – Kindow Rollerblinds vs. state-of-the-art alternatives

1 Synopsis

This report discusses the results of a series of simulation studies carried out by researchers at Eindhoven University of Technology. The study analyses the performance of rollerblinds using an advanced solar-tracking control strategy – Kindow Rollerblinds [Kindow, 2019] – in comparison to commercially available automated shading systems like external and internal roller shades with façade irradiance sensors. The results are analysed in terms of energy consumption and visual comfort. The performance of the investigated system is examined in relation to shading material properties and settings for the control parameters. The simulations are run for a test office building of $27m^2$ area and 80% WWR for a South orientation in Amsterdam.

The comparison with conventional shading systems shows that careful combination of shade materials with reflective properties and the Kindow Rollerblind control strategy can lead to 6.5% energy savings compared to external shading and 20% against internal shading systems. A common rule-of-thumb in the building industry states that “indoor shading is not effective for reducing energy demand, because the heat is already trapped inside”. This study provides clear indications that this conventional wisdom can be refuted with carefully chosen material properties and modern-day control technology. The results furthermore show that the application of the Kindow Rollerblind strategy can lead to an average increase of up to 65% (sDA300/50) in the amount of daylight entering the building. Furthermore, the simulation studies showed an increase of 22% in the operating time with an unobstructed view for the occupant. In terms of glare, the Kindow Rollerblind system has a 5 – 9% reduction to a conventional system.

2 Simulation Setup and Methodology

The reference office space developed by the International Energy Agency (IEA) Task 56 (2018) was used in this study [D'Antoni et al, 2018]. The office model has an area of 27m^2 and a South facing façade with a window to wall ratio of 80%. Table 1 illustrates all the assumptions made for the reference office. The differences amongst the cases are due to variations in shade materials, shade positioning and control strategy. In order to compare and benchmark the performance of Kindow Rollerblinds, the following case studies were considered.

- Case 1: External roller shades with reflective material properties (shade 1).
- Case 2: External roller shades with non-reflective material properties (shade 2).
- Case 3: Internal roller blinds with reflective material properties (shade 1).
- Case 4: Internal roller blinds with non-reflective material properties (shade 2).
- Case 5: Internal roller blinds with the Kindow control strategy (shade 1).

Cases 1 to 4 are the baseline cases which are chosen in such a way to represent the performance of conventional automated shading systems available in the market. Case 5 uses the same reflective shade material as case 1 and 3, but with the advanced Kindow control algorithm. The control strategies (Figure 1) are elaborated below:

- The industry standard control strategy where the roller shades are either in up or down position based on a threshold value of 200W/m^2 façade irradiance value.
- The latest Kindow Rollerblind control strategy where the rollerblind movement is based on sun tracking and senses high light and low light condition to control shade movement.
  To elaborate more on this, the system calculates the time and location of the sun at every moment. If the sun is behind the façade, the roller blind will be fully opened to allow daylight and view to enter. If the sun does fall into the field of vision of the facade, the system will try to determine whether there is a cloudy sky or a clear sky. If it is a cloudy sky, the blinds are fully opened. But when the sun is in sight and there is a clear sky, the system will lower the roller blind to such an extent that the sun is kept out of sight of the user. The height of the roller blind is determined based on the calculated position of the sun. This prevents glare from direct sunlight and reflections from the workplane. At the same time, the uncovered part of the window still allows daylight to enter the room and allows the user to retain part of his view to the outside. It is one of the more comprehensive control strategies available for Kindow products.

Performance of advanced solar shading systems depends on the interaction between the thermal and visual domains of physics. This study, therefore, uses a co-simulation method in which advanced models for thermal performance and daylight access are linked.

The co-simulation model (Figure 2) uses a link between four existing software environments where information is exchanged between the different models during simulation. EnergyPlus, a dynamic building simulation program developed on behalf of the U.S. Department of Energy, is used to simulate the thermal behaviour and energy performance of the building. The co-simulation model uses Radiance to describe the behaviour of daylight. Radiance is a collection of programs which uses 'backward raytracing' to make accurate predictions about daylight access, glare and the amount of artificial lighting required. Matlab, a mathematical programming environment, was used to implement the Kindow control algorithm. The information exchange within the co-simulation model is made possible by the software environment BCVTB (visualized by arrows in Figure 2).

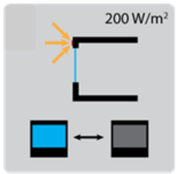

$I_{g;v}$ >200 W/m² – shades down
$I_{g;v}$ <200 W/m² – shades up

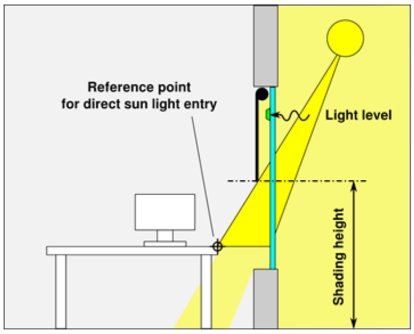

- Light level sunny: Dynamic shade height based on solar zenith and azimuth angle
- Light level cloudy: Shades are open

Figure 1: Baseline strategy and latest Kindow Rollerblind control strategy

Table 1: Modelling assumptions for the reference office for test cases.

		EnergyPlus	**Radiance**
	Dimensions	width: 4.5m; depth: 6m; height: 3m (27 m2)	
Geometry	**Window to wall ratio:**	80%	
	Type:	Solar Coating (pos. 3) double glazing with argon cavity filling,	
Fenestration	**Glazing:**	Ugl: 1.12 W/m2K Uframe: 1.5 W/m2K, SHGC: 0.306, CEN	Tvis: 0.688
	Shade 1 (Reflective):	Tsol: 0.02, Rsol: 0.74, Tvis: 0.01, Rvis: 0.72	
	Shade 2 (Non-Reflective):	Tsol: 0.02, Rsol: 0.48, Tvis: 0.01, Rvis: 0.45	
Facade		Rc = 4.5 m2K/W	rvis = 0.5
Ceiling, walls, floor		Mixed: heavy weight floor/ceiling, lightweight walls	Ceiling: rvis = 0.8, Wall: rvis = 0.5
			Floor: rvis = 0.2
	People:	3 (variable occupancy). 120 W/pers.	
Internal gains	**Occupancy:**	Weekdays: 8:00-19:00 (2860 hours/year)	
	Lighting:	10.9 W/m2 Dimming (linear between 0-500 lux) Two sensors (Figure 1) each control 50% of loads	
	Equipment:	7.0 W/m2	
	Infiltration:	ACH: 0.15	
	Ventilation:	Demand driven, 40 m3/(h*pers.), ACH: 1 (average)	
		Sensible heat recovery, eff: 70%	Sensor grid: 5x25
HVAC and settings	**Setpoints:**	Lower set point: 21°C, Upper set point: 25°C (constant)	V: -ab 12 -ad 5·104 -lw 2·10-6,
		Idealised: unlimited capacity and ideal response	D: -ab 2 -ad 103 -lw 5·10-4 -c 3000
	System efficiencies	ηe = 0.39, ηcool,deliv = 0.7, COPcool = 3, ηh = 0.95	
		Anisotropic optical model for shade	s and D: MF3
		5 min. time step	hourly time step
Weather		IWEC, Amsterdam	
Orientation		South	

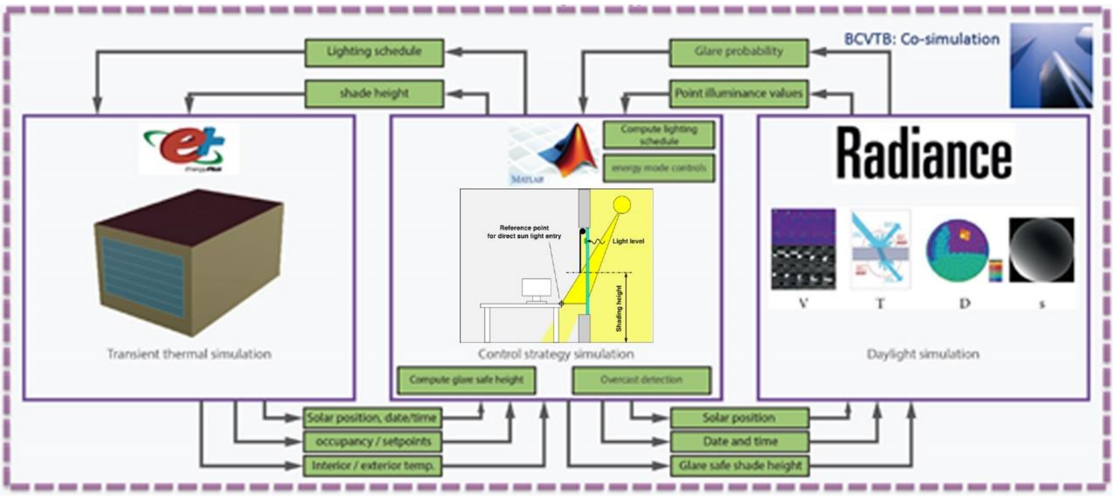

Figure 2: The co-simulation model

2.1 Performance indicators

In this study, energy performance is assessed on the basis of the energy demand for lighting, cooling and heating at room level in combination with an estimate of the primary energy consumption based on a number of system efficiency assumptions. The energy demand at room level provides an insight into the savings potential in general. It can be used to estimate the actual energy and cost savings when the Kindow Rollerblind control system is applied in combination with specific shade materials. In order to gain insight into the environmental savings potential, the primary energy consumption is also taken into account. The following reference figures have been used for this purpose. (Beck et al. 2010; Aa van der 2012).

$$E_{Prim} = \frac{E_{Light}}{\eta_e} + \frac{E_{cool}}{\eta_e \eta_c COP} + \frac{E_{heat}}{\eta_h} \quad \text{met: } \eta_e = 0.39, \;\; \eta_c = 0.7, \;\; COP = 3, \;\; \eta_h = 0.95$$

In order to assess the performance of the shading systems, a series of performance indicators have been selected. In order to quantify the degree of daylight access, this study will use daylight autonomy (DA) and spatial daylight autonomy (sDA). Daylight autonomy can be interpreted as the percentage of time that a measuring point receives 'sufficient' daylight. For this indicator, the abbreviation DA300 is often used, where 300 stands for the number of lux that is set as a limit value. Spatial daylight autonomy enables us to express daylight access to a room as a whole in one number. It is defined as the percentage of the floor area with a daylight autonomy higher than fifty percent. Spatial daylight autonomy can be interpreted as the fraction of the floor area that receives sufficient daylight most of the time (Reinhart, Mardaljevic, and Rogers 2006). For this indicator, the abbreviation sDA 300/50 is often used, where 300 stands for the limit value in lux and 50 for the required exceeding percentage of the usage time.
In this report, 'daylight glare probability simplified' (DGPs) is used as an indicator to assess the risk of glare (Wienold 2009). Although much is still unknown in the field of glare perception and assessment, it is certain that glare is associated with high luminance differences in the field of view, with the total luminance at eye level, as well as with the position of glare sources in relation to the focus area of the eye task. The DGPS indicator is primarily based on vertical illuminance but neglects the influence of peak glare sources. In this report, a DGPs limit of 0.40 has been considered for occupied hours when the glare is weaker than ‘disturbing’. And the DGPs values are considered at the two sensor points as shown in figure 3, one has a viewing angle of 45 degrees and the other at 0 degrees meaning it is directly facing the wall. The maximum value

out of the two sensor points is considered at each timestep and then the DGPs is evaluated for the whole year.

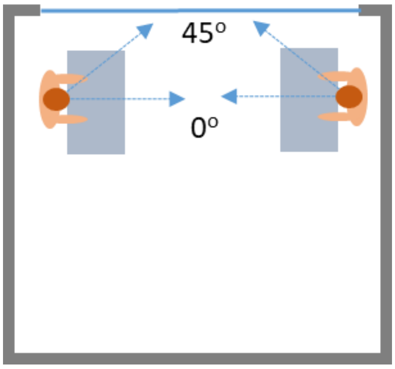

Figure 3: Positioning of the sensor point and the viewing angles considered for dgp calculations

3 Results

3.1 Energy Performance

Figure 4 shows the comparison of energy demand of the different cases considered for a south-facing office space in Amsterdam. The external shading system has much lower cooling demands in comparison to the internal shading systems as it can keep the solar radiation from entering the test space, but this also increases their heating demand considerably. Simple changes like the choice of using reflective shading material instead of the conventional non-reflective one can have quite an impact on the performance of these systems. For external shades (cases 1 and 2), this change accounts for 5.0% and 12.5% reduction in lighting and cooling demands. For internal shades (case 3 and 4), use of reflective shade material leads to 6.5% and 24.0% reduction in lighting and cooling demands respectively. The reductions seen in lighting demands is due to the angular behaviour of the reflective material which leads to difference in transmittance. And reduction in cooling is due to the reflectance property of the material, hence the reduction in cooling demand is more apparent for internal shades than external ones.

Since case 1 to 4 (conventional indoor and outdoor shading systems) use the same control strategy based on façade irradiance, the lighting demand is comparable for all these cases. Although at a closer look, one can notice a 5 – 6% reduction in lighting demand because of the use of reflective shades in cases 2 (baseline_externalshade) and 4 (baseline_internalshade) respectively. Case 5 (Kindow Rollerblind control), which uses the same reflective shading material as case 2 and 4, has an improved heating and lighting demand in comparison to the rest of the cases. For example, heating demand is reduced by an average of 25% in comparison to internal shades (case 3 and 4) and by an average of 50% against external shades (case 1 and 2). And lighting demand is reduced by an average of 44% against all cases 1 - 4. This improvement is because of its use of the complex sun tracking algorithm that considers sun position and sky brightness for its positioning during occupied hours.

On the other hand, there is also a 25% increase in cooling demand in comparison to case 4 (baseline_internalshade_reflective), as the current version of the control strategy allows more time with its shades up and unobstructed view of the outdoors to the occupant. This increase in cooling demands is less decisive for the total primary energy consumption and the influence of lighting is relatively large due to the system efficiency factors associated to meeting different types of loads.

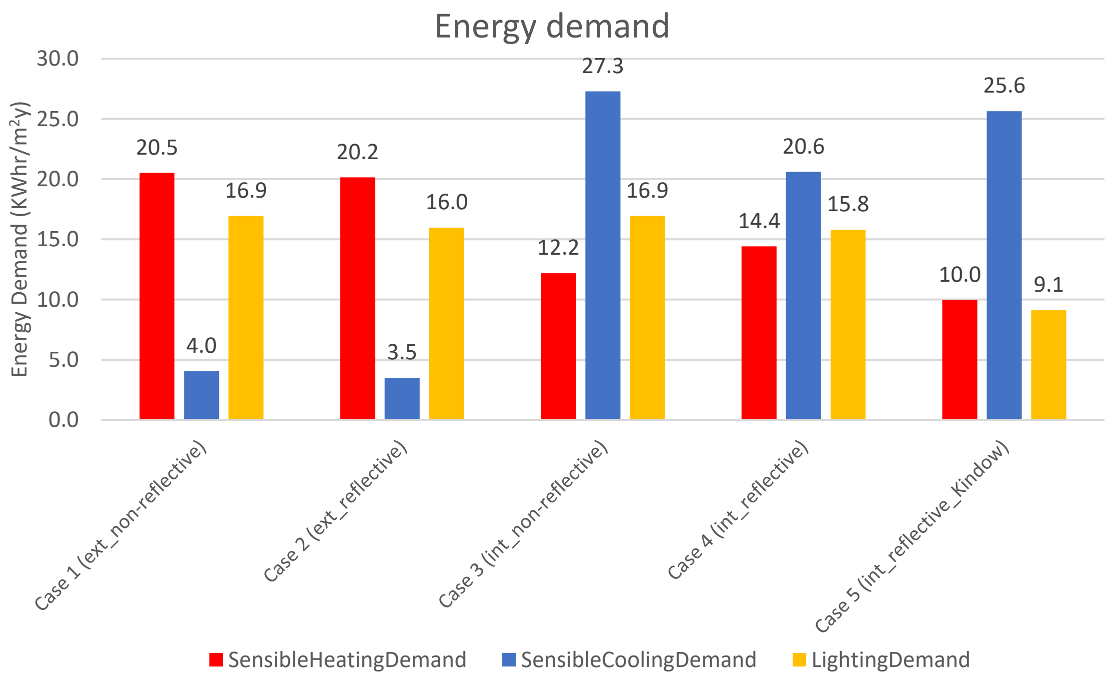

Figure 4: Annual energy demand comparison

As we can see in figure 5, the primary energy consumption shows that indoor shading systems with careful combination of shading material and control strategy (case 5) can outperform external shading systems (case 2) by a 6.5%.

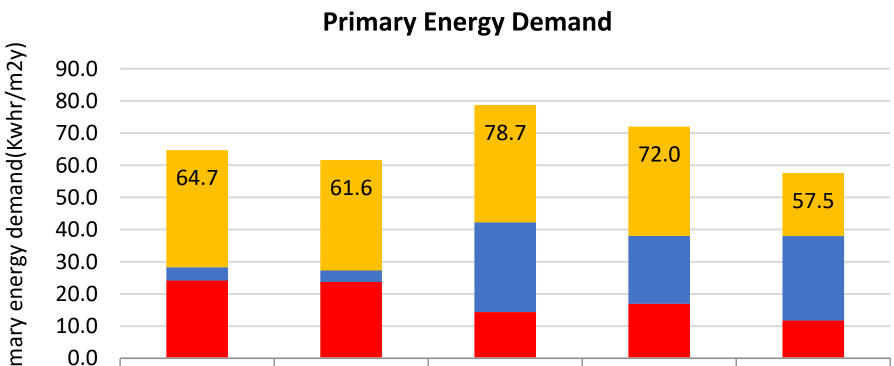

	Case 1 (ext_non-reflective)	Case 2 (ext_reflective)	Case 3 (int_non-reflective)	Case 4 (int_reflective)	Case 5 (int_reflective_Kindow)
LightingPrimEn	36.4	34.3	36.4	34.0	19.6
SensibleCoolingPrimEn	4.1	3.6	27.9	21.1	26.3
SensibleHeatingPrimEn	24.1	23.7	14.3	17.0	11.7

SensibleHeatingPrimEn SensibleCoolingPrimEn LightingPrimEn

Figure 5: Primary energy demand

It can also be seen that the use of Kindow Rollerblind control strategy (case 5) leads to an average 40% reduction in primary lighting energy demand in comparison to the rest of the cases. This also highlights that lighting energy has a greater influence on overall energy consumption compared to heating or cooling loads.

As the visible transmittance of both shade materials were kept identical at 0.012, the variation in reflective and non-reflective shading did not have a significant impact on visual performance. There is, however, a remarkable difference because of the change in control strategy.

3.2 Visual Performance

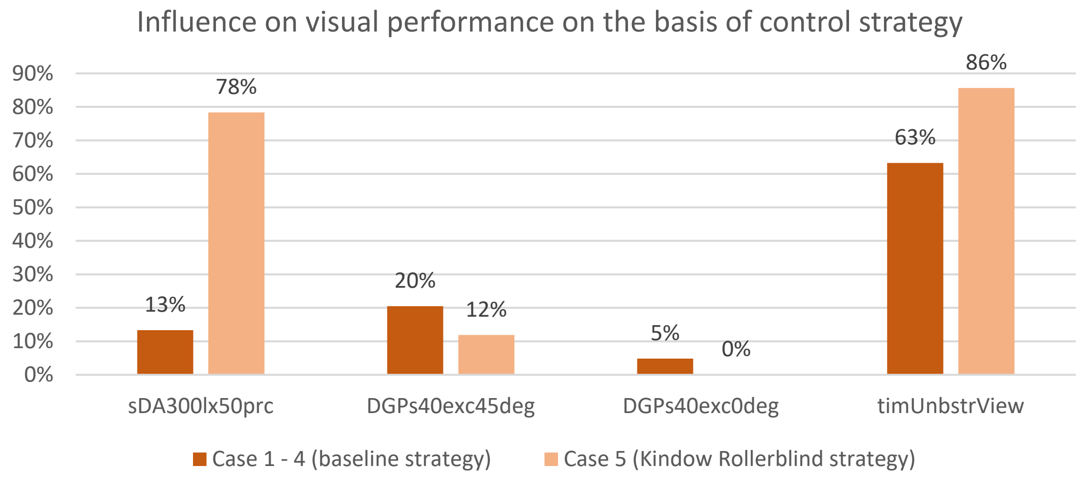

Figure 6: Influence of control strategy on visual performance.

There is a 65% increase in spatial daylight autonomy and 23% increase in percentage of time with an unobstructed view. An Unobstructed view means whenever the shades are above the height of the occupant's eyelevel. The Kindow Rollerblind strategy allows the shades to be more open than the baseline strategy thereby causing this remarkable improvement in the daylighting gains and view in the space. Also, its strategy for obstructing direct sun and instances of high illuminance sky conditions has resulted in 8% reduction in Glare values for 45º viewing angle and complete removal of glare problems when the occupant is sitting parallel to the window (0º).

3.3 Conclusion

From this study it can be concluded that use of reflective materials and the Kindow Rollerblind control strategy has great potential to optimise automated indoor shading systems according to building characteristics, user preferences and objectives. The possibilities in terms of energy saving and optimizing user comfort can be significantly increased. Primary energy consumption is reduced by 6.5% in comparison to external shading systems whereas there is a 20% drop in primary energy demand when compared to indoor shading systems. The use of the Kindow Rollerblind strategy greatly improves the amount of daylight entering the space. As much as 65% increase in terms of spatial daylight autonomy and 9 and 5% decrease in glare probability for viewing angles 45 and 0 degrees respectively. It also questions the common rule-of-thumb that outdoor shading systems perform better as it keeps the solar radiation out before it enters the building through the glazing. And also illustrates that such conception doesn't necessarily guarantee good building performance. The study provides clear pointers that that careful combination of glazing and shading properties, and control strategies is important for optimal energy performance. Using reflective shade material instead of conventional non-reflective ones is likely the first step to improving energy demands. Consequently, major improvements in visual performance as well as energy demands can be obtained by using a refined and complex control strategy as used by Kindow.

4 Reference

1. Aa van der, R. 2012. "NEN 7120+ C2: Energieprestatie van gebouwen-Bepalingsmethode." In. Delft: Stichting Nederlands Normalisatie-instituut (NEN/CEN).

2. Beck, W, D Dolmans, G Dutoo, A Hall, and O Seppänen. 2010. "Solar Shading. REHVA Guidebook 12." In.: Forssa, Finland.

3. D'Antoni, Matteo, Paolo Bonato, David Geisler-Moroder, Roel Loonen, and Fabian Ochs. 2018. "IEA SHC T56 - System Simulation Models: part C." In. Paris: IEA.

4. Kindow B.V. 2019. Last accessed 27 august 2019. http://www.kindowblinds.com/

5. Reinhart, Christoph F, John Mardaljevic, and Zack Rogers. 2006. 'Dynamic daylight performance metrics for sustainable building design', Leukos, 3: 7-31.

6. Wienold, J. 2009. Daylight glare in offices. (Fraunhofer and Universität Karlsruhe (TH): Freiburg, Germany).

System Simulation Results

IEA SHC TASK 56 | Building Integrated Solar Envelope Systems for HVAC and Lighting

System Simulation Results

Deliverable DC.2

Authors: Ochs Fabian, Magni Mara, Hauer Martin, Geisler-Moroder David, Bonato Paolo, de Vries Samuel, Loonen Roel, Venus David, Abdelnour Nermeen, Calabrese Toni, Venturi Elisa, Maccarini Alessandro, Häringer Simon, Bueno Bruno, Ioannidis Zissis, Rounis Efstratios

April, 2020
DC.2, DOI: 10.18777/ieashc-task56-2020-0005

IEA Solar Heating and Cooling Technology Collaboration Programme (IEA SHC)

The Solar Heating and Cooling Technology Collaboration Programme was founded in 1977 as one of the first multilateral technology initiatives ("Implementing Agreements") of the International Energy Agency. Its mission is *"To enhance collective knowledge and application of solar heating and cooling through international collaboration to reach the goal set in the vision of solar thermal energy meeting 50% of low temperature heating and cooling demand by 2050."*

The members of the IEA SHC collaborate on projects (referred to as Tasks) in the field of research, development, demonstration (RD&D), and test methods for solar thermal energy and solar buildings.

Research topics and the associated Tasks in parenthesis include:

- Solar Space Heating and Water Heating (Tasks 14, 19, 26, 44, 54)
- Solar Cooling (Tasks 25, 38, 48, 53)
- Solar Heat for Industrial or Agricultural Processes (Tasks 29, 33, 49, 62, 64)
- Solar District Heating (Tasks 7, 45, 55)
- Solar Buildings/Architecture/Urban Planning (Tasks 8, 11, 12, 13, 20, 22, 23, 28, 37, 40, 41, 47, 51, 52, 56, 59, 63)
- Solar Thermal & PV (Tasks 16, 35, 60)
- Daylighting/Lighting (Tasks 21, 31, 50, 61)
- Materials/Components for Solar Heating and Cooling (Tasks 2, 3, 6, 10, 18, 27, 39)
- Standards, Certification, and Test Methods (Tasks 14, 24, 34, 43, 57)
- Resource Assessment (Tasks 1, 4, 5, 9, 17, 36, 46)
- Storage of Solar Heat (Tasks 7, 32, 42, 58)

In addition to our Task work, other activities of the IEA SHC include our:

- International Conference on Solar Heating and Cooling for Buildings and Industry
- SHC Solar Academy
- Solar Heat Worldwide annual statics report
- Collaboration with solar thermal trade associations

Country Members

Australia	France	South Africa
Austria	Germany	Spain
Belgium	Italy	Sweden
Canada	Netherlands	Switzerland
China	Norway	Turkey
Denmark	Portugal	United Kingdom
European Commission	Slovakia	

Sponsor Members

European Copper Institute	ECREEE
International Solar Energy Society	RCREEE
EACREEE	SACREEE

For more information on the IEA SHC work, including many free publications, please visit www.iea-shc.org

Contents

2.2.6 Kindow sun tracking vertical blinds

Samuel de Vries[a], Roel Loonen[a]

[a]Eindhoven University of Technology, Eindhoven (The Netherlands)

Goal of this case study

Different façade solutions each come with different investments, operational costs and benefits. In designing facades and selecting glazing and solar shading systems, the competing performance aspects of visual comfort, daylighting performance, thermal comfort, costs and energy performance will therefore need to be balanced. This task is complicated by the fact that the effects of glazing and shading solutions on building energy performance are increasingly being determined by interactions between the thermal and the visual domain. The traditional approach in the building industry has been to treat these two physical domains as separate design and engineering problems but with the advent of daylight dimming, high reflectance metal coatings and advanced solar shading controls, these domains are becoming increasingly interlinked.

The goal of this case study is to illustrate how simulations can be used to find balanced trade-off solutions considering the multitude of conflicting performance aspects in the selection of solar shading and glazing technologies. Additionally, this case study will explore how the design space for such solutions can evolve as a result of changes in the technical and economic context. In this study, the performance of the Kindow sun tracking vertical blind system (DA.1+2 page 67) will be assessed in relation to other conventional solutions for controlling the admission of solar heat gains and daylight.

Approach

In this study, two conventional control approaches (both titled baseline) for roller blinds will be compared to three different versions of the Kindow sun tracking blinds strategy (**Table 2-20**). For both the baseline and the Kindow control strategy multiple variations to the main control approach will be evaluated. These variations relate to different control settings which can be chosen to admit more or less daylight.

The baseline strategies fully raise or lower the roller blind in response to a sensor threshold. Here two alternatives are used which either prioritise visual comfort (vertical indoor illuminance sensor [E_v] and a 6400 lux threshold) or the admission of daylight (vertical exterior irradiance sensor [$I_{g;v}$] and a 200 W/m^2 threshold).

The Kindow blind system is developed by the company Kindow B.V. in the Netherlands. The Kindow system (**Figure 2-71**) utilises vertical blinds made out of a fabric with a high solar reflectance metal coating on one side. The blinds are operated in relation to the position of the sun and indoor daylight conditions. Under bright sky conditions the blinds track the sun to prevent occupants from perceiving glare from direct sunlight whilst admitting daylight and views to the outdoors. Under overcast conditions, or when the sun is not in view of the façade, the system fully opens.

Three variations to the Kindow strategy will be evaluated:

- The first variation, titled Low+High, employs the most closed form of sun tracking which prioritises visual comfort over daylighting performance;
- The second variation, titled Low+Mid+High, prioritises the admission of daylight and tracks the sun in a way which allows for a greater visibility of the sky;
- The third strategy is identical to the second one with the exception that this strategy employs a slightly wider slat such that the edges of the blind overlap in a fully closed position. The overlapping blinds help prevent visual disturbance from direct sunlight being visible during small dangling movements of the blinds. In this alternative a full rotation of the blinds is not possible because the width of the slats is larger than their individual spacing. In this strategy both sides of the blind have to therefore be used in order to track the sun and the metallised side is facing the sun only during the morning.

The admission of solar radiation depends on interactions between the glazing and solar shading system. Important factors are the position of the solar shading system, its solar reflectance and transmittance, the type of glass coating that is used and its position inside the glazing system. In this study, three alternatives will be assessed (**Table 2-21**): high solar gain glazing (low reflectance low-E coating in position 2) in combination with a metallised interior shading system, solar control glazing (high reflectance low-E coating in position 2) in combination with a metallised interior shading system, and high solar gain glazing (low reflectance low-E coating in position 3) in combination with a non-metallised exterior shading system. All shading fabrics have an identical visual and solar transmittance. The three alternatives each offer a distinct set of visual and thermal properties and have different investment and maintenance costs associated to them.

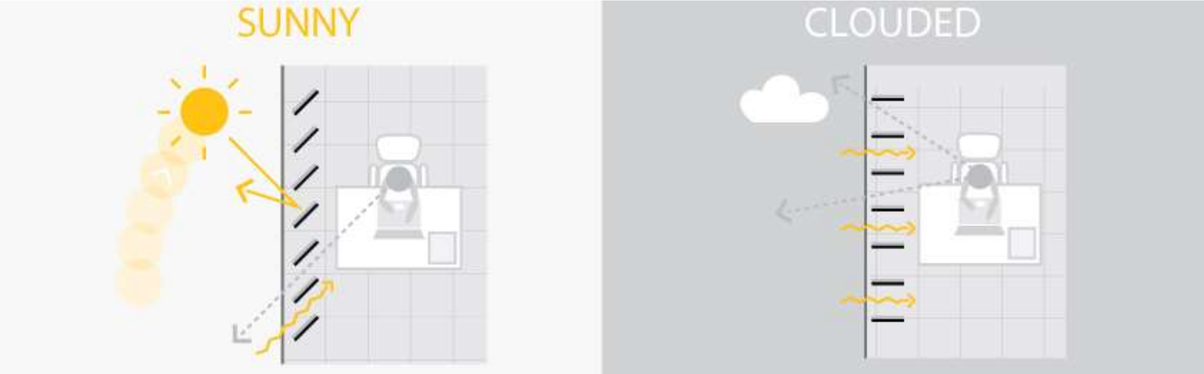

Figure 2-71 The Kindow sun tracking vertical blinds system

The reference office that is used in this case study largely follows the description given in DC.1. **Table 2-20** and **Table 2-21** give an overview of the assumptions in this case study that differ from the general description of the reference office building reported in the report DC.1.

Table 2-20: Solar shading control strategies and assumptions

Shading strategy	Control approach
Conventional roller blind (BL: Baseline)	Conventional: Down if $I_{g;v}$ > 200 W/m^2 else up Conventional: Down if E_v > 6400 lux else up
Kindow sun tracking vertical blinds (Kindow verticals)	Most closed sun tracking (Low+High), always reflecting Most closed and more open sun tracking (Low+Mid+High), always reflecting Most closed and more open sun tracking (Low+Mid+High), reflect in morning

Window to wall ratio	80%, South facing window
Climate	Amsterdam, the Netherlands (IWEC database)
Daylight dimming	None or linear dimming (500 lux target work plane E_h) using two lighting zones
HVAC conventional	Gas furnace and low efficiency air-source compression cooling. $\eta_{cool,deliv}$ = 0.7 (air system eff. cooling), COP_{cool} = 3, η_h = 0.85 (heating system eff.)
HVAC all-electric	Air source heat pump for heating and cooling as described in appendix 0
Primary energy ratios (PER)	EU_{total} $2.5_{constant}$, $10\text{-}10\text{-}10_{non\text{-}ren.,varying\ monthly}$, $10\text{-}30\text{-}30_{non\text{-}ren.,varying\ monthly}$ (see Appendix A.1 in report DC.1)

Table 2-21: Glazing and shading parameters

Glazing types	High solar gain glazing P2[7] (LoE)	High solar gain glazing P3[7] (LoE)	Solar control glazing P2[8] (SC)
	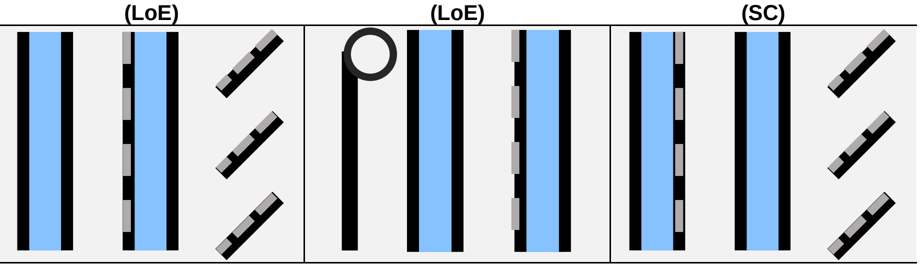		
SHGC	0.60	0.62	0.31
T_{vis}	0.82	0.82	0.70
Investment [€/m^2_{facade}]	40	40	70
Lifetime	50	50	50
Type of solar shading	**Interior, metallised fabric, Rs:80%**	**Exterior, regular fabric, Rs:55%**	**Interior, metallised fabric, Rs:80%**
SHGC	G:0.60, G+S: 0.19[9]	G:0.62, G+S: 0.06[9]	G:0.31, G+S: 0.11[9]
T_{vis}	G:0.82, G+S: 0.01[9]	G:0.82, G+S: 0.01[9]	G:0.70, G+S: 0.01[9]
Investment [€/m^2_{facade}]	BL:70, Kindow:80	BL: 166	BL:70, Kindow:80
Maintenance [€/y·m^2_{facade}]	4	8	4
Lifetime [Years]	12	20	12

Table 2-22: Shading / fenestration technology design space

Glazing + shading	**Shading control**				
	Kindow verticals			**Conventional**	
	Low, High, Reflect always	Low, Mid, High, Reflect always	Low, Mid, High, Reflect in morning	Baseline: $I_{g;v}$ > 200 W/m2	Baseline: E_v > 6400 lux
Low-E P2, Internal fabric	S.1 DD[10]	S.2 DD[10]	S.3 DD[10]Error! Bookmark not defined.	S.4 DD[10]	S.5 DD[10]
SC P2, Internal fabric	H.1 DD[10]	H.2 DD[10]	H.3 DD[10]	H.4 DD[10]	H.5 DD[10]
Low-E P3, External fabric				P.4 DD[10]	P.5 DD[10]
Low-E P3, External fabric				C.4 no-DD[7]	C.5 no-DD[11]

Table 2-22 gives an overview of the full design space of glazing, shading and control alternatives that is evaluated in this study. Two additional alternatives are included which do not include daylight dimming of artificial lighting. These alternatives are otherwise identical to the conventionally controlled alternatives with external shading. The two alternatives without daylight dimming are most similar to the DC.1 description and they are included to assess what performance gains can be attributed to the daylight dimming system alone.

For assessing visual (dis)comfort, DGPs (DC.1 5.4 and DC.2 2.1.2), and the fraction of occupied time with at least disturbing glare (DGPs ≥ 0.4) will be used. Here a distinction is made between two viewing directions: one where the occupants are facing the window at 45 degrees and one where the occupants are facing a side-wall. For each viewing direction, two seating positions are used; one facing east and one facing west. At each time step, the maximum DGPs value of both positions is used. Daylighting performance is operationalised using $sDA_{300lx/50\%}$ (DC.1 5.4). Energy performance is assessed using the primary energy consumption for heating, cooling, lighting, ventilation and equipment. The effects of two different HVAC concepts and three different primary energy ratio (PER) scenarios are evaluated (**Table 2-20**). The economic costs and benefits over the entire lifetime of the different solutions is evaluated using total annual costs as an indicator. In this approach the investment costs of technologies with different lifespans are computed into Equivalent Annual Costs using an assumed annual interest rate according to the method presented in DC.1 chapter 5.5 and summed with operational energy and maintenance costs. In this study, the costs for glazing, shading, daylight dimming and cooling and ventilation systems are included (**Table**

[7] Coating in position 3 (outside of inner glass pane)
[8] Coating in position 2 (inside of outer glass pane)
[9] G: Glazing only, G+S: Glazing with fully closed shading
[10] DD: With daylighting dimming of artificial lighting
[11] no-DD: Without daylighting dimming of artificial lighting

2-23). The sizing dependent costs of cooling and ventilation are estimated for each alternative using a load duration curve and 125 allowed temperature exceedance hours as a criterion. The uncertainty related to assumptions regarding costs, lifespan, interest rates, and energy prices is evaluated by varying the assumptions using ranges taken from 2.2.2 which are shown in **Table 2-23**. For assessing the aforementioned performance indicators the co-simulation model, discussed in chapter 2.1.4.2, is used [11].

Table 2-23: Other costs and parameters for economic performance assessment

	Investment:		Lifetime:	
Daylight dimming system (TL-5 not included)	12	€/m^2_{floor}	20	years
Variable sizing dependant costs of cooling and ventilation:	518	€/kW	30	years
Revenue per employee (3 in room)	50000	€/year		

	Min:	Median:	Max:	
Assumed productivity increase from Kindow	0%		1%	
Uncertainty ranges for life time, investment and maintenance costs	90%	100%	110%	
Annual interest rates	2%	3%	4%	
Average electricity price over period			0.23412	€/kWh
Average gas price over period			0.5805	€/nm^3
Uncertainty ranges for energy costs	80%	100%	120%	

Results

Figure 2-72 shows the daylighting and glare performance of the investigated solar shading and glazing solutions. Using this graph the following can be concluded:

- Conventionally controlled alternatives (numbers 4 and 5) lead to poor daylighting performance (0-24% sDA300lx/50%) whilst the Kindow strategies offer a very desirable daylighting performance (74-99% sDA300lx/50%) which comes close to the daylighting performance without any shading system (100%, yellow markers).

- The Kindow strategies (numbers 1-3) are each designed to prevent 'disturbing' glare at all times in the most critical viewing angle, where the occupants are facing the wall. For this viewing direction, the Kindow strategies perform significantly better than the baseline 200W/m^2 strategy (5-8% less DGPs0.4 exceedance).

- For the viewing direction facing the window, the Kindow strategies perform better to slightly worse as the baseline 200W/m^2 strategy (number 4), depending on which Kindow alternative is chosen. Although the control threshold can be chosen more stringently in the conventional strategies, such that glare is always prevented (number 5: baseline 6400lx), doing so would have a severe negative impact on daylighting performance (0% sDA300lx/50%).

- The trade-off between prohibiting visual discomfort and maximizing the admission of daylight is more desirable for Kindow than it is for the conventional approaches.

- Choosing for solar controlled glazing (hexagrams) can improve visual comfort (0-6% decrease in DGPs0.4 exceedance) and have a negative effect on daylighting performance (5% decrease in sDA300lx/50%). These effects are, however, very small in comparison to the effects that can be achieved by choosing a particular shading control strategy.

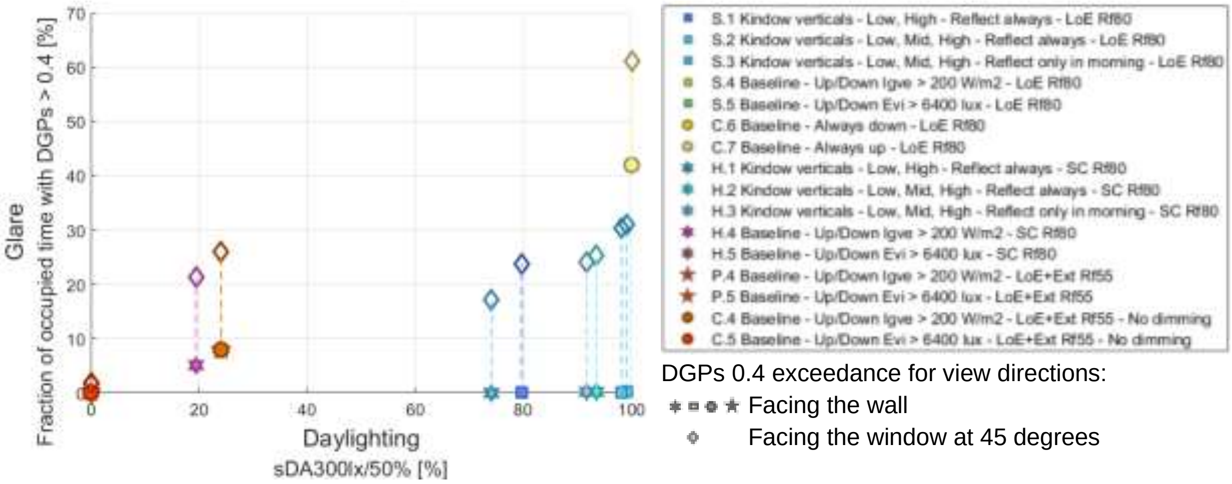

Figure 2-72: Daylighting and glare performance of different shading strategies and glazing systems. Glare is expressed as the fraction of occupied hours with DGPs > 0.4 for two viewing directions

In **Figure 2-73**, the energy performance and costs associated with each glazing and solar shading alternative are explored in relation to different scenarios for the primary energy ratio of electricity and in combination with two HVAC concepts. In each individual graph, primary energy consumption and total costs are expressed as a difference between each alternative and a common baseline. Here, the alternative with daylight dimming, an external shading device, and the baseline$_{6400lux}$ control approach (prioritises visual comfort) is chosen as the common baseline (orange pentagram) and is plotted at the origins of each axis. In these graphs, positive values for ΔPE and ΔTotal annual costs indicate that the alternative in question offers a reduction in primary energy consumption and total annual costs, respectively. The vertical dashed lines in this graph represent the spread in total costs as a result of variations in underlying assumptions regarding investment costs, lifespan, interest rates and energy prices. The marker in this graph is placed at the median of all ΔTotal annual costs outcomes. It should be noted that the plotted spread gives the degree of uncertainty in the difference between a particular solution and the common baseline. This spread given for a particular alternative is therefore indicative of the uncertainty in the predicted costs of both that alternative as well as that of the baseline.

Figure 2-73 A shows the results for a conventional low-efficiency HVAC system and assuming the EU-2.5 total primary energy ratio. These assumptions are in line with current building codes and the electrical primary energy ratios in the Netherlands in the past decade. By comparing the conventionally controlled approaches (numbers 4 and 5) in combination with different glazing/shading configurations (S: squares, H: hexagrams, P: pentagrams), the following can be observed:

- Metallised indoor solar shading (S and H) is more beneficial in terms of total costs. This difference in costs can be primarily attributed to the lower maintenance costs of indoor solutions but their lower initial investment costs also contribute strongly.
- The energy performance of the high solar gain (S), solar control (H), and exterior shaded glazing (P) shows that reducing solar heat gain appears to improve overall energy performance.
- Using solar controlled glazing with a metallised indoor shading fabric (H) gives the most beneficial trade-off between total costs and primary energy consumption. This solution offers a lower energy consumption for similar total costs as using high solar gain glazing (S) with indoor shading. Compared to the external shading device alternative (P), the solar control glazing solution has a slightly higher primary energy consumption but it is significantly less expensive.
- Implementing a daylight dimming device (pentagrams P in relation to circles C) significantly improves energy performance. The effects on primary energy consumption are of the same order of magnitude as the choices made concerning the glazing/shading configuration.
- Implementing a daylight dimming device has a positive effect on total costs. This effect is much smaller, however, than the difference between indoor and outdoor shading.

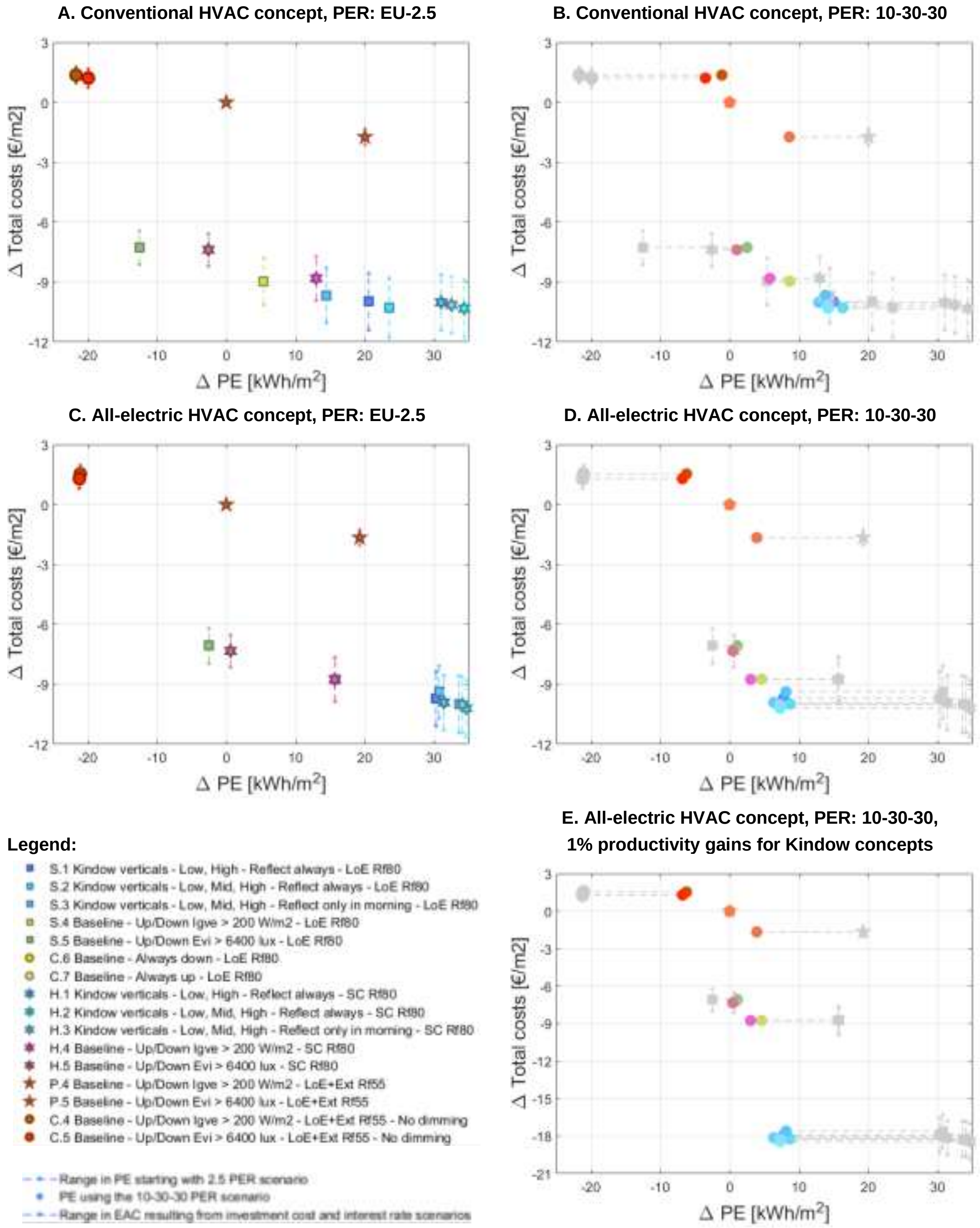

Figure 2-73: Difference in primary energy consumption (ΔPE) and total annual costs (ΔTotal costs) of different shading strategies and glazing systems compared to the outdoor roller blind baseline.

From a comparison of the Kindow control concepts with the alternative approaches the following can be concluded:

- Kindow (S and H numbers 1-3) offers significant reductions in terms of primary energy consumption for similar costs as the other indoor solution solutions (S and H numbers 4-5).
- Kindow with high solar gain glazing (S.1-3) leads to similar energy performance as conventionally controlled exterior solar shading (P.4-5) but does so at much lower total annual costs.
- Using a Kindow solar shading system together with solar control glazing (H.1-3) gives offers the most optimal overall performance.

Figure 2-73 C shows the same comparison as in **Figure 2-73 A,** but now for the all-electric HVAC concept. Compared to the conventional HVAC concept the following aspects change in the all-electric concept:

- Increased heating and cooling efficiency reduce the overall primary energy consumption for all alternatives. For most alternatives, however, the differences with the common baseline (ΔPE) remain largely unchanged.
- The energy performance of the high solar gain glazing alternatives (S) improves relative to the solar control glazing (H) and exterior shading alternatives (P).
- This can be explained by the higher efficiency of cooling equipment which reduces the impact that undesired solar gains have on overall energy performance. The electrification of heating, in combination with a high PER, increases the relative importance of heating and desired solar gains in the heating season.

The graphs **B** and **D** in **Figure 2-73** show the same evaluations as in **A** and **C** but now assuming the 10-30-30 primary energy ratio scenario. In these graphs the following can be observed:

- The differences in primary energy consumption become smaller in absolute terms.
- Alternatives which reduce solar heat gains no longer offer superior energy performance. The low primary energy ratios associated to the abundance of renewable electricity during the summer months reduce the importance of cooling.
- The choice in glazing/shading configuration hardly affects energy performance. Daylight dimming and the solar shading control strategy do still affect energy performance significantly. The hierarchy of solutions in terms of energy performance shown in graphs **C** and **D** reflects the daylighting performance of the different alternatives.

Discussion and conclusion

Some aspects of this case-study require elaboration and place some limitations on the interpretation of its conclusions. This study focussed on a south facing perimeter office in the Dutch context.

The way in which total costs are operationalised in this study allows for a comparison of solar shading and glazing solutions on the basis building related costs but it omits the operational benefits that improved visual comfort and exposure to daylight and views could have on the well-being and productivity of office workers. Although there is sufficient research indicating that such benefits exists, it is difficult to translate these findings into quantifiable improvements from specific daylighting technologies ([35], [36], [37], [38], [39]). Considering that, for a typical office building, building related costs constitute only 10% of the total operating expenses and salary and employee related costs can be as high as 80% ([37], [40]), it is likely that potential productivity improvements will have a very strong effect on total costs. **Figure 2-73 E** illustrates the extent to which potential productivity gains might influence the total costs presented in this study. Here the assumption is made that the improved visual comfort and daylighting performance would lead to an increase in productivity of 1% compared to the conventional shading control alternatives

This assumption can be considered as a conservative estimate in comparison to what is reported in the aforementioned literature. The graph shows that, even with a conservative estimate, the effects of including productivity gains in the total cost are as large as the difference between the best and the worst conventionally controlled alternatives.

From this study, the following can be concluded:

- The Kindow solar shading concept offers superior daylighting, visual comfort and energy performance compared to conventional automated solar shading solutions. This conclusion is robust with respect to different assumptions regarding PER scenarios, HVAC concepts and glazing systems.
- The presence of a daylight dimming system is an essential condition for the Kindow system to offer improvements in energy performance over conventional automated control approaches.
- With regards to building related costs, the Kindow system performs similar to other indoor solar shading solutions.

- More efficient cooling systems and improvements in the PER of electricity will decrease the relative importance of energy performance in relation to other performance aspects in the selection of glazing and solar shading systems.

- If daylight dimming systems and more efficient cooling systems become more ubiquitous, and the presence of renewable electricity from PV gives rise to favourable PER in the summer months, reducing solar heat gains will become less important in the selection of glazing and the control of solar shading systems. Effective daylighting becomes the most defining aspect in improving energy performance.

- For daylighting technologies, the financial benefits of an improved visual environment are likely to be large in comparison to differences in terms of other operational costs. Although more research is needed in order to quantify these financial benefits, there is sufficient evidence to weigh potential improvements in the visual environment strongly in relation to energy performance and building related costs.

Coupled design optimization of façade design and automated shading control for improving visual comfort in office buildings

Kim Bodde | 1273329

Department of the Built Environment
Unit of Building Physics and Services
Eindhoven University of Technology

Supervisor
Prof.dr.ir. J.L.M. (Jan) Hensen | Eindhoven University of Technology
Dr.ir. R.C.G.M. (Roel) Loonen | Eindhoven University of Technology
Ir. S.B. (Samuel) de Vries | Eindhoven University of Technology

Eindhoven, 2 March 2020

Summary

Solar shading is an important feature of high-performance building design, as these systems can determine the access of natural daylight illuminance, prevent glare, enable view to outside and have an impact on the energy balance of a building. Research shows that daylight and view to the outside can improve the occupant well-being, workplace productivity and satisfaction by positively influencing various psychological and physical processes. Given that most working adults spend the majority of their time indoors, it is important that we optimize the indoor environmental quality. Appropriate design and control of solar shading systems can play a prominent role in this respect, by finding balanced trade-off solutions among the various competing performance aspects.

Various shading systems have merits and disadvantages. Static shading solutions offer interesting opportunities for architectural integration but they have the drawback that they cannot respond to changing weather conditions. Dynamic shading systems such as verticals blinds or a roller blind, on the other hand, can be adapted to outside conditions and occupant preferences, bringing more flexibility for energy and comfort management during building operation. However, their control can be complex, and dynamic shading system significantly limit the admission of daylight views to outside. Whereas horizontal shading systems can block effectively the summer sun around mid-day, vertical shading is more preferable in the early morning and late noon.

Based on: i) the aspiration to maximize the positive influence of daylight and view, ii) the application-specific strengths and weaknesses of the various shading typologies, and iii) the promising potential of novel automated control strategies, it is hypothesized that the visual comfort in office buildings can be improved through coupled design optimization of façade design and automated shading control. Two simulation studies are performed to evaluate and compare the visual performance of dynamic and static shading, individually and combined. Both studies focus on finding synergies in the combination of horizontal and vertical shading topologies. The first case study regards an interior roller blind and exterior fins. The second case study focuses on interior vertical blinds and an overhang. Both studies are performed for a south-oriented test office building of 27m² area in Amsterdam with a window-to-wall ratio of 80%.

Three performance indicators are considered for evaluating of the visual comfort: Daylight Glare Probability Simplified (DGPs) for glare, spatial Daylight Autonomy (sDA) for daylight utilization and View Fraction for view to the outside. A multi-criteria performance-based control strategy is used by embedding the DGPs, sDA and View Fraction in a penalty function. The most appropriate state of the dynamic shading for each time-step is selected by finding the state with minimum penalties. For evaluation of the results for the different shading solutions, a threshold value for glare is specified to narrow down the solution space and to assist in decision-making trade-offs.

The two case studies show that static shading combined with performance-based controlled dynamic shading has potential to improve visual comfort in comparison to both systems as individual shading solutions. This can be assigned to the fact that blocking of the sun by static shading results in an higher uncovered window fraction for dynamic shading. It leads to a more beneficial daylight performance (16% – 31%) in terms of spatial daylight autonomy in comparison to dynamic shading as individual shading solution. The impact on view depends strongly on: i) the size of view obstruction by the static shading, ii) the improvement of the view through increase of the uncovered window fraction for dynamic shading and the iii) occupant-related assumptions (e.g. occupant position, view direction).

By using a performance-based control strategy in both case studies for concurrent optimization of static shading design and dynamic shading, it was possible to make a tight coupling between façade design and the operational aspect. This leads to more beneficial values for daylight and view performance in comparison with the results for the rule-based control strategy and a larger facade design space with near-optimal performance. This larger design space could offer benefits in terms of performance aspects (e.g. energy use, thermal comfort), which were not explictly addressed in this study. In addition, it leads in one of the case studies to the ability to use a different design solution, which generates number of benefits, such as cost-reduction and material saving.

This study shows the potential of coupled design optimization of static shading and performance-based controlled dynamic shading to improve the visual comfort. Application of this approach in practice asks for a tailored approach from the design team. In the first place, it requires conscious choices regarding the façade as a static element. Therefore, the façade design must result from a careful process in the early phase of an integral design process. Secondly, the use of an advanced control strategy requires an expression of the performance of the shading through a set of clearly defined criteria and also a definition of acceptance thresholds for dynamic evaluations. A final recommendation is to use objective performance information to assist in decision-making trade-offs.

Acknowledgements

I want to thank prof. Jan Hensen, Roel Loonen and Samuel de Vries for their continuous advice and suggestions in the supervision of this project. Their questions, feedback and support were essential for the successful completion of this thesis. I am grateful that you were willing to share your knowledge with me. Samuel, I greatly appreciate your patience and support during the weekly meetings. Your suggestions, enthusiasm and guidance throughout the entire thesis were fundamental for completing my thesis. Roel, thank you very much for sharing you knowledge with me and challenging me with your questions and ideas. Finally, I would like to thank prof. Jan Hensen for the monthly progress meetings. His suggestions and feedback were very helpful for this thesis.

"It's okay to not be perfect.
It's okay to make mistakes.
It's okay to do something that
you wish you hadn't done,
because if we don't do those
things we never grow."

– Dawn Stanyon

Contents

Acronyms

BPS	Building performance simulation
DGP	Daylight glare probability
DGPs	Daylight glare probability simplified
H-sDA	Hourly spatial daylight autonomy
HSA	Horizontal shading angle
IEA	International Energy Agency
PBC	Performance-based control
RBC	Rule-based control
sDA	Spatial daylight autonomy
VB	Vertical blinds
VF	View fraction
VSA	Vertical shading angle
WWR	Window-to-wall ratio

1. Introduction

Effective use of daylight in buildings is an important consideration for minimizing the carbon impacts and for creating an high indoor environment quality. A growing number of studies demonstrate that access to daylight and window view have a range of impacts on health, well-being, productivity and job satisfaction of building occupants. *[Ward, Rockcastle, Kline, & Wymelenberg, 2019; Al Horr, Arif, Mazroei, Katafygiotou, & Elsarrag, 2016; WGBC, 2014]*. The importance of view is increasingly recognized over the last years by the introduction of multiple design guides regarding view by, for example, the Leadership in Energy and Environmental Design (LEED), the Chartered Institution of Building Services Engineers (CIBSE) and New European Daylighting Standard EN 17037. Beside the impact on health, view and daylight also play a significant role in the market price of real estate since people are often willing to pay a premium for attractive views and more daylight *[Turan, Chegut, & Reinhart, 2020; Damigos & Anyfantis, 2011]*.

Solar shading is an important feature of high-performance building design to achieve a good balance between daylight admission, views to outside and solar gains. Especially with the often highly glazed façades nowadays. In terms of visual comfort, an “ideal” façade, would continuously provide: i) sufficient levels of well-distributed daylight illuminance, ii) absence of discomfort glare for all occupants and iii) view to the outside. *[Loonen, 2018; Ruck, et al., 2001]*. In this context, various shading solutions have their merits and disadvantages. Static shading solutions offer interesting opportunities for architectural integration and are able to block the direct sun while keeping daylighting view to the outside (Figure 1)

Figure 1. Examples of façades with static shading: 1) Head office ING Amsterdam [source: Rollecate, 2019]; 2) Office Tower Amsterdam [source: Rafel Viñoly Architects, 2005], 3) Office DUO Groningen [source: UN Studio, 2011], 4) Residential building Amadeus Den Haag [source: BNA, 2019]

Application of static shading results for selective hours in an higher daylight utilization and more view in comparison to dynamic shading. However, static shading has the drawback that it cannot respond to changing weather conditions. Extreme dimensions for fixed solar shading devices may be necessary to prevent discomfort glare all year long. Another disadvantage is that it also limits the exposure to positive aspects of daylight utilization, for example on cloudy days. (Figure 2)

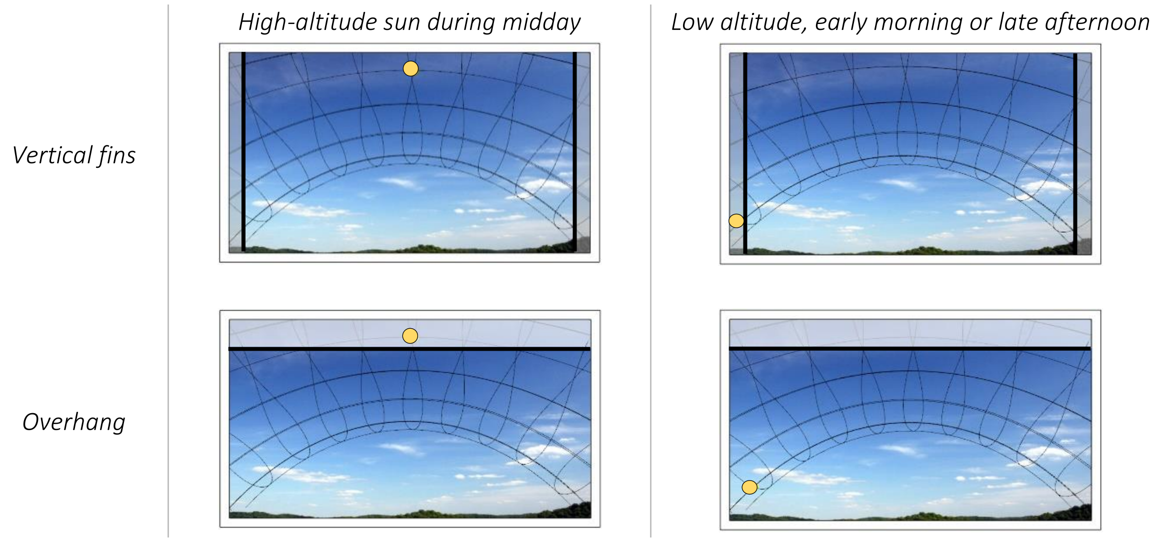

Figure 2. Strength and weakness of static shading systems in relation to the sun position

Dynamic shading systems such as venetian blinds or a roller blind, on the other hand, can be adapted to outside conditions and occupant preferences. However, their control can be complex, and dynamic shading system can significantly limits the admission of daylight views to outside. (Figure 3)

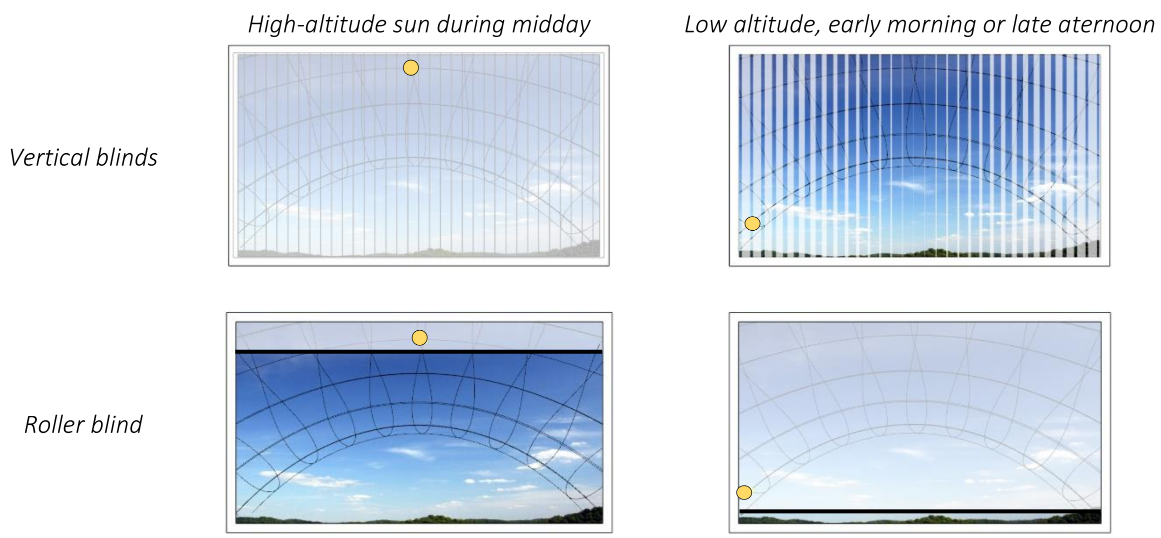

Figure 3. Strength and weakness of dynamic shading systems in relation to the sun position

Horizontal shading is preferable during summer 12h00 (Figure 4). On these moments, vertical fins aren’t able to prevent glare and vertical blinds needs to be fully closed. Vertical shading is preferable in the early morning and late afternoon. On these hours, the roller blind needs to be fully lowered to prevent glare and an overhang isn’t able to prevent glare.

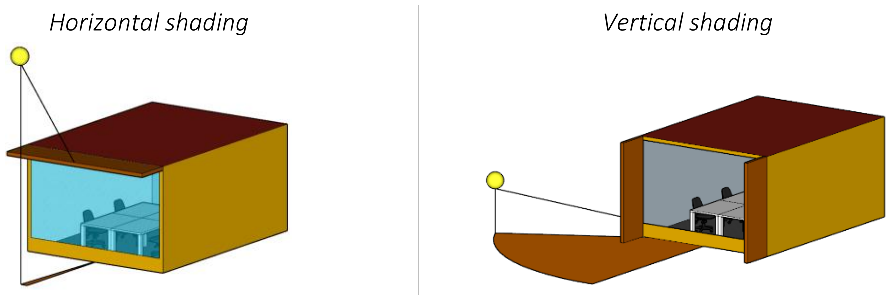

Figure 4. Effectiveness of horizontal (left) and vertical (right) shading in relation the sun position

1.1. Hypothesis
Based on: i) the aspiration to maximize the positive influence of daylight and view, ii) the application-specific strengths and weaknesses of the various shading typologies, and iii) the promising potential of novel automated control strategies, it is hypothesized that the visual comfort in office buildings can be improved through coupled design optimization of façade design and automated shading control.

1.2. Background studies
The number of studies regarding combined static and dynamic shading is limited. Lee and Tavil (2007) considered façade designs with overhangs combined with electrochromic window control strategies and so show the potential for optimization of the energy and comfort by combining dynamic and static shading *[Tavil & Lee, 2006]*.

Over the last years, breakthroughs in material science opened up a range of new possibilities for building designers to influence the conflicting performance goals of visual comfort, daylighting and energy consumption in a more dynamic way. Switchable reflection/ transmission materials, intelligent lighting systems and advanced control strategies are three examples of promising opportunities through their adaptability *[Favoino, Jin, & Overend, 2017; Jeong, Choi, & Sung, 2016; Kheybari & Hoffmann, 2018; Creemers, Loenen, Aarts, Chraibi, & Lashina, 2014; Loonen & Hensen, 2014]*.

1.3. Research question
The primary objective of this research is to explore the potential of coupled design optimisation of fixed building characteristics, static shading and automated shading control in terms of visual comfort. Thereby, this study focuses on finding synergies in the combination of horizontal and vertical shading topologies, where the one is static, and the other is controlled in a dynamic way. In order to fulfil this objective, the following main question will be answered:

- Could the application of static and automated controlled shading mutually enhance each other, to combine their strengths, while mitigating the weaknesses in terms of visual comfort and daylight performance?

This research addresses the following sub-questions:

- What is the performance gain compared to individual shading solutions?
- What is the impact of the control strategy on the performance?

1.3. Methodology

This research makes use Building Performance Simulation (BPS). Thereby, two case studies will be performed to explore the potential of coupled design optimization of static and dynamic shading systems in comparison to the performance for dynamic and static shading as individual solutions. This research follows the majority of the steps indicated by Loonen et al., who mapped out the different fundamental stages for simulation based support or product development of adaptive building technologies *[Loonen, Singaravel, Trčka, Cóstola, & Hensen, 2014]*. The resulting steps, which add structure to the simulation in this research and to the structure of this report, are:

1. Determining performance indicators
2. Developing an appropriate modelling and simulation strategy
3. Identification of (un)certainties and quality assurance
4. Defining test case models
5. Presenting and discussing the results

1.4. Thesis outline

Figure 5 shows a graphical representation of the way this thesis is structured. Chapter 2 presents the simulation strategy to be used for exploring the potential of coupled design of static shading automated shading control for optimization of visual comfort. This chapter also presents model's assumptions and explains the approach for the advanced-control strategy. The reliability of the simulation model and model's assumptions is examined in chapter 3. Chapter 4 describes the outcomes of the two simulation studies. Finally, chapter 5 concludes with summarizing the findings of the entire study and provides recommendations for future work.

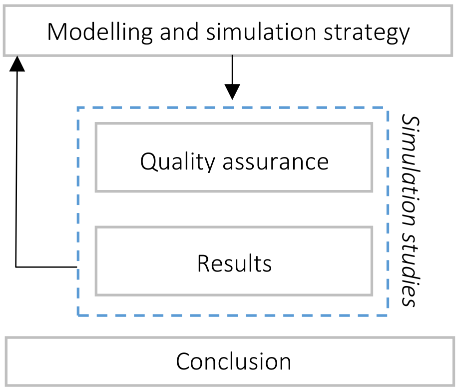

Figure 5. Structure of the thesis

2. Modelling and simulation strategy

In this chapter, the modelling and simulation strategy for the BPS in this research is presented in six steps: 1) performance indicators, 2) building test case model, 3) static shading, 4) dynamic shading, 5) simulation method and 6) shading control.

2.1. Performance indicators

In this research are glare, daylight and view to the outside considered for evaluation of the visual performance.

Glare

The 'daylight glare probability simplified' (DGPs) is used as indicator to assess the discomfort glare. *[Wienold, 2009]*. The DGPs indicator is primarily based on vertical illuminance (E_v). In this report, the DGPs has been considered at the four sensor points as shown in Figure 6, whereby the occupants look under an angle of 45 degrees in the direction of the window. The maximum value out of the four sensor points is considered at each timestep. Four different categories according to the classification of *[Wienold, 2009]* are considered: intolerable (DPGs > 0.45), disturbing (0.40 > DGPs ≤ 0.45), perceptible (0.35 > DGPs ≤ 0.40) and imperceptible (DPGs < 0.35). The DGPs 95th percentile is used for the annual glare performance *[Mardaljevic, Andersen, Roy, & Christoffersen, 2012]*.

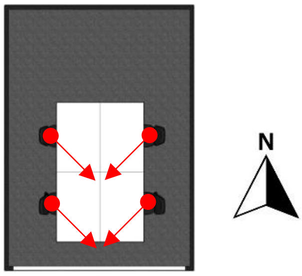

Figure 6. Floor plan with the seating of the four occupants and their view direction

Daylight

Spatial daylight autonomy (sDA) is used as an indicator for the daylight quality. In this report, the $sDA_{300/50\%}$ is defined as the percentage of floor area that receives at least 300 lux for more than 50% of the occupied hours *[Illuminating Engineering Society, 2012]*. The hourly daylight illuminance sufficiency is assessed by the Hourly Spatial Daylight Autonomy (H-sDA_{300}). This is the percentage of the floor area that receives more than 300 lux for a particular point in time *[Wagdy, Fathy, & Altomonte, 2016]*.

View to the outside

There is no standard method or set of metrics to evaluate view. Over the years, researchers have developed multiple methods to evaluate view, based on: vector raytracing in 3D models *[Mardaljevic, 2019; Turan, Reinhart & Kocher 2019]*, answering multiple choice questions about the view content *[Hellinga & Hordijk, 2014]*, geometric quantification of view access *[Pilechiha, Mahdavinejad, & Rahimian, 2020; Konstantzos & Tzempelikos, 2017]* and quantification of the area-weighted occupant's view preference *[Wenting & Samuelson, 2020]*. An overview with the description of each method is attached as appendix I to this report.

Although the visual perception of the user and the effects on visual performance are difficult to quantify, it is believed that improve of: i) view quantity and ii) the view quality (*what* is seen, *where* and *how* points of interest relate to one another) can affect these aspects in a positive way. The view quantity depends on multiple variables such as the seating position, view direction, window size, glazing type and properties of shading material.

View quality depends on a variety of highly subjective parameters, including scenery, location and the human visual perception. This research focus only on the view quantity. The objective of this research is to quantify and evaluate to what extent the different shading solutions have impact on the view quantity. The view quantity is assessed as the portion of the occupant's visual field (Figure 7) that has a direct line of sight to the exterior. This approach makes the view performance dependent on the shading solution, observers position and view direction. The shading fabrics are assumed to be fully opaque. The Ladybug Grasshopper plug-in is used for vector raytracing in the building model and so calculation of the fraction of rays in the visual field which beam through the window without intersect with the shading system. (Figure 7) *[Sadeghipour Roudsari, Michelle, & Smith, 2013].* The component makes use of the Tregenza sky subdivision, which divides the hemisphere into 145 patches of approximately equal solid angle. The accuracy of this division is increased by dividing up the sky patches (Figure 8).

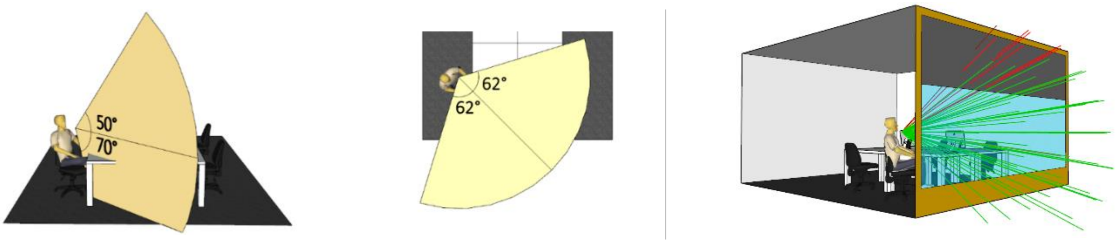

Figure 7. Left: human cone of vision in two directions, horizontally and vertically; Right: Rays cast from position of occupant eye within the human cone of vision for a façade with and without roller blind

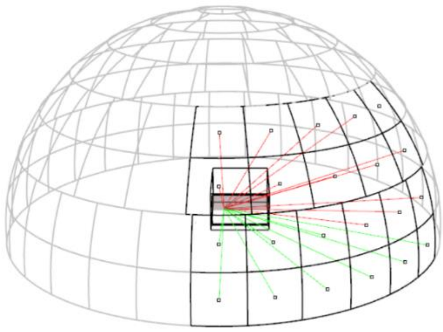

Figure 8. Rays cast from position of occupant eye, within the human cone of vision, to the centre point of the Tregenza sky patches

The occupants are simulated as small grids (0.5 x 0.5m; 25 points) instead of one point to mitigate differences in view at a short distance from the occupant's eye level (Figure 9). This assumption is based on an explorative study which is attached as appendix II to this research. The view quantity is determined for each shading configuration by defining the fraction of rays with unobstructed view to the outside within the vision field. This is called the View Fraction. The average view fraction is taking over the all the grid-points of the four grids.

$$VF = \frac{1}{100} * \frac{1}{N} * \sum_{i=1}^{100} \sum_{j=1}^{N} A_j$$

N: number of rays

$$A: \begin{cases} 1, \text{ if ray intersect with window, but not with shading system } \textit{(green rays)} \\ 0, \text{ else} \end{cases}$$

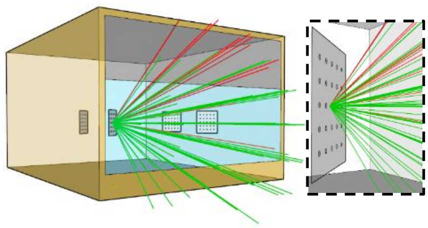

Figure 9. Left: Defining equation for View Fraction (VF); Right: rays cast from position of one of grid points.

2.2. Building test case model

This research used the reference office building for evaluating building integrated solar envelope systems, developed within IEA SHC Task 56 with some minor adjustments *[D'Antoni, Bonato, Geisler-Moroder , Loonen, & Ochs, 2017]*. Details of this south facing perimeter office cell and the associated modelling assumptions are given in Table 1. The office is assumed to be occupied by four persons on working days, which are present from 8:00 to 18:00. The total number of occupied hours in this study is 2860.

Table 1. Reference office building details and modelling assumptions

Geometry	Dimensions	4.5m x 6m x 3m (W x D x H)
	Orientation	South
	Window-to-wall ratio	80%
Fenestration	Type	Low-E double glazing with argon cavity filling
	Glazing	SHGC: 0.637, T_{vis}: 0.785
Separations	Ceiling	r_{vis} = 0.8
	Walls	r_{vis} = 0.5
	Floor	r_{vis} = 0.2
Weather		IWEC, Amsterdam, The Netherlands

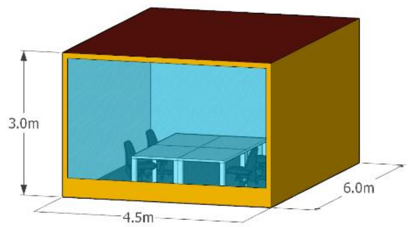

2.3. Static shading

The static shading design is in this research specified by using the vertical shading angle (VSA) for the overhang and horizontal shading angle (HSA) for the fins (Figure 10).

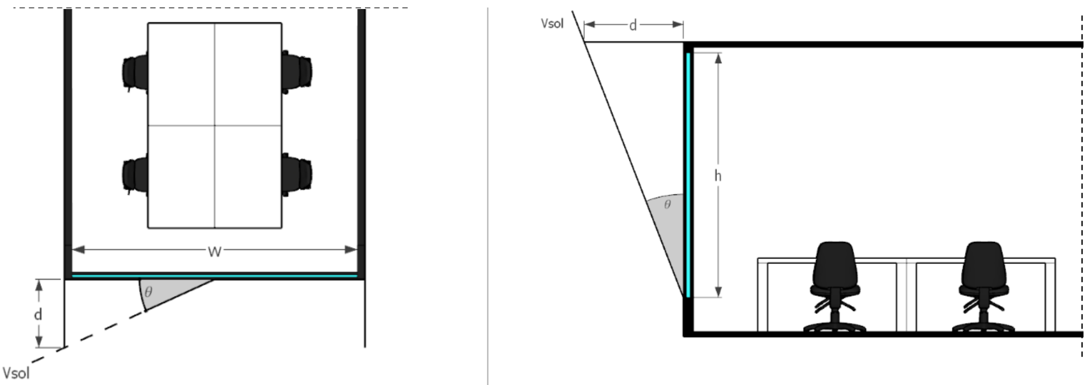

$$HSA = \frac{d}{0.5 \cdot \theta} \qquad VSA = \frac{d}{h}$$

Figure 10. Defining images for the horizontal (left) and vertical (right) shading angle

The design of static shading with the HSA and VSA gives the possibility to freely change between different shading device typologies. Many configurations, shapes, and sizes are possible for exterior shading systems. One large or several small static shading elements may give the same shading angle (Figure 11). This study uses an abstraction, where only a simple horizontal overhang at the top of the window opening and two simples vertical fins on both sides of the window are considered. The intention is that it can be used to extract general design principles. These can then be used as input for architectural design concepts that may (or may not) have more geometric complexitiy and asethetic appeal that the test solutions.

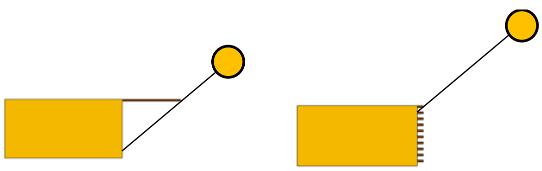

Figure 11. Different shading designs for the same shading angle

Different designs for the overhang and fins are generated by increasing the shading angle with steps of 10°. The shading angle is increasing by increasing the depth of the shading device. Multiple small shading devices in combination with the imprecise representation of the direct sun component through averaging over relatively large sky solid angles could lead to blurry and featureless interior shadows *[Ward, Mistrick, & Lee, 2011]*.

Simulation of fins

The fins are is modelled as two vertical surfaces on each side of the window and with a reflection value of 0.2. Eight different designs are generated by assuming a discrete possible range of vertical shading angles (10°, 20°, 30°, 40°, 50°, 60°, 70°, 80°) (Figure 12). The height of the fins is assumed to be equal to three times the office height. This assumption will be explained in section 3.

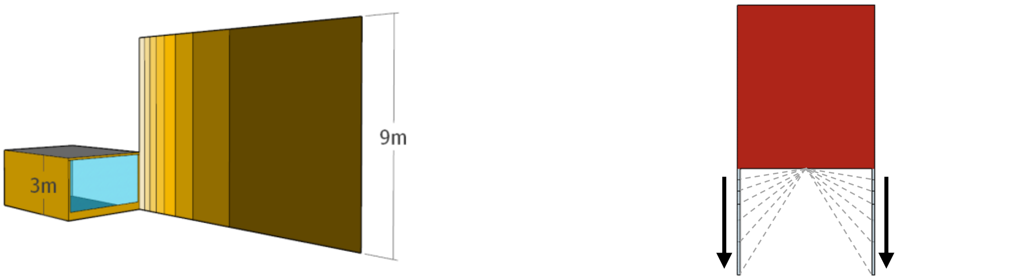

HSA	10°	20°	30°	40°	50°	60°	70°	80°
Fin depth [m]	0.40	0.82	1.30	1.89	2.68	3.90	6.18	12.76

Figure 12. The eight façade designs for fins, characterised by their HSA, fin depth and visualized with colours

Simulation of overhang

The overhang is modelled as one horizontal surface with a reflection value of 0.2 on top of the window. Six different designs are generated by assuming a discrete possible range of vertical shading angles (10°, 20°, 30°, 40°, 50°, 60°). (Figure 13). The extrusion for the overhang is assumed to be equal to two times the office width. This assumption will be explained in section 3.

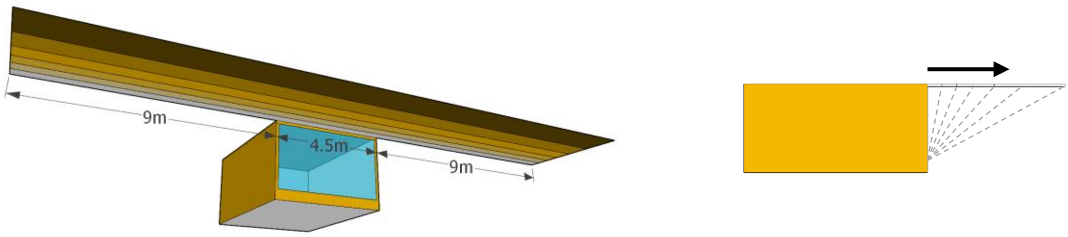

VSA	10°	20°	30°	40°	50°	60°
Overhang depth [m]	0.44	0.91	1.44	2.09	2.97	4.31

Figure 13. The six façade designs for an overhang, characterised by their VSA, overhang depth and visualized with colours

2.4. Dynamic shading

Vertical blinds and roller blind, as dynamic shading systems in this research, are modelled by assuming a range of discrete shading states for both shading systems.

Roller blind

The roller blind is assumed as dense shade with a visible reflection outside of 0.74, light transmission of 4% and an openness factor of 2%. The roller blind shading system is modelled by dividing the window into ten horizontally oriented equal segments which are either fully shaded or unshaded. This resulted in eleven shading states as shown in Figure 14.

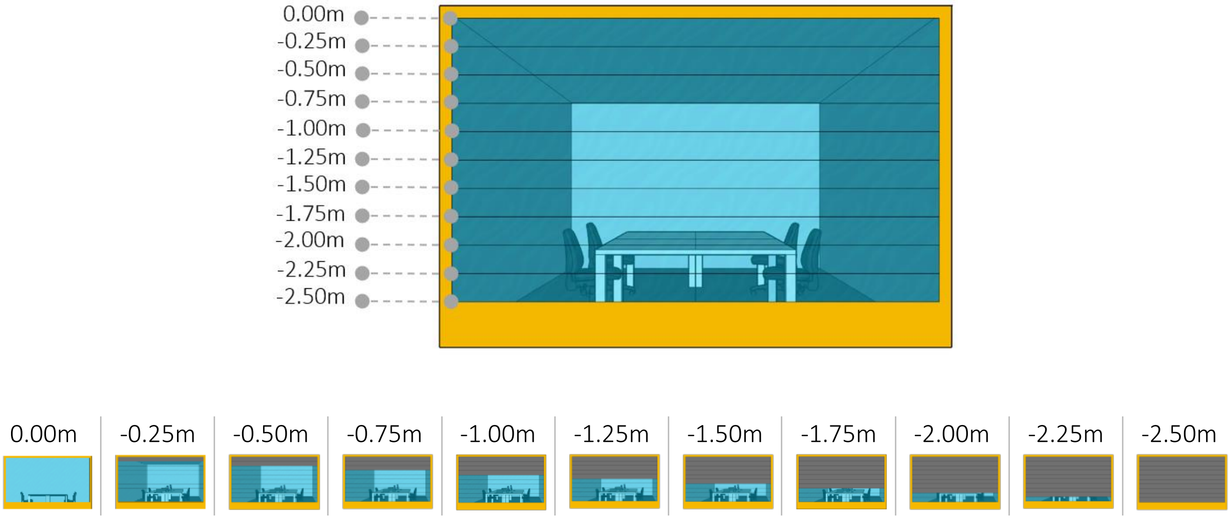

Figure 14. The eleven modelled shading states for the roller blind with their shade height

Vertical blinds

Vertical blinds are assumed as flat slats (slat width: 127mm, spacing: 127 mm) with a solar reflection value of 0.75 (front) and 0.50 (back) . The variable slat angle of the blinds is assumed as the discrete possible range of eight different angles (-67.5°, -45°, -22.5°, 0°, 22.5°, 45°, 67.5°, 90°). The slat angle α is defined as the angle between the glazing outward normal and the slat outwards normal, where the outwards normal points away from the front of the slat. The different slat angles for the vertical blinds are visualized in (Figure 15).

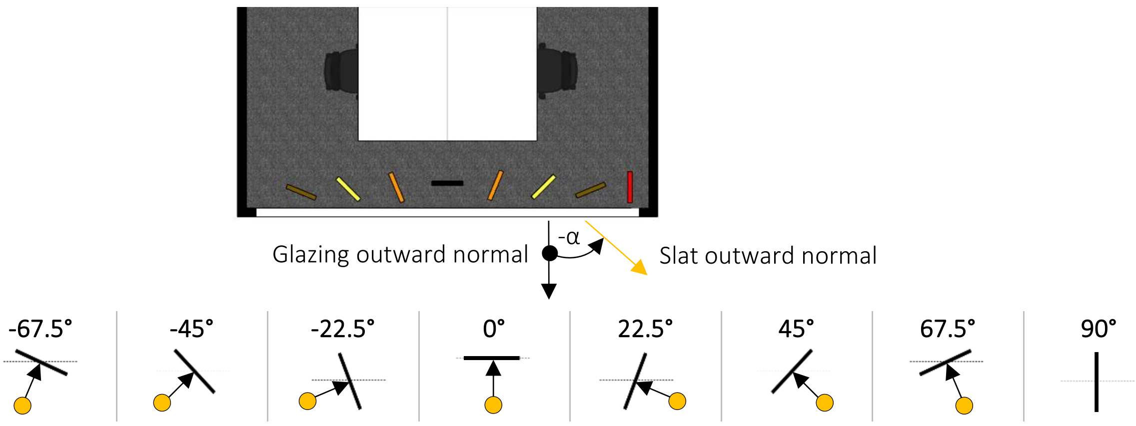

Figure 15. The eight slat angles for the vertical blinds

2.5. Simulation method

The Radiance three-phase method is used for daylighting and glare performance assessments. This validated method separates light transport between the sky and the sensor points into three phases: exterior transport (sky matrix), fenestration transmission (transmission matrix) and interior transport (view matrix). Each phase of light transport is simulated independently and stored in a matrix form. The resulting climate-based indoor illumination is obtained using matrix multiplication *[McNeil & Lee, 2013]*. The main reason for using the three-phase method in this research is the possibility for analysing the dynamic performance of multiple shading configuration in a quick, yet accurate way. The shading state can be changed without simulating the entire light path, simply by substituting a new fenestration transmission matrix *[Subramaniam, 2018]*. The spatial daylight autonomy in the office is determined by modelling a grid of 70-sensor points on work plane height (Figure 16). The vertical illuminance at the eye of the observer is modelled by modelling four sensors at the position of the observer with the view direction facing the window at 45° to assess glare probability.

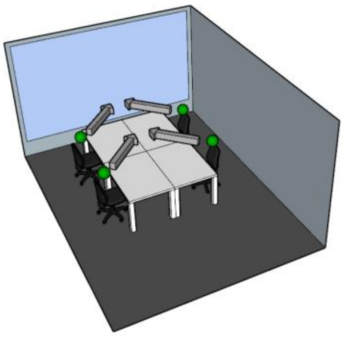

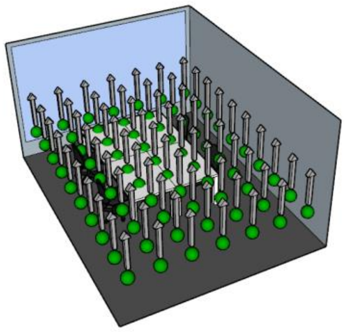

Figure 16. Four points grid for glare and daylight (left) and seventy points sensor grid for daylight (right)

2.6. Shading control

The control strategy is very important for the performance of dynamic shading during operation. This research makes use of different control strategies which are elaborated below.

Rule-based control strategies

Rule-based control (RBC) strategies connect measurements by sensors to actions via rules of the kind "*if* condition *then* action" *[Loonen, 2018]*. Two different RBC strategies are used in this research to control the roller blind and vertical blinds. The roller blind is controlled using an outdoor global horizontal irradiance sensor on the roof of the office where the shade is either fully raised or lowered in response to a threshold of 200 W/m². The vertical blinds are controlled by using sun tracking behaviour. In this strategy, the cut-off angle of the slats is determined in relation to the sun's position (azimuth angle) to exclude direct sunlight from entering the office.

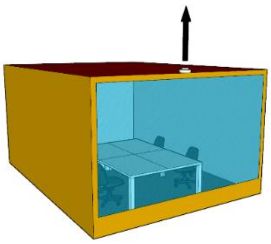

Figure 17. Office with outdoor global horizontal irradiance sensor on the roof

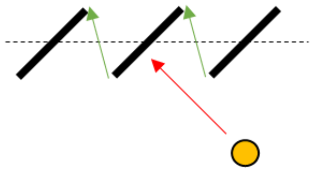

Figure 18. Vertical blind "cut-off" angle

Performance-based control strategy

The control actions for the performance-based control (PBC) strategy in this research follows from comparing the visual performance for the different dynamic shading states for each time-step and selecting the best state. The selection of the best shading state is driven by an optimization function that ranks the visual performance for each shading state. This strategy couples the façade design with the operational aspects of the dynamic shading and so allow coupled-design optimization.

This strategy consists of three steps:

1. Simulation of all possible states of the shading system to get the hourly values for daylight, glare and view

2. Evaluation of the performance of all possible shading states by using weighted penalty functions. When the required criteria are not achieved, the unacceptable cases are rejected by applying penalties for the different components: DGPs (P_{glare}), H-sDA$_{300}$($P_{daylight}$) and view (P_{view}). The threshold values for glare, daylight and view are indicated in (Figure 19). The priority of daylight, glare and view can be set separately by different weighting factors (W_{glare}, $W_{daylight}$, W_{view}).

Main penalty function: $P_{total} = W_{glare} \times P_{glare} + W_{daylight} \times P_{daylight} + W_{view} \times P_{view}$

3. Selection of the most appropriate shading state at every time-step by selecting for every timestep the shading state with the minimum main penalty (P_{total}). The outcome is a schedule which contains the shading states with the best performance at every timestep.

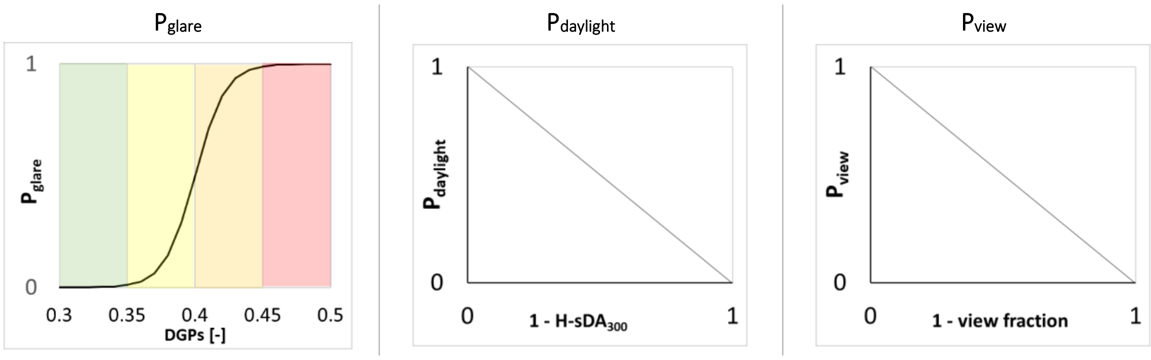

Figure 19. Penalty functions for glare, daylight and view

The weights (W_{glare}, $W_{daylight}$, W_{view}) represent the relative importance of glare, daylight and view. Multiple test runs are performed to evaluate the impact of different penalty functions on daylight performance. This resulted in five different penalty functions by making different assumptions for the weighting factors W_{glare}, $W_{daylight}$ and W_{view} (Table 2**Fout! Verwijzingsbron niet gevonden.**).

Table 2. Five penalty functions

Function	W_{glare}	$W_{daylight}$	W_{view}
P1	0.33	0.33	0.33
P2	0.44	0.56	0.00
P3	0.56	0.33	0.11
P4	0.67	0.33	0.00
P5	0.95	0.05	0.001

These five penalty functions are developed based on two sets of criteria. The first criteria is that the annual glare performance, in the form of 95th percentile, is divided over the different glare classes (see appendix III). The second criteria is that sometimes (e.g. low illuminance), glare and daylight are not sufficient for the control to make a meaningful decision. In this context, the role of view differs between the five penalty function by giving the weighting factor an value of 0 for P2 and P4 and an value larger than zero for P1 and P3. P5 is a preconditioned penalty function whereby view to the outside is only of interest after the performance criteria for glare (DPGs ≤ 0.35) has been met. By giving view a relatively low weight, the penalty function tends to select solutions that maximize openness of the façade while not compromising on glare discomfort and daylight illuminance (Figure 20**Fout! Verwijzingsbron niet gevonden.**).

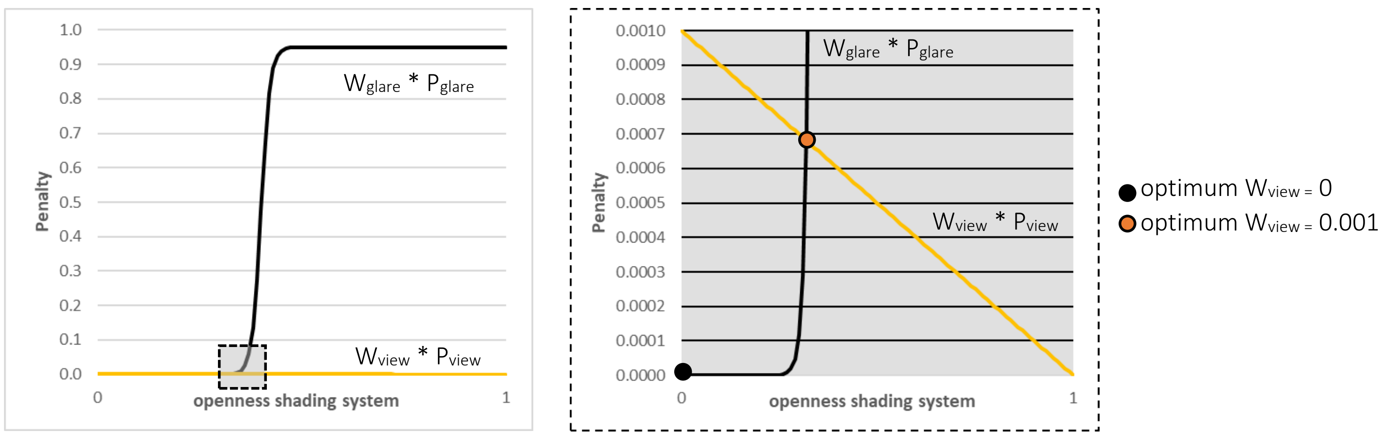

Figure 20. A relatively low weight for Wview leads to nudging of solution towards a solution that maximize openness of the shading system while not compromising on glare

As summary of the performance-based control strategy is given in (Figure 21).

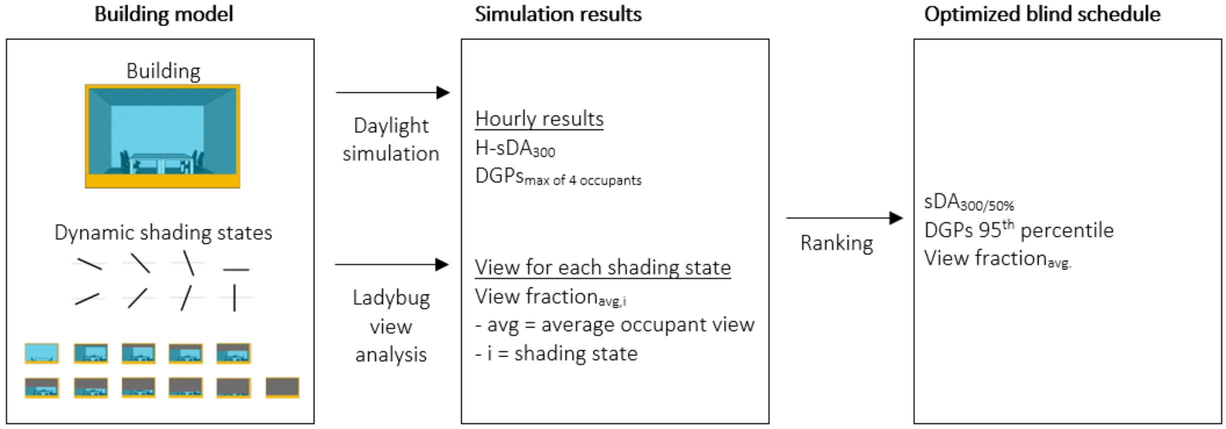

Figure 21. Summary of the PBC strategy

3. Quality assurance

It is important to examine whether the simulation model behaves in a manner - like a real building. Due to unavailability of measurement and experiment data it is not possible to perform empirical validation, but only to increase the level of confidence *[Hensen & Lamberts, 2019]*. This chapter examines the reliability of simulation-based predictions by:

1. Testing assumptions that are made regarding static shading by performing sensitivity analysis
2. Comparing the computer predictions of shading behaviour with expectations
3. Comparing the simulation results with data from comparable studies

3.1. Sensitivity analysis

Effect of fin height

A simulation study is performed to explore the impact of the extrusion for static fins on the annual glare performance, whereby the geometry is changed by setting the height of the exterior fins equal to one, two and three times the office height. The results show a minimum impact on glare for a fins with an extrusion of two times the office height. See appendix IV for more information about this study (Figure 22). This situation is representative for an office cell which is part of a larger building, whereby static shading devices of upper neighboring cells result in additional shading.

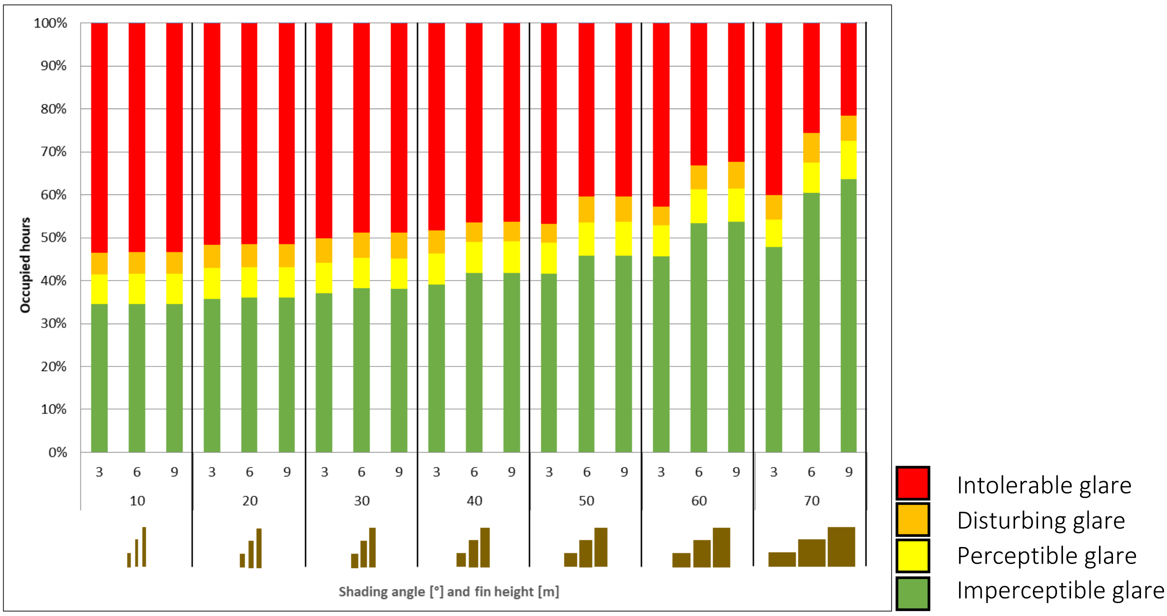

Figure 22. Difference in annual glare performance for fins with one(3) , two (6) or three times (9) the reference office height (for more see appendix IV)

Effect of number of overhangs, reflection value and ground reflection

A simulation study is performed for the overhang to explore the impact of: i) the number of horizontal devices, ii) the reflection value and iii) the ground reflection on the annual glare performance when it is combined with vertical blinds. Whereas the impact of the number of fins is minimal, increase of the reflection value results in an increase of glare (see appendix V). The ground reflection as a surface doesn't seem to have much impact on the results for visual comfort (Figure 23).

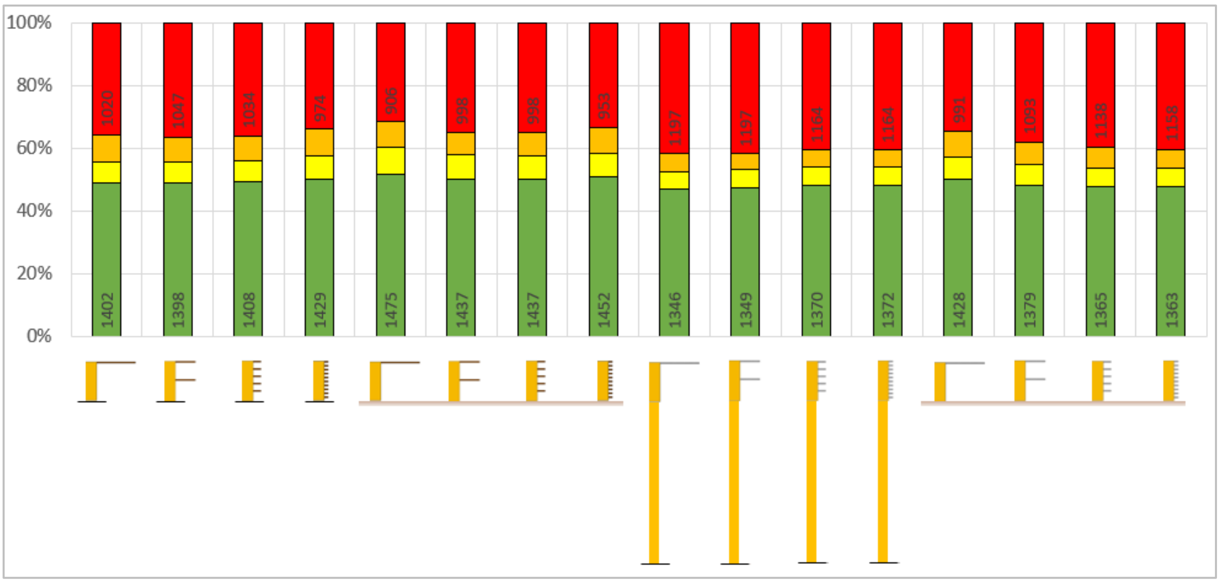

Figure 23. Impact of number of overhangs, reflection value and ground reflection on glare performance (for more see appendix V)

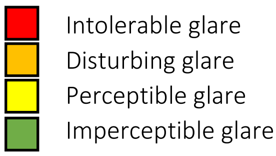

3.2. Model testing

Model testing is performed to see if the results for the modelled shading systems are in line with the expectations. To put this into practice, the impact of the different static shading designs, for both the overhang and fins, and dynamic shading states, for both the VB and roller blind, on the spatial illuminance distribution over the work plane is analysed. The hourly spatial illuminance results for all the different shading states (dynamic shading) and static shading designs for all the occupied hours are gathered for a clear sunny day (31 March). The expectations and results for each of the four shading systems in this research will be discussed below together with three spatial maps. All the spatial maps are attached as appendix VI to this report.

Roller blind

A roller blind controls daylight by varying the effective window aperture and so changing the luminous flux through the window. In case of dense shade material (2% openness), the majority of the diffuse daylight is blocked when the roller blind is deployed. Lowering of the roller blind results in reduction of the daylight penetration in the back of the office. The spatial maps show that pulling down of the roller blind leads to initially to an area with less daylight than desirable back in the room. Further lowering of the roller blind results in an increase of this area to the front of the office. Figure 24 gives an impression of the reduction of the penetration depth by lowering the roller blind.

12h00 (azimuth: 177°, altitude: 41°)

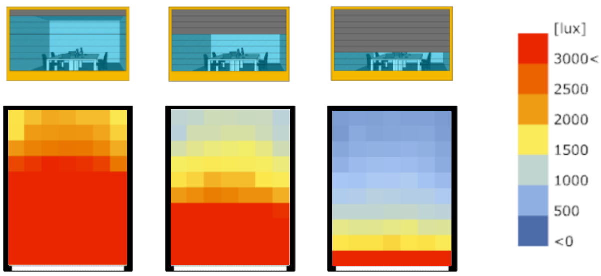

Figure 24. Spatial maps with the illuminance distribution on the work plane for three roller blind states

Vertical blinds

Vertical blinds block direct sunlight, while redirecting diffuse light and maintaining daylight performance within the space. Elimination of direct sunlight and view over a wide range of annual sun angles and sky conditions requires intermittently adjusting of the slat angles and may result in blinds that are rotated to a closed state, thus eliminating daylight and view along with glare. Figure 25 shows the spatial maps for the vertical blinds (VB) at 15h00 and confirms the relation between the redirecting behaviour of the slats, the openness of the slats and the illuminance distribution over the work plane.

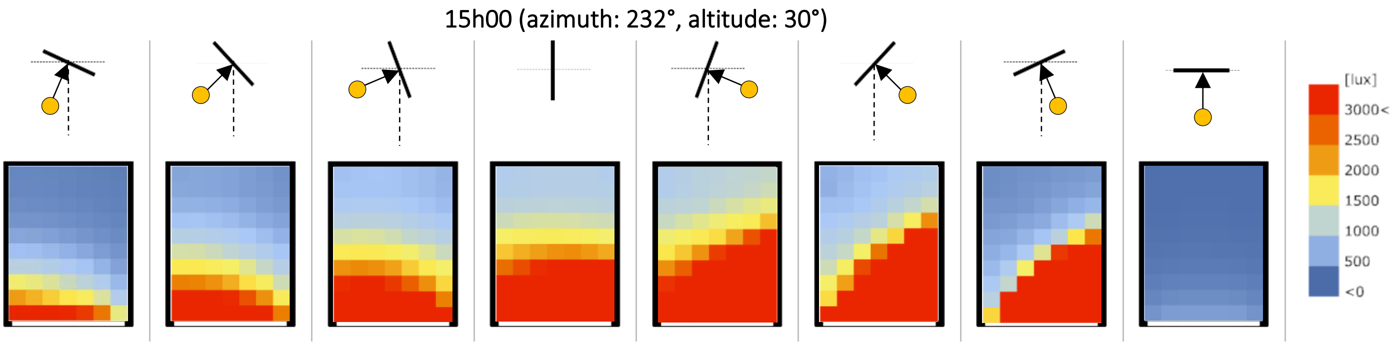

Figure 25. Spatial maps with the illuminance distribution on the work plane for different slat angles

Overhang

An horizontal surface on top of the window blocks the direct solar radiation from entering the window in case of high altitude sun. Diffuse radiation will partially be blocked. The amount of daylight in the back of the room will be decreased by increasing the depth of shading device. The simulation results for the different overhang geometries for 12h00 are shown in Figure 26. These spatial maps show that application of an overhang, with an reflection value of 0.2, results initially in reduction of the daylight penetration in the back of the office. Increase of the overhang depth results in an enlargement of this area to the front of the office.

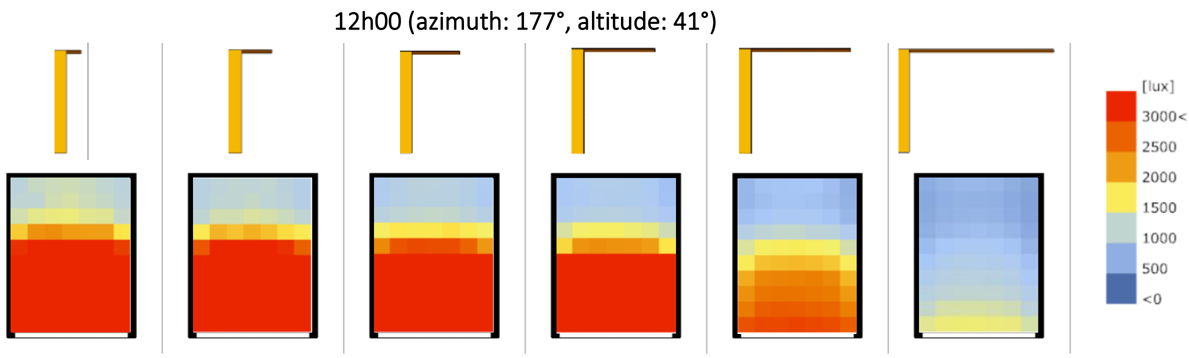

Figure 26. Spatial maps with the illuminance distribution on the work plane for six overhang depths

Fins

Vertical exterior fins are most effective at blocking sun positions with a high surface-solar azimuth and low altitude. The deeper the fins, the longer they are able to block sun in the morning and the earlier the sun in the afternoon. But fins are not able to block the sun when it is positioned perpendicular to the south-oriented window during noon, the moment of the day when solar irradiation is often highest. The simulated spatial maps confirm the blocking of the early morning and late evening sun. The results, for fins with an reflection value of 0.2, show also a decrease of the daylight penetration depth by increasing the fin depth. In comparison with the overhang, a larger shading angle for the fins is necessary to lower the maximum illuminance on the work plane (Figure 27).

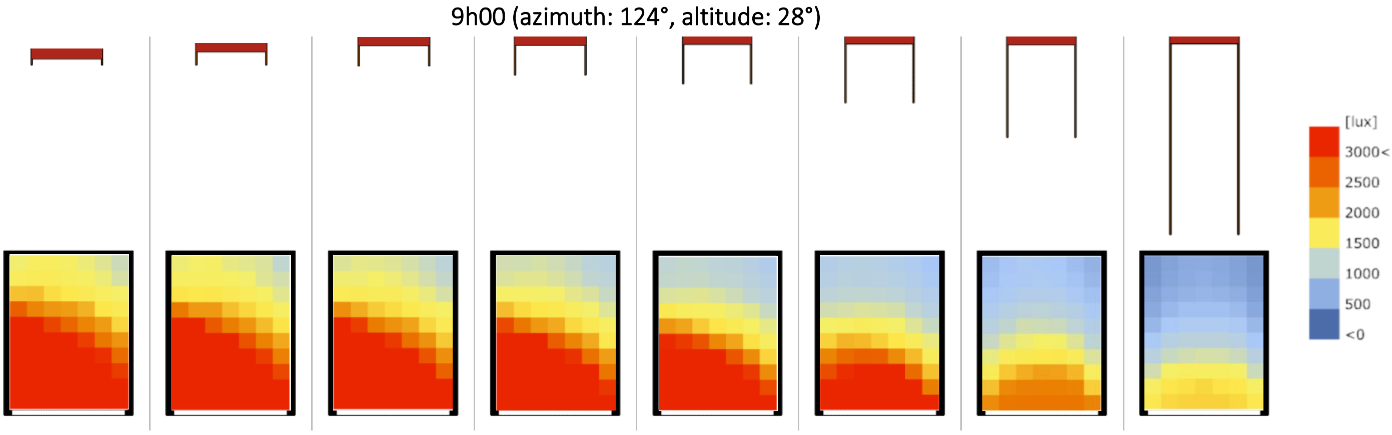

Figure 27. Spatial maps with the illuminance distribution on the work plane for eight fin depths

3.3. Comparative validation

The results of daylight simulations for the reference office with interior roller blind are compared with simulation data, obtained from one published and one yet-to-be-published research article *[de Vries, Loonen, & Hensen, 2019; de Vries, Loonen, & Hensen]*. The two studies also make use of IEA SHC Task 56. Also Radiance three-phase method is used for simulation. Table 3 shows the details of this reference space and the associated modelling assumptions for the two studies, whereby the titles of the studies are:

- **Research 1 - title:** Sensor selection and control strategy development support for automated solar shading systems using building performance simulation
- **Research 2 - title:** A screening method for sensor selection and control strategy development of automated solar shading systems using building performance simulation

Table 3. Comparative overview with the simulation details and modelling assumptions for the two studies and this research

		Research 1	Research 2	This study
Geometry	Dimensions	4.5m x 6m x 3m	4.5m x 6m x 3m	4.5m x 6m x 3m
	WTW-ratio	85%	80%	80%
Fenestration	Type	Low-E double glazing with argon cavity filling	Low-E double glazing with argon cavity filling	Low-E double glazing with argon cavity filling
	Glazing	SHGC: 0.62, T_{vis}: 0.82	SHGC: 0.62, T_{vis}: 0.82	SHGC: 0.64, T_{vis}: 0.79
	Shade	Indoor roller blind OF: 0.04	Indoor roller blind OF:0.008	Indoor roller blind OF: 0.04
Visible reflection	Ceiling	0.8	0.8	0.8
	Walls	0.5	0.5	0.5
	floor	0.2	0.2	0.2
Weather		IWEC, Amsterdam	IWEC, Amsterdam	IWEC, Amsterdam

Three control scenarios are discussed. A situation where the roller blind is always up (AU), a situation where the shades are always down (AD) and control strategy where roller blind is controlled using an outdoor sensor where the shade is either fully raised or lowered in response to a threshold of 200 W/m² (BL).

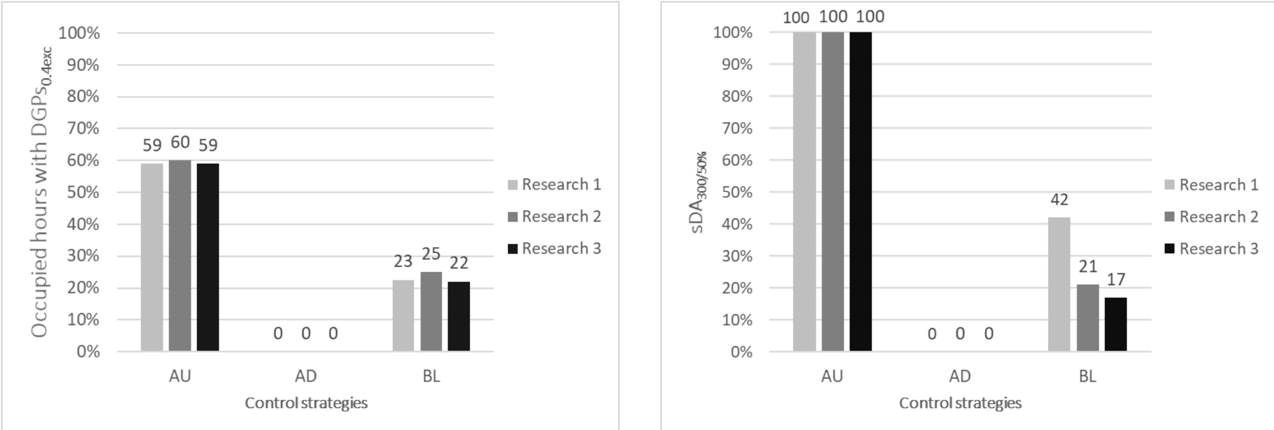

Figure 28. Summary of glare (left) and daylight (right) performance for the three researches and the three strategies. AU: always up, AD: always down, BL: Baseline E-ig; 200 W/m².

Figure 28 shows a building performance summary comparing the AU, AD and BL strategies as well as the glare and daylight performance for all the three researches. Glare performance is shown as the percentage of occupied hours that a DGPs of 0.40 is exceeded using the maximum of the view directions. Daylight performance is presented as the $sDA_{300/50\%}$. Figure 28 shows that the difference between all the three studies for both glare and daylight are very equal. Regarding daylight performance, the BL strategy shows the biggest discrepancies between the studies, especially between this study and research study 1. An explanation for this difference could be the different orientation of the shading control sensor. Overall, the simulations results of this study are very comparable with the results of the other two studies.

4. Results

This chapter presents0 two case studies to explore the potential of coupled design optimisation of fixed building characteristic, static shading and automated shading control in terms of visual comfort. In the first case study, we make use of a roller blind as interior, horizontal, dynamic shading solution and exterior vertical fins in the façade. For the second case study, an overhang is assumed in the façade and vertical blinds as interior dynamic shading system. In both studies, the visual performance for different static façade solutions and dynamic shading, both individually and in combination, are tested. Each case study can be divided into 3 parts (a-c):

a) **Static shading**: testing the visual performance for different static façade solutions
b) **Dynamic shading**: testing the visual performance for the dynamic shading system and evaluate the effect of using different control strategies
c) **Static and dynamic shading**: testing the visual performance for the different combinations between the static façade solutions and the different control strategies for dynamic shading

Table 4 presents the structure for the performed simulation studies and represents also the structure in this chapter.

Table 4. Structure of the two case studies

			Horizontal shading	Vertical shading
Case study 1	a:	Static shading		Fins
	b:	Dynamic shading	Roller blind	
	c:	Static and dynamic shading	Roller blind	Fins
Case study 2	a:	Static shading	Overhang	
	b:	Dynamic shading		Vertical blinds
	c:	Static and dynamic shading	Overhang	Vertical blinds

The comparison of the visual performance for the different shading solutions and the optimization process for visual comfort seeks to improve three performance aspects at the same time; glare, daylight and view. In this study, the performance for the different shading solutions is explored by analysing the trade-offs between glare and daylight and glare and view. Thereby, a DGP 95th percentile of maximum 0.35 (perceptible glare) is assumed as a constraint and indicated with a dashed line ($DGPs_{thr.}$) in the different scatter plots in this chapter.

4.1. Case 1 - Roller blind combined and fins

4.1.1. Case 1A - Fins

Figure 29 shows the trade-offs between glare and daylight for fins with different shading angles. Even though the $sDA_{300/50\%}$ levels are high, vertical fins lead to a high risk of intolerable glare discomfort. If we assume a DGP 95th percentile of max. 0.35, all the static shading solutions for the fins are clearly unacceptable. Only the application of 80°-fins lead to a small reduction in glare, contrary to the other dots who are all positioned under each other in the right-upper corner of the plot. Blocking of direct sunlight for all the annual occupied hours will lead to extremely large shading systems. To create visual comfort, an additional shading solution needs to be applied.

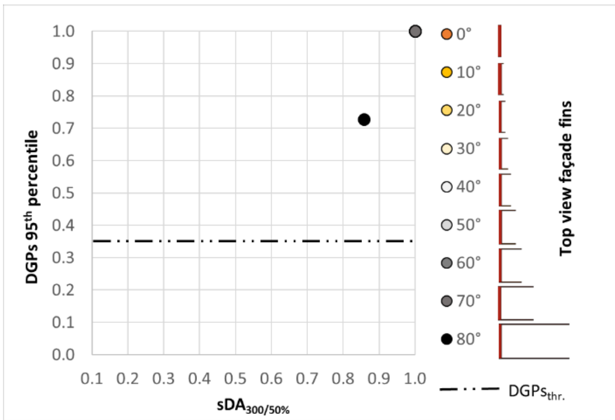

Figure 29. The trade-offs between the annual glare and daylight performance for the fins with different shading angles.

4.1.2. Case 1B - Roller blind

Figure 30 and Figure 31 show the annual performance of the roller blind in case of different control strategies. The dots represent the five penalty functions. The diamond is representative for the RBC strategy, which is based on a control sensor with a threshold of 200 W/m² positioned on the roof of the office. The figures show that:

- RBC *(diamonds)* strategy for the roller blind leads to a high risk of intolerable glare discomfort. That can be assigned to the fact that the roller blind is either fully raised or lowered in response to a threshold of 200 W/m². In addition, the advance strategy has the possibility to control the roller blind in way that best responds to the dynamically changing conditions and is able to find a more beneficial balance between the glare, daylight and view. This makes the PBC strategy controlled roller blind able to prevent glare all year long.
- Application of PBC strategy results a 41 - 47% reduction of the DGP 95th percentile value compared to the RBC strategy
- If a maximum DGP 95th percentile of 0.35 is assumed, P5 gives the most beneficial trade-off between glare and daylight and between glare and view. Glare could be reduced further, but always at the expense of view and daylight.
- P1 – P5 contain different weights for glare, daylight and view and so have different priorities for glare, daylight and view. This results in a different order of the five dots between the two plots below.

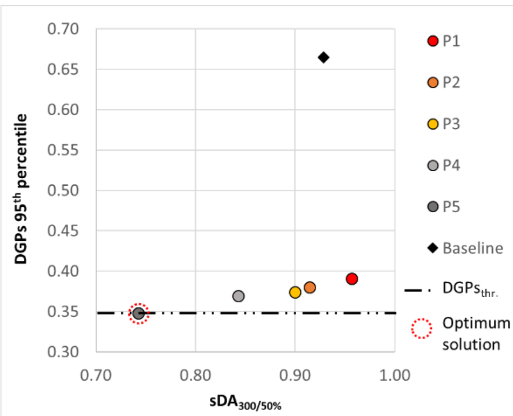

Figure 30. The trade-offs between the annual glare and daylight performance for the roller blind with different control strategies.

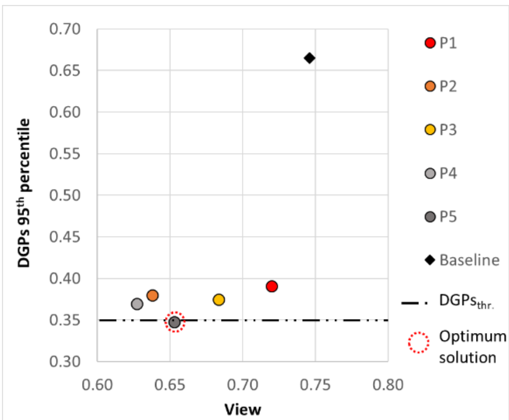

Figure 31. The trade-offs between the annual glare and view performance for the roller blind with different control strategies.

4.1.3. Case 1C - Roller blind with fins

Glare and view performance

Figure 32 shows a scatter plot with the annual performance for glare and view for all the possible combinations between the static fin designs (i.e. façade designs) and the different control strategies for the roller blind as dynamic shading system. The orange-grey colour gradient is based on the value for the shading angle of the overhang. Figure 33 zooms in on the trade-offs in case of a performance-based control strategy. The 5 penalty functions (P1-P5) together with 9 overhang angles (0° - 80°) provide 45 dots. The figures show that:

- The addition of static fins in the façade doesn't lead to a more beneficial trade-off between glare and view fraction for both control strategies, RBC *(diamonds)* and PBC (*dots*).
- If a maximum DGP 95th percentile of 0.35 is assumed, the optimum design in case of an RBC-strategy is 70° fins. A façade without fins is the optimum design in case of a PBC control strategy.

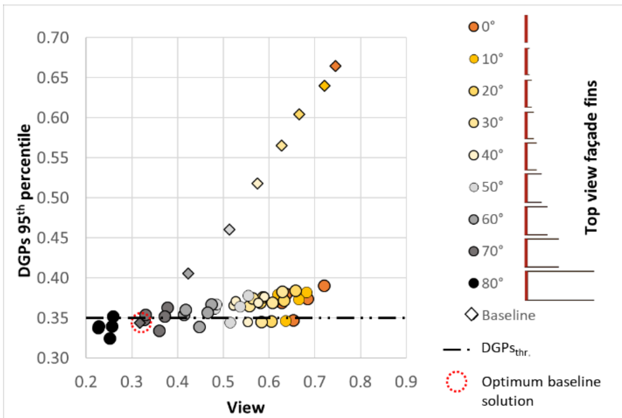

Figure 32. The trade-offs between the annual glare and view performance for the different combinations between façade designs and the roller blind..

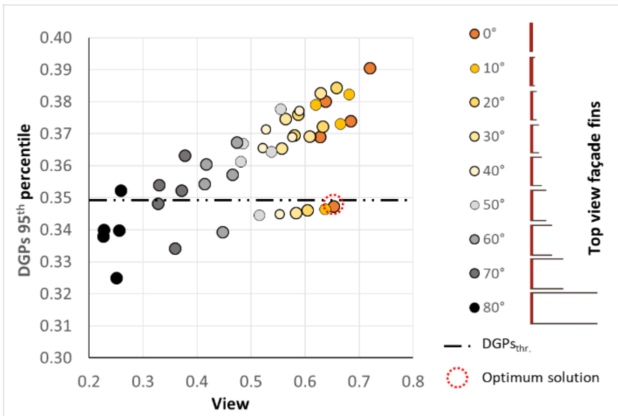

Figure 33. The trade-offs between the annual glare and view performance for the different combinations between façade designs and the PBC controlled roller blind.

Glare and daylight performance

Figure 34 shows a scatter plot with the annual performance for glare and daylight for all the possible combinations between the static fins angles (i.e. façade designs) and the different control strategies for the roller blind as dynamic shading system. Figure 35 zooms in the trade-offs in case of a performance-based control strategy. The figures show that:

- Application of the RBC *(diamonds)* strategy results in decrease of $sDA_{300/50\%}$ by increase of fin depth.
- PBC *(diamonds)* strategy shows potential for coupled optimization.
- The larger spread of the diamonds in comparison to the dots indicates that the RBC is more sensitive to the choices in the early design phase regarding the static façade design than the PBC. This results in more freedom for the designers in comparison to the RBC-strategy in case of an assumed glare requirement.
- If a maximum DGP 95th percentile of 0.35 is assumed, optimization in the early design phase with the RBC or PBC not will lead to different façade solutions. For both, the optimum design contains 70°-fins in the façade. Note that in case of 0.37 or 0.38 as maximum for glare would lead to other façade design.
- The difference between the PBC and RBC-strategy for daylight is large. This finding could probably lead to different design decisions if other performance aspects (e.g. energy use, thermal comfort) and design parameters are taken into account in the comparison.

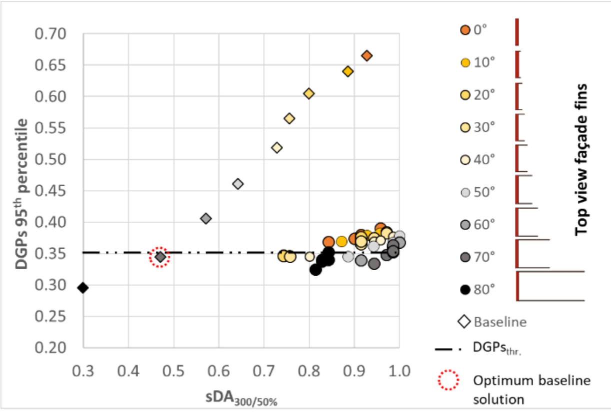

Figure 34. Scatter plot with performance for glare and daylight for the different combinations between façade designs and the roller blind. The colours are based on the value for the shading angle

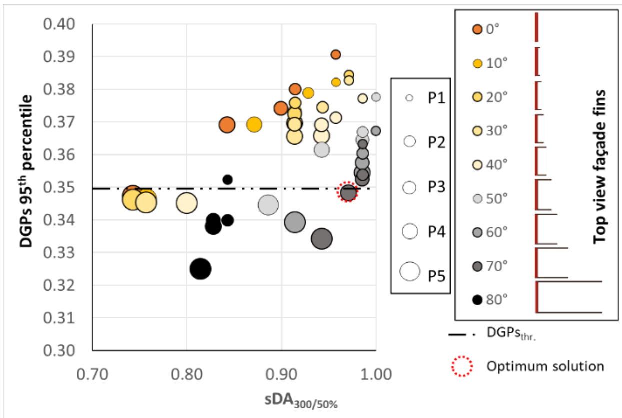

Figure 35. The trade-offs between the annual glare and view performance for the different combinations between façade designs and the PBC controlled roller blind.

The optimum in Figure 35 contains 70°-fins in the façade and shows an increase of the $sDA_{300/50\%}$ with 31% (from 0.74 to 0.97) compared to the optimum controlled roller blind and an increase of more than 100% (from 0.47 to 0.97) compared to the optimum conventional controlled roller blind combined with 70°-fins. This improvement in daylight performance can be assigned to an higher uncovered window fraction for the roller blind. (Figure 36)

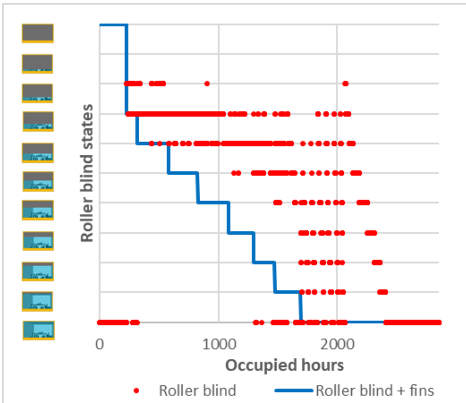

Figure 36. The openness duration curve for the optimum controlled roller blind as individual shading solution and with the addition of 70°-fins

Figure 38 shows the difference in roller blind states for the optimum controlled roller blind as individual shading solution and with 70°-fins. The hours with a large decrease of the roller blind are the consequence of the characteristics of the penalty function P4. This function excludes view from the penalty function by $W_{view} = 0$ with the consequence that P4 tends to select solutions with the minimum glare during hours with minimum daylight. The largest increase of the roller blind is in the early morning and late afternoon, when the fins are most effective. The associated impact on daylight and view is shown in Figure 39 and Figure 40.

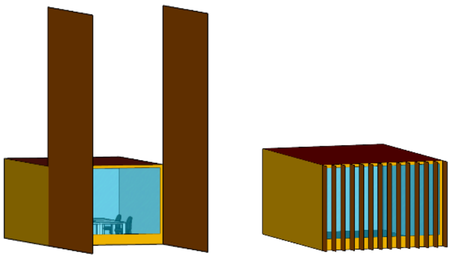

Figure 37. Simulated façade (left) and a variant design (right) for a façade with 70°-fins

The three maps together show a clear relationship between the impact of the fins, the change in roller blind state and the impact on the daylight. Figure 39 shows that the visual obstruction due to the fins does not outweigh the increase of the roller blind with as result a decrease of the VF for the majority of the occupied hours. The assumed fixed view positions and directions for occupants make that only for a couple of hours in the early morning and late afternoon, when Δ state is very high, a small increase of the VF is visible.

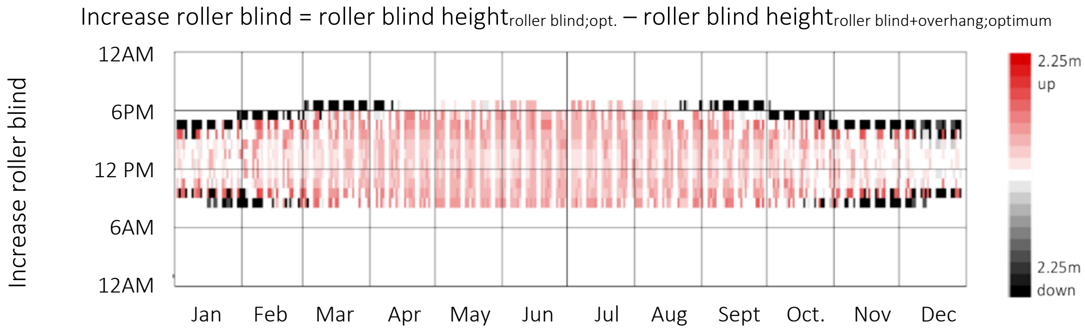

Figure 38. Difference in roller blind state between PBC controlled roller blind with and without 70°-fins

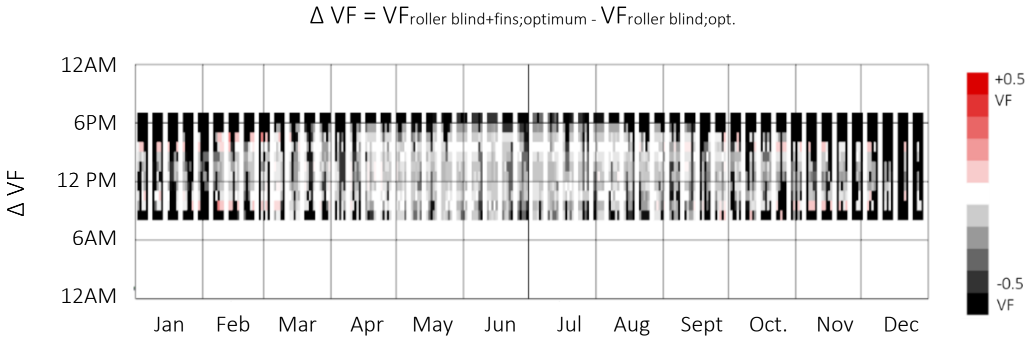

Figure 39. Difference in value for VF between PBC controlled roller blind with and without 70°-fins

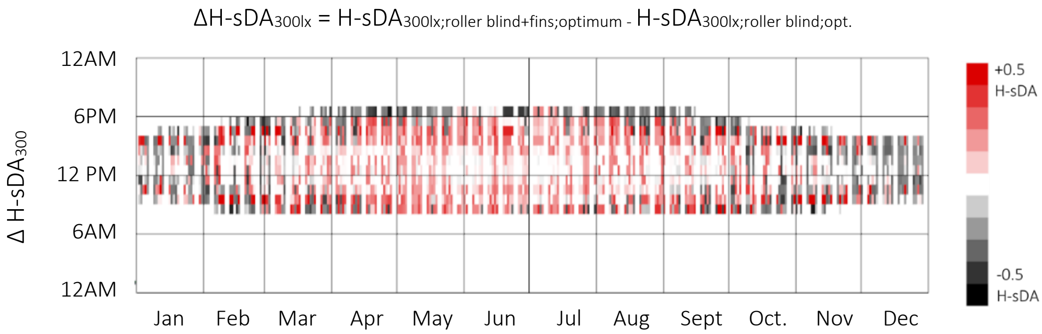

Figure 40. Difference in value for VF between PBC roller blind with and without 70°-fins

Figure 40 shows that the large increase of the roller blind in the early morning and late afternoon also results in a large increase of the H-sDA. See appendix VII for a more explorative analysis. The addition of fins is not beneficial for all occupied hours, because of their angular selectivity in blocking of the direct radiation and restriction of the daylight access during overcast sky conditions. During cloudy hours, for example, it is desired to allow solar radiation in to the office as much as possible. In the maps, such hours show a decrease of the H-sDA. The positive and negative impact of the fins is further analysed by zooming on a representative spring week in Figure 41.

On sunny days, the application of fins results in an increase of the roller blind between the 1 and 2 metres with as result an increase of the H-sDA (from acceptable to high). The view fraction as indicator for view shows small increase for a couple of these hours, but overall the presence of fins is at the expense of the view fraction. During the morning and evening hours on overcast days, the presence of fins does not change the roller blind height with an decrease of the H-sDA (from high to acceptable) and view as result.

For all the five days, the penalty function suggests a small increase of the roller blind height during noon. Dependent of the weather conditions, this results in a positive or negative impact on the daylight utilization. A possible explanation for this phenomenon is the choice of DGPs as glare indicator which is based on the vertical illuminance.

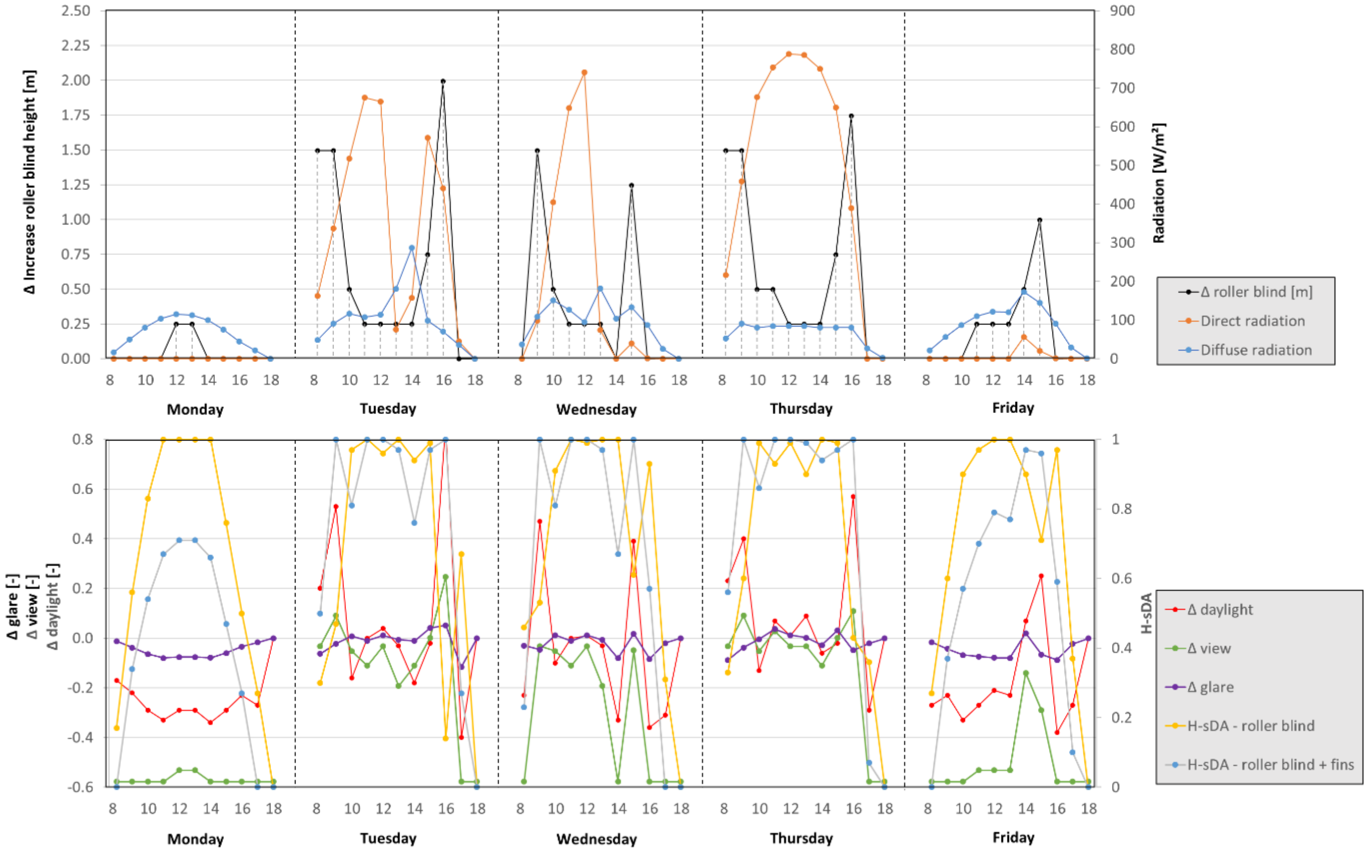

Figure 41. Up: Increase of roller blind after application of fins (70°) in the façade for a spring week together with the direct and diffuse radiation [W/m²]. Down: Impact of application of fins (70°) on glare, daylight(H-sDA$_{300}$) and view.

4.2. Case 2 - Vertical blinds and overhang

4.2.1. Case 2A - Overhang

Figure 42 shows the trade-off between glare and daylight for an overhang with different shading angles. Even though the $sDA_{300/50\%}$ levels are high, overhangs lead to a high risk of intolerable glare discomfort. Only the extreme case (80°-overhang) leads to a small reduction. All cases are clearly unacceptable. Blocking of direct sunlight for all the annual occupied hours will lead to extremely large shading systems. To create visual comfort, an additional shading solution needs to be applied.

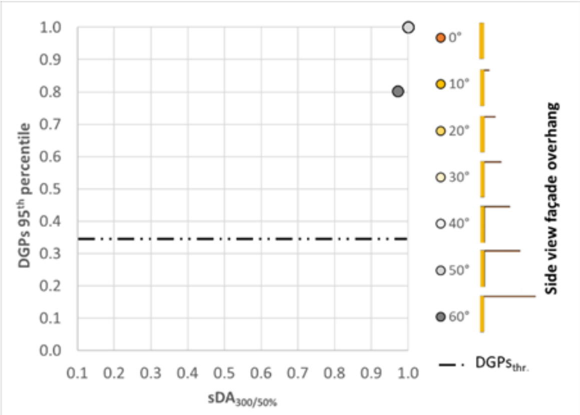

Figure 42. The trade-offs between the annual glare and daylight performance for the overhang with different shading angles.

4.2.2. Case 2B - Vertical blinds

Figure 43 and Figure 44 show the annual performance of the vertical blinds (VB) in case of different control strategies. The dots represent the five penalty functions. he diamond is representative for the RBC strategy, using a sun-tracking control strategy. The figures show that:

- Application of the RBC *(diamonds)* strategy leads to a high risk of intolerable glare discomfort. This can be assigned to that fact that such a sun-tracking control approach does not necessarily eliminate all occurrences of glare. For example, during moment with bright sky conditions.
- Performance-based controlled VB are able to prevent glare.
- In terms of glare, application of a PBC leads to 25 - 35% reduction compared to a conventional control strategy.

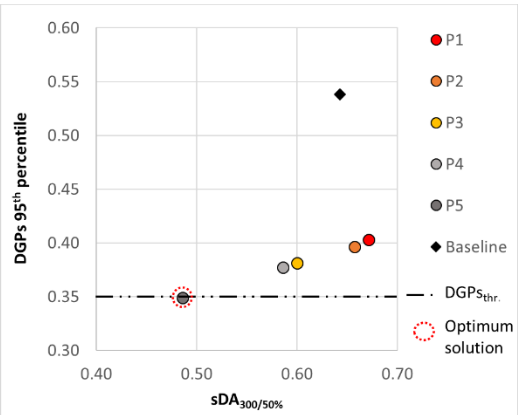

Figure 43. The trade-offs between the annual glare and daylight performance for the VB with different control strategies.

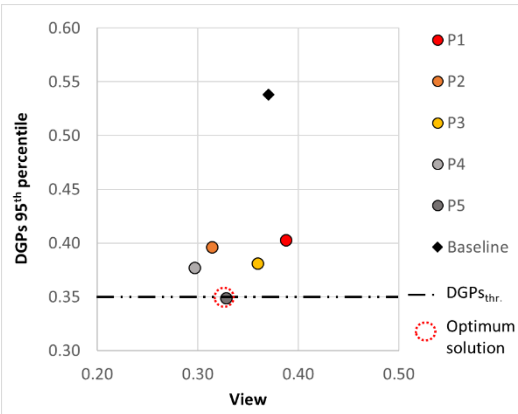

Figure 44. The trade-offs between the annual glare and view performance for the VB with different control strategies.

- If a maximum DGP 95th percentile of 0.35 is assumed, P5 gives the most beneficial trade-off between glare and daylight and between glare and view. Glare could be reduced further, but always at the expense of view and daylight.
- P1 – P5 contain different weights for glare, daylight and view and so have different priorities for glare, daylight and view. This results in a different order of the five dots by comparison Figure 43 and *Figure 44*.

4.2.3. Case 2C - Vertical blinds with overhang

Glare and view performance

Figure 45 shows a scatter plot with the annual performance for glare and view for all the possible combinations between the static overhang designs (i.e. façade designs) and the different control strategies for the VB as dynamic shading system. The orange-grey colour gradient is based on the value for the shading angle of the overhang. Figure 46 zooms in on in the trade-offs in case of a performance-based control strategy. The 5 penalty functions (P1-P5) in combination with 7 overhang angles (0° - 60°) provide 35 dots. The figures show that:

- Application of the RBC *(diamonds)* strategy results in a decrease of view by increase of overhang depth
- If a maximum DGP 95th percentile of 0.35 is assumed, the optimum façade design for a RBC-strategy contains a 50°-overhang
- If a maximum DGP 95th percentile of 0.35 is assumed, the optimum façade design for PBC contains a 30°-overhang. Important to note is that the difference in view performance with no overhang is small (±0.02 VF)
- The two groups (Figure 46) of dots are formed as result of the weights for view in the five penalty function. The left group (*blue dotted circle*) contains the trade-offs for the penalty function with a W_{view} of 0 (P2, P4) The right group (*red dotted circle*) contains the trade-offs for the other three penalty functions

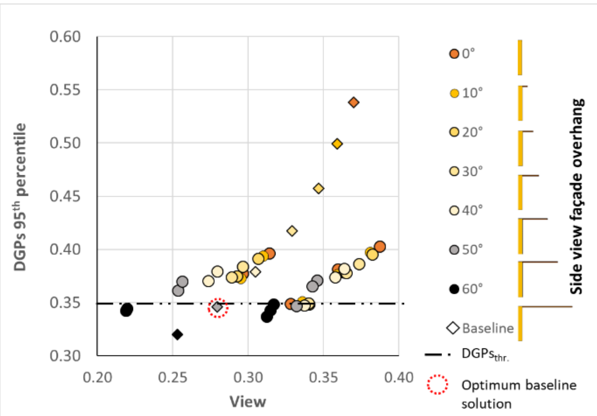

Figure 45. The trade-offs between the annual glare and view performance for the different combinations between façade designs and the VB

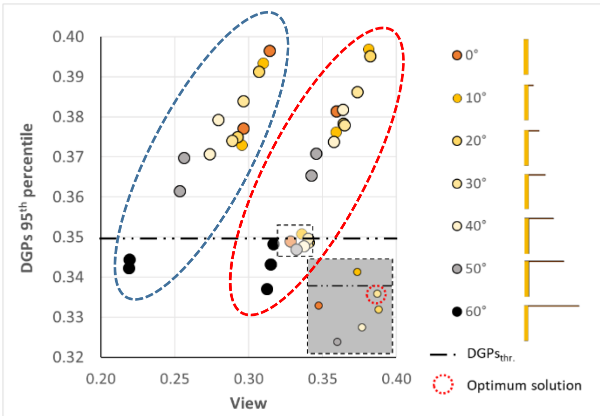

Figure 46. The trade-offs between the annual glare and view performance for the different combinations between façade designs and the performance-based controlled VB.

Glare and daylight performance

Figure 47 shows a scatter plot with the annual performance for glare and daylight for all the possible combinations between the shading angles for the overhang (i.e. façade designs) and the different control strategies for the VB as dynamic shading system. Figure 48 zooms in on in the trade-offs in case of a performance-based control strategy. The figures show that:

- Application of the RBC *(diamonds)* strategy results in decrease of daylight by increase of overhang depth.
- The PBC *(diamonds)* strategy shows potential for coupled optimization.
- The larger spread of the diamonds in comparison to the dots indicates that the RBC is more sensitive to the choices in the early design phase regarding the static façade design than the PBC. This gives more freedom for the designers in comparison to the RBC-strategy in case of an assumed glare requirement.

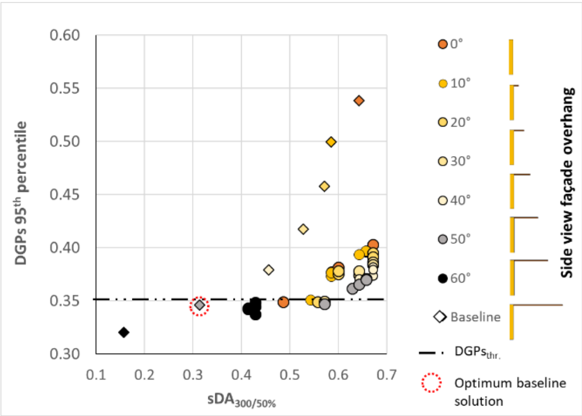

Figure 47. Scatter plot with performance for glare and daylight for the different combinations between façade designs and the VB.

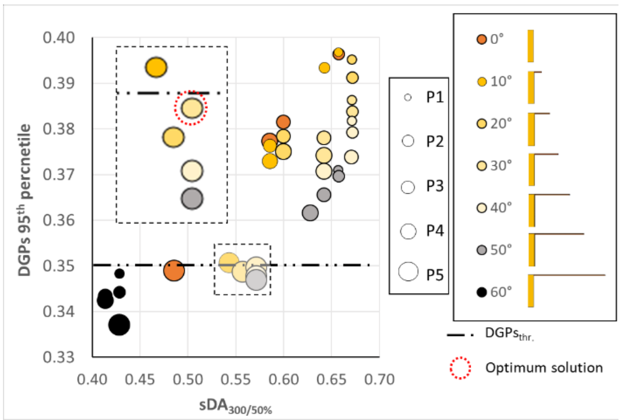

Figure 48. The trade-offs between the annual glare and daylight performance for the different combinations between façade designs and the performance-based controlled VB.

- If a maximum DGP 95th percentile of 0.35 is assumed, the optimum façade design for a RBC-strategy contains a 50°-overhang. In case on PBC strategy, the most optimal design range is an overhang with a shading angle of 20°-50°.
- Optimization of the façade in the early design phase with the RBC (50°-overhang) will lead to minimal differences in annual performance for daylight (±0%) and view (1-2%) if later PBC is installed.
- Optimization of the façade in the early design phase with the RBC will lead to a façade design with an 20°- or 30°-overhang. Application of this design instead of the 50°-overhang (based on RBC optimization) can lead to benefits as cost-reduction and material saving.
- The difference between the PBC and RBC-strategy for view (±8%) and daylight (±25%) is large. This finding could probably lead to different design decisions if other performance aspects (e.g. energy use, thermal comfort) and design parameters are taken into account in the comparison. For example, the benefits for the PBC strategy could lead to a change in window size.

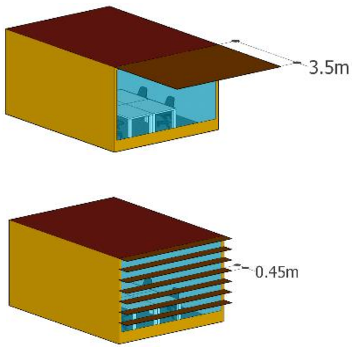

Figure 49. Simulated façade (up) and a variant design (down) for a façade with 50°-fins

Combined shading with an overhang in the range of 20°-50° results in an increase of the $sDA_{300/50\%}$ with 16% (from 0.49 to 0.77) compared to the optimum controlled VB and an increase of 84% (from 0.31 to 0.57) compared to the optimum conventional controlled VB. This improvement in daylight performance can be assigned to an higher uncovered window fraction for the vertical blinds Figure 50.

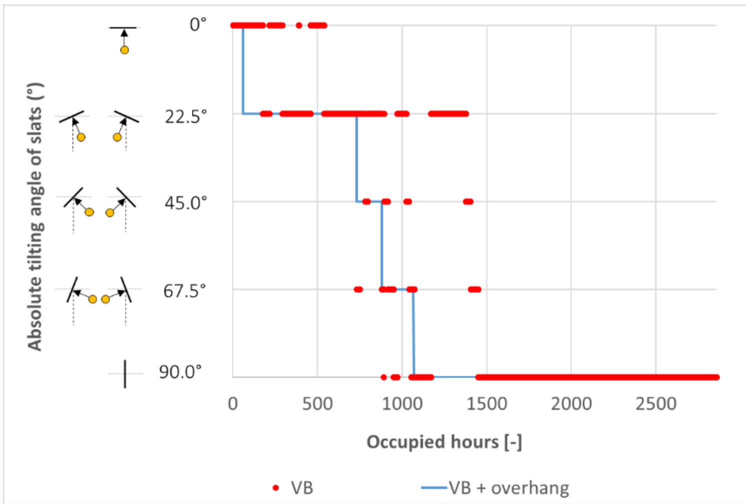

Figure 50. Openness duration curve for optimum controlled VB with and without addition of 30°-overhang

The openness duration curves show that combined shading leads to a more open state for the VB. Increase of the shading angle for the overhang from 30° to 50° results in a rotation of the slats to a more open position, especially during midday when the overhang is most effective (Figure 51). The associate impact on daylight and view is shown in Figure 52 and Figure 53. The three maps together show a clear relationship between the impact of the overhang, the change in slat position and the associated impact on daylight and view. See appendix VIII for more information.

The addition of the overhang is very beneficial for daylight and view during midday in summer, but has also negative consequences. The overhang causes restriction of the daylight access during overcast sky conditions, but this effect is limited in comparison to the previous case study. This result for a small number of hours even a rotation of the slats to a more close position, caused by the low daylight utilization in combination with the sigmoid curve for P_{glare}. Also the VF decreases for the hours when the slats do not rotate to a more open position.

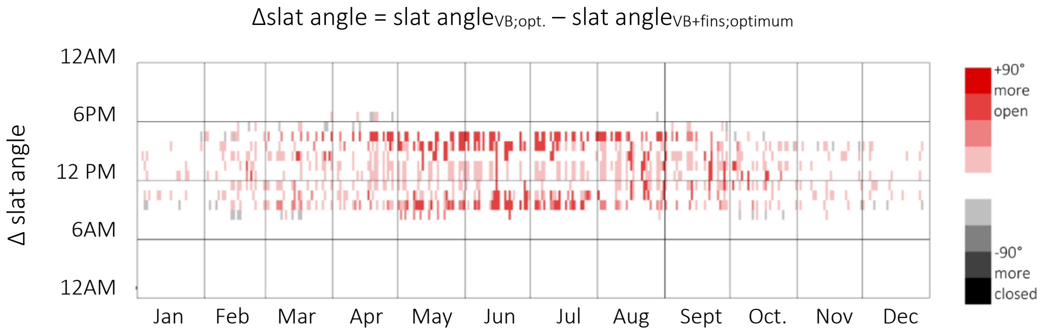

Figure 51. Difference in VB between performance-based controlled VB with and without 30°-overhang

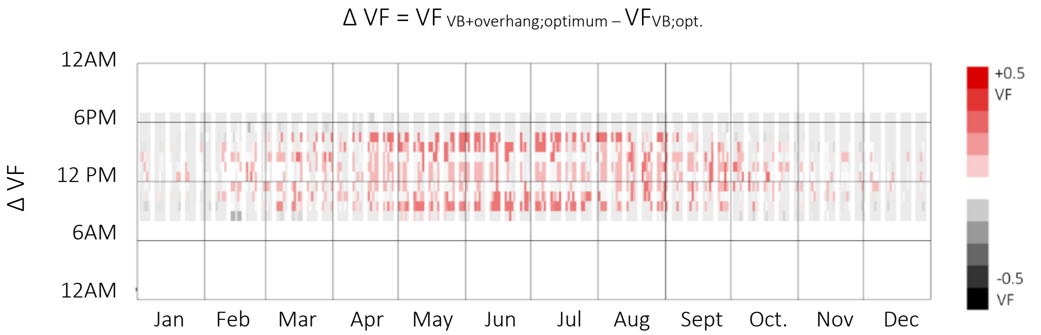

Figure 52. Difference in value for VF between performance-based controlled VB with and without 30°-overhang

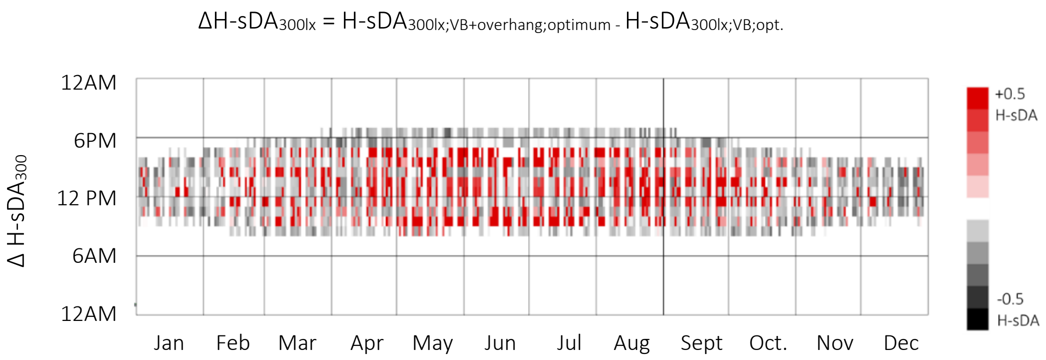

Figure 53. Difference in value for H-sDA$_{300}$ between performance-based controlled VB with and without 30°-overhang

The relationship between façade design, shading control and daylight performance is further analysed by zooming in on a summer week which contains hours with increase and decrease of H-sDA$_{300}$ after application of the overhang (30°). Remarkable is that the largest positive change in slat position happens for just before and after 12h00 in the summer. It is expected, that the biggest increase of the VB-slats and the associated visual comfort would occur at 12h00. However, the results for combined shading with an 50°-overhang are more in line with the expectations and so show the largest positive rotation of the slats during 12h00. The reason for this phenomenon could be the choice of DGPs as glare indicator in combination with the penalty function. The larger overhang results in a lower vertical illuminance at glare sensors which, in combination with the sigmoid function for P_{glare}, results in a significant more open state for the VB. (see matrices, appendix VIII).

Figure 54 shows that application of 30°-fins results in a large rotation of the slats in the morning and afternoon. These hours show also large improvements for daylight utilization and view. At 12h00, the rotation is relative small with 22.5° but on the other hand, the associated impact on daylight and view is relative large, especially on Tuesday. During overcast hours, the presence of overhang doesn't change the slat angle, but is responsible for a decrease of H-sDA$_{300}$ and view as result. The hourly spatial daylight autonomy change on these hours from high to acceptable.

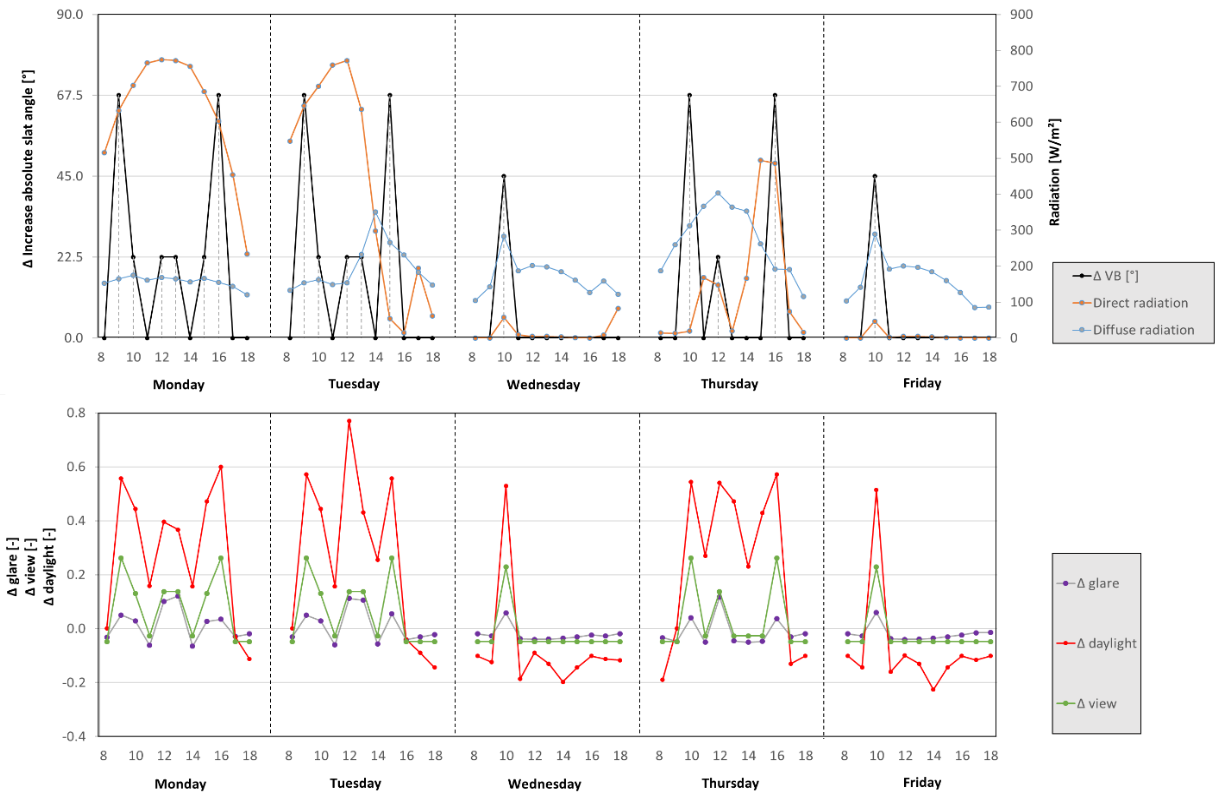

Figure 54. Up: increase of openness of VB after application of 30°-overhang in the façade for a summer week together with the direct and diffuse radiation [W/m²]. Down: the impact of on glare, daylight(H-sDA$_{300}$) and view

5. Discussion and conclusion

This chapter discusses limitations of this work, provides directions for future research and summarizes the main outcomes of this study.

5.1. Limitations and future work

- **Three-phase method + DGPs as glare indicator**: An identified drawback of the 3-phase method is the imprecise representation of the direct sun component through averaging over relatively large sky solid angles. The DGPs as illuminance baed metric for the assessment of the glare performance is less reliable in predicting contrast glare when there is direct sunlight in the field of view. *[Wienold, et al., 2019; Konstantzos, Tzempelikos, Murchison, & Proctor, 2016]*. The three phase-method in combinatino with the choice for DGPs as glare indicator might lead to an underestimation of glare. The consequence is that the performance-based controlled dynamic shading chooses a position which is too open with as result an overestimation of the daylight performance.

- **Time-step**: the case studies are performed with an hour as time-step of recording. A limitation for a smaller time-step is the hourly weather data. Actual outdoor daylight conditions show much more sub-hourly variability than what is represented by the used weather data. Nevertheless, a smaller timestep will drastically increases the computational time.

- **Limited scope:** the selection of shading systems, the use of simple architectural shading devices, weather condition and orientation are examples of the multiple scope limiting assumptions that are made in the simulation approach of this research. All these factors have influence on the performance. The potential of combined shading is application-specific and context dependent, which makes the scope of the two case studies very limited. In addition, this study is only limited to the visual performance. Coupled design optimization of façade design and automated shading control has also consequences for other performance aspects (e.g. energy use, thermal comfort), which were not explictly addressed in this study. For example, the increase of daylight utilization will probably lead to decrease of the energy demand for artificial lighting.

- **Modelling resolution of dynamic shading:** that the dynamic shading systems are modelled with a limited resolution. For example, the roller blind is modelled by dividing the fenestration system into ten horizontally oriented segments which are eater fully shaded or unshaded. The sensitivity analysis of de Vries et. al (2019) showed that performance is sensitive to these assumption

- **View:** Given the benefits and preference for daylight and view, there is interest in understanding and evaluating them. Yet, there is also no standard method or set of metrics to evaluate view. This research used the view fraction as indicator to quantify view. This indicator has his drawbacks and is very dependent on the assumptions regarding the view direction and position of the occupants. More research is also necessary to:
    - fully understand the relationship between daylight, view and health
    - to get more insight in the relationship between view content variables and landscape preference variables and their impact on view quality in a way which can be operationalised for the development of control strategies for façade design.

5.2. Practical implementation

- Multiple studies have shown that performance-based control strategies can offer an improved building performance. Their implication in practice however is complicated. More research and development is necessary to develop practical design solution in this direction to bridge the gap between research and practice.

- It is questionable if the performance benefits of coupled design-optimization in relation to a dynamic shading as individual shadings solution during operation might outweigh the costs. After all, the purchase of an extra shading system is necessary.

5.3. Conclusions

It is hypothesized that the visual comfort in office buildings can be improved through coupled design optimization of façade design and automated shading control. The previous chapters presented two simulation studies for a south-oriented test office building in the Netherlands to explore this potential. The analysis of both studies leads to the following conclusions:

- Static shading combined with performance-based controlled dynamic shading has potential to improve visual comfort in comparison to both systems as individual shading solutions. This can be assigned to the fact that blocking of the sun by static shading results in an higher uncovered window fraction for dynamic shading. The associated impact on the visual comfort is:
    - Significant improvement of the daylight performance in terms of spatial daylight autonomy
    - Contradictory impact on view. Whereas the uncovered window fraction for dynamic shading increases, static shading obstructs the view. The view performance depends strongly on:
        - the size of view obstruction by the static shading
        - the improvement of the view through increase of the uncovered window fraction for dynamic shading
        - occupant-related assumptions (e.g. occupant position, view direction).

- Concurrent optimization of static shading design and dynamic shading control could lead to different design decision if other aspects (e.g. energy use, thermal comfort) are taken in to account and/or to a number of benefits, such as cost-reductions and material-saving.

- Performance-based control integrates the façade design to the control of the dynamic shading and so is an important requirement for concurrent optimization. The benefits are:
    - more beneficial values for daylight and view performance in comparison the results for the rule-based control strategy
    - A larger facade design space with near-optimal performance. This larger design space could offer benefits in terms of performance aspects which were not explictly addressed in this study.

Application of combined shading in practice asks for a tailored approach from the design team. In the first place, it requires conscious choices regarding the façade as a static element. Therefore, the façade design must result from a careful process in the early phase of an integral design process. In addition, an advanced control strategy for dynamic shading is required. Thereby it is recommended to beforehand express the performance of the shading through a set of clearly defined criteria which can be used in dynamic evaluations and define acceptance thresholds for dynamic evaluations. Finally, it is recommended to use objective performance information to assist in decision-making trade-offs.

References

Al Horr, Y., Arif, M., Mazroei, A., Katafygiotou, M., & Elsarrag, E. (2016). Occupant productivity and office indoor

BNA. (2019). Beste gebouw van het jaar 2019. Opgehaald van BNA: https://www.bna.nl/gebouw-van-het-jaar/

Creemers, P., Loenen, E. v., Aarts, M., Chraibi, S., & Lashina, T. (2014). Acceptable Fading time of a Granual Controlled Lighting System for Co-workers in an Open Office. *Proceedings of Experiencing Light 2014 : International Conference on the Effects of Light on Wellbeing*.

Damigos, D., & Anyfantis, F. (2011). The value of view through the eyes of real estate experts: a Fuzzy Delphi approach. *Landscape and Urban Planning*, 171-178.

D'Antoni, M., Bonato, P., Geisler-Moroder , D., Loonen, R., & Ochs, F. (2017). *IEA SHC T56 - System Simulation Models.* Michigan: IEA SHC.

de Vries, S., Loonen, R., & Hensen, J. (2019). Sensor selection and control strategy development support for automated solar shading systems using building performance simulation. *Paper presented at Building Simulation 2019.* Rome: TUe.

EnergyPlus. (2001). *Weather Data by Location*. Retrieved from EnergyPlus: https://energyplus.net/weather-location/europe_wmo_region_6/NLD//NLD_Amsterdam.062400_IWEC

Favoino, F., Jin, Q., & Overend, M. (2017). Design and control optimisation of adaptive insulation systems for office buildings. Part 1: Adaptive technologies and simulation framework. *Energy*, 301-309.

Hellinga, H., & Hordijk, T. (2014). The D&V analysis method: a method for the analysis of daylight access and view quality. *Building and Environment*, 101-114.

Hensen, J., & Lamberts, R. (2019). *Building Performance Simulation for Design and Operation.* Abingdon: Routledge.

Heschong Mahone Group. (2003). *Windows and Offices: A Study of Office Worker Performance and the Indoor Environment.* California: California Energy Commission.

Hoes, P., Loonen, R., Trčka, M., & Hensen, J. (2012). *Performance Prediction of Advanced Building Controls in the Design Phase Using ESP-R, BCVTB and Matlab.* Loughborough, UK: Proceedings of Building Simulation and Optimization.

Illuminating Engineering Society. (2012). Spatial daylight autonomy. *IES Approved Method: Spatial Daylight Autonomy (sDA) and Annual Sunlight Exposure (ASE)*.

Jeong, K.-Y., Choi, A.-S., & Sung, M. (2016). A mock-up study for validation of an improved control algorithm for automated roller shade. *Indoor and Built Environment*, 17-28.

Kheybari, A. G., & Hoffmann, S. (2018). Exploring the Potential of The Dynamic Facade: Simulating Daylight and Energy Performance of Complex Fenestration Systems (Venetian Blinds). *Exploring the Potential of The Dynamic Facade: Simulating Daylight and Energy Performance of Complex Fenestration Systems (Venetian Blinds).* Kaiserslautern, Germany: TU Kaiserslautern.

Konstantzos, I., & Tzempelikos, A. (2017). A holistic approach for improving visual environment in private offices. *Procedia Environmental Sciences*, 372-380.

Konstantzos, I., Chan, Y.-C., Seibold, J., Tzempelikos, A., Proctor, R., & Protzman, J. (2015). View clarity index: A new metric to evaluate clarity of view through window shades. *Building and Environment*, 206-214.

Lee, E., Geisler-Moroder, D., & Ward, G. (2018). Validation of the Five-Phase Method for Simulating Complex Fenestration Systems with Radiance against Field Measurements. *15th International Conference of the International Building Performance Simulation Association*.

Loonen, R. (2018). *Approaches for computational performance optimization of innovative adaptive façade concepts.* Eindhoven: Roel Loonen.

Loonen, R., & Hensen, J. (2013). Dynamic sensitivity analysis for performance-based building design and operation. *Conference of International Building Performance Simulation Association*, 26-28.

Loonen, R., & Hensen, J. (2014). Smart windows with dynamic spectral selectivity - a scoping study. *14th Conference of International Building Performance Simulation Association*.

Loonen, R., Singaravel, S., Trčka, M., Cóstola, D., & Hensen, J. (2014). Simulation-based support for product development of innovative building envelope components. *Automation in Construction*, 86-95.

Mardaljevic, J. (2019). Aperture-Based Daylight Modelling: Introducing the "View Lumen". *Presented at the 16th IBPSA International Conference & Exhibition Building Simulation 2019*.

Mardaljevic, J., Andersen, M., Roy, N., & Christoffersen, J. (2012). Daylighting metrics: is there a relation between useful daylight illuminance and daylight glare probability. *First Building Simulation and Optimizatino Conference*, 189-196.

McNeil, A., & Lee, E. (2013). A validation of the radiance three-phase simulation method for modelling annual daylight performance of optically complex fenestration systems. *Journal of Building Performance Simulation*, 24-37.

Ochoa, C., Aries, M., Loenen, E. v., & Hensen, J. (2012). Considerations on design optimization criteria for windows providing low energy consumption and high visual comfort. *Applied Energy*, 238-245.

Pilechiha, P., Mahdavinejad, M., & Rahimian, F. P. (2020). Multi-objective optimisation framework for designing office windows: quality of view, daylight and energy efficiency. *Applied Energy*.

Rafel Viñoly Architects. (2005). Mahler 4 Office Tower. Opgehaald van Viñoly: https://vinoly.com/works/mahler-4-office-tower/

Rao, S., & Tzempelikos, A. (2010). The Impact of Exterior Overhang on the Daylighting Performance Office Spaces. *International High Performance Buildings Conference*.

Rollecate. (2019). ING HQ 'Cedar'. Opgehaald van Rollecate: https://www.rollecate.nl/projecten/ing-hq

Ruck, N., Aschehoug, Ø., Aydinli, S., Christoffersen, J., Courret, G., Edmonds, I., . . . Michel, L. (2001). *Daylight in Buildings. A Source Book on Daylighting Systems and Components.* Washington, D.C.: IEA.

Sadeghipour Roudsari, M., Michelle, P., & Smith, A. (2013). Ladybug: a parametric environmental plugin for grasshopper to help designers create a environmentally-conscious design. *13th Conference of International Building Performance Simulation Association, Chambéry, France, August, 26-28*.

Sargent, J. A., Niemasz, J., & Reinhart, C. F. (2011). Shaderade: combining rhinoceros and energyplus for the design of static exterior shading devices. *Proceedings of Building Simulation 2011: 12th Conference of International Building Performance Simulation Association, Sydney*.

Subramaniam, S. (2018). *Parametric modeing strategies for efficient annual analysis of daylight in buildings* . Pennsylvania: Sarith Subramaniam.

Tavil, A., & Lee, E. (2006). Effects of Overhangs on the Performance of Electrochromic Windows. *Architectural Science Review*.

Turan, I., Chegut, A., & Reinhart, C. (2020). The value of daylight in office spaces. *Building and Environment*.

Turan, I., Reinhart, C., & Kocher, M. (2019). Evaluating Spatially-Distributed Views in Open Plan Work Spaces. *Evaluating Spatially-Distributed Views in Open Plan Work Spaces.*

Tzempelikos, A., & Shen, H. (2012). *Energy and daylighting interaction in offices with shading devices .* Retrieved from IBPSA: http://www.ibpsa.org/proceedings/BSA2013/40.pdf

UN Studio. (2011). Education Executive Agency & Tax Offices. Opgehaald van UN Studio: https://www.unstudio.com/en/page/12100/education-executive-agency-tax-offices

Vries, S. d., Loonen, R., & Hensen, J. (2019). Sensor selection and control strategy development support for automated solar shading systems using building performance simulation. *Building simulation 2019, Rome*.

Vries, S., Loonen, R., & Hensen, J. (2019). *A screening method for sensor selection and control strategy development of automated solar shading systems using building performance simulation.* Eindhoven: TUe.

Wagdy, A., Fathy, F., & Altomonte, S. (2016). PLEA 2016 Los Angeles - 32th International Conference on Passive and Low Energy Architecture. . *Evaluating the Daylighting Performance of Dynamic Façades by Using New Annual Climate-Based Metrics.* Los Angeles: PLEA 2016.

Ward, G., Mistrick, R., & Lee, E. (2011). Simulating the Daylight Performane of Complex Fenestration Systems Using Bidirectional Scattering Distribution Functions within Radiance. *Leukos*.

Ward, P., Rockcastle, S., Kline, J., & Wymelenberg, K. V. (2019). Illuminating Engineering Society Annual Conference. *The impact of lighting and views on the workplace of the future* (pp. 1-15). Louisville: University of Oregon.

Wenting, L., & Samuelson, H. (n.d.). A new method for visualizing and evluating views in architectural design. *Journal Pre-proof*.

WGBC. (2014). *Health, Wellbeing & Productivity in Offices, The next chapter for green building.* World Green Building Council.

Wienold, J. (2009). Eleventh International IBPSA Conference: Building Simulation. *Dynamic daylight glare evaluation*, (pp. 944-951). Glasgow, Scotland.

Appendices

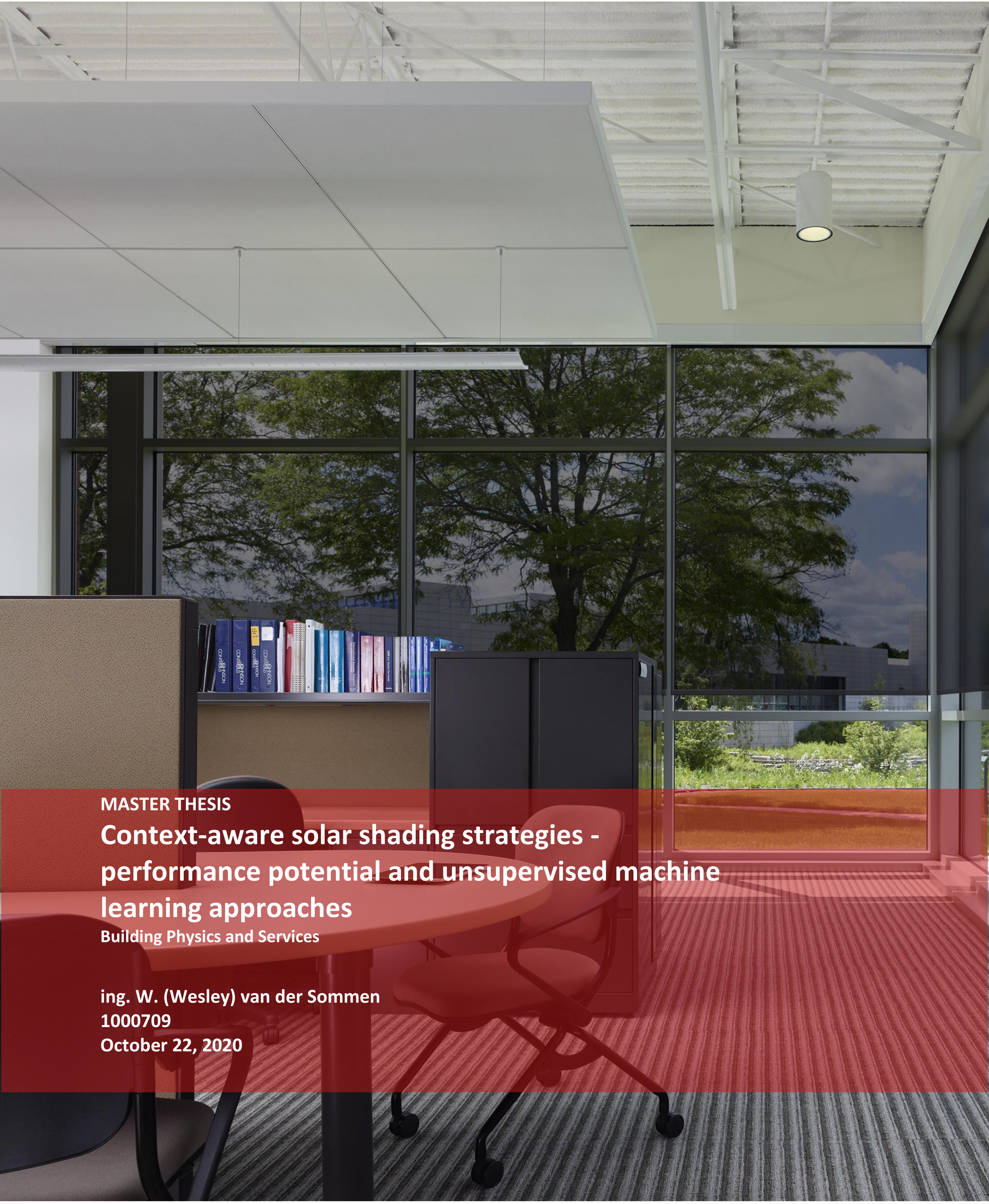

MASTER THESIS

Context-aware solar shading strategies - performance potential and unsupervised machine learning approaches

Building Physics and Services

ing. W. (Wesley) van der Sommen
1000709

October 22, 2020

EINDHOVEN UNIVERSITY OF TECHNOLOGY

Context-aware solar shading strategies - performance potential and unsupervised machine learning approaches

MASTER THESIS BUILDING PHYSICS AND SERVICES

EINDHOVEN UNIVERSITY OF TECHNOLOGY

Built Environment
Building Physics and Services
Building Performance

w.v.d.sommen@student.tue.nl
1000709

www.tue.nl

Date
October 22, 2020

Author
ing. W. (Wesley) van der Sommen

Supervisors
prof.dr.ir. J.L.M. (Jan) Hensen
Dr.ir. R.C.G.G (Roel) Loonen
Ir. S.B. (Samuel) de Vries

Abstract

This study focused on improving the positive effects of shading control strategies by extracting and utilizing information about the surrounding environment. Developing sensor strategies for advanced solar shading systems which automatically adapts to the surroundings minimizes the need for human interaction and allows for a simpler commissioning process. This is done by exploring the potential of obstruction detection and developing an unsupervised method to do so. Threshold calculations using confusion matrices with reference illuminance sensor data and DGPs values have been done for varying case studies to quantify the number of 'false' decisions made by the solar shading system. Manual obstruction isolation was done to create a best-case scenario regarding obstruction detection. Assigning separate thresholds to the obstructed and non-obstructed data points resulted in a very minimal decrease of wrong shading positions during office hours, making the potential of obstruction detection very limited. A method is proposed to automatically identify and predict local obstructions as seen from the user space by comparing the measured illuminance to their simulated equivalent and generalizing the results with the use of machine learning. The accuracy of the method is dependent on the length and start date of the commissioning period. As the prediction is dependent on solar positions, gathering sufficient training data can take up to a year. The obstruction detection model can then be used to assist in predicting obstruction events to aid automatic solar shading systems in their decision making regarding the effects from urban context. A daylight glare probability method evaluation has been conducted to assess the accuracy of the obstruction detection potential results. The evaluation concludes that DGPs often overestimates the glare probability compared to the most accurate DGP method, implying DGPs is not the best glare indicator for the obstruction detection potential assessment. A potential use-case for the SVM obstruction prediction model could be to be a part of a model predictive control (MPC) system. In a MPC system, the model should have an idea of the surroundings. Employing the support vector machine obstruction prediction model allows the urban context to be detected automatically. To further improve the confidence and accuracy of the prediction model, LiDAR data may be implemented in the model to provide additional information about the surroundings.

Contents

1 Introduction

1.1 Solar shading in high-performance buildings

Previous studies explored and confirmed that the energy performance of buildings is highly dependent on the design and size of the transparent façades in buildings [1], [2]. Automatic solar shading systems have the ability to respond to various indoor and outdoor conditions and can significantly improve the performance of a building [3]. Effective use of daylight has an impact on energy usage [4], [5], thermal comfort [6] and visual comfort [7]. Daylight is also an important factor in the wellbeing of workers in office spaces. It produces positive psychological effects and stimulates the visual and circadian system [8]. In order to effectively control solar shading, the following must be considered: direct sunlight should be cut to reduce cooling load and discomfort glare, daylight should contribute to task illuminance to reduce electricity for lighting, and the outside view should be preserved as much as possible [9]. It has been emphasized that the balance between these aspects should be an important issue in any solar shading control strategy, where glare protection is an essential part in office spaces since workplaces tend to be fixed and workers often cannot change their position or viewing direction [10], [11]. Several recent studies deal with the potential of automated control systems in achieving a balance between the ambition to maximize energy savings and the necessity to control the admission of daylight and to avoid glare and overheating [12], [13].

The obstruction of sunlight due to nearby buildings reduces natural daylight and could negatively impact the performance and effectiveness of a daylight linked control strategy. This leads to a common desire for more information on the energy performance of buildings affected by various degrees of sky obstruction when daylight linked strategies are implemented. Effective building design considering shading from urban context is fundamental to optimize energy performance [14]. Blind control strategies are often used for the specific location and orientation of the building it is designed for. However, studies have rarely considered urban context impacting the performance of solar shading systems [15]. Conventional methods for improving indoor daylight conditions and visual comfort often do not consider surrounding buildings. When direct sunlight is blocked by urban context, blinds can be opened to benefit from indirect sunlight, reducing heating and lighting demand while visual comfort is maintained. Existing blind control systems that use a feedback controlled strategy with sensors for measuring illuminance or solar irradiance are not able to differentiate whether direct sunlight is blocked by urban context or not [16].

This background leads to the awareness that possible changes in control strategies due to surrounding buildings should be considered for automated blind control. Therefore, the installed or proposed shading system and its use pattern should be considered as well.

This thesis focusses on developing a control strategy which automatically adapts based on the effect of the surrounding built environment. The various effects to consider related to (urban) obstructions for solar shading control are direct, indirect and reflected sunlight.

1.2 Current solar shading control systems

Current automated solar shading systems using daylight linked control strategies are categorized as simple or state of the art. Simple systems use multiple sensors inside and outside the office space to assess and control daylighting. State of the art modelling systems use varying physics-based models to predict daylight conditions, often combined with a sensor to assess and control daylighting.

1.2.1 Simple automated solar shading system

Simple automated solar shading systems (Figure 1) control shading based on illuminance determined by sensor input [17]. The functionality and performance of a simple solar shading system is affected by many parameters. An example is a system controlled by a rooftop sensor where the difference between horizontal and vertical irradiance is larger due to urban context. During the design process of the solar shading, the designer has to take many factors into account that influence the performance of the system. The control strategy must be decided, as well as the sensor type depending on spectral and spatial response. The sensors have to be correctly located into the space, luminaires have to be grouped in different control zones and compatible hardware has to be identified [18]. A major drawback of this system is that this can become challenging to commission and hard to calibrate, which in turn introduces errors in decision making [19].

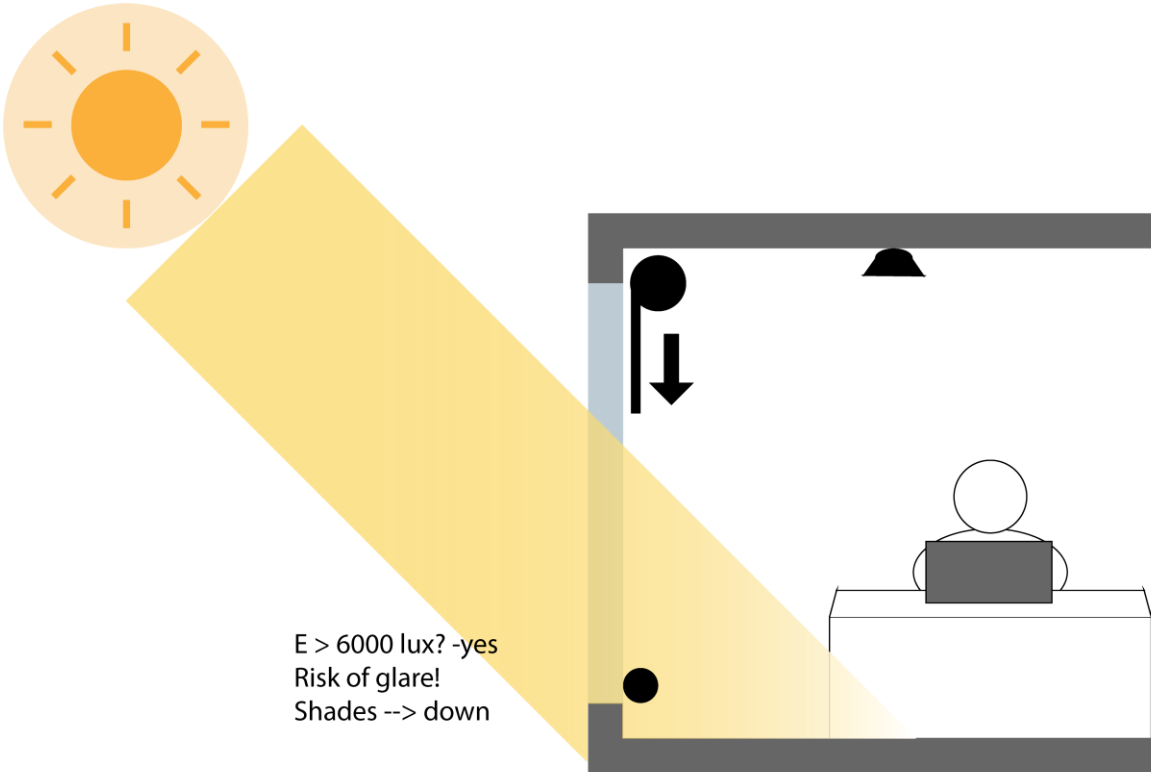

Figure 1 Automatic solar shading system

1.2.2 State of the art automated solar shading systems

Rule based strategies

The current state of the art in automated shading control systems employing advanced rule based control strategies use varying approaches employing a series of externally mounted sensors to measure sky conditions, brightness from a buildings' rooftop and several façade orientations. Rule based control strategies rely on predefined instructions based on the difference between measured and set-point values. At every timestep, the inputs are filtered through a set of rules with an 'if...then' decision structure in order to evaluate the current room situation and decide on the appropriate control decision [20].

Model predictive control (with sky modelling)

Model predictive control systems (MPC) use a simulations assisted sensor strategy to assess the impact of daylighting on blind control. Using this method it is possible to reduce the number of sensors, but challenges are introduced regarding the slow response of the control system performing real time daylight simulations that may be time consuming. Another challenge is the lack of fast daylight simulation tools able to be integrated in the control process [21]. Virtual sensors use simulation to predict conditions at predetermined locations. Such sensors can potentially replace physical sensors for controlling automated building systems and permitting sensor locations that would not be feasible for physical devices [22]. Dynamic daylight simulations not only calculate indoor daylight availability, but are also able to determine energy savings for different control strategies. Researchers underlined a drawback of dynamic daylight simulations, which is that despite their reliable daylight simulation, there are limits in simulating photosensors and electric lighting characteristics [18]. Evaluation of artificial lighting demand is based on control points, which ideally corresponds to a photosensor selected as an illuminance sensor. However, this way spectral and spatial responses are neglected. Finally the relation between photosensor signal and light output ratio are not considered and absorbed power is neglected [18].

1.3 Problem definition

The current control strategies show that the complicated and expensive calibration process involved in advanced daylighting systems is among the several other challenges to make daylighting strategies feasible in typical sensor demanding systems. The number of sensors can be limited using model predictive control strategies involving real time simulation studies, but this introduces several drawbacks.
In an ideal situation, the solar shading system is controlled directly using performance aspects like glare, daylight availability and unobstructed outside view. However, measuring this actively introduces an intrusiveness problem for occupants, as it is not acceptable to have sensors on occupants' bodies. Therefore it is necessary to make control decisions based on non-intrusive sensors. A drawback of these inexpensive physical sensors is that they typically provide a single value without considering the size, intensity and direction of the potential glare source. A small specular reflection from a neighbouring building is likely to cause only a small increase in the value reported by an illuminance sensor while still causing a significant amount of glare.
When an obstruction is introduced, direct sunlight is blocked. The sensor threshold of automatic solar shading systems may be exceeded by indirect sunlight only, resulting in a situation where the shades will go down even though there is no risk of glare. This will result in unnecessary loss of daylight and an increased artificial lighting usage. Automated shading system manufacturers have added the ability to take shadowing from the urban context into account [23]. However, these measures are often expensive and include time consuming measurements and manual adjusting/setup of sensor settings. This results in that most automatic solar shading strategies are not able to take surrounding buildings in account, leading to incorrect decisions, glare and insufficient daylight. This often results in that proposed improvements on the indoor climate are not met.

1.4 Research objectives

The problem definition translates into the following research objectives:

(1) To explore the potential of augmenting automatic solar shading systems with knowledge about the urban context for a more effective operation;
(2) To develop and test an unsupervised method for obstruction detection.

The main objective of this graduation project is to improve the positive effects of shading control by extracting information about the surrounding environment. The proposed control algorithm aims to influence the behavior of the solar shading system based on knowledge of the built environment, leading to better building performance. Developing sensor strategies for advanced solar shading systems which automatically adapts to the surroundings minimizes the need for human interaction and allows for a simpler commissioning process. The proposed method aims to reduce glare and increase daylight in (office) spaces that experience hindrance in daylight quality caused by surrounding buildings. The approach aims to be scalable since it only requires common available data from a single photometer with no further need for human intervention.

1.5 Hypothesis

As shown in Figure 2, during periods when neighbouring obstructions cast shadows on the building facade, indirect sunlight can still trigger the basic solar shading threshold even though there is no risk of glare. Initial, explorative simulations using confusion matrices showed an area of wrong decisions based on sensor illuminance and glare potential in the position of obstructions. This is further explained in section 4.2. Separating the obstruction allows to introduce a second threshold which is only used for data points where the sun is behind the obstruction. During periods where there is no risk of glare, daylight usage can be increased and artificial lighting usage can reduce. Threshold optimization can aid in the reduction of noise in measurement data. The potential constraints introduced by obstructions may be resolved using machine learning, discussed in chapter 5.

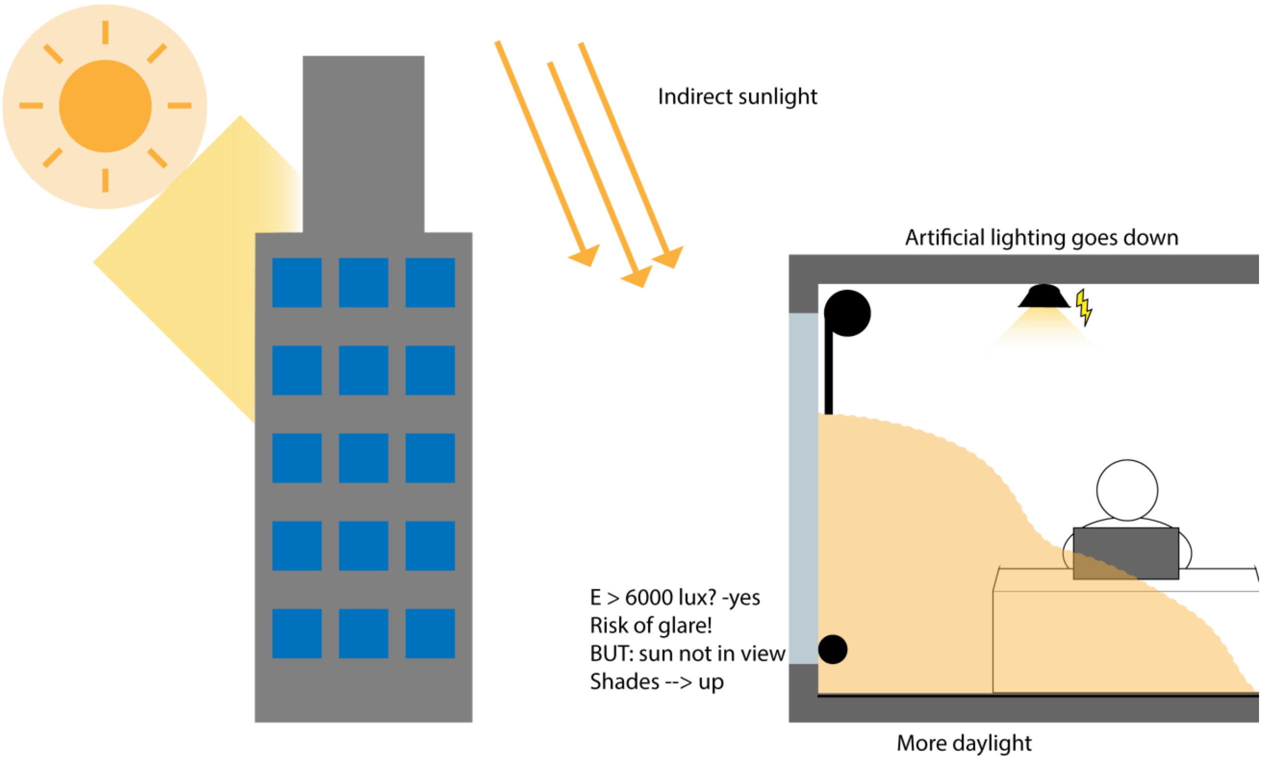

Figure 2 hypothesis example

1.6 Thesis outline

Section 2 discussed the research methodology used to explore the research objective. The case studies used to analyse the hypothesis are explained in detail in section 3. Section 4 discusses the obstruction detection potential, utilizing different manual strategies to isolate obstructions. To make the method unsupervised, section 5 describes the proposed model making use of machine learning. The daylight performance of the manual and automated model are discussed in section 6. A glare potential method has been evaluated and discussed in section 7, after which the conclusion and discussion will take place in section 8.

2 Research methodology

The research objective will be explored with multiple case studies using simulations. Glare and illuminance studies are simulated using Daysim with a 15-minute timestep. The obstruction detection potential discussed in chapter 4 starts with threshold calculations, which are carried out using confusion matrices and are discussed in section 4.1. Section 4.3 explores the potential of obstruction isolation and the application of multiple thresholds. To automate the obstruction detection, and develop an unsupervised method, section 5 proposes a workflow which uses machine learning to predict obstruction events. The analysis on the performance of the sensor strategy is based on performance indicators discussed in section 2.1. Figure 3 shows an overview of the research methodology.

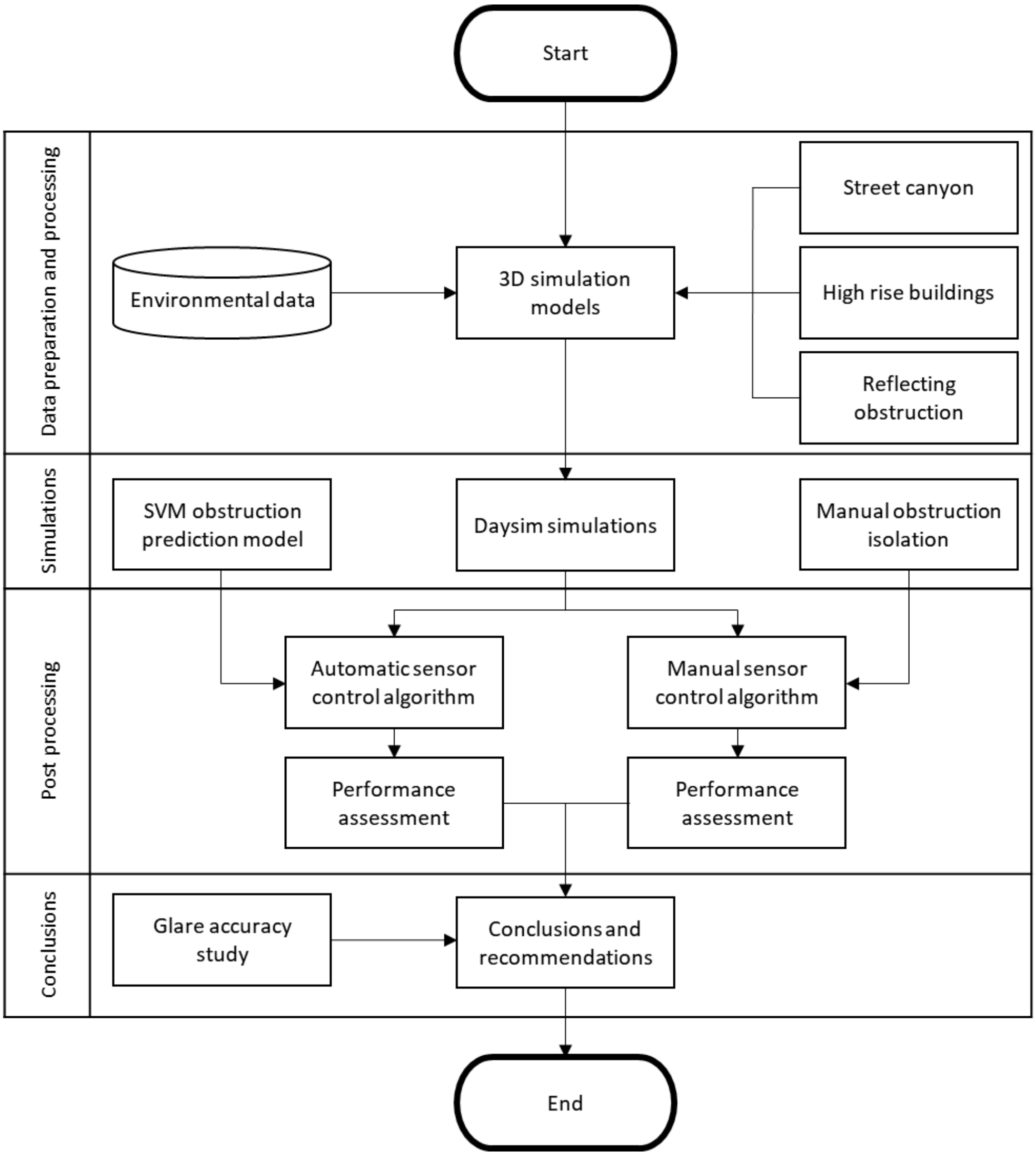

Figure 3 Research methodology overview

2.1 Performance indicators

The performance indicators where the analysis of the proposed sensor strategy will be based on are:

$sDA_{300lx,50\%}$: Spatial daylight autonomy 300 lux 50% sDA refers to the percentage of the area where daylight illuminance is higher than the target level for more than a specified occupied period in a year. It allows for the characterization of daylight quantity using a single value.

DGPs: In order to assess the glare, simplified Daylight Glare Probability is used. The normal DGP method is based on the evaluation of a picture. To overcome the large computational effort required to generate pictures at every time step of the simulations, a simplified method to calculate the DGP is investigated. It was shown that the vertical illuminance at eye level (E_v) shows a reasonable correlation to the glare perception in instances where occupants are not exposed to direct sunlight [24]. From this publication, the DGPs could be derived with equation 1:

$$DGPs = 6.22 \cdot 10^{-5} \cdot E_v + 0.184 \tag{1}$$

This equation doesn't take the influence of individual glare sources into account, and therefore cannot be used in case of direct sun or when specular reflection hits the eye of the observer. Table 1 shows the glare categories that have been defined based on user assessments results gathered within a comprehensive user assessment study in test rooms done by Wienold [25]. These DGP limits should not be exceeded in more than 5% of office time.

Table 1 DGPs categories

Glare rating	DGP value
Imperceptible	< 0.33
Perceptible	0.40
Disturbing	0.45
Intolerable	> 0.45

Energy consumption: Another performance indicator used in this study is the annual artificial lighting demand for electric lighting. This is calculated using a closed loop strategy using two ceiling-mounted lamps with integrated illuminance sensors facing towards the floor. These lamps are positioned two and five meters from the window. As soon as the work plane illuminance falls below the threshold, the lamp immediately provides the needed illuminance to maintain the threshold. For this study, the threshold is set at 500 lux and the light power is set at 10.7W/m^2. The annual energy is then computed using equation 2:

$$AALD = \frac{\sum A * \frac{Lux_i}{thr} * P}{A * ts} \tag{2}$$

Where:

$AALD\ =\ Annual\ Artificial\ Lighting\ Demand\ in\ kWh/m^2\ for\ occupied\ hours$
$A\ =\ Surface\ that\ the\ light\ source\ illuminates\ in\ m^2$
$Lux\ =\ Illuminance\ value\ of\ each\ gridpoint\ i\ in\ lux$
$thr\ =\ Threshold\ in\ lux$
$P\ =\ Power\ of\ light\ source\ in\ Watt$
$ts\ =\ Number\ of\ (occupied)\ timesteps$

2.2 Software

During this research, yearly illuminance data was not readily available from measurements. Therefore the illuminance data was simulated using the Radiance-based simulation environment Daysim. Daysim needs a description of the geometry and materials, which have been modelled in Rhinoceros. Secondly Daysim needs a description of the light sources for each timestep. In this study only daylight is used, which is described with a sky luminance distribution.

2.2.1 Illuminance simulations using Daysim

The illuminance simulation with a 15-minute interval are run using Daysim with the DDS method. This method is appropriate for cases where sensors experience rapid changes in solar exposure, for example in urban canyons [26]. Daysim is a simulation engine using Radiance and combines its daylight coefficient approach with the Perez sky model. The Radiance lighting simulation engine uses a hybrid approach of Monte Carlo and deterministic ray tracing to achieve a reasonably accurate result in a reasonable time [27]. The Perez all-weather sky model is a mathematical model used to describe the relative luminance distribution of the sky. Daysim makes use of diffuse and direct raytracing, as well as a ground model for ground reflections. Daysim has fast calculation times since it uses the daylight coefficient method and is together with Radiance integrated in the simulation environment Honeybee/Ladybug [28]. The weather file used for the simulations is based on the hourly IWEC Amsterdam (The Netherlands, latitude = 52.30°, longitude = -4.77°) weather file [29], which is linearly interpolated to an interval of 15 minutes.

3 Case studies

The proposed method is analysed using case studies. The studies will compare different obstructions and orientations based on the performance indicators mentioned in section 2.

3.1 Reference office

The reference office used for simulation is the IEA SHC Task 56 reference office for building integrated solar envelope systems [30]. It has dimensions of 6.0m (length) x 4.5m (width) x 3.0m (height), resulting in a rectangular floor plan with a gross floor area of 27m^2 and volume of 81m^3. The space has one window of 4.10m (length) x 2.65m (height). The reflection coefficients of the ceiling, walls and floor were set as 0.8, 0.5 and 0.2 respectively, the reflection coefficient of the exterior ground was set at 0.2. The office has been modelled in Rhinoceros, from where it is used by Grasshopper and Ladybug for illuminance simulations. The grid of 108 measurement points used for daylight calculations has a spacing of 0.5m. Grid points were distributed equally on the workplane 0.75m above the floor. Figure 4 shows the dimensions of the space and the arrangement of the calculation grid. For the glare assessment four measurement points (sensor 109-112) were used 1.2m above the floor as shown in Figure 5. Finally two measurement points facing outside are placed 1.2m above the floor just in behind and in front of the glass pane of the window (sensor 113 and 114).

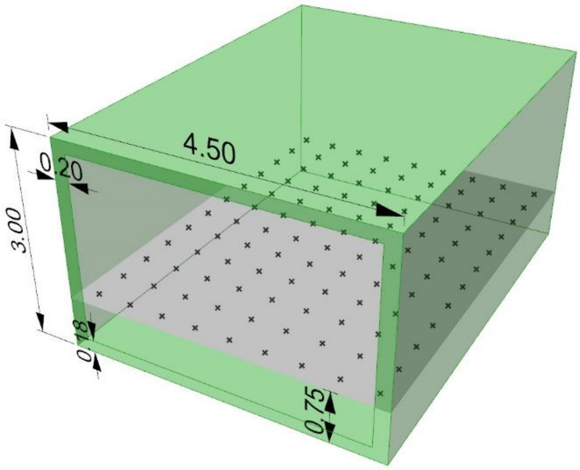

Figure 4: Reference office with calculation grid

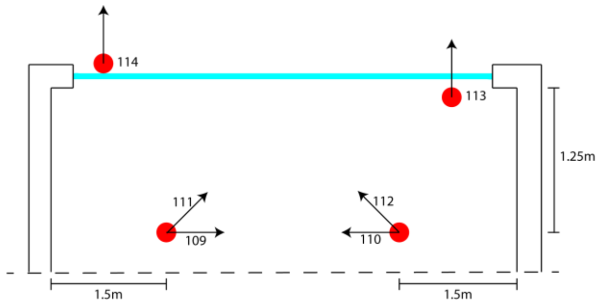

Figure 5 Sensor locations

3.2 Obstructions

The obstructions used to analyse the method are based on a common occurrence, a street canyon. The simulated street canyon has a width of 17m with obstructions varying from 10m to 15m in height. Two situations have been considered, a full street canyon and an asymmetrical obstruction as seen on Figure 6. The obstruction consists of a material with a red, blue and green reflectance of 0.35, a roughness of 0.05 and a specularity of 0. The glazing, used to assess reflections, has a red, blue and green reflectance of 0.713, a roughness of 0 and a specularity of 0.1.

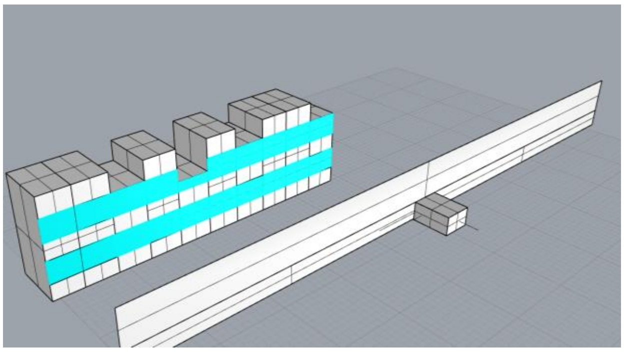
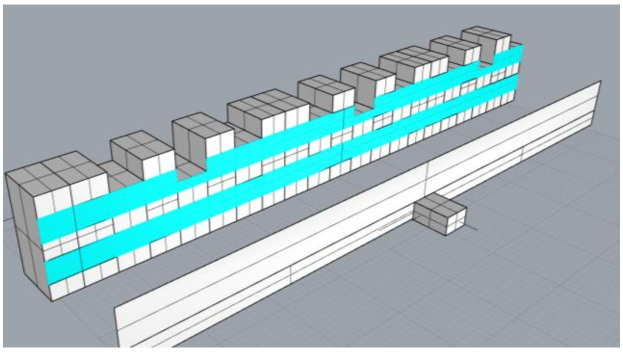

Figure 6 Asymmetrical obstruction (left) and full street canyon (right)

3.2.1 Reflective case

To test the further impact of reflections, an extreme obstruction is introduced. Figure 7 shows a large building with a glass façade causing reflections towards the office space. The glazing also uses a red, blue and green reflectance of 0.713, a roughness of 0 and a specularity of 0.1.

3.2.2 High rise case

To further analyse the rapid changes in solar exposure the model has to react to, a more extreme case with high rise buildings is used. Figure 8 shows the case study with a mix of low and high rise buildings, with open areas in between as well.

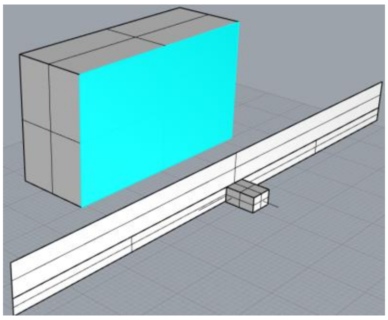

Figure 7 Reflection obstruction

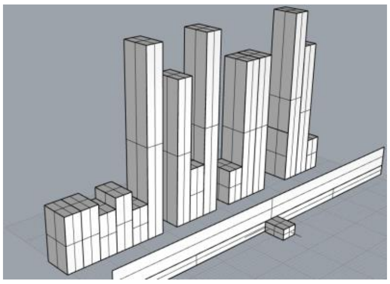

Figure 8 High rise obstructions

3.3 Glazing and solar shading system

The glazing used in the case study represents a low emission double glazing with an argon filled cavity. For the assessment including a solar shading system, a roller blind system is used which either can be fully opened or fully closed. The values shown in Table 2 represent a homogeneous diffusing shade.

Table 2 Fenestration and solar shading system assumptions

Glazing	Red, Green, Blue Transmittance	0.770
	Refractive index	1.520
Fenestration with solar shading	Red, Green, Blue Transmittance	0.010
	Refractive index	1.520

4 Obstruction detection potential

In the introduction it was mentioned that when direct sunlight is blocked by urban context, blinds can be opened to benefit from indirect sunlight, reducing heating and lighting demand while visual comfort is maintained. To assess the potential of obstruction detection, threshold calculations have been conducted to evaluate the performance of the system, quantifying the amount of right and wrong decisions. The potential assessment is based on information and results manually collected from data and simulations where the obstruction location and silhouette is known.

4.1 Threshold calculation

The goal of the threshold calculations is to find a control threshold that matches well with potential glare problems and daylight performance without too many wrong decisions. An example how indoor illuminance sensors can be used as input is shown in Figure 9. Using a confusion matrix, the strategy can determine the threshold where the reference sensor can safely assume the shading can be raised or closed without causing glare. The graph is based on the results from the illuminance simulation for a south orientation. It shows the DGPs values for two viewing directions, plotted as a function of the reference sensor behind the window (sensor 113). For both the viewing position towards the wall (sensor 109 and 110) and the viewing position towards the window (sensor 111 and 112), the maximum value of both positions is used. The graph shows the effectivity of a sensor threshold detecting the conditions where a risk of glare can occur. The limit where glare starts to be disturbing is above a DGPs of 0.4, indicated by a horizontal line in the graph. A threshold is then determined based on the data and visualized using a vertical line. An offset can be used to allow some glare, in favour of reducing the time the shading is down, admitting more daylight. Detecting a risk of glare is called 'positive' in this graph. The four quadrants of the confusion matrix are used to indicate the performance of the sensor threshold. True positives are moments where the chosen threshold correctly assumes there is a risk of glare, resulting in the solar shading going down. False positives are moments where the sensor threshold causing the solar shading to go down when there is no risk of glare, resulting in unnecessary loss of daylight. True Negatives are moments where the threshold rightly assumes there is no risk of glare and the solar shading can be raised. Finally, false negatives indicate moments where the threshold leads to a wrong decision where the solar shading is raised while there is a risk of glare, resulting in a situation where disturbing glare occurs.

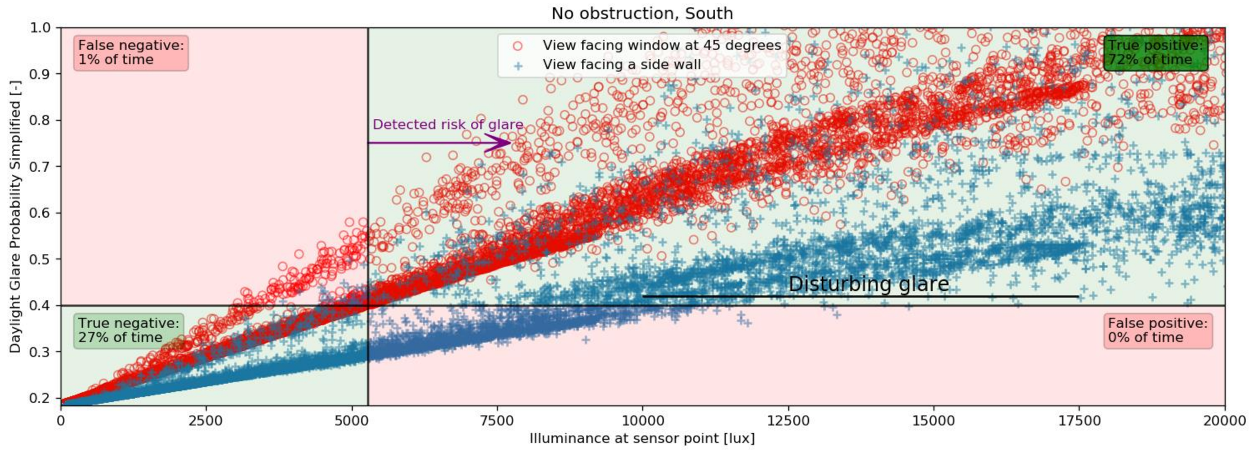

Figure 9 DGPs for two viewing position versus vertical illuminance sensor for a case facing south

4.2 Single threshold

The results from the confusion matrix can be plotted in a sun chart map. A sun chart map can be used as a scatter plot with the solar azimuth and elevation in combination with a value for a certain moment. Figure 11 shows a Cartesian sun chart scatter plot with the results of the south orientated study without an obstruction, for a viewing position facing a window on a 45 degrees angle. The plot uses a grid with the solar azimuth on the x-axis and the solar elevation on the y-axis. The grid represents the solar positions as seen from the reference illuminance sensor. It is filtered for a sun elevation greater than 0, meaning only moments when the sun is up. Furthermore it is filtered for office hours from 08:00 until 17:00.

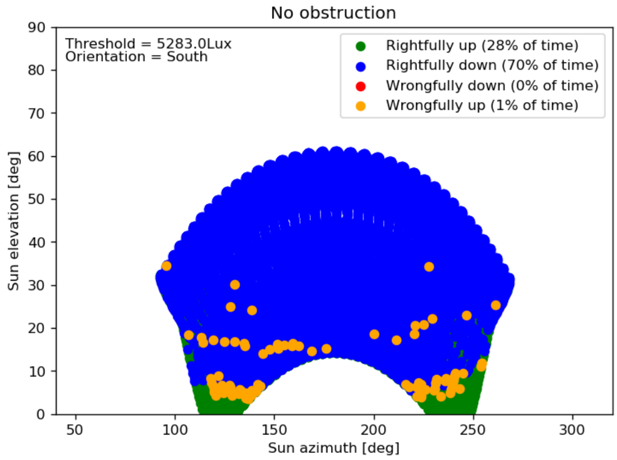

Figure 11 Cartesian sun chart map from threshold calculation south orientated

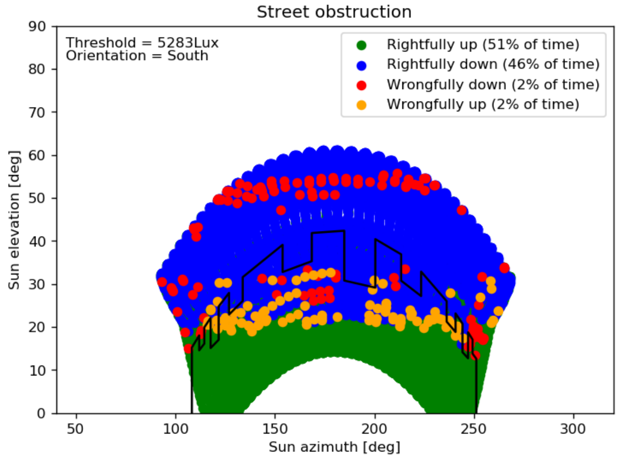

Figure 10 Cartesian sun chart map from threshold calculation south oriented

The calculated threshold acts as a baseline that can be used for other cases. Figure 10 shows the performance of the sensor threshold of 5,283 lux used for the street canyon case study. The used threshold corresponds to a false negative of 2% and a false positive of 2%, with the majority of false decisions in the area of the obstruction. The increase of wrongfully up positions indicate additional glare moments occurring. These moments are problematic since glare distracts users from work, resulting in lowering the blinds and therefore reduce natural daylight throughout the day. However, an increase of 1% is not considered significant. When a more extreme obstruction is introduced with the high rise case study, more wrong decisions occur because of the changes in solar exposure due to the obstruction. Figure 12 shows the results for the high rise case study, in which there is a majority of wrongfully down positions, indicating the solar shading could have been up without glare occurring. These points can be explained for incidences behind the obstruction, since direct sunlight is blocked. Since the wrong decisions are not consistently located inside the obstruction outline, knowledge about the obstruction will only result in a small decrease of wrong decisions.

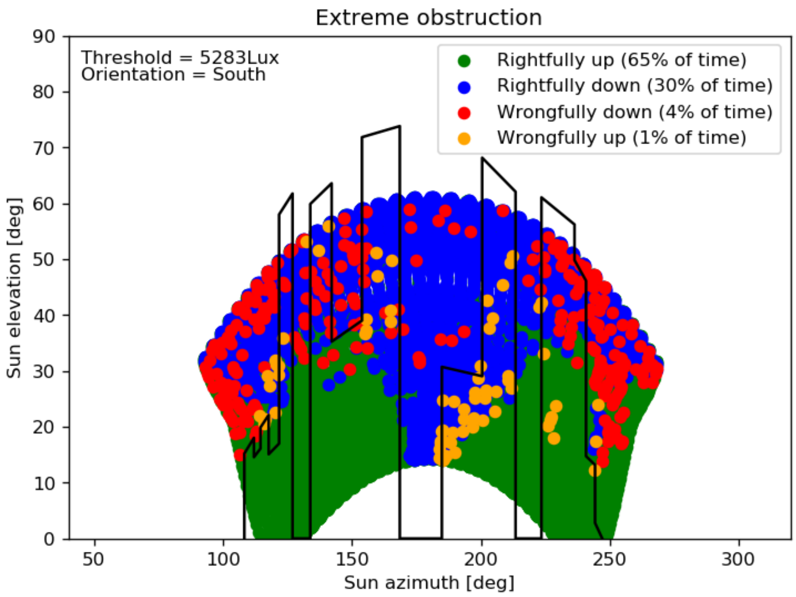

Figure 12 Cartesian sun chart map from threshold calculation south oriented high rise case

4.3 Multiple thresholds

The hypotheses stated that obstruction detection aids in the performance improvement of the office space. Since the majority of false decisions is located in the area of the obstructions, assigning a different threshold to that area can influence the number of wrong decisions during the year. When the sun is behind the obstruction the data point of that given time lies in the obstruction area.

4.3.1 Manual obstruction isolation

The data points have been separated manually to assess the best case scenario of isolating the obstruction area and assign a separate threshold to the moments the sun is behind an obstruction. As seen in Figure 13, thresholds for both the obstruction points and free-view data points have been calculated using separate confusion matrices which can then be combined to calculate the results. The separate calculations show a small decrease of 1.5% in wrong decisions during office hours. As a result, for this case, multiple thresholds can reduce the amount of wrongfully up moments, minimizing glare. However, the improvement is very minimal. Results using the high rise case study show a decrease of 1% in wrong decisions, resulting in a low potential of obstruction detection improving the solar shading system.

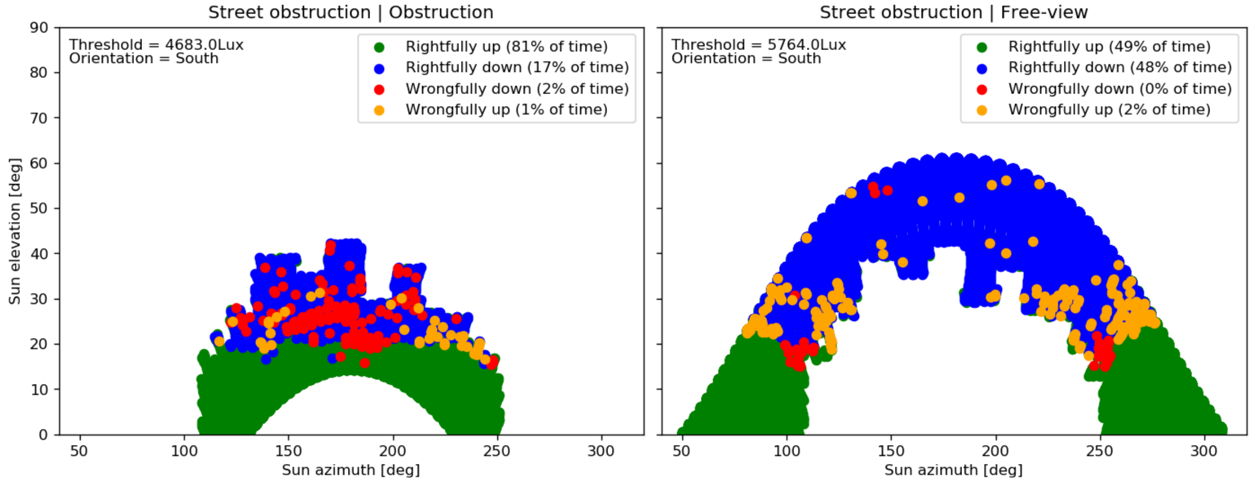

Figure 13 Manual obstruction isolation

4.4 Reflections

Looking at reflections, the threshold has been calculated for a case without an obstruction facing north. The sensor threshold is then applied to the reflective case study, resulting in the confusion matrix shown in Figure 14. The narrow, linear line indicates an accurate performance regarding illuminance and glare probability due to reflections. As a result, for this case study, obstruction detection regarding reflections is superfluous.

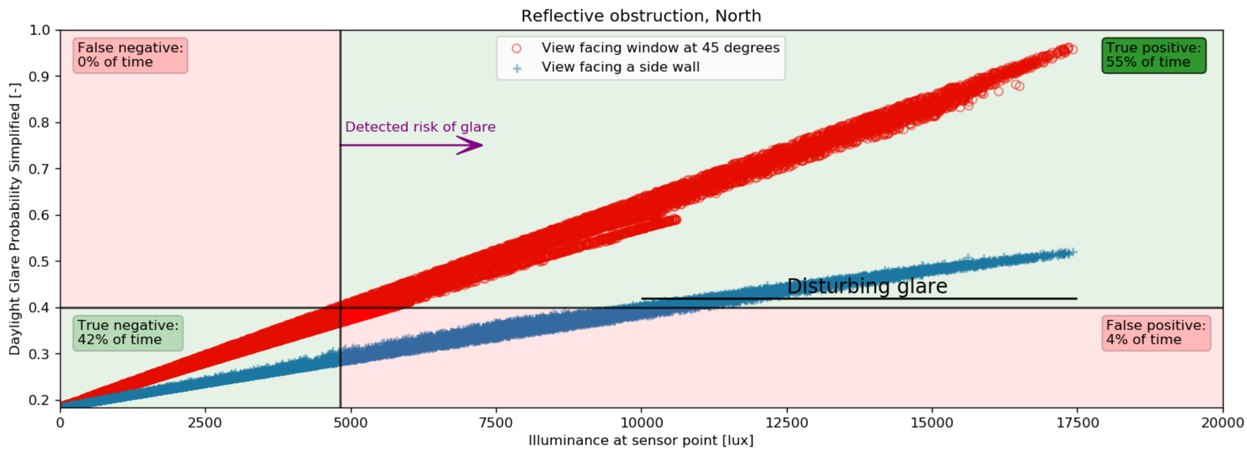

Figure 14 DGPs for two viewing position versus vertical illuminance sensor for reflective case facing north

5 Support Vector Machine obstruction prediction model

In order for the sensor strategy to be unsupervised as projected in the research objective, the process of detecting the obstruction has to be automated. A method inspired from Bógnar et al. [31] is proposed to identify and predict local obstructions as seen from the user space by comparing the measured illuminance to their simulated equivalent and generalizing the results with the use of machine learning. Illuminance data was gathered from the simulations and post-processed using Python. The obstruction detection model is written in Python and is using the Support Vector Machine classification with the radial basis (RBF) kernel. This is implemented using the Scikit-learn package [32]. A step-wise procedure is shown in Figure 15, where the process is split in two general parts: the commissioning period and the operation period.

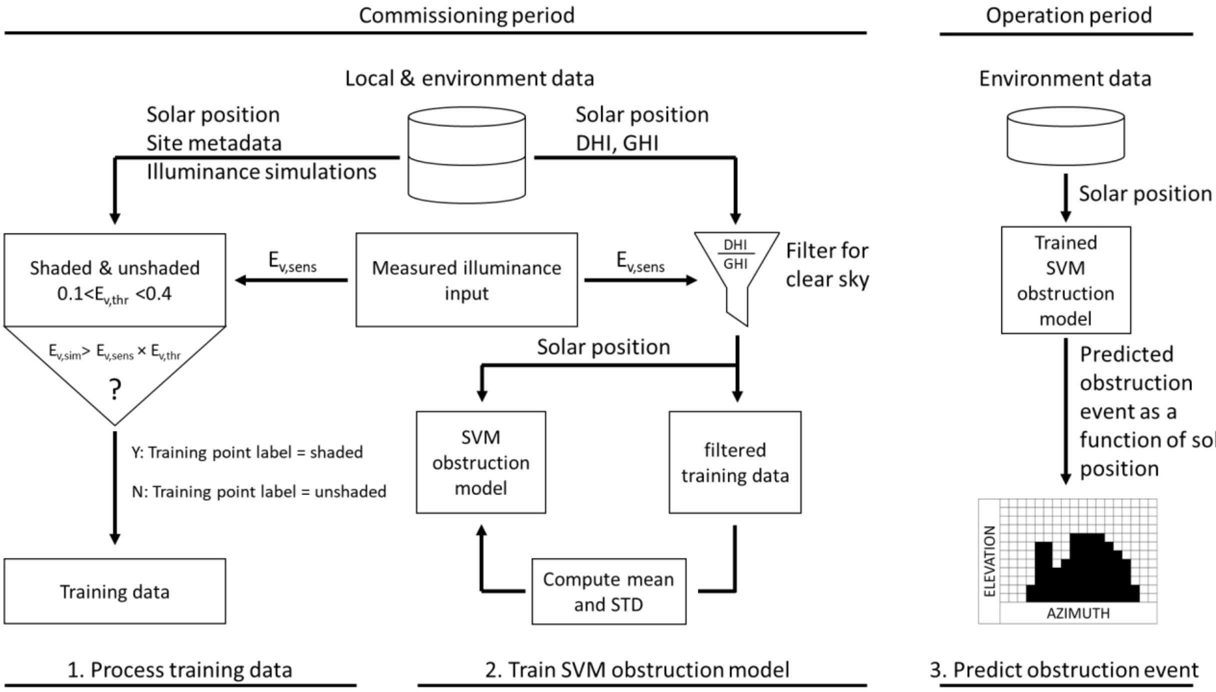

Figure 15 SVM obstruction model flowchart

5.1.1 Commissioning period

In order to be able to differentiate obstructions from free-view, local and environmental data is used as input for an illuminance simulation which is then compared with measured illuminance representing operational sensor input. Using historical data allows the model to have a reference for the data to fit to. The data is filtered for the intent of only using moments where the sky is clear from clouds for the training purposes of the Support Vector Machine (SVM). If illuminance measured by the photosensor is lower than the in the simulated results on these moments, this is concluded to be caused by an obstruction. Clearsky days are categorized using a clearsky index (CSI), calculated by dividing the direct horizontal irradiance (DHI) by the global horizontal irradiance (GHI). During fully clouded moments, DHI and GHI values are equal. On fully clear sky days, the DHI values are typically between 10-20% of the GHI values. The diffuse fraction is obtained by dividing DHI by GHI. When the CSI is near 1, the sky is fully clouded, values near 0.2 represent a fully clear sky.
For this case, the dataset consists of two features, shaded (+) and unshaded (-). These data points are used to train the SVM and construct a hyperplane dividing the datasets in two classes. The RBF kernel used to determine the shape of this hyperplane allows for a non-linear soft-margin classification using the C and γ parameter. The C value allows to disregard misclassifications by simplifying the decision curve between the two classes. A low C results in a smooth decision curve whereas a high C aims to classify all training points correctly as shaded or unshaded. The γ value defines how far the influence of a single training data point reaches, with low values for γ meaning 'far' and high values for γ meaning 'low'. The classification takes place on a grid, in this case a 2D grid using the solar azimuth on the x-axis and the solar elevation on the y-axis. The grid represents the solar

positions as seen from the reference illuminance sensor on which the new data points are projected as obstructed (+) and not obstructed (-). Combining all the points classified as obstructed results in the obstruction detected and predicted by the SVM.

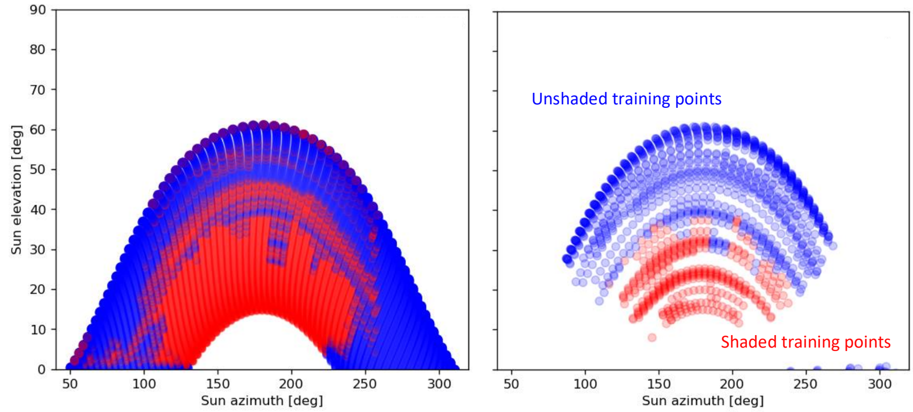

Figure 16 Training data for street canyon case, unfiltered (left) and filtered for clearsky (right)

5.1.2 Operation period

Once training the SVM is complete, the decision curve can be extracted and used to classify new data points to the (+) or (-) class based on their features and position on the grid. From an evaluation of all parameters that influence the SVM results, the C and γ values have the biggest influence on the decision curve. These two parameters have been analyzed more carefully using a range of values applied to the street canyon case. Figure 17 shows the results from the parameter analysis, with training points and the actual obstruction outline added as a comparison. From this it can be seen that the C value should be around 100 and γ values around 2.5 for the street canyon study.

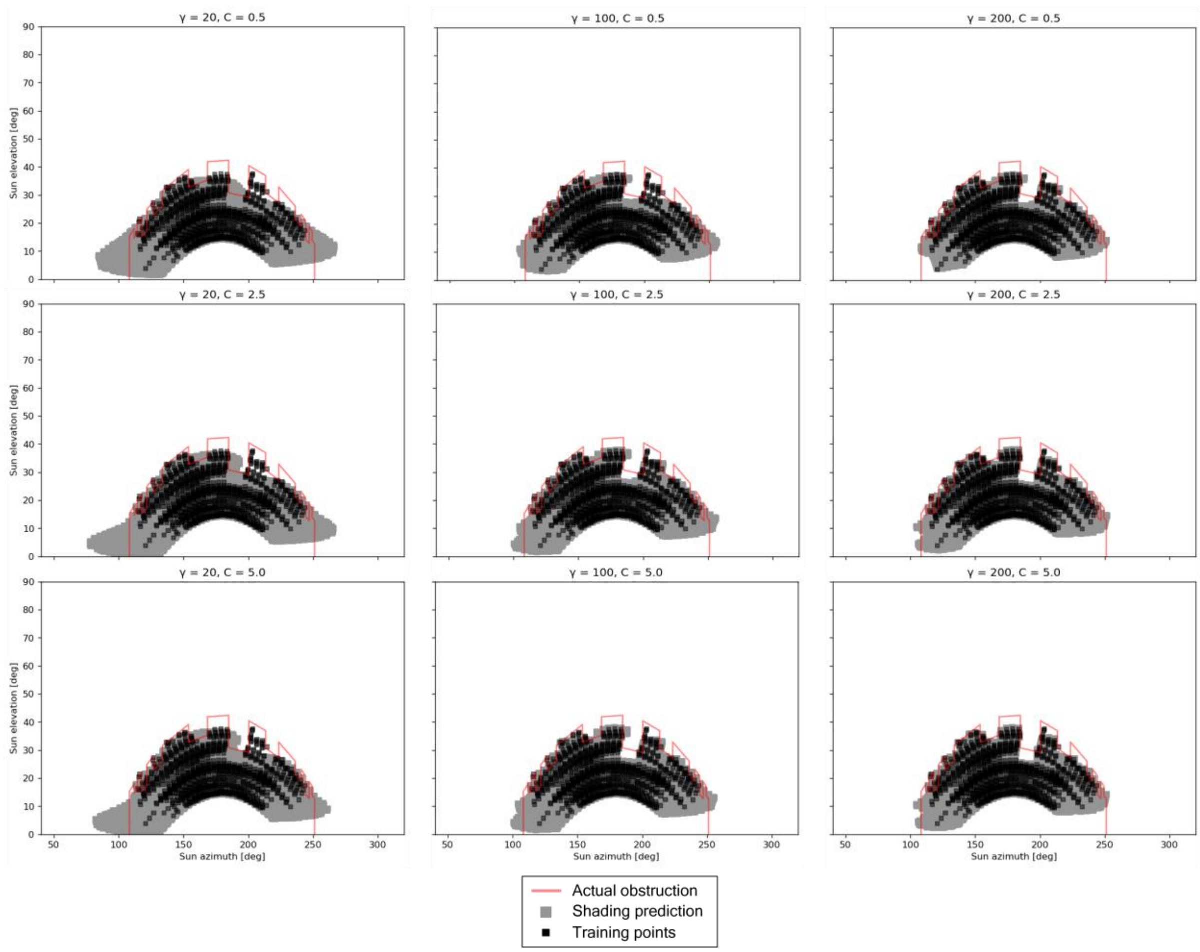

Figure 17 C and γ parameter analysis

5.2 Performance of the SVM in detecting obstructions

Looking at the high rise case study, results from the SVM obstruction model show the limitation that is introduced when using sun positions as input. Figure 18 shows that for tall obstructions, the detected height is limited to the sun positions during the commissioning period. Openings between neighbouring buildings are mostly incorrectly classified as obstructed. This problem arises in the training data due to the discretization of sun positions by Daysim, meaning changing SVM parameters will not drastically change the classification in these openings.

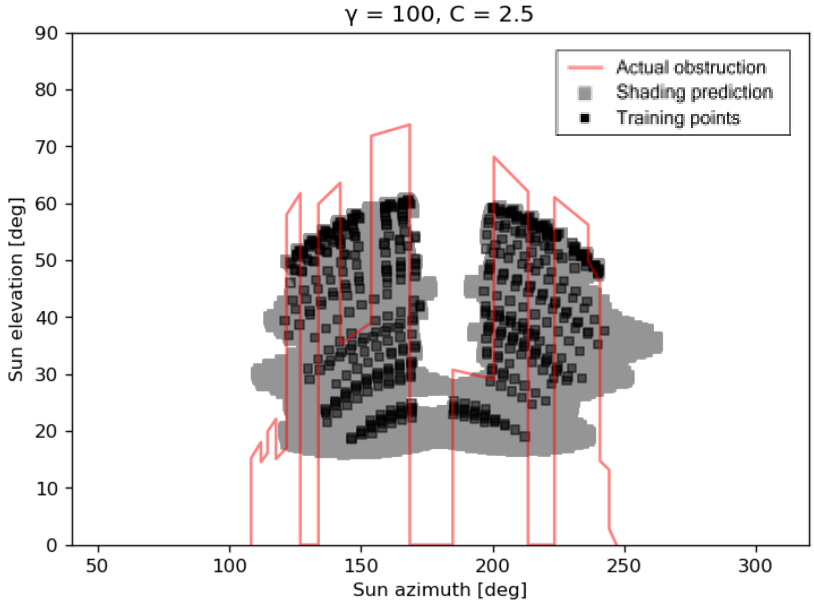

Figure 18 SVM obstruction model results for high rise case

To reduce the minimal commissioning phase duration as much as possible, less data can be used as training data input. Again, the training data relies on sun positions, and therefore the minimal commissioning period is dependent on the obstruction height and start date. Figure 19 shows an example of the SVM obstruction model using three months of training data from January up to and including March. The results for the street canyon case show a reasonable prediction after three months, while for the high rise case tree months of training data does not suffice.

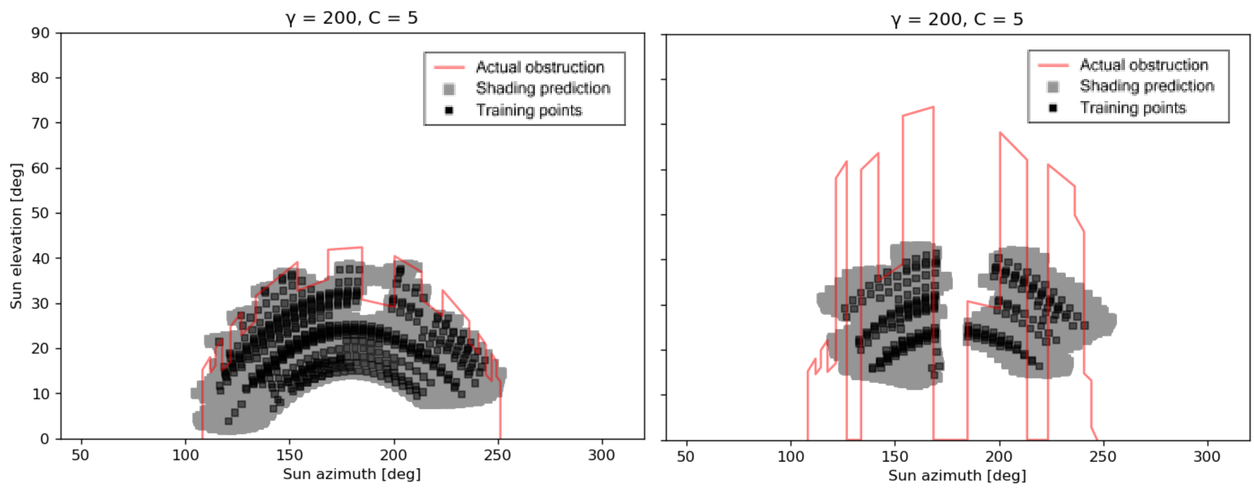

Figure 19 SMV obstruction model using limited training data, for street canyon (left) and high rise (right) case studies

6 Performance assessment

This chapter discusses the performance assessment of a context-aware suntracking strategy using manual obstruction detection discussed in section 4 and automatic obstruction detecting through the SVM model discussed in section 5. Note that for the SVM results, the north facing cases have no results. This is due to the lack of shaded classified data in the area the sun positions reach for that orientation.

6.1 Glare

Throughout this research DGPs is used to express the potential glare issues. To evaluate glare performance, an overall assessment within a time period is needed to judge a solution not only for specific situations. Figure 20 shows the DGPs performance of the street canyon case study for both a single threshold and multiple thresholds. The data has been filtered for office hours from 08:00 until 17:00. The images show a distinctive overlap between the two methods for both a South and West oriented case study.

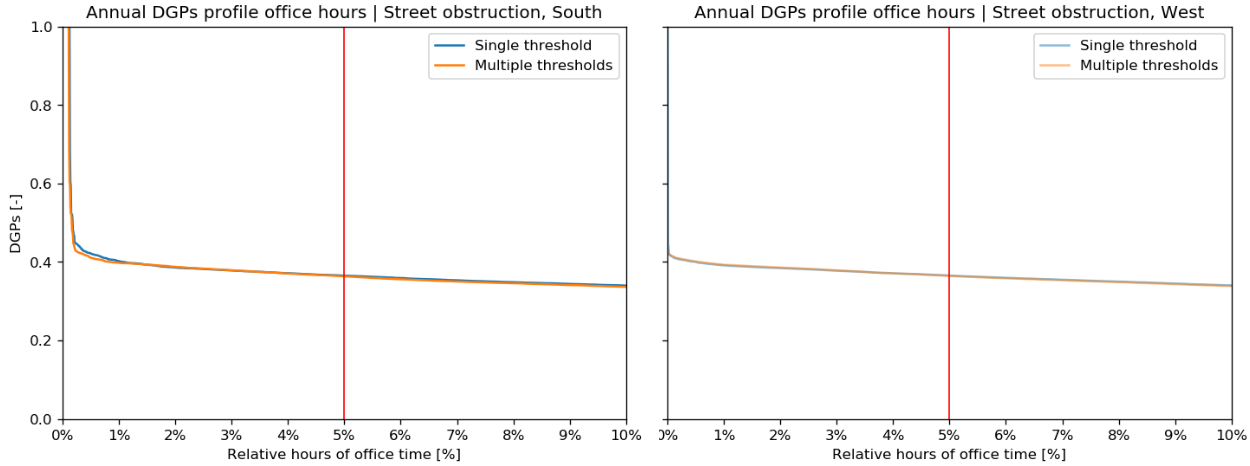

Figure 20 Annual DGPs profile for office hours. Street canyon oriented South on the left, West on the right

Table 3 shows the DGPs value within 5% of office time and the amount of hours where the DGPs threshold of 0.40 is exceeded for the different case studies, orientations and threshold calculations during occupied times. The results show a very minimal decrease in glare during 5% of office time utilizing multiple thresholds. The larger decrease in glare exceeding hours for the SVM model results from a stricter threshold, increasing the amount of time that the solar shading is down. However, this occurs on the expense of the other performance indicators and the results do not indicate a more beneficial performance trade-off from the context-aware SVM approach.

Table 3 DGPs results

Case study	Orientation	DGPs value within 5% office time			Exceeding hours per year, occupied		
Threshold(s)		Single	Multiple manual	Multiple SVM	Single	Multiple manual	Multiple SVM
Street canyon	North	0.38	0.38	-	50	43	-
	East	0.38	0.38	0.37	65	57	29
	South	0.37	0.36	0.36	37	22	20
	West	0.38	0.38	0.37	65	56	28
Asymmetrical obstruction	North	0.38	0.38	-	48	40	-
	East	0.38	0.38	0.37	77	68	40
	South	0.38	0.37	0.36	76	58	25
	West	0.38	0.37	0.37	46	35	18

6.2 Spatial Daylight Autonomy and energy usage

The daylight performance in Table 4 is presented using the Spatial Daylight Autonomy with a threshold of 300lux during at least 50% of occupied time. Energy usage is assessed using a closed-loop system with two light sources, and presented in Table 5. The results show a minimal decrease in performance employing manual and predicted obstruction detection and applying multiple thresholds. The decrease in overall performance using the proposed strategy suggest that daylight entrance is restricted during periods that are beneficial to the $sDA_{300lx,50\%}$ and artificial lighting demand. The decrease in $sDA_{300lx,50\%}$ and increase in energy usage implies the SVM prediction model in combination with multiple thresholds is not a suitable strategy to increase the performance of automated solar shading systems.

Table 4 Spatial Daylight Autonomy results

Case study	Orientation	$sDA_{300lx,50\%}$ [%]		
Threshold(s)		Single	Multiple manual	Multiple SVM
Street canyon	North	30.2	29.8	-
	East	29.6	29.3	27.5
	South	27.4	26.8	25.4
	West	29.3	28.9	26.8
Asymmetrical obstruction	North	28.9	28	-
	East	22.6	22.3	20.5
	South	21.3	20.5	18.6
	West	28.7	27.8	26.4

Table 5 Annual Artificial Lighting Demand results

Case study	Orientation	Annual energy usage [kWh/m^2]		
Threshold(s)		Single	Multiple manual	Multiple SVM
Street canyon	North	13.4	13.5	-
	East	13.9	14	14.4
	South	13.4	13.5	13.8
	West	13.4	13.5	13.9
Asymmetrical obstruction	North	14.1	14.3	-
	East	15.5	15.6	16
	South	14.3	14.5	14.8
	West	13.5	13.7	14

7 Daylight Glare Probability method evaluation

This chapter discusses the accuracy of using the simplified Daylight Glare Probability (DGPs) as indicator for glare during this research.

7.1 Alternatives

The alternatives for evaluating the risk of glare embodied in the used simulation environment are:
Enhanced simplified Daylight Glare Probability: The enhanced simplified Daylight Glare Probability (DGPs_e), uses a simplified image that includes the main glare source, without spending too much effort in calculating the exact luminance distribution within the room. This allows for a rapid simulation of DGP values.
Daylight Glare Probability: The most accurate method for calculating potential glare is the Daylight Glare Probability (DGP). The conventional DGP calculation method uses Radiance rendering routines to analyse a full 180° image for every timestep of the simulation using Evalglare. This method is very time consuming mainly due to bouncing reflection calculations within the scene.

7.2 Performance

The three methods for determining the risk of glare are compared during various circumstances. Important to note is that the DGP has been calculated once for every hour. Using a south facing case without an obstruction in Figure 21, the three DGP methods are compared with each other for office hours on April 5th. The results for this fully clouded day show an overestimation of glare probability using DGPs compared to the most accurate DGP calculation method.

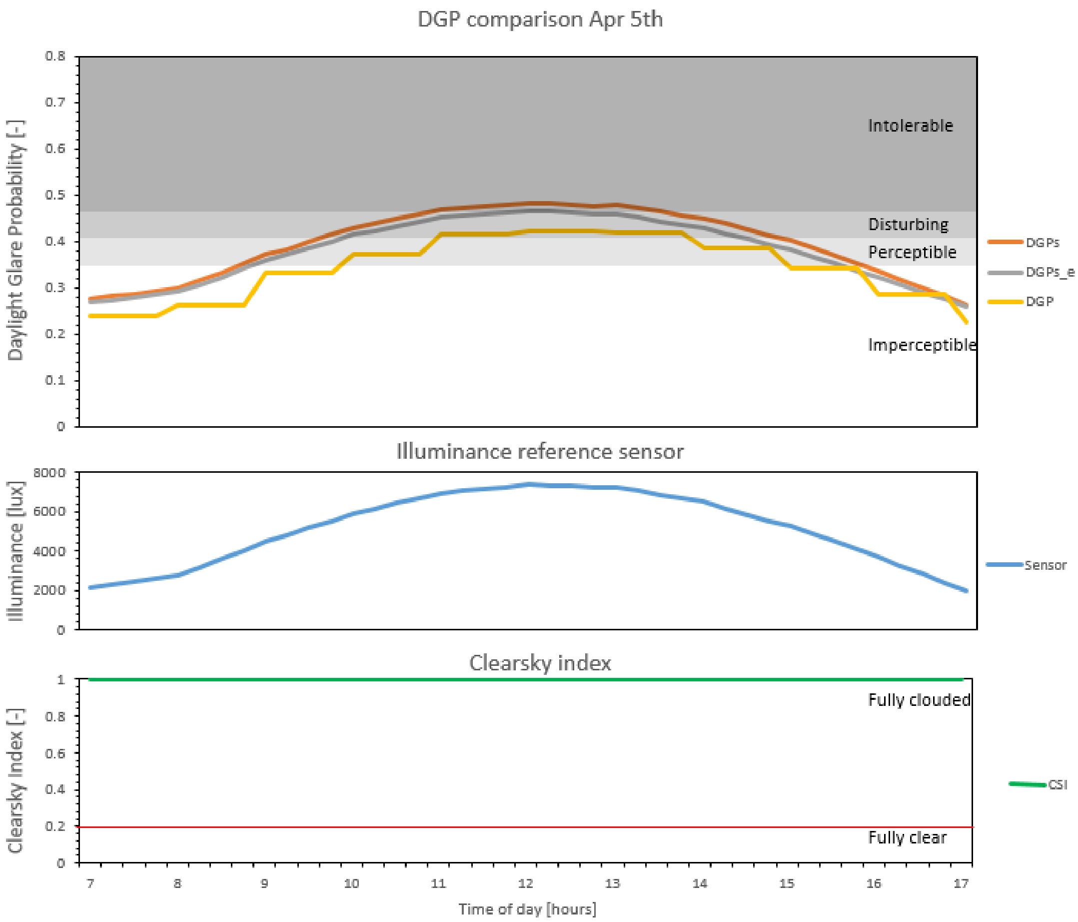

Figure 21 DGP method comparison for case without obstruction facing South, on April 5th during office hours

Figure 22 shows the results for the high rise case on March 31st. During this clear day, the sun is obstructed multiple times by the neighbouring buildings. Similarly to the non-obstructed case, DGPs values are often categorised different from the most accurate DGP method, indicating a difference in risk of glare.

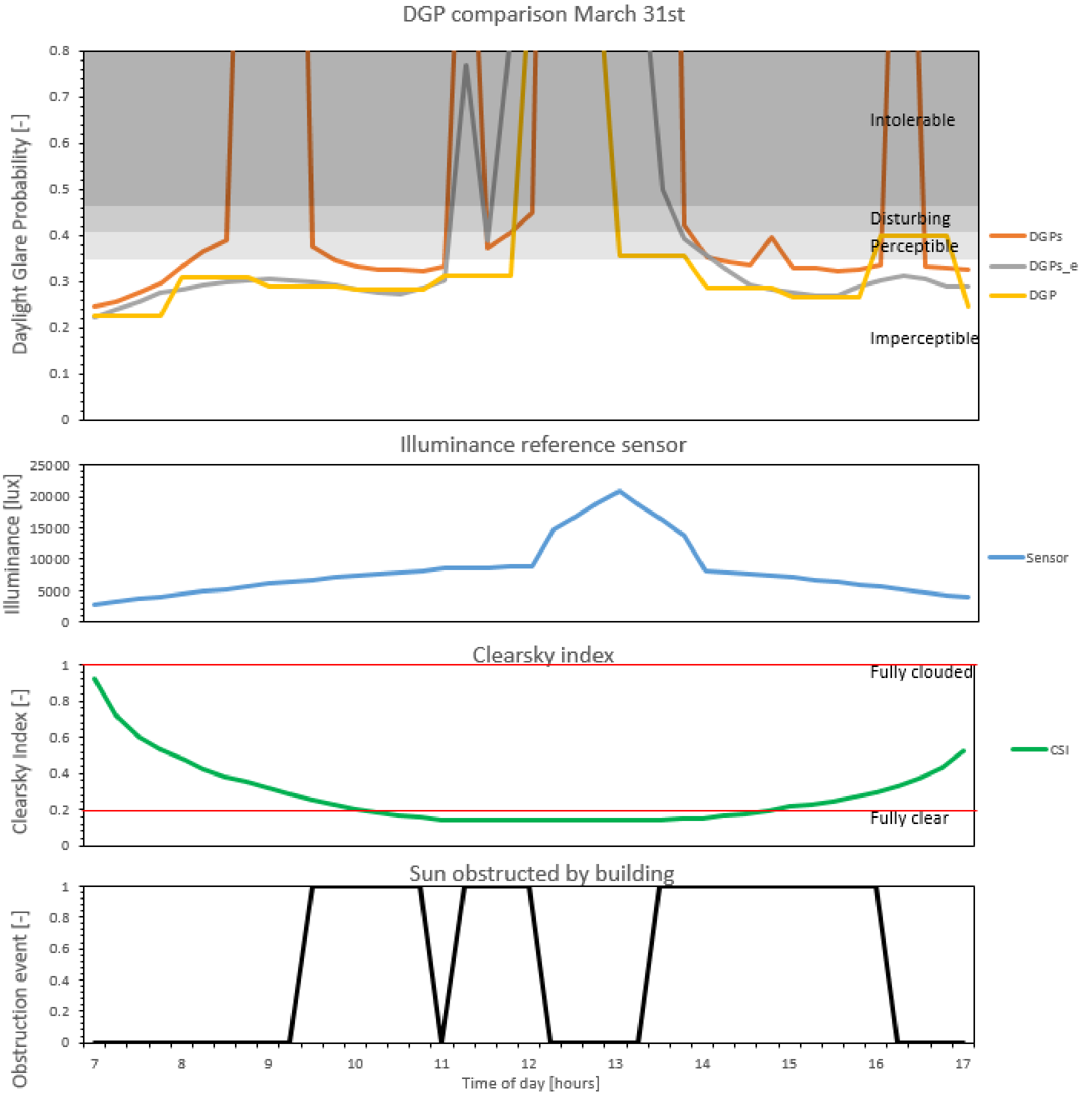

Figure 22 DGP method comparison for high rise case without facing South, on March 31st during office hours

Figure 23 shows an example of the DGP results for the high rise case study on March 31st, for a viewing position 45 degrees towards the window. At 11:00 the sun is partially blocked by the obstruction, resulting in a glare probability of 0.31, indicating imperceptible glare. At 12:00 the sun is not obstructed by the building, resulting in a maximum DGP of 1.0, indicating intolerable glare.

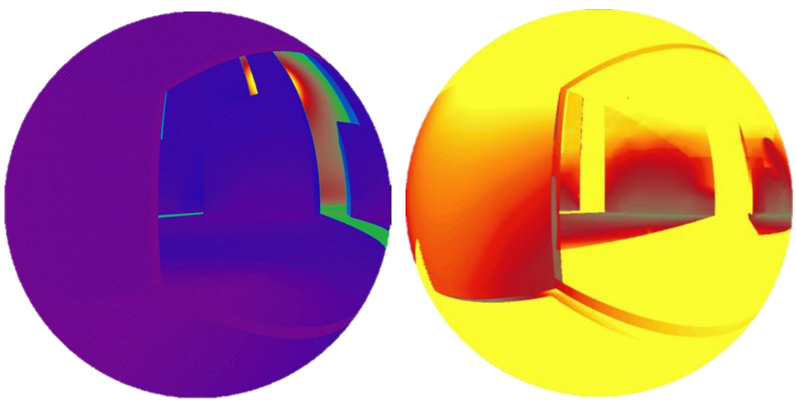

Figure 23 DGP result high rise case, on March 31st at 11:00 (left) and 12:00 (right)

8 Conclusion and discussion

8.1 Conclusions

This study focused on improving the positive effects of shading control strategies by extracting and utilizing information about the surrounding environment. The results from the confusion matrix for the street canyon case study showed a majority of wrong shading positions in the area of the obstruction, implying obstruction detection has the potential of optimizing the decision making of automated solar shading systems. However, manual obstruction isolation was done to create a best-case scenario regarding obstruction detection. Assigning separate thresholds to the obstructed and non-obstructed data points has no substantial influence on the number of wrong decisions, resulting in a low potential to improve the performance of advanced solar shading systems. Since the results turned out not to be as promising as expected in the hypothesis, a daylight glare probability method evaluation has been conducted to assess the accuracy of the results. The evaluation concludes that DGPs often overestimates the glare probability compared to the most accurate DGP method. Therefore, the accuracy of the potential of obstruction detection is uncertain since DGPs appears to not be the best indicator to judge the results of the research objective.

To achieve unsupervised obstruction detection, a method is proposed to identify and predict local obstructions as seen from the sensor position by comparing the measured illuminance to their simulated equivalent and generalizing the results with the use of machine learning. The method consists of two steps: the commissioning period and the operation period. The approach aims to be scalable since it only requires common available data from a single photometer with no further need for human intervention. When complex obstructions containing gaps in between buildings are introduced, the model is unable to predict openings where sun exposure is only partially obstructed, like in the high rise case study. The accuracy of the method is dependent on the length and start date of the commissioning period. As the prediction is dependent on solar positions, gathering sufficient training data can take up to a year. The obstruction detection model can then be used to assist in predicting obstruction events to aid automatic solar shading systems in their decision making regarding the effects from urban context.

8.2 Discussion

Using DGPs as performance indicator for glare during this thesis has not been the best indicator for the research objective. DGPs has been proven to be a reliable indicator for glare in cases where the sun is not in the direct view of an occupant. This thesis included obstructions that cause rapid changes in solar exposure due to the sun partially being blocked. Sun position discretization in combination with the timestep used are responsible for wrong assumptions. Once the sun is not obstructed, direct sunlight is the main cause of glare, being in the direct view of an occupant. For these situation DGPs is not the best indicator for glare. Additionally, perception of glare can still occur due to direct sunlight being visible through a fabric roller shade, even when not indicated by sensors.

A critical look on the SVM obstruction prediction model shows several limitations. The dependency on solar position during clear sky periods makes the model less than ideal regarding commissioning time. The best fitting values for the C and γ have to be investigated for each sensor and case individually, requiring a lot of manual labour. This questions the unsupervised aspect of the research objective as the optimal values for the C and γ are sensitive to the density of training data. Using less data or a different timestep may result in a necessity to re-evaluate the parameter values. Small objects and cavities between buildings cannot be predicted by the SVM obstruction detection model proposed in this research, but are important regarding potential glare conditions. Therefore, an alternative method exploiting LiDAR data to identify smaller objects may be implemented to provide additional information about the surroundings impacting the performance of solar shading systems.
The potential of obstruction detection was assessed using a best-case scenario where the obstruction can be detected with a 100% accuracy. The performance using the SVM obstruction prediction model varies between performance indicators. Where glare exceeding hours are lower, the $SDA_{300lx,50\%}$ is also lower and energy usage is higher. This is expected when a different strategy is used in which solar shading is more often closed

compared to the best-case scenario. This implies that a 100% accuracy is not necessary to benefit from the SVM obstruction model. However, the minimum accuracy needed has not been investigated. A close look at the unfiltered training data shows the obstruction outline is similar to the results from the SVM obstruction model. Using the 'shaded' data points as input for sensor strategies is possible. However the training data also classifies data as 'shaded' during partially overcast sky conditions, resulting in a necessity to filter these moments. The training data after the filter is scattered, and the SVM obstruction model aids in combining the data to a more realistic obstruction shape. Additionally, the commissioning phase can be repeated to account for changes in the urban context.

8.2.1 Further research

A potential use-case for the SVM obstruction prediction model could be to be a part of a model predictive control system. In a MPC system, the model should have an idea of the surroundings. Employing the SVM obstruction model allows the urban context to be detected automatically. Certain sensors are expensive and generally installed once per building or façade, like pyranometers and HDR sky scanners. These central sensors are unable to predict effects from local shading on the room level. Employing cheap, local illuminance sensors combined with the SVM obstruction detection model, knowledge of central sensors can be combined to make predictions on floor or room level. To further improve the confidence of the prediction model, LiDAR data may be implemented in the model to provide additional information about the surroundings. LiDAR-based approaches are capable of detecting smaller objects impacting the daylight performance like foliage or antennas. Additionally, implementing LiDAR-based models may increase the accuracy of detecting small gaps in-between buildings previously classified as shaded. More research is required to accurately differentiate reflections from shaded classified data points. As of now, the reflecting surfaces are part of the obstruction. The ability to distinguish reflecting surfaces allows the introduction of a third class in the SVM obstruction prediction model: reflections. To further increase the resolution of the obstruction maps, increasing the timestep may result in a more accurate description of sun positions. An important factor that has to be taken in account is sun position discretization. If a sun position is used for multiple timesteps, the accuracy of the model decreases.

9 References

[1] M. Perino and V. Serra, “Switching from static to adaptable and dynamic building envelopes: A paradigm shift for the energy efficiency in buildings,” *J. Facade Des. Eng.*, vol. 3, pp. 143–163, 2015.
[2] H. Poirazis, Å. Blomsterberg, and M. Wall, “Energy simulations for glazed office buildings in Sweden,” *Energy Build.*, vol. 40, no. 7, pp. 1161–1170, Jan. 2008.
[3] S. Y. Koo, M. S. Yeo, and K. W. Kim, “Automated blind control to maximize the benefits of daylight in buildings,” *Build. Environ.*, vol. 45, no. 6, pp. 1508–1520, Jun. 2010.
[4] A. Tzempelikos and A. K. Athienitis, “The impact of shading design and control on building cooling and lighting demand,” *Sol. Energy*, vol. 81, no. 3, pp. 369–382, Mar. 2007.
[5] R. Lollini, L. Danza, and I. Meroni, “Energy efficiency of a dynamic glazing system,” *Sol. Energy*, vol. 84, no. 4, pp. 526–537, Apr. 2010.
[6] A. Tzempelikos and H. Shen, “Comparative control strategies for roller shades with respect to daylighting and energy performance,” *Build. Environ.*, vol. 67, pp. 179–192, Sep. 2013.
[7] E. S. Lee *et al.*, “A Post-Occupancy Monitored Evaluation of the Dimmable Lighting, Automated Shading, and Underfloor Air Distribution System in The New York Times Building,” 2013.
[8] M. B. C. Aries, J. A. Veitch, and G. R. Newsham, “Windows, view, and office characteristics predict physical and psychological discomfort,” *J. Environ. Psychol.*, vol. 30, no. 4, pp. 533–541, Dec. 2010.
[9] L. G. Bakker, E. C. M. Hoes-van Oeffelen, R. C. G. M. Loonen, and J. L. M. Hensen, “User satisfaction and interaction with automated dynamic facades: A pilot study,” *Build. Environ.*, vol. 78, pp. 44–52, Aug. 2014.
[10] S. A. Sadeghi, P. Karava, I. Konstantzos, and A. Tzempelikos, “Occupant interactions with shading and lighting systems using different control interfaces: A pilot field study,” 2016.
[11] D. Abigail and C. Pool, “A Comprehensive Evaluation of Perforated Façades for Daylighting and Solar Shading Performance: Effects of Matrix, Thickness and Separation Distance,” *J. Daylighting*, vol. 6, pp. 97–111, 2019.
[12] H. Shen and A. Tzempelikos, “Daylighting and energy analysis of private offices with automated interior roller shades,” *Sol. Energy*, vol. 86, no. 2, pp. 681–704, Feb. 2012.
[13] H. Shen and A. Tzempelikos, “Sensitivity analysis on daylighting and energy performance of perimeter offices with automated shading,” *Build. Environ.*, vol. 59, pp. 303–314, Jan. 2013.
[14] I. G. Capeluto, “The influence of the urban environment on the availability of daylighting in office buildings in Israel,” *Build. Environ.*, vol. 38, no. 5, pp. 745–752, May 2003.
[15] W. J. Chung, C. Liu, and Y.-B. Seong, “Potential lighting and thermal demand reduction in office buildings using blind control considering surrounding buildings,” *J. Asian Archit. Build. Eng.*, vol. 18, no. 3, pp. 262–270, May 2019.
[16] Y.-B. Seong, “*HELIOS-EX* : Blind control simulator and method with a consideration of adjacent buildings,” *Indoor Built Environ.*, vol. 24, no. 1, pp. 37–51, Feb. 2015.
[17] S. Berman, J., Berman, J., Greenspan, A. and Hebeisen, “Automated Shade Control Method and System,” 7,417,397, 2008.
[18] L. Bellia, F. Fragliasso, and E. Stefanizzi, “Why are daylight-linked controls (DLCs) not so spread? A literature review,” *Building and Environment*, vol. 106. Elsevier Ltd, pp. 301–312, 01-Sep-2016.
[19] E. S. Lee *et al.*, “Demonstration of Energy Efficient Retrofits for Lighting and Daylighting in New York City Office Buildings,” 2017.
[20] A. Katsifaraki, B. Bueno, and T. E. Kuhn, “A daylight optimized simulation-based shading controller for venetian blinds,” *Build. Environ.*, vol. 126, pp. 207–220, Dec. 2017.
[21] S. Jain and V. Garg, “A review of open loop control strategies for shades, blinds and integrated lighting by use of real-time daylight prediction methods,” *Building and Environment*, vol. 135. Elsevier Ltd, pp. 352–364, 01-May-2018.
[22] C. Humann and A. Mcneil, “Using HDR Sky Luminance Maps to Improve Accuracy of Virtual Work Plane Illuminance Sensors.”
[23] A. McNeil, “A photographic method for mapping angular locations of exterior solar obstructions,” *J. Build. Eng.*, vol. 29, p. 101170, May 2020.
[24] J. Wienold and J. Christoffersen, “Evaluation methods and development of a new glare prediction model for daylight environments with the use of CCD cameras,” *Energy Build.*, vol. 38, no. 7, pp. 743–757, Jul. 2006.
[25] J. Wienold, “DYNAMIC DAYLIGHT GLARE EVALUATION.”
[26] D. Bourgeois, C. F. Reinhart, and G. Ward, “Standard daylight coefficient model for dynamic daylighting simulations,” *Build. Res. Inf.*, vol. 36, no. 1, pp. 68–82, Jan. 2008.

[27] “Detailed Description — Radsite.” [Online]. Available: https://www.radiance-online.org/about/detailed-description.html. [Accessed: 20-Aug-2020].

[28] M. S. Roudsari and M. Pak, “LADYBUG: A PARAMETRIC ENVIRONMENTAL PLUGIN FOR GRASSHOPPER TO HELP DESIGNERS CREATE AN ENVIRONMENTALLY-CONSCIOUS DESIGN.”

[29] “Amsterdam Weather data.” [Online]. Available: https://energyplus.net/weather-location/europe_wmo_region_6/NLD/NLD_Amsterdam.062400_IWEC. [Accessed: 22-Aug-2020].

[30] “IEA SHC TASK 56 | Building Integrated Solar Envelope Systems for HVAC and Lighting System Simulation Models.”

[31] Bognár, R. C. G. M. Loonen, R. M. E. Valckenborg, and J. L. M. Hensen, “An unsupervised method for identifying local PV shading based on AC power and regional irradiance data,” *Sol. Energy*, vol. 174, pp. 1068–1077, Nov. 2018.

[32] F. Pedregosa FABIANPEDREGOSA *et al.*, “Scikit-learn: Machine Learning in Python Gaël Varoquaux Bertrand Thirion Vincent Dubourg Alexandre Passos PEDREGOSA, VAROQUAUX, GRAMFORT ET AL. Matthieu Perrot,” 2011.

Simulation-based Performance Evaluation of Buildings with Window-frame Integrated Ventilation and Advanced Solar Shading

Anqi Shi - Student ID 1306375

Graduation Project Sustainable Energy Technology (7SE45)

Unit Building Physics and Services, Department of the Built Environment,

Eindhoven University of Technology

Supervisors:

prof.dr.ir. J.L.M. (Jan) Hensen, dr.ir. R.C.G.M. (Roel) Loonen, ir. S.B. (Samuel) de Vries

November 30th, 2020

Abstract

This research evaluates the potential of a novel window-frame integrated ventilation concept for improving the energy performance of office buildings. The study focuses on glazed façades with interior roller blinds optimized for daylighting and visual comfort. The convective solar gains in the cavity between the roller blinds and the glazing can cause overheating of the room. The window-frame integrated ventilation concept is developed to extract the convective heat in the cavity and provide night ventilation. The building performance simulation tool EnergyPlus is used to assess the potential of this system to reduce the energy consumption in office buildings. The study is divided into three parts: (1) concepts study, which focuses on specifying ventilation configurations and control strategies that are used in this study, (2) preparation of the modelling methods, which focuses on choosing the modelling method to implement different ventilation configurations and control strategies using simulation software, and (3) energy performance evaluation of an office building in Amsterdam, which focuses on assessing the performance of different decentralized ventilation strategies. Two different modelling methods for the cavity ventilation were analyzed in this study, namely two zone airboundary model and one zone heat removal model. The outputs are compared in terms of temperature and heat transfer through the façade. The findings of this research provide guidance on how to model the cavity ventilation for interior solar shading devices. Both cavity ventilation and night ventilation strategies were evaluated in terms of annual energy consumption and heating/cooling loads. Assuming the ventilation rate that is feasible for a window-frame integrated ventilator is $50m^3/h$, the results show that cavity ventilation not only protects from summer overheating but also has a potential to reduce 17% primary energy consumption compared to the baseline case without cavity ventilation nor night ventilation. With the same ventilator, the night ventilation can contribute to 21.6% reduction of the primary energy demand on the cost of increased heating loads.

Keywords: decentralized ventilation; exhaust air façade; interior shading; multifunctional facades; EnergyPlus

Table of Contents

1 Introduction

1.1 Background

The building envelope is a key element for achieving building energy efficiency and indoor human comfort. In the past, efforts were mainly focused on increasing thermal insulation of the envelope components to reduce heating demand. However, these features may lead to overheating phenomena, especially in office buildings [1]. Static and single function facades are no longer sufficient for tackling various challenges that the designers of modern buildings are facing: growing consciousness toward environmental problems and the dissatisfaction of the occupants' comfort [2].

Adaptive facade modules typically include energy generation or conversion systems, act as an element in ventilation (as air heat exchangers, air preheaters, ventilation outlets/inlets, ducts, etc.) and are integrated with the heating/cooling/lighting equipment. In contrast with conventional, static facades which are usually insensitive to the environmental changes, adaptive facades are able to respond to the day-night patterns and the changing seasons which can lead to significant energy savings as well as comfort improvements [2].

In addition, facade integrated ventilation systems are able to reduce space requirements for HVAC equipment while allowing local control and more responsiveness to user comfort. Decentralized systems are usually easier to install and control than centralized ones, which in many cases imply achieving a lower primary energy consumption. [3]. Many studies have analyzed the benefits of air-exhaust Double Skin Façade consisting of an external insulated glazing plus an internally ventilated glazing [4]. However, the air-exhaust cavity is also possible for façade with interior solar shading [5]. This study presents an adaptive façade concept that allows decentralized window-frame integrated ventilation.

1.2 Physee SmartSkin

The integration of photovoltaic solar components into building envelopes represents a significant step towards improving the energy performance of buildings. SmartSkin technology, composed of PowerWindows, SMART, EESY and SKIN has been developed by Physee to lower energy consumption whilst simultaneously generating electricity. PowerWindows are patented and transparent double- or triple-paned windows that convert part of the sunlight into electricity. SMART integrates sensors that measure light intensity, temperature, pressure and air quality into the window-spacers. EESY is a combination of local power storage, connectivity to the servers, big data and connection to control systems. SKIN offers opportunities for collaboration with existing third-party façade applications using the electricity and data generated from the window. As shown in Figure 1, The window generates electricity from the integrated solar cells in the glass and stores the electricity in the batteries. The data from the sensors can be accessed and analyzed through an online platform [6]. The indoor & outdoor data from the sensor and the electricity generated from the facade create opportunities for the SmartSkin to be combined with other devices such as sun-blinds and window-frame integrated ventilation systems. The sun-blinds applied in this study will be introduced in the next section 1.3 Kindow Rollers, and the ventilation concepts will be specified in the 0 Research Objective and Scope.

1.3 Kindow Rollers

Kindow Rollers are interior roller blinds that automatically adapt to the position of the sun. The latest Kindow Rollers control strategy was developed based on sun tracking from the light sensor as shown in Figure 2. The blinds are fully opened under a cloudy sky or lowered to an extent that prevents glare from direct sunlight under a clear sky. Meanwhile, the uncovered part of the window still allows daylight entering the room and allows the occupants' view to the outside. The system calculates the time and location of the sun at every moment.

Previous research shows that, compared with external roller blinds, the interior roller shades with careful combination of shading material and control strategy can decrease the primary energy demand of a building by 6.5% for a case study in the Netherlands [7]. In comparison with conventional automated shading systems available in the market, the Kindow Rollers control strategy saves lighting and heating energy while increasing the cooling demand, as the current version of the control strategy allows more time with its shades up and provide unobstructed view of the outdoors to the occupants which lead to higher solar heat gains [7].

Figure 1 PHYSEE SmartSkin [6]

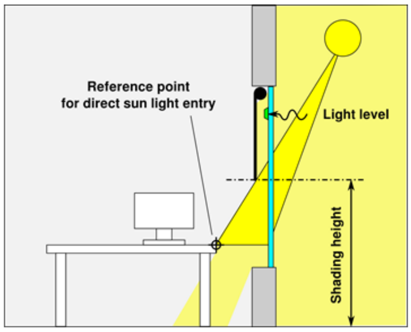

- Light level sunny: Dynamic shade height based on solar zenith and azimuth angle
- Light level cloudy: Shades are open

Figure 2 Kindow Rollers Control Strategy [7]

The active cavity transition (ACT) façade concept shown in Figure 3 provides an option to extract the heated air between the roller blinds and the glazing to prevent overheating of the room. An optimized operation of the ACT Facade is likely to be controlled by a building automation system while being possible to be taken over by the occupants. In addition, the ACT facade is said to be more cost efficient due to energy and operation efficiency and gain of maximized rentable space as compared to Double-Skin-Facades [8].

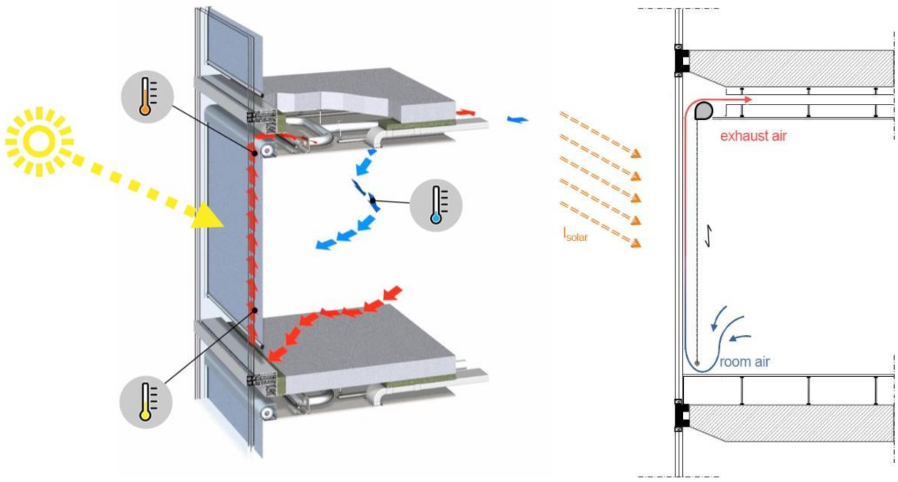

Figure 3 Active Cavity Transition (ACT) Façade [5] [9]

1.4 Research Objective and Scope

The goal of this project is to evaluate the potential performance improvement of combining a window-frame integrated ventilator with Physee SmartSkin and Kindow Rollers. In this façade system, Kindow interior shading and the ventilation unit can utilize the electricity generated from Physee Smart Skin. The feasible configurations and control strategies for the decentralized ventilation needs to be developed, and it is necessary to establish a suitable simulation model to evaluate the energy performance of different strategies. This study uses several existing ventilation products to provide reference for sizing, airflow rates and fan energy consumption as listed in Table 1. The ventilation flow rate varies from 10 m^3/h to 300 m^3/h. 10 m^3/h is usually the flow rate of a grill integrated with the window-frame at natural ventilation, and 300 m^3/h is the maximum flow rate of a large façade-integrated ventilation. The product has a nominal flow rate of 50 m^3/h. The specific fan power used is 0.07 W/(m^3/h) of the fan with 35*35*12cm measurements [10].

Table 1 Example of Facade Ventilation and Flow Rates

Ventilation Type	Grill integrated with the window-frame [11]	Mechanical Vent integrated with the window-frame [12]	Façade-integrated Ventilation [13]
Picture	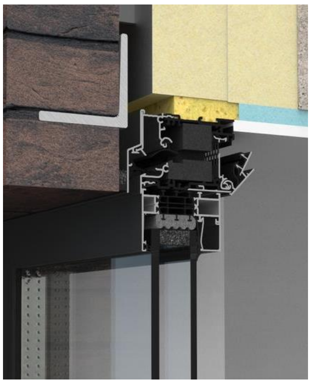		
Ventilation Airflow Rate	10-30 m^3/h	50 m^3/h	Maximum: 300 m^3/h

A concept inspired by the ACT façade will be investigated: cavity ventilation (CV). With ACT facades, the cavity is ventilated by the indoor air, and the exhaust air from the cavity is extracted by the HVAC system as shown in Figure 3. The cavity ventilation concept, on the other hand, ventilates the cavity with outdoor air. The exhaust air from the cavity is extracted by the façade ventilation to the outside as shown in

Figure 4.

The same ventilation configuration can be used for night ventilation as shown in Figure 5. The night mechanical ventilation (NMV) induces the cold ambient air to cool the exposed building thermal mass and save cooling energy for the next day. As sufficient cooling energy should be stored in thermal mass at night, the minimum indoor air temperature setpoint is relatively low, which may cause an overcooling penalty [14]. To obtain an optimum NMV control strategy, research should include various indicators and take the building configuration and climate into consideration [15]. In this study, night ventilation is possible through the façade and the night heating setpoint will be varied to evaluate the influence on the energy performance.

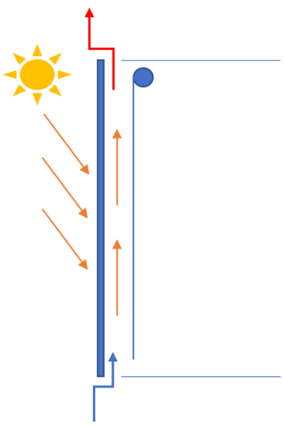

Figure 4 Cavity ventilation Operation Mode

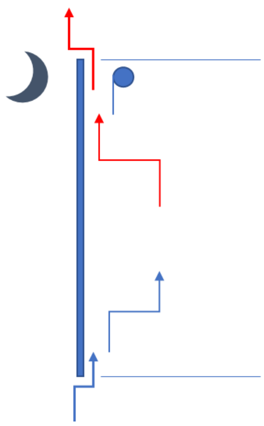

Figure 5 Night Ventilation Operation Mode

1.5 Methodology

Figure 6 shows an overview of the research methodology in this project. The software EnergyPlus is used to simulate the building performance, and MATLAB is used to process and visualize the simulation results.

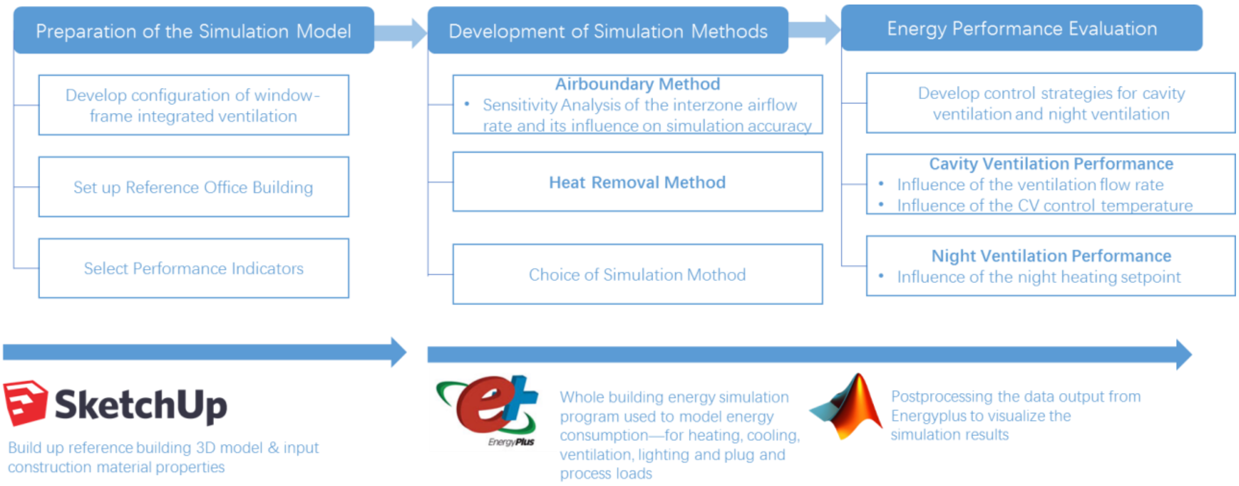

Figure 6 Schematic Overview of the Research Methodology

2 Development of modeling and simulation strategy

2.1 Reference office

The building model that is used in this study is based on the reference office from Task 56 of the Solar Heating and Cooling Programme of the International Energy Agency [16].Task 56 describes three different options for the thickness of the insulating material in the external wall and for the window properties, based on three different climate zones. In this study, a climate file of Amsterdam is used, so the set of construction properties from Task 56 for the climate zone of Stuttgart are used, as this climate resembles the Dutch climate the most. Several modifications were made to the model of Task 56, in order to make the model suitable for this study.

The two-person office is part of a larger office building, with the floor, ceiling and three of the walls connected to other offices. These constructions are assumed adiabatic. The south-facing wall is an external wall and contains one large window, instead of three separate windows as in Task 56 as shown in Figure 7. This was done to represent a PHYSEE fully glazed façade. The properties of the glazing are listed in Appendix A.

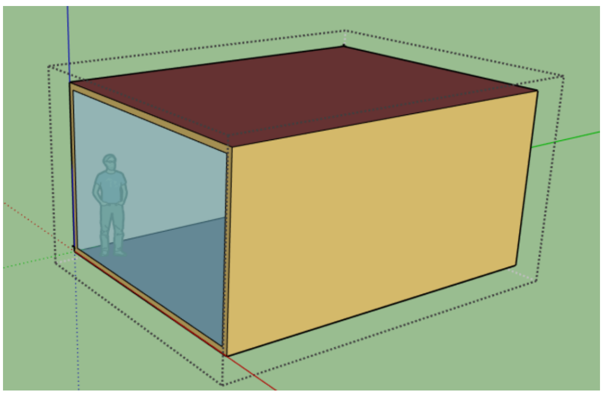

Figure 7 Reference Office

The solar shading system used in Task 56 is not implemented, as the roller blinds material by Kindow is used instead. The Kindow smart shading control adjusts the shading height according to the position of the sun. The shading control strategy used in this study is simplified for the sake of the calculation of convective heat removal by the cavity ventilation. The shade is fully lowered if the vertical solar irradiance on the facade exceeds 120 W/m^2.

All properties for the internal gains due to occupants and lighting are based on Task 56 as listed in Appendix A. The HVAC system is set to keep the indoor temperature between the heating setpoint of 21°C and the cooling setpoint of 25°C. Only during weekends, there is a setback for the heating and cooling setpoints. They are changed to 18°C and 28°C respectively.

2.2 Performance Indicators

The first performance indicator that is evaluated is the annual primary energy demand. The primary energy demand is investigated for heating, cooling and fan energy consumption for the façade ventilation, based on the equation (1) [17] and the conversion factors listed below. The annual primary energy demands for heating, cooling and ventilation are divided by the floor surface area and expressed in kWh/m^2.

$$E_{primary} = \frac{E_{cool}}{\eta_e \eta_c COP_{cool}} + \frac{E_{heat}}{\eta_h} + \frac{E_{fan}}{\eta_e} \quad (1)$$

$E_{primary}$: primary energy consumption
E_{cool}: cooling energy demand, E_{heat}: heating energy demand, E_{fan}: ventilation fan electricity demand
COP_{cool} = 3.00, chiller coefficient of performance [17]
η_h = 0.95, overall heating system efficiency [17]
η_c = 0.70, cooling delivery system efficiency [17]
η_e = 0.49, site to source primary energy ratio for electricity [18]

The second performance indicator is the cooling load. The cooling load is investigated by the peak cooling and the cooling load duration curve in this study.

2.3 Modelling Methods

By default, EnergyPlus has limited options for modelling airflow between shading devices and the inner pane of glazing systems. The airflow in such cavities is limited to buoyancy driven mass flow which cannot be controlled. It is therefore not possible to investigate air exchange between the cavity and the outside (Table 2). Therefore, two different modelling methods were tested to develop a suitable workaround method for model for the cavity ventilated façade. The building properties in these tests were the same as mentioned in Section 2.1, except that the shading control is set to be 'always on', to to test whether the modelling methods function as intended.

Table 2 Comparison of Validation Model, Airboundary Model and Heat Removal Model

Validation Model (cavity ventilation limited to buoyangcy driven)	Airboundary Model (cavity ventilation off mode)	Heat Removal Model (cavity ventilation on mode)
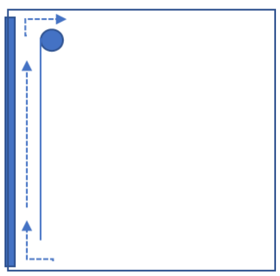	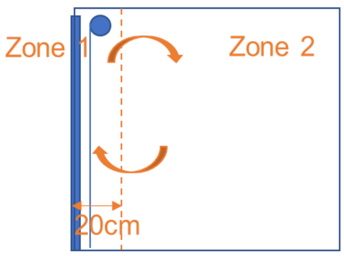	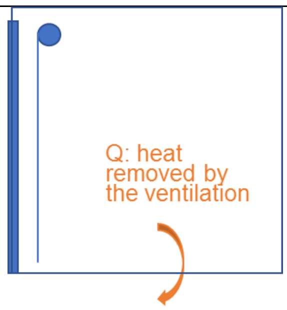

2.3.1 Two Zone Airboundary Model Validation

Modelling Method 1 uses a function in EnergyPlus 9.3 called "Airboundary" to separate and connect two zones in the room. The width of zone 1 (blue lined zone in Figure 8 left) is 20cm as shown in Figure 8, which includes the cavity between the glazing and shading device. Zone 2 represents the rest of the room. In the cavity ventilation operation mode, it is possible to exchange the air from the cavity (zone 1) with the air from the outdoor. When the cavity ventilation is off, it is desirable that the two-zone model has the same energy performance as the validation model. More specifically, the airboundary that connects the two zones (green area in Figure 8 right) should transfer shortwave solar radiation, longwave thermal radiation and convective heat so that the two-zone model acts the same as the validation model.

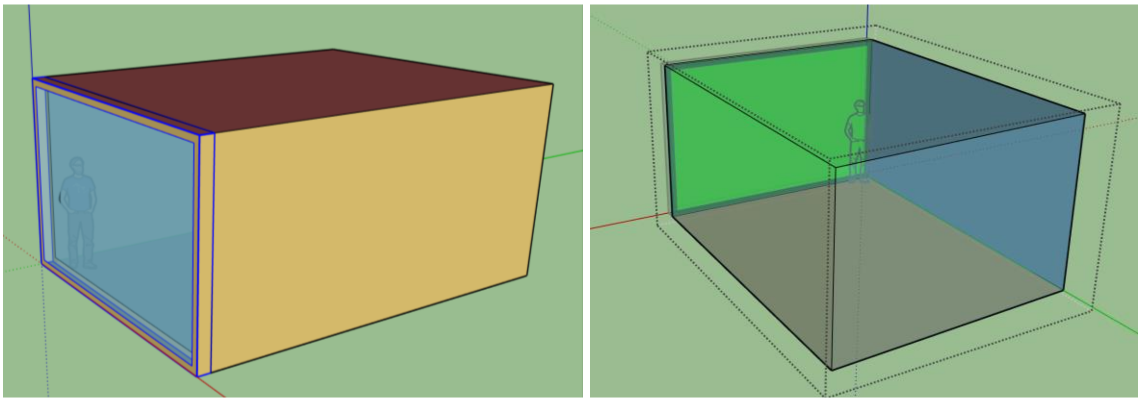

Figure 8 Two zone Airboundary Model

In the two zone airboundary model, convective heat between two zones is transferred by a pair of interzone airflow. A sensitivity analysis of the airflow rate is performed to find the optimum airflow rate which will output the most similar thermal behaviour with the validation model in cavity ventilation off mode when the shade is down. The interzone airflow rate is first varied by 0.1, 1, 10 and 100 m^3/s to obtain a quick comparison with the validation model and the rough range of the optimum airflow rate. Figure 9 shows the annual heating and cooling demand results from these interzone air flow rates in the airboundary model. The interzone airflow rate range from 0.1 to $1m^3/s$ was then investigated further for its influence on heating and cooling. From Figure 9 it can be observed that the interzone airflow rate and the energy demand does not have a linear relationship. When the interzone airflow rate is at 0.2 or 0.3 m^3/s, the annual heating and cooling demand are the closest to the validation model. The difference in cooling demand is about 1.5% while the difference in heating demand is about 10% between the airboundary model at 0.3 m^3/s and the validation model.

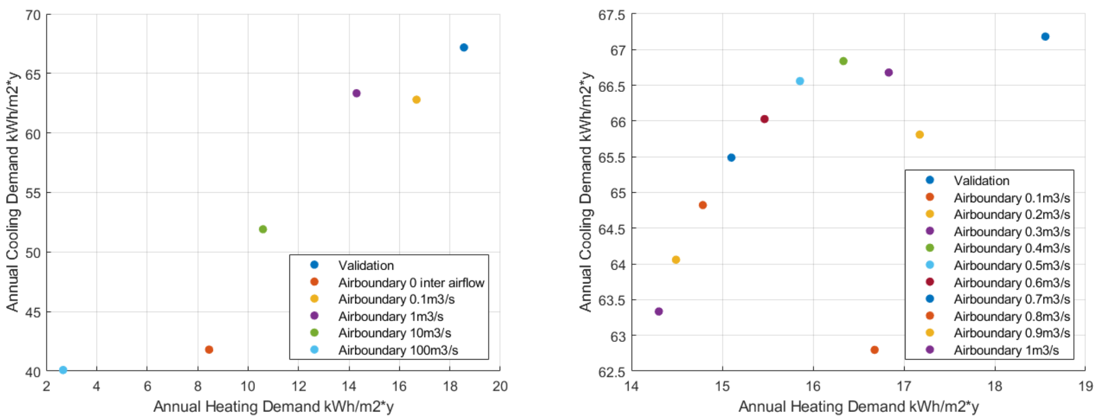

Figure 9 Sensitivity of Annual Heating and Cooling Demand to Interzone Airflow Rate in Two Zone Airboundary Model

Table 3 Heat Transfer in Operation Modes of the Modelling Methods, generated from [19]

<table>
<tr><th></th><th>Cavity Ventilation Off Mode (bouncy driven mass flow in the cavity)</th><th>Cavity Ventilation Operation Mode</th><th>Validation</th></tr>
<tr><td>Validation Model: One zone without CV setting</td><td>Buoyancy driven mass flow of the cavity
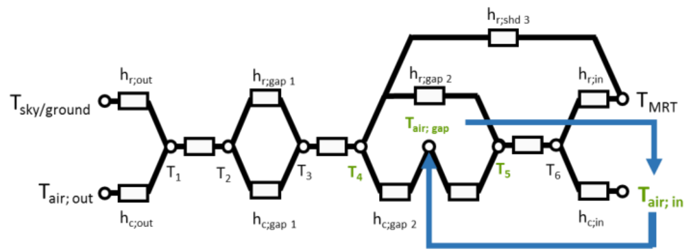
</td><td>Not possible because EnergyPlus only supports buoyancy driven mass flow of the cavity</td><td></td></tr>
<tr><td>Two Zone Airboundary Model</td><td>Airboundary connecting zone 1 and zone 2
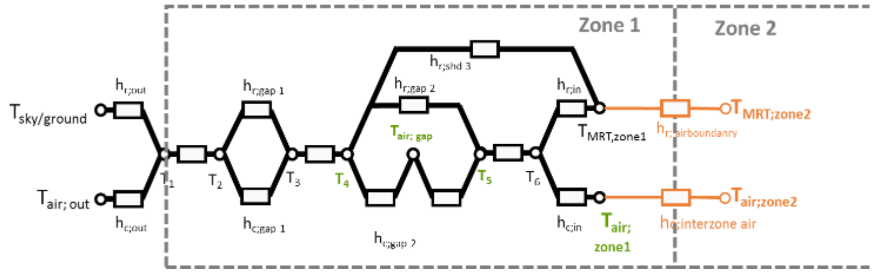
</td><td>Air exchange between zone 1 & outside
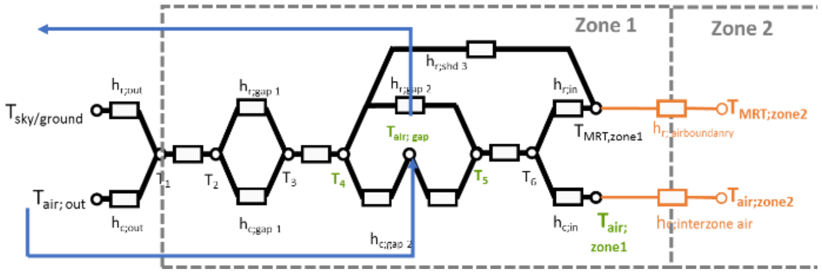
</td><td>Investigating whether the thermal behavior is the same as validation model in <u>CV off mode</u></td></tr>
<tr><td>One Zone Heat Removal Model</td><td>Buoyancy driven mass flow of the cavity Same as the Validation Model
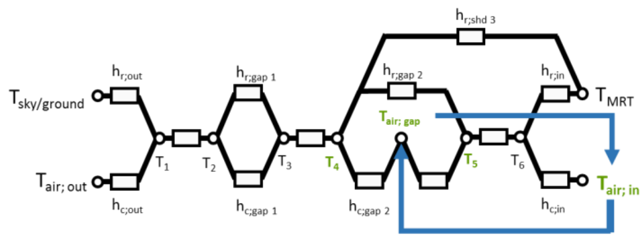
</td><td>Scheduled Heat Removal
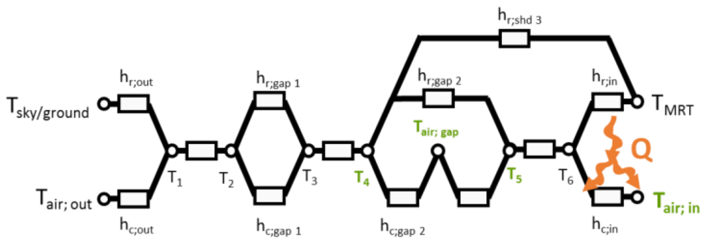
</td><td>Investigating whether the heat removal can be controlled according to expectations in <u>CV operation mode</u></td></tr>
</table>

In order to understand how the airboundary transfers radiative and convective heat and to investigate why the difference in energy demand occurs, the heat balance graphs in a spring day were generated as shown in Figure 10 (all heat balance graphs for airflow rates from 0 to 1 m^3/s can be found in Appendix B). When interzone airflow rate is set at 0.3 m^3/s, the heat from the window is mostly transferred to zone 2 by the interzone airflow.

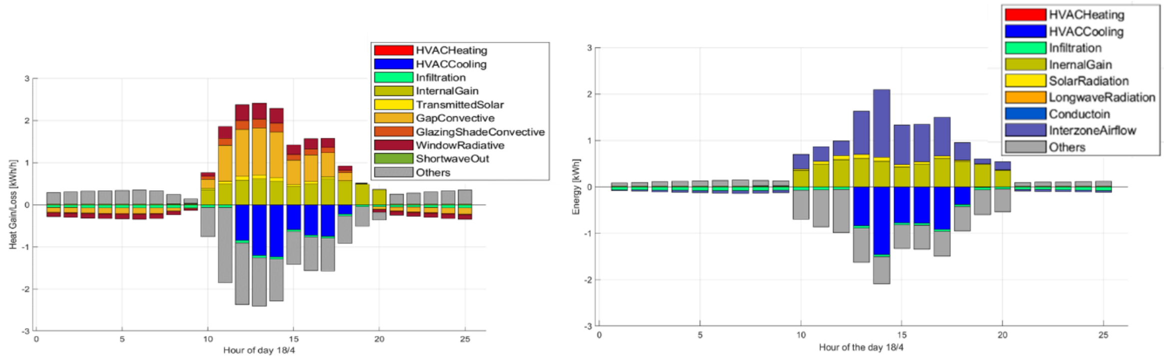

Figure 10 Heat Balance Graph Comparison Baseline (above) & Airboundary Model (below)

Figure 11 shows that the air temperature in zone 2 of the airboundary model is similar with the air temperature of the one zone validation model, but the temperature of the shade surface is 2°C higher than the validation model at noon. This indicates that more heat is trapped on the roller blinds as radiative energy in the airboundary model instead of transferred as convective heat to the cavity.

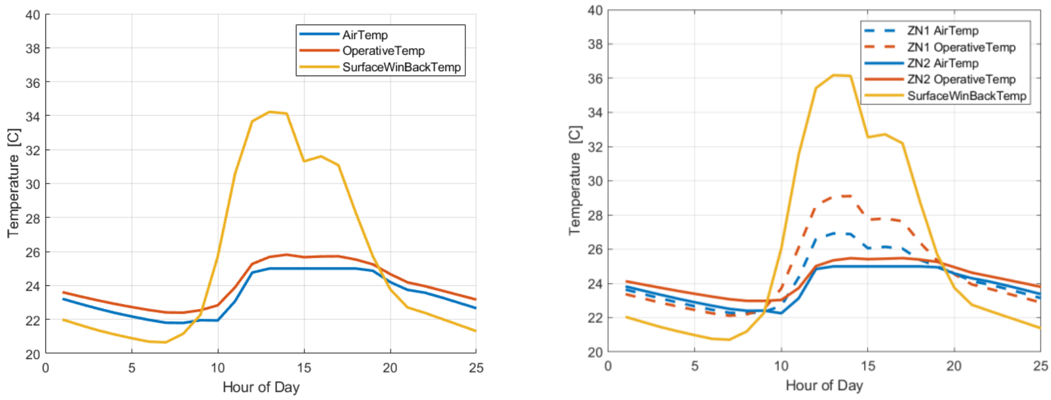

Figure 11 Zone Temperature Comparison Validation Model (left) & Airboundary Model (right)

Heat transferred through the façade elements is calculated as the sum of transmitted solar radiation and convective heat and longwave radiation transferred from the glazing and the shade to the zone at the inside glazing. Table 4 and Figure 12 shows the window heat transfer in baseline and airboundary models. It can be observed that window heat transfer is close to each other. From the table it is observed that the solar radiation transferred through the window is the same, but the airboundary model transferred less convective heat and higher radiative heat.

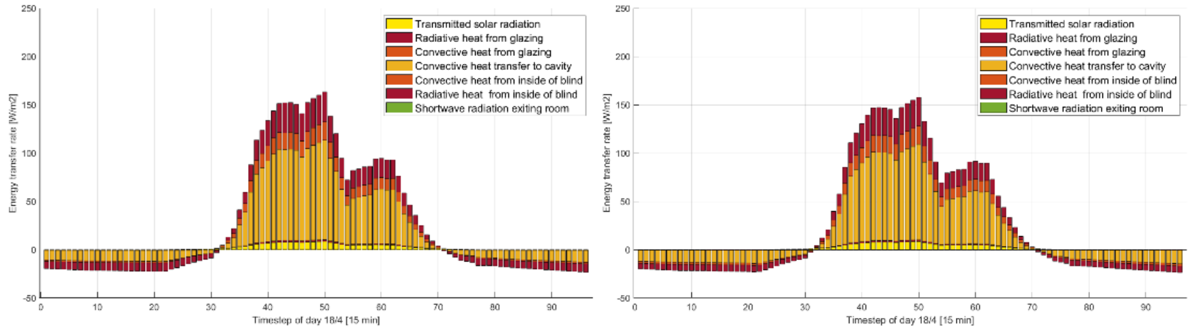

Figure 12 Window heat transfer Graph Comparison Baseline (above) & Airboundary Model (below)

Table 4 Annual Window Heat Transfer Comparison between Validation Model and Airboundary Model

Energy (GJ/y)	Solar Radiation	Convective heat to cavity	Glazing & Shade long wave radiation	Glazing / Shade Transferred Convective Heat	Net Window Transferred Heat
Validation Modle	0.55	3.51	0.52	0.85	5.42
Airboundary Model	0.55	3.15	0.68	0.76	5.12

In summary, the comparison between the two-zone airboundary model and one zone validation model shows that the airboundary does not transfer heat between zone 1 and zone 2 as expected in the cavity ventilation off mode.

2.3.2 One Zone Heat Removal Model Validation

Modelling Method 2 uses a scheduled heat removal Q to represent the convective heat removed by the ventilation at the facade. The schedule and value of the heat removal Q can be controlled. Figure 13 shows the heat balance comparison between the baseline model and the heat removal model when the heat removal Q is set to be equal to the convective heat in the gap, i.e. the fan extracts all the convective heat in the gap to the outside. Note that in the heat removal model, the heat removal Q (purple part) is not exactly same as the convective heat in the gap Qgap,conv (orange part) because in EnergyPlus the simulation

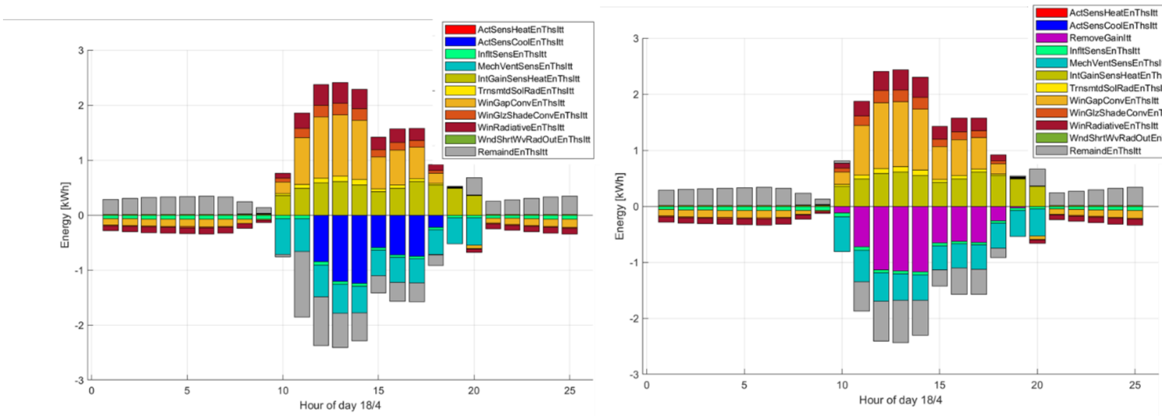

Figure 13 Heat Balance Graph Comparison Validation Model (left) & Heat Removal Model (right)

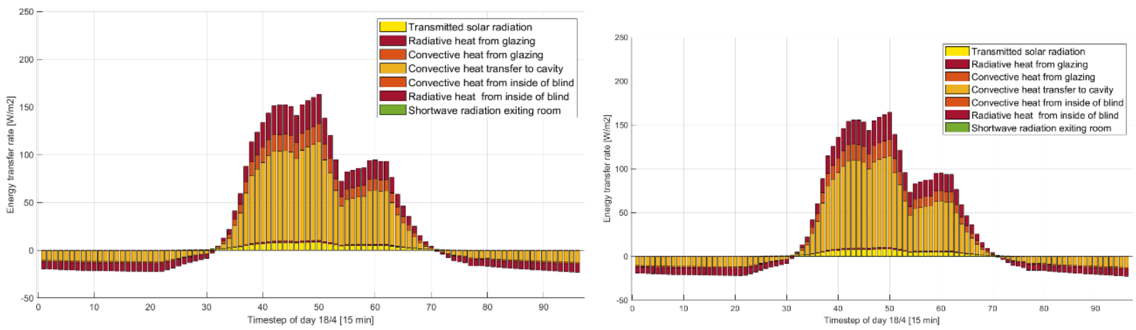

Figure 14 Heat Balance Graph Comparison Validation Model (left) &Heat Removal Model (right)

2.3.3 Choice of modelling strategy

The scheduled heat removal model is easier to configure while the two-zone model is more flexible. It is more straightforward to add heating or cooling elements in the cavity inlet and outlet region in the two-zone airboundary model than in the case of the one zone heat removal model. However, the imbalance of interzone airflow heat transfer leads to discrepancy of heating energy demand (about 10% when interzone airflow is set at the optimum). The heat balance of the heat removal model is almost identical to baseline one zone model. The discrepancy of the window heat transfer as shown in is relatively small (3.0%) compared to airboundary model (5.5%) as shown in Figure 15. Although the scheduled heat removal model cannot influence the cavity directly by airflow, it is chosen as the modelling strategy for its better accuracy in energy performance which is of interest in this project.

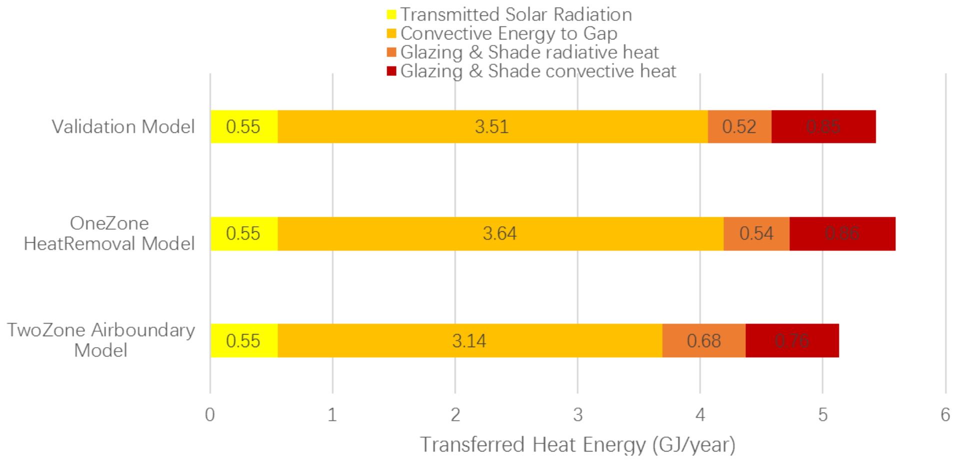

Figure 15 Annual Window Heat Transfer

3 Energy performance evaluation of the proposed window-frame ventilation concepts

3.1 Cavity Ventilation

The cavity ventilation models are compared with baseline models with the settings shown in Table 5. Baseline 1 represents a room with interior shading and no cavity ventilation which offers a comparison on how cavity ventilation influences the performance of interior shading. Baseline 2 and 3 are models with exterior shading and no cavity ventilation which offers comparison between interior and exterior shading. Meanwhile the comparison between Baseline 2 and 3 will indicate the influence of reflectance of shading material on the energy performance.

Table 5 Cavity Ventilation Comparison Models

	BL1 No Vent	BL.2 Exterior Shade1	BL.3 Exterior Shade2	CV.1 Constant	CV.2 Temperature Controlled
Shading Type Configuration	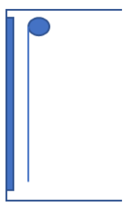 InteriorShade	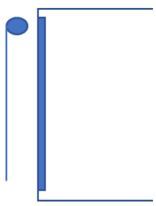 ExteriorShade	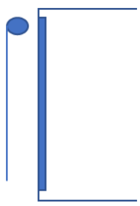 ExteriorShade	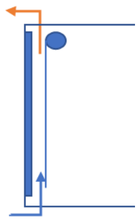 ExteriorShade	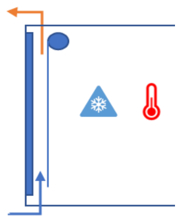 ExteriorShade

Shade Material	Kindow Rollers	Kindow Rollers	Task 56 Generic	Kindow Rollers	Kindow Rollers
Shading Material Properties	Tv:3% Rsol:81%	Tv:3% Rsol:81%	Tv:30% R:60%	Tv:3% R:81%	Tv:3% R:81%
Shade Control	120 W/m^2 Threshold	120 W/m^2 Threshold	120 W/m^2 Threshold	120 W/m^2 Threshold	120 W/m^2 Threshold
Ventilation control	Never	Never	Never	Always outward	Outward if T_{indoor}>23
CV Flow Rate	0	0	0	10, 50, 100, 200, 300 m^3/h	10, 50, 100, 200, 300 m^3/h

The CV1 and CV2 model is ventilated by an exhaust fan ventilating the air towards the outside and a supply fan ventilating the outside air to the cavity. In CV1, the cavity ventilation is switched on when the shade is down. Figure 16 shows how heating and cooling load changes with the indoor and outdoor temperature. In CV 2, the cavity ventilation is switched on when the shade is down and the indoor temperature is above 23 degree to avoid admitting cold outdoor air inside during winter.

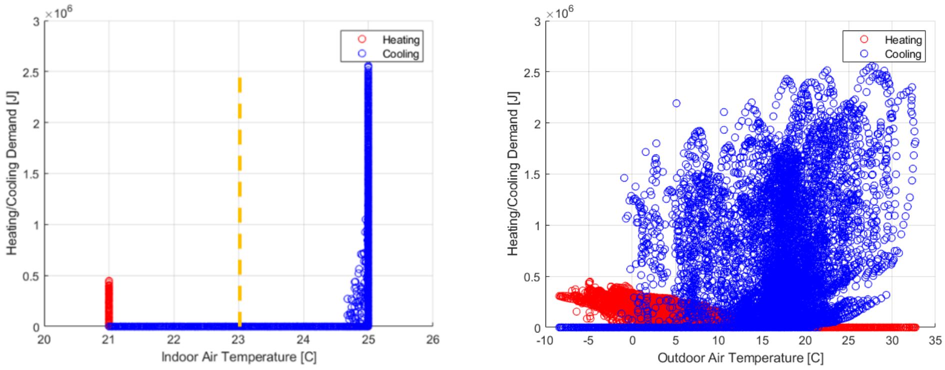

Figure 16 Heating and Cooling Load – Temperature in Baseline Model

The exterior shade offers natural air exchange between the cavity and the outdoor air. There is no mechanical cavity ventilation in the exterior shade model. Two different shading materials were implemented in the exterior shade model: Kindow Rollers and the generic shading material from Task 56 reference building. The shading material properties are listed in Appendix A shading screen properties.

3.1.1 Implementation of Cavity Ventilation (CV)

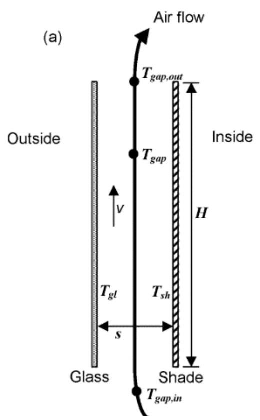

Figure 17 Model of the cavity of an Interior shade system [30]

For the cavity ventilation, equation (2) is the calculated heat removal capacity by the fan $Q_{fan,calculated}$ when the air is passing through the cavity at the airflow rate m. In reality, the temperature T_{gap} is inconsistent within the cavity. In order to simplify the calculation of the heat removal in the cavity, T_{gap} is assumed to be consistent and the same as the temperature of the shading material T_{sh}. The Equation (3) is how the heat removal is calculated in this study.

$$Q_{fan,calculated} = m * C_p * (T_{gap} - T_{outdoor}) \quad (2)$$
$$Q_{fan,calculated} = \rho v * C_p * (T_{sh} - T_{outdoor}) \quad (3)$$

$Q_{fan,calculated}$: heat removal capacity by the fan driven mass flow
m: fan driven mass flow rate ρ: Outdoor air density
v: Fan driven air flow rate C_p: specific heat capacity of air

T_{gap}: air temperature in the cavity T_{sh}: temperature of shading material surface $T_{outdoor}$: outdoor air temperature

The heat removal in the cavity Q is determined as the smaller value between convective heat accumulated in the cavity $Q_{gap,conv}$ and the calculated fan capacity $Q_{fan,calculated}$. Figure 18 shows how the heat removal Q changes during the first week in July. When the cavity ventilation flow rate is at 10m^3/h, the capacity of the fan is not enough to ventilate all convective heat gain during the day. Therefore, the actual heat removal Q is equal to the $Q_{fan,calculated}$ when $Q_{fan,calculated} < Q_{gap,conv}$. When the air flow rate increases to 300 m^3/h, the fan can extract all the convective heat accumulated in the cavity.

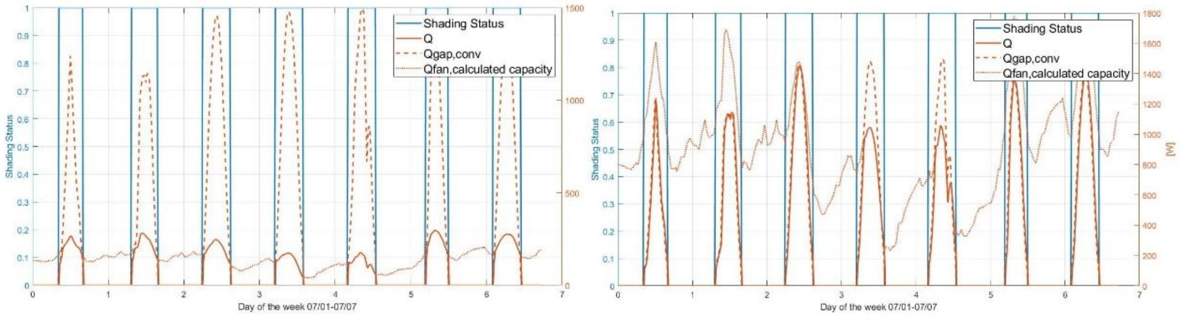

Figure 18 Cavity Ventilation Control Strategy for Interior Shade, Constant CV at 50 m^3/h (left) and 300 m^3/h (right)

A shown in Figure 19, the temperature controlled CV at 50 m^3/h operates the same as the constant CV at 50 m^3/h during the first week of July because the indoor temperature in summer is usually above 23°C when the shade is down. In winter, the indoor temperature is usually lower than 23°C, therefore the CV ventilation is only switched on in day 4.

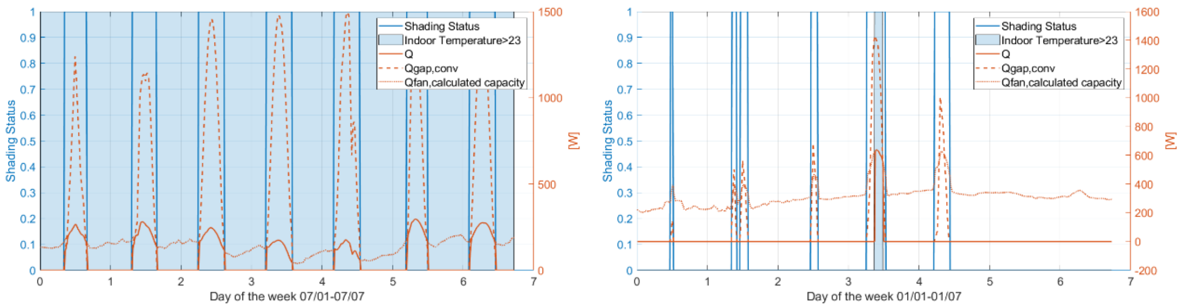

Figure 19 Cavity Ventilation Control Strategy for Interior Shade, Constant CV at 50 m^3/h summer (left) and winter (right)

3.1.2 Cavity Ventilation Simulation Results

Figure 20 and Figure 21 show the annual heating, cooling and fan energy demand and primary energy consumption of all the alternatives. Compared with the baseline no ventilation model, cooling demand has decreased, and heating demand has increased with all types of cavity ventilation control strategies. It can also be observed that the fan energy consumption is very low even at the maximum air flow rate compared to heating and cooling energy demand.

The results show that higher ventilation rates lead to lower cooling demand and higher heating demand. This is because the cavity ventilation may bring cold outdoor air inside which cools the space that reaches the heating setpoint in spring or autumn. However, the positive influence on the cooling demand is much higher than the negative influence on the heating demand. When the fan is running at 10 m^3/h, the influence in cooling and heating are smaller than 10%. When the fan is running at nominal flow rate 50 m^3/h, the cooling demand decreased 27% and the heating demand increased 8.6%. It is noticeable that the ventilation flow rate at 200 m^3/h has a close performance to the ventilation flow rate at 300 m^3/h.

The temperature-controlled CV results in slightly higher cooling energy demand and slightly lower heating demand as compared to constant CV. The fan consumption of the temperature-controlled models and constant ventilation models are almost the same which means that the fan operating time are very close in both strategies. Controlling the cavity ventilation with a temperature of threshold 23 degree did not improve the heating and cooling to a significant amount compared with constant cavity ventilation strategy.

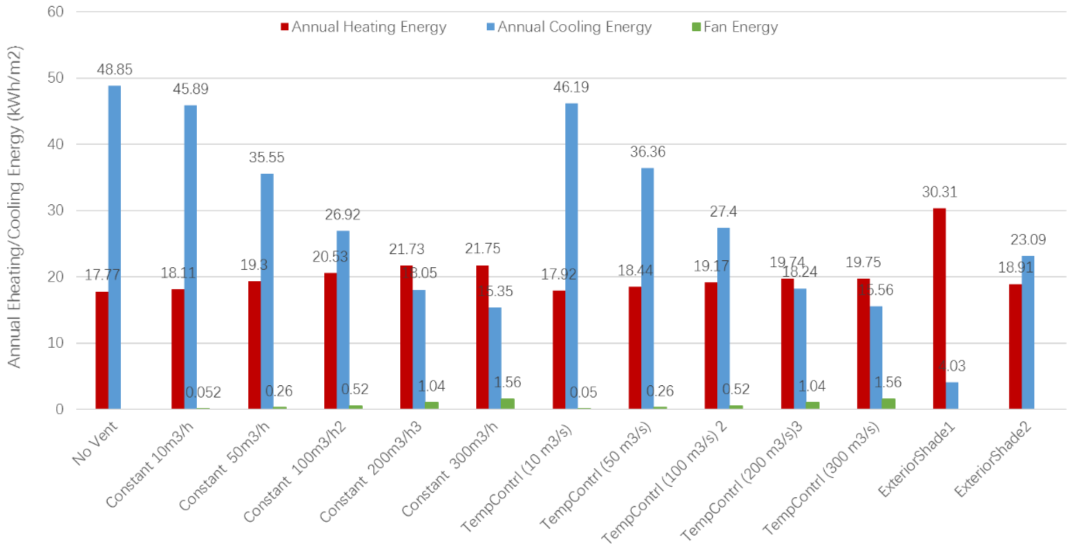

Figure 20 Cavity Ventilation Comparison Models - Energy Demand

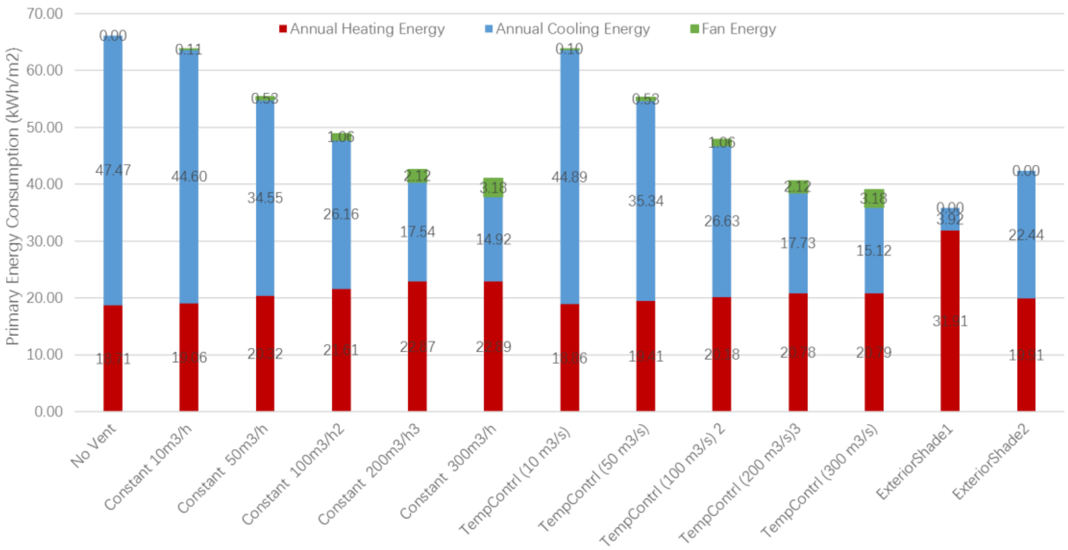

Figure 21 Cavity Ventilation Cases - Primary Energy Consumption

As for the cooling load which will influence the sizing of the HVAC, higher ventilation rates lead to lower peak cooling load as shown in Figure 22 and Figure 23. The CV controlled by temperature at 300 m^3/h has the lowest peak cooling load among all the interior shading models. Again, the cooling load of the 200 m^3/h model is close to the 300 m^3/h model. For exterior shading, the Kindow shading material results in lower peak cooling and total cooling demand than the Task 56 generic shading material due to its higher reflectance and lower transmittance properties.

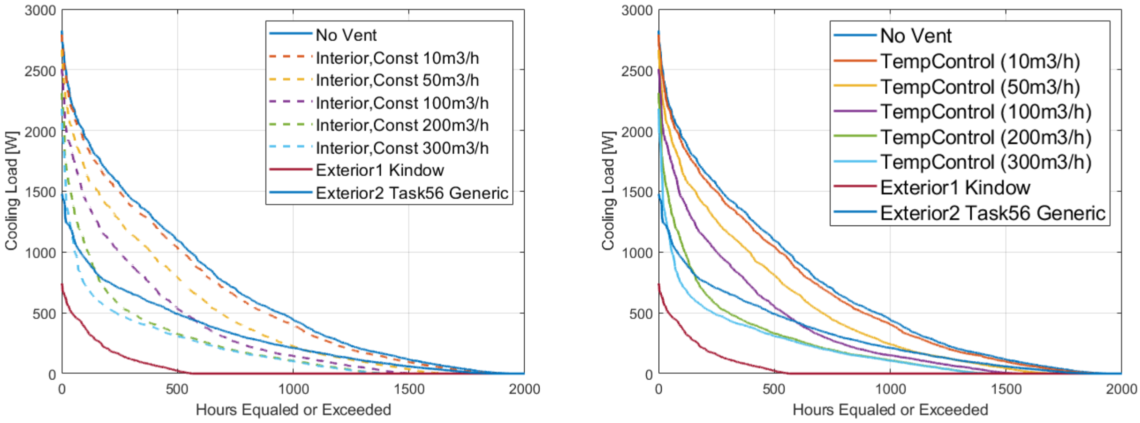

Figure 22 Cooling Load Duration Curve– Constant Flow Rate (left) Temperature Controlled Flow Rate (right)

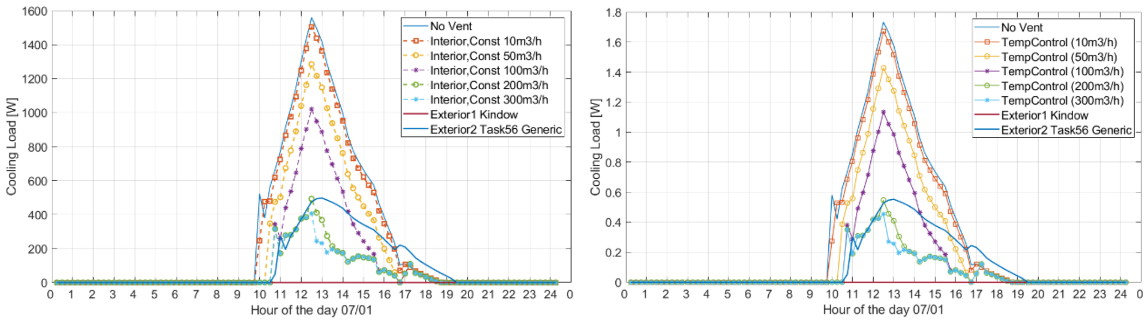

Figure 23 Cooling Load Summer Day July 1st – Constant Flow Rate (left) Temperature Controlled Flow Rate (right)

3.2 Night Ventilation (NV)

3.2.1 Implementation of Night Ventilation (NV)

Table 6 shows the ventilation configurations and control strategies of the models tested for night ventilation. There are three configurations investigated: no night ventilation (baseline), night mechanical ventilation modelled by heat removal (NV1), and night ventilation modelled by infiltration (NV2). The no night ventilation model acts as a baseline for observation of the influence of night ventilation. The infiltration rate in NV2 model is developed with an equivalent air exchange volume to the ventilation flow rate in NV1 model. The energy performance of NV1 should be close to that of NV2 to verify the heat removal modelling approach.

Night heating setpoints of 21°C and 18°C are implemented in each configuration. 21°C is the heating setpoint during the daytime. 18°C night heating setpoint is lower than the daytime setpoint which allows the building to cool down further at night without causing undesired heating. Equation (3) is used to calculate the heat removed by the mechanical ventilation in the NV1 model:

$$Q = \rho v * C_p * (T_{indoor} - T_{outdoor}) \quad (3)$$

Q: heat removal by the fan driven mass flow
ρ: Outdoor air density
v: Fan driven air flow rate
C_p: specific heat capacity of air
T_{indoor}: indoor air temperature
$T_{outdoor}$: outdoor air temperature

Table 6 Night Ventilation Comparison Models

	Baseline: No Night Ventilation	NV1: night mechanical ventilation modelled by heat removal	NV2: night mechanical ventilation ventilation modelled by infiltration
Configuration	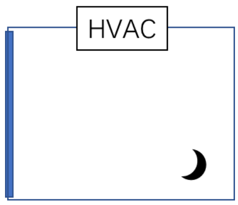	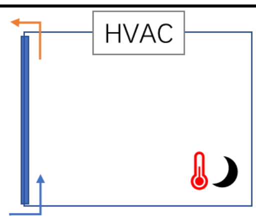	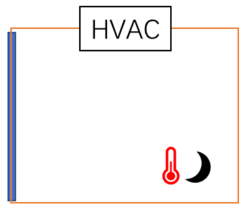
Night Heating Setpoint (HS)	18, 21	18, 21	18, 21
Air Flow Rate	0	50 m^3/s	0.62ACH

Figure 24 shows the night ventilation control strategies through in NV1 and NV2 models. When the façade ventilation is set to be the nominal air flow rate 50 m^3/h for the 81 m^3 room, the equivalent infiltration rate is 50/81 = 0.62ACH. Considering the infiltration setting is constantly at 0.15ACH for the NV1 model during the daytime, the infiltration rate should be 0.15+0.62=0.77ACH for the NV2 model to result in the same air exchange volume during the night.

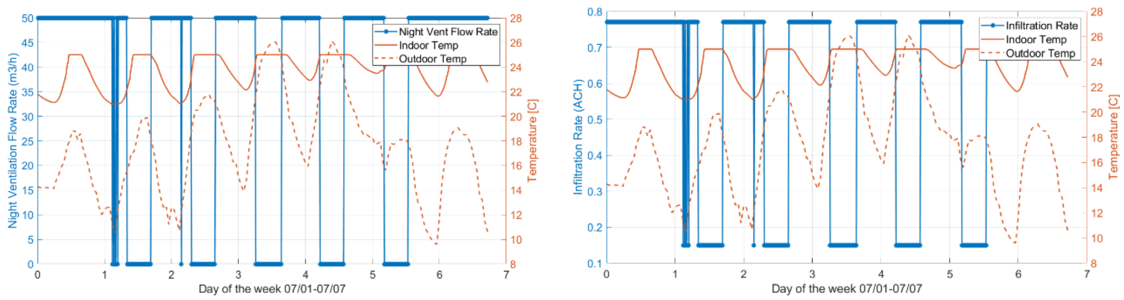

Figure 24 Night Ventilation Control Strategy - Through Mechanical Ventilation (left) Through Infiltration (right)

3.2.2 Night Ventilation (NV) Simulation Results

As shown in Figure 25, the outputs of the NV through mechanical ventilation models are close to the output of the night infiltration models the same air exchange volume as the NV models. When the night heating setpoint is at 21 °C (same as during the daytime), the heating demand increases significantly due to the low night temperature when night mechanical ventilation operates at the temperature above 21°C.

As the night heating setpoint decreases to 18 degree, the heating energy also decreased, which allows the room to cool down at night. It is worth noticing that the heating demand dropped 30% by only changing the heating setpoint at night to 18 degree without night ventilation. With 18 degree night heating setpoint, the cooling demand dropped 25% with extra night mechanical ventilation through the façade compared to no night ventilation.

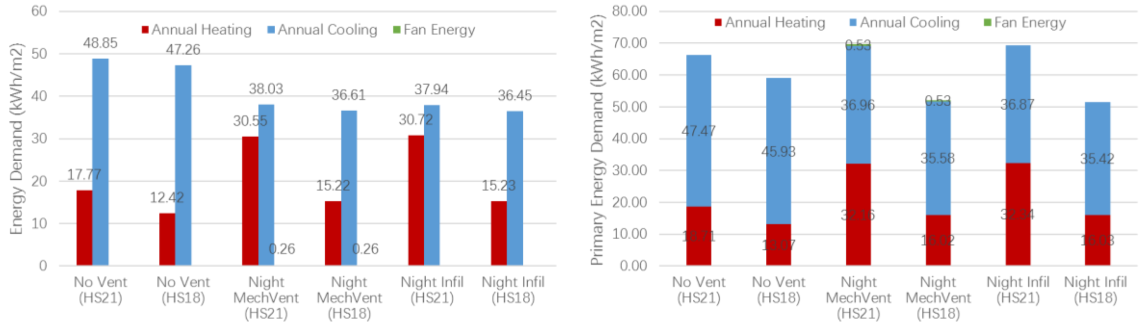

Figure 25 Night Ventilation Models - energy demand (left) Primary Energy Consumption (right)

The cooling load duration curves of NV1 also resemble the NV2 as shown in Figure 26. The maximum cooling load are similar with and without night ventilation. Assuming the HVAC system has a cooling capacity of 2000W, it can be observed from Figure 26 that the hours exceedance decreased from around 100 to around 70hours. This is also reflected on the cooling demand graph in Figure 27. The cooling starts after 9:30am for no night ventilation model and 11:30am for night ventilation models.

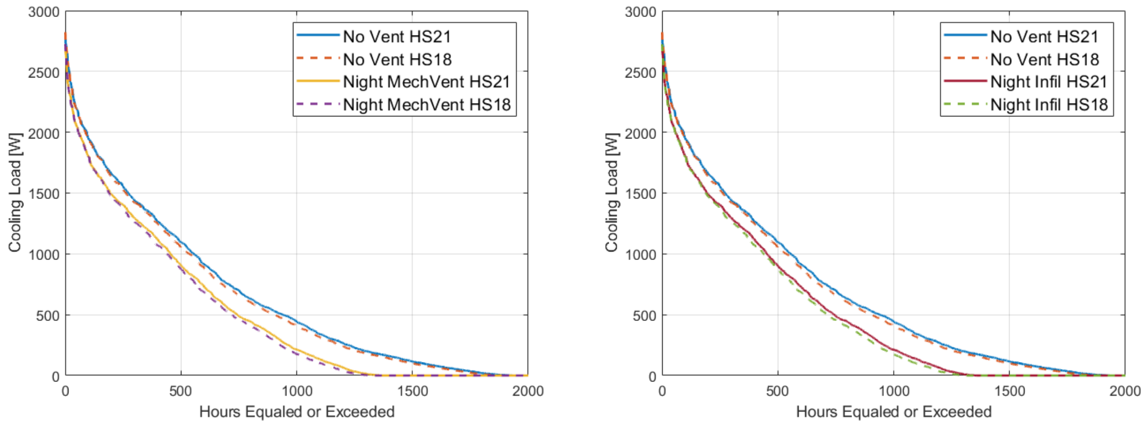

Figure 26 Cooling Load Duration Curve – NV1 modelled by heat removal (Left) NV2 modelled by Infiltration (right)

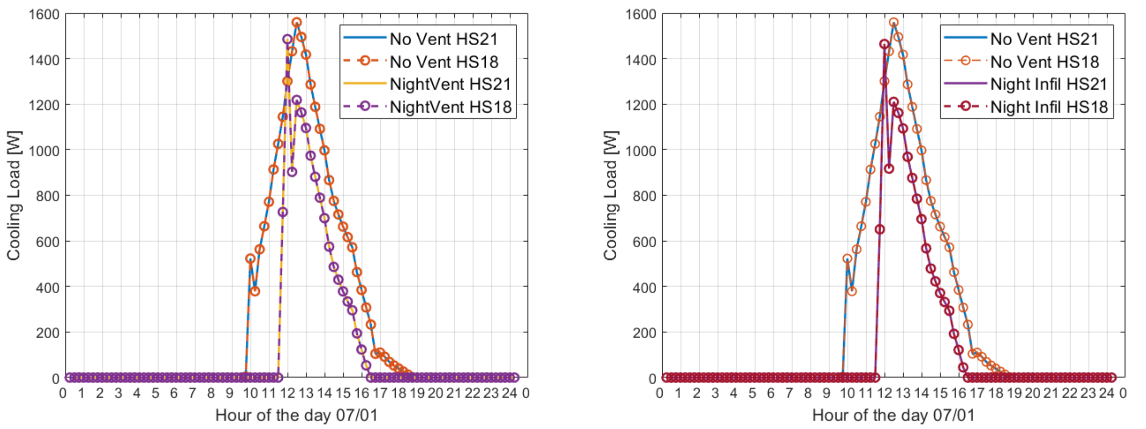

Figure 27 Cooling Load Summer Day July 1st– NV1 modelled by heat removal (Left) NV2 modelled by Infiltration (right)

Figure 28 shows the temperature changes throughout the summer day of no ventilation and night mechanical ventilation models at the night heating setpoint 21 degree. (Graphs for all other modes can be found in appendix D). The indoor temperature is 24 degree when the day starts without night ventilation and can be decreased to 21 degree with the night ventilation. The time lag for active cooling is approximately 2 hours.

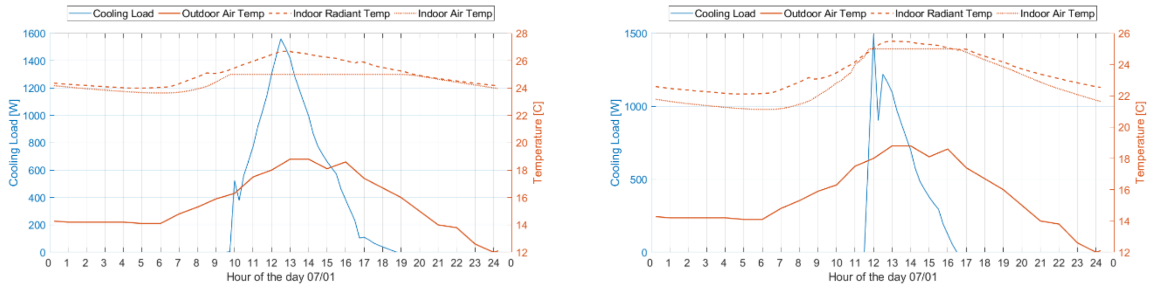

(a) Baseline: No Night Ventilation HS21 (b) NV1 modelled by heat removal HS21

Figure 28 Cooling Load and Temperature Through a Summer Day July 1st

Figure 29 shows the maximum heating load increased by more than twice with the night heating setpoint at 18 degree with or without the night ventilation. This is due to the night heating setpoint is 18 degree when there is no occupancy for the whole night. During the first occupied hour of the day the heating setpoint increased to 21 and the heating load was increased suddenly in Figure 30. In order to shave the peak heating, further strategies can be implemented such as increase the night ventilation setpoint and decrease the night ventilation duration. If the night ventilation stops few hours before the first occupant arrives, there will be longer warmup period for the building to reach the temperature above the heating setpoint

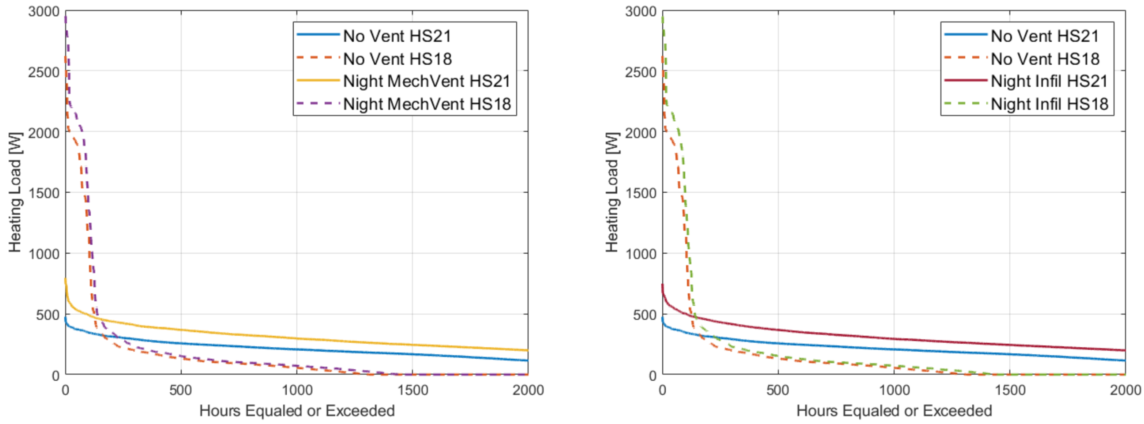

Figure 29 Heating Load Duration Curve

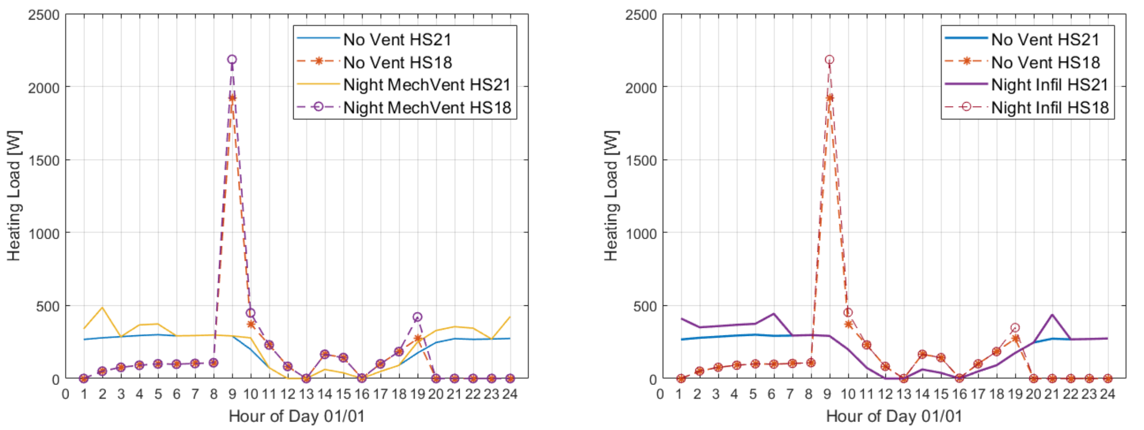

Figure 30 Heating Load in Winter Day 01/01

4 Conclusions

In this report, simulation models for fully glazed facades with interior roller blinds and window-frame integrated ventilation are developed, and evaluated in terms of the potential to improve the energy performance in office buildings.

First of all, the study compares two modelling methods for cavity ventilation of interior shading systems: the two zone airboundary method and the one zone heat removal method. For the airboundary method, the sensitivity analysis shows that the interzone airflow rate has a critical impact on the accuracy of the heat balance. With the optimum airflow rate setting at 0.3 m3/s, the airboundary model still has a 10% discrepancy in annual heating, possibly due to the insufficient radiative heat transfer. Since the study focuses on the energy performance of the building, the one zone heat removal approach was chosen for its better accuracy of heat transfer, even though the amount of heat removal is an approximate calculation.

The interior shading with cavity ventilation at the nominal air flow rate of a window-frame integrated ventilation (50m^3/h) leads to 27% decreased cooling load as compared to the no CV model. The total energy saving amounts to 17% although there is slightly increased heating and electricity consumption by the ventilation. The maximum air flow rate of the façade-integrated ventilation (300m^3/h) can decrease the cooling load by more than 60%, but 300 m^3/h may not be feasible considering the human comfort and the size of the ventilation unit. The sensitivity analysis of the airflow rate shows that 200 m^3/h cavity ventilation rate has a very close performance with the 300 m^3/h, which indicates that smaller ventilation unit may bring similar energy savings. Implementing a temperature threshold of 23 for the cavity ventilation results in no significant energy savings compared to the cavity ventilation without temperature control.

For the night ventilation strategies, the results first verify the heat removal modelling method by comparing the energy performance of NV1 with the energy performance of NV2, which is night ventilation modelled by infiltration with the same air exchange volume. Decreasing the night heating setpoint from 21°C to 18 °C without extra night mechanical ventilation leads to 10.8% energy saving. The primary energy consumption is further decreased by 11.6% when night ventilation at the nominal flow rate is implement. However, the schedule for the heating setpoint needs to be adjusted to prevent overcooling of the room and drastic increase of the heating load in winter.

There are several limitations and discrepancies in this study resulting from the modelling method:

- The ventilation modelling approach can only be used for simulating thermal energy. The scheduled heat removal influences directly on the heat balance instead of influencing the air mass in reality. It does not influence the humidity and other characteristics of the air in the room; therefore the humidity related comfort indicators are not applicable in this approach.
- When the heat removal method is applied to cavity ventilation modelling, it is assumed that the temperature inside of the cavity is unified and the same as the shading surface temperature due to the unavailability of cavity temperature output in EnergyPlus. The shading surface temperature is mostly higher than the cavity temperature during the day. This will lead to higher calculated heat removal than the actual heat removal at the same ventilation flow rate, which means the energy performance improvement in this study could be overestimated.
- Comparing with the Kindow smart shading control, the control strategy in this study is simplified with a threshold of 120 W/m^2 façade irradiance. The Kindow smart shading control has a more complex control strategy which adjust the shading height according the position of the sun to avoid glare. During the day, there will be situations that the shade is not fully down when the façade irradiance exceeds 120 W/m^2, but positioned at a higher shading height. This will lead to less convective heat accumulated in the cavity and more solar gains in the room. The cavity ventilation will have less impact on the energy performance of rooms with smart shading control than the simplified control strategy. During the night, Kindow Rollers operates according to heating and

cooling demand. Cooling demand is minimized when the shade is fully up (summer), and heating demand is minimized by fully lowering the shade (winter). Therefore, the night ventilation is expected to have the same impact on the cooling energy demand during summer, since the shades are also always up during the night in the simplified control strategy. However, the heating energy during winter will be lower with the smart control strategy.

Future work of this window-frame integrated ventilation concept can further evaluate and improve the energy performance of the system by the following aspects:

- As described in 1.3, Physee SmartSkin generates data by the sensors and electricity by the solar cells which can be used to power and control the ventilation unit. In order to form a completely autonomous system, it is worth investigating whether the PV production can meet the electricity consumption and storage needs of the ventilation and shading system
- The schedule for the night heating setpoint needs could be shorter and the temperature setpoint of the night ventilation could be higher to prevent overcooling of the room. The night ventilation control strategy in this study leads to drastic increase of the heating load during the first occupied hour. It can be prevented by stop the night ventilation few hours before the first occupant arrives or by increase the night ventilation setpoint so that the room temperature is higher in the morning.

Literture

[1] M. Perino and V. Serra, "Switching from static to adaptable and dynamic building envelopes: a paradigm shift for the energy efficiency in buildings," *Journal of Facade Design and Engineering,* vol. 3, p. 143–163, 2015.

[2] D. Aelenei, L. Aelenei, R. Loonen, M. Perino and S. Valentina, "Adaptive Facades," in *Handbook of Energy Efficiency in Buildings: A Life Cycle Approach*, Elsevier, 2019, pp. 384-411.

[3] J. P. L. B. E. S. M. K. F. Meggers, "Evaluating and adapting low exergy systems with decentralized ventilation for tropical climates," *Energy Build.,* vol. 67 , pp. 559-567, 2013.

[4] M. ,. S. T. P. C. B. Bruno Buenoa, "A co-simulation modelling approach for the assessment of a ventilated double-skin complex fenestration system coupled with a compact fan-coil unit," *Energy and Buildings,* vol. 151, no. 15, pp. 18-27, 2017.

[5] P.-R. Denz, "ACT Façade – Interior sun shading for energy efficient fully glazed façades.," in *Final conference of COST TU1403 "Adaptive Facades Network"*, Lucerne, 2018.

[6] "PHYSEE PRODUCTS," Physee, [Online]. Available: https://www.physee.eu/products. [Accessed 5th January 2019].

[7] O. Ghosh, S. d. Vries and R. Loonen, "Energy performance analysis of advanced interior solar shading systems – Kindow Rollerblinds vs. state-of-the-art alternatives," 27 August 2019. [Online]. Available: https://kindowblinds.com/wp-content/uploads/downloads/Energy%20performance%20analysis%20of%20advanced%20interior%20solar%20shading%20systems-Revised.pdf. [Accessed 5th January 2020].

[8] Pridmann, "Passende Parameter," 2016. [Online]. Available: https://www.v-f-t.de/images/Publikationen_von_Mitgliedern/W.Priedemann_2016-07_FT_03.pdf. [Accessed 7 January 2020].

[9] P. F. Experts, "New Development in Solar Thermal Facade," [Online]. Available: https://aee-intec.at/0uploads/dateien1459.pdf. [Accessed 15 January 2019].

[10] "ClimaRad S-Fan," [Online]. Available: https://www.climarad.nl/files/downloads/documentatie/climarad_s-fan.pdf. [Accessed 16 11 2020].

[11] "Invisivent COMFORT," RENSON, [Online]. Available: https://www.renson.eu/en-gb/producten-zoeken/ventilatie/raamverluchtingen/roosters-op-het-raam/invisivent-comfort. [Accessed 16 11 2020].

[12] RENSON. [Online]. Available: https://www.renson.eu/gd-gb/products/ventilation/mechanical-ventilation. [Accessed 23 11 2020].

[13] P. Bonato, M. D. Antoni and R. Fedrizzi, "Modelling and simulation-based analysis of a façade-integrated decentralised ventilation unit," *Journal of Building Engineering ,* no. 101183, p. 29, 2020.

[14] G. Rui, H. Yue, L. Mingzhe and H. Per, "Optimal Night Mechanical Ventilation control strategy in office buildings," in *IOP Conference Series: Materials Science and Engineering*, 2012.

[15] Y. H. M. L. P. H. Rui Guo1, "Optimal Night Mechanical Ventilation control strategy in office buildings," in *IOP Conf. Series: Materials Science and Engineering* , 2019.

[16] Judkoff and Neymark, "International Energy Agency Building Simulation Test (BESTEST)," 1995.

[17] D. D. G. D. A. H. O. S. W. Beck, "Solar Shading: How to integrate solar shading in sustainable buildings," in *REHVA Guidebook* , 2010, p. 12.

[18] "Primaire fossiele energiefactor elektriciteit op bovenwaarde (HHV) voor toepassing in de energieprestatienorm NTA8800," ECN TNO, 2018.

[19] S. B. d. Vries, *Computational Analysis and Optimization of Innovative Shading Strategies.*

[20] "KINDOW ROLLERS," Kindow, [Online]. Available: https://kindowblinds.com/products/kindow-rollers/. [Accessed 5th January 2019].

[21] R. Loonen, M. Trčka, D. Cóstola and J. Hensen, "Climate Adaptive Building Shells: State-of-theArt and Future Challenges," *Renewable and Sustainable Energy Reviews ,* pp. 483-93, 2013.

[22] Z. Wang, L. Yi and F. Gao, "Night ventilation control strategies in office buildings,," *Sol. Energy.,* vol. 83, pp. 1902-1913, 2009.

[23] I. Gaetani, P.-J. Hoes and J. L. M. Hensen, "Occupant behavior in building energy simulation: towards a fit-for-purpose modeling strategy," *Energy and Buildings,* 2016.

[24] J. Clarke and J. Hensen, "Integrated building performance simulation: Progress, prospects and requirements," *Builidng and Environment,* vol. 91, pp. 294-306, 2015.

[25] B. Vidrih, C. Arkar and S. Medved, "Generalized model-based predictive weather control for the control of free cooling by enhanced night-time ventilation," *Appl. Energy.,* vol. 168, pp. 482-492, 2016.

[26] F. Goia, M. Haase and MarcoPerinoa, "Optimizing the configuration of a facade module for office buildings by means of integrated thermal and lighting simulations in a total energy perspective," *Appl Energy,* vol. 108, pp. 515-27, 2013.

[27] XuXu and S. V. Dessel, "Evaluation of an active building envelope window-system.," *Build Environ,* vol. 43, no. 11, p. 1785–91, 2008.

[28] F. Favoino, F. Goia, M. Perino and V. Serra, "Experimental assessment of the energy performance of an advanced responsive multifunctional fac¸ade module," *Energy Build,* vol. 68, pp. 647-59, 2014.

[29] K.-U. Ahn and C. S. Park, "Different occupant modeling approaches for building energy prediction," *Energy Procedia,* vol. 88, no. 1, pp. 721-724, 2016.

[30] L. Wu, J. Zhao and Z. Wang, "Night ventilation and active cooling coupled operation for large supermarkets in cold climates," *Energy Build.,* pp. 1409-1416, 2006.

[31] P. Roach, F. Bruno and M. Belusko, "Modelling the cooling energy of night ventilation and economiser strategies on façade selection of commercial buildings," *Energy Build.,* vol. 66, pp. 562-570, 2013.

[32] P. Bonato, D. Matteo and R. Fedrizzi, "Demand-controlled ventilation through a decentralized mechanical ventilation unit for office buildings," in *Society for Modeling & Simulation International (SCS)*, Delft, 2018.

[33] [Online]. Available: https://bigladdersoftware.com/epx/docs/9-3/engineering-reference/window-heat-balance-calculation.html#solving-for-gap-airflow-and-temperature.

[34] "Low-tech ventilation for double-glazed facades," [Online]. Available: https://www.detail-online.com/article/low-tech-ventilation-for-double-glazed-facades-31800/. [Accessed 16 11 2020].

Appendices

A. Model Properties

Window Properties

Shading Material	Solar		Visible		U (W/m^2K)
	Transmittance	Reflectance	Transmittance	Reflectance	
PHYSEE Glass	0.55	0.13	0.76	0.15	1.0

Shading screen properties

Shading Material	Solar		Visible		Emissivity	Infrared Transmittance	Thickness (mm)	Conductivity (W/mK)
	Transmittance	Reflectance	Transmittance	Reflectance				
Kindow Rollers	0.03	0.81	0.03	0.81	0.54	0.0164	5	0.3
Task 56 Generic	0.3	0.6	0.3	0.6	0.9	0	2.5	221

B. Modelling Method Validation: Heat Balance of Airboundary Model at 0.1-1 m^3/s interzone airflow rate

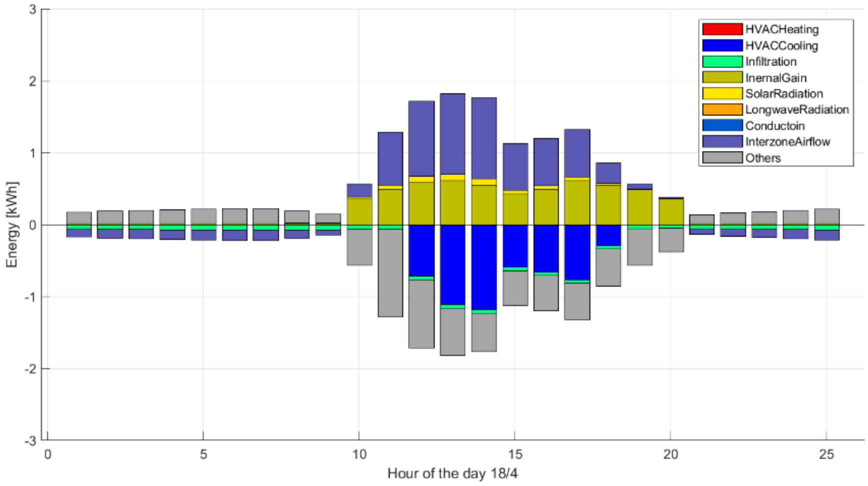

$0.1 m^3/s$

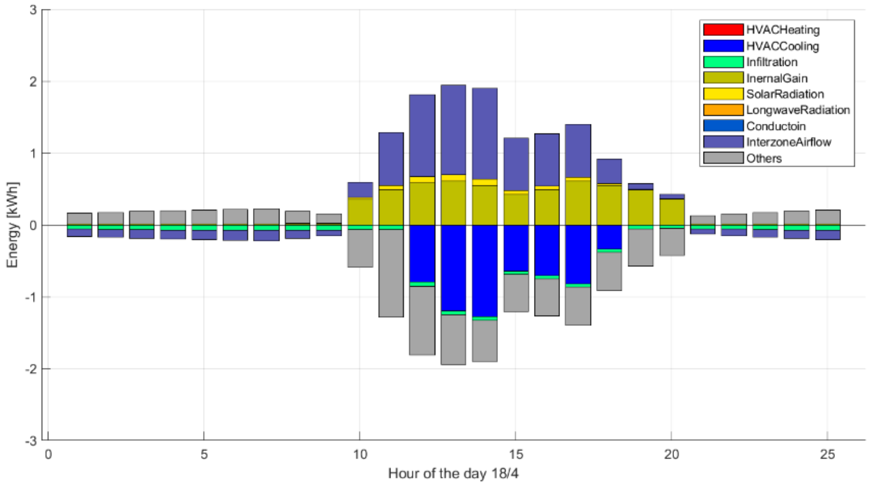

$0.2 m^3/s$

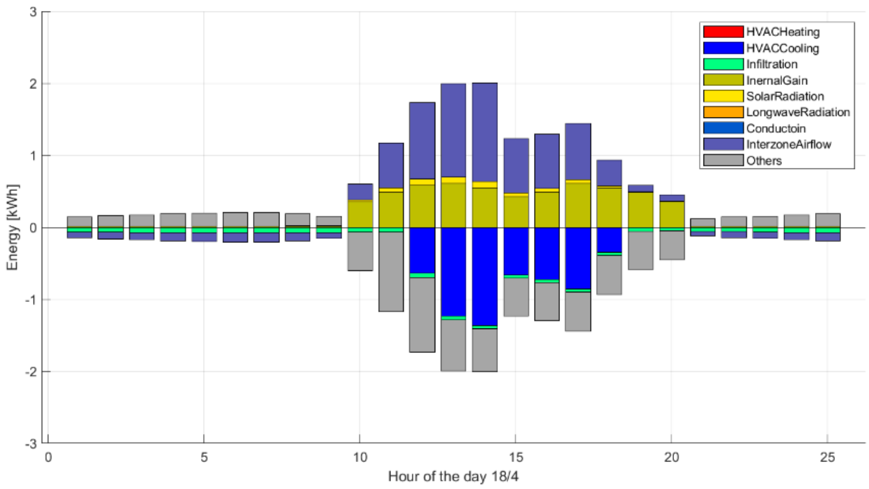

$0.3 m^3/s$

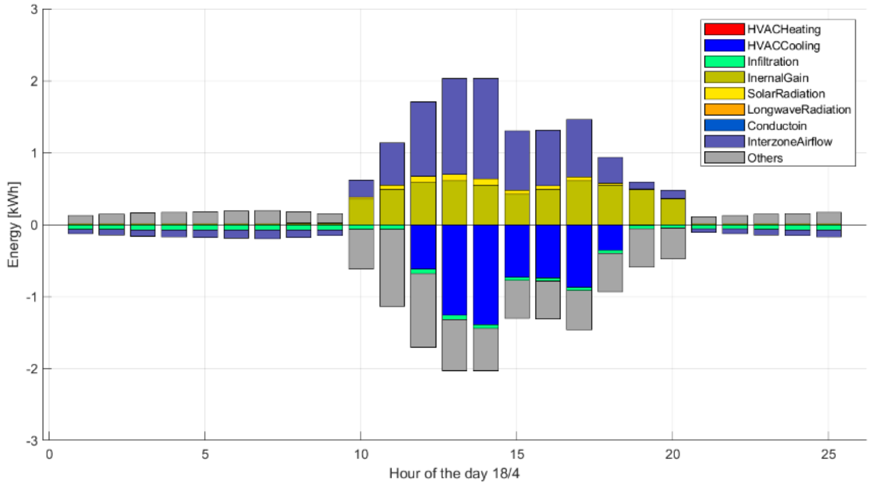

0.4 m^3/s

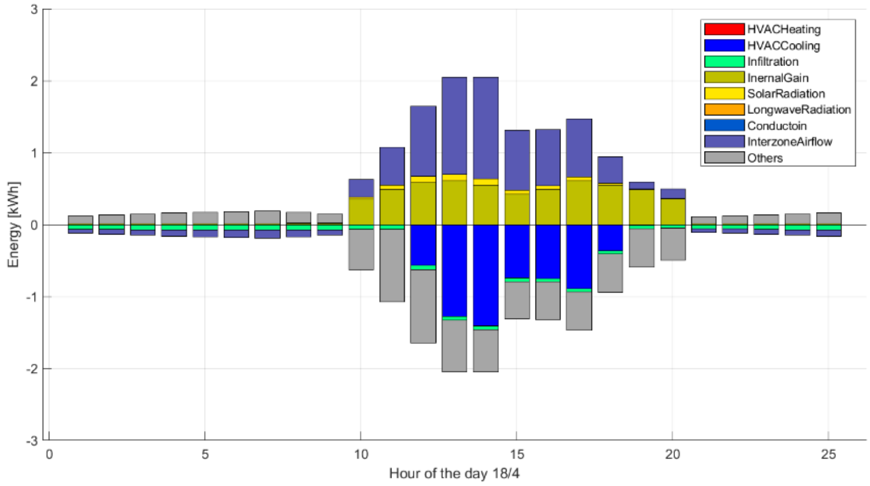

0.5 m^3/s

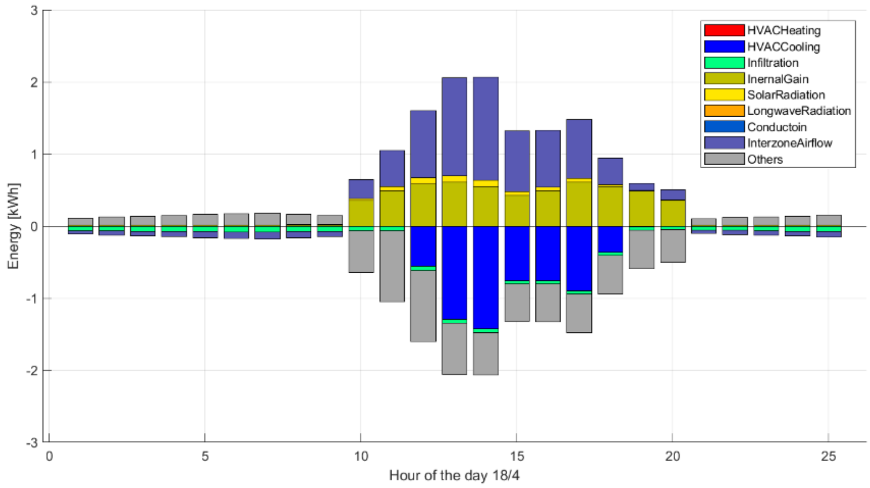

0.6 m^3/s

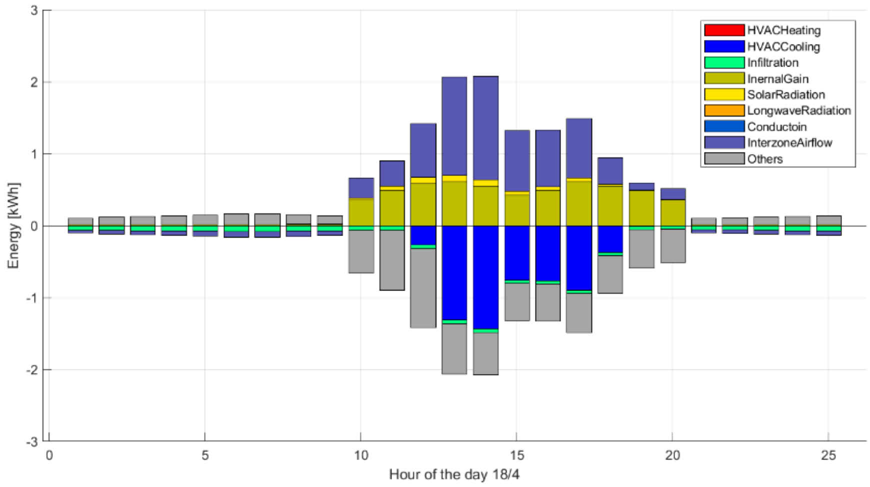

0.7 m^3/s

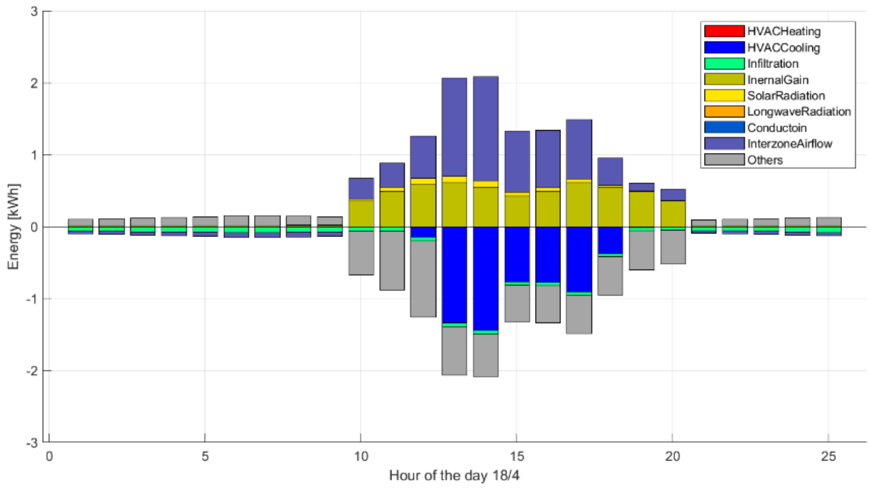

0.8 m^3/s

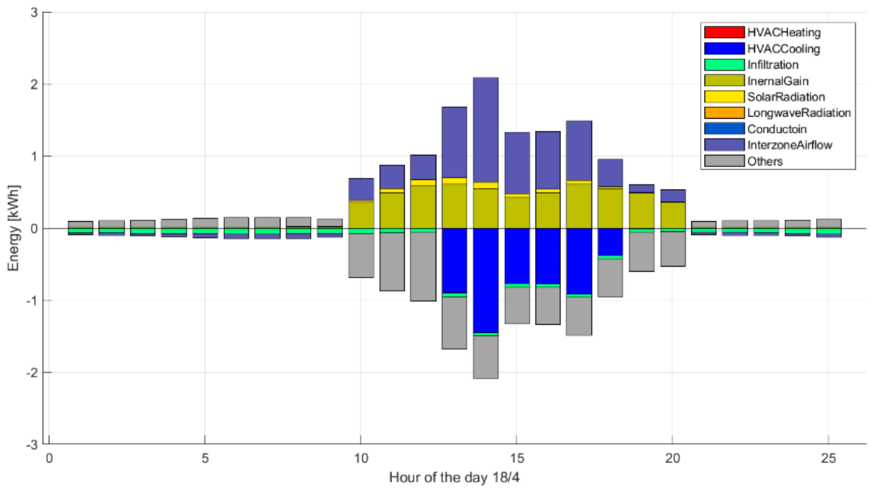

0.9 m^3/s

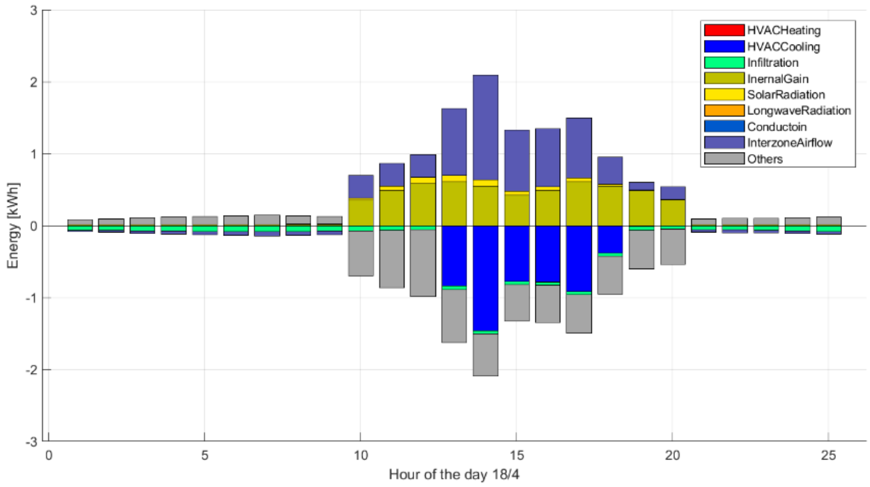

HVACHeating
HVACCooling
Infiltration
InernalGain
SolarRadiation
LongwaveRadiation
Conductoin
InterzoneAirflow
Others
Energy [kWh]
Hour of the day 18/4

1.0 m^3/s

C. Cavity Ventilation Peak Heating/Cooling Load Results

VentStrategy (flow rate)	BL1	BL2	BL3	CV1 10	CV1 50	CV1 100	CV1 200	CV1 300	CV2 10	CV2 50	CV2 100	CV2200	CV2 300
Peak Heating Load (kW)	0.50	0.57	0.51	0.50	0.51	0.52	0.52	0.52	0.50	0.50	0.51	0.51	0.51
Peak Cooling Load(kW)	2.84	0.75	1.52	2.81	2.69	2.54	2.38	2.26	2.81	2.68	2.54	2.38	2.26

D. Night Ventilation Results

Peak Heating/Cooling Load

VentStrategy	NoVent HS21	NoVent HS18	NV1 HS21	NV1 HS18	NV2 HS21	NV2 HS18
Peak Heating Load (kW)	0.50	6.23	0.97	0.62	0.93	0.6.23
Peak Cooling Load(kW)	2.84	2.84	2.74	2.74	2.74	2.74

Cooling Load & Temperatur Graph

No Vent HS21

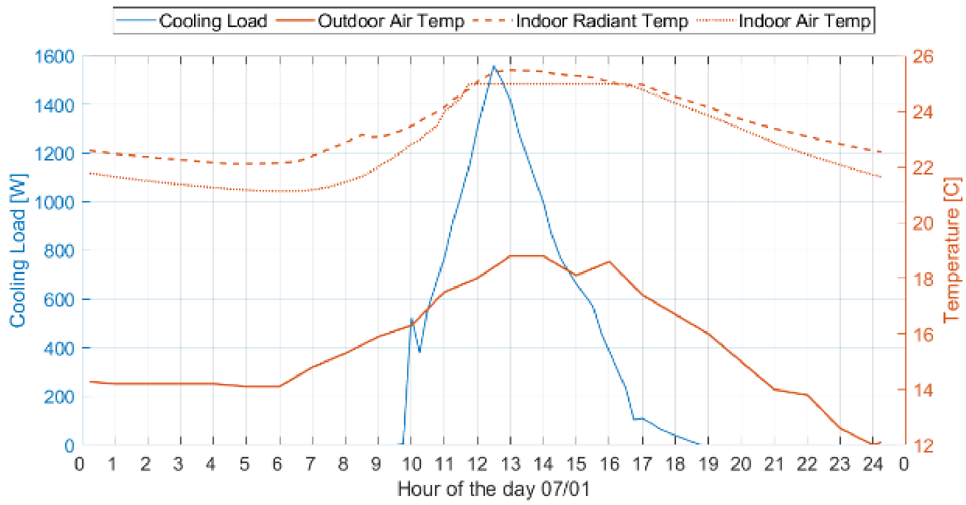

No Vent HS 18

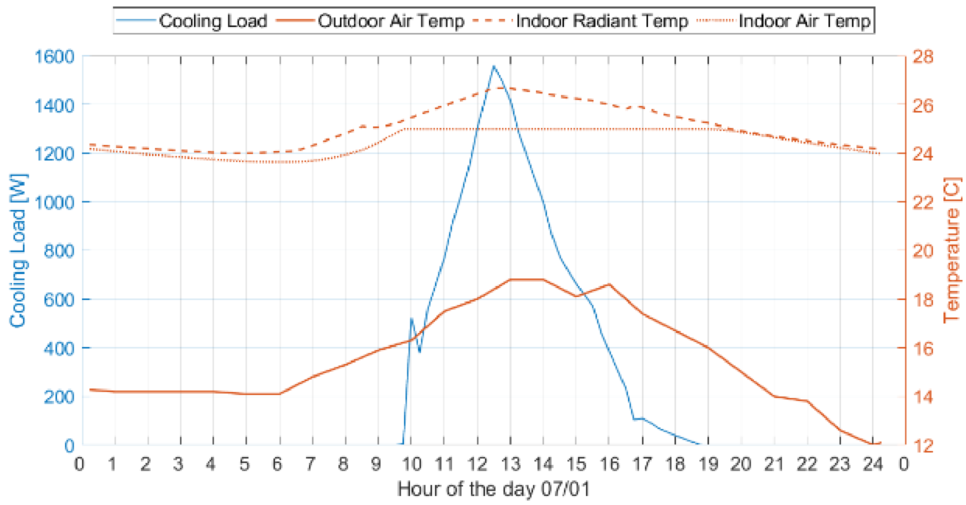

Night MechVent HS21

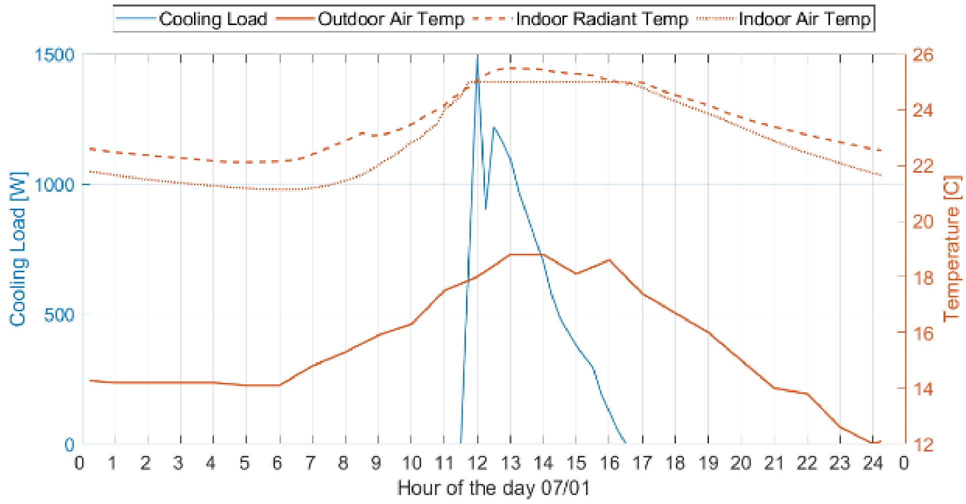

Night MechVent HS18

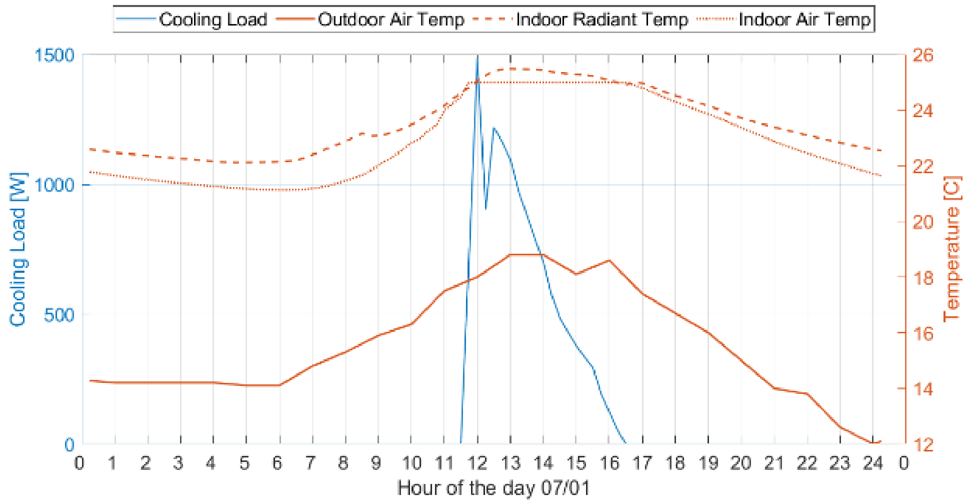

Night Infil HS21

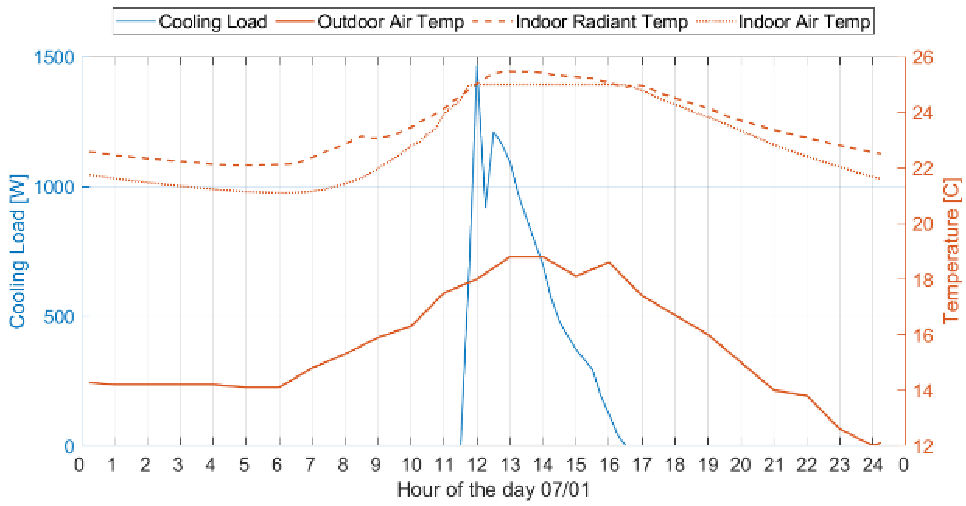

Night Infil HS18